

Organization TC-1600 Bldg./Room Kensen

U. S. DEPARTMENT OF COMMERCE

COMMISSIONER FOR PATENTS

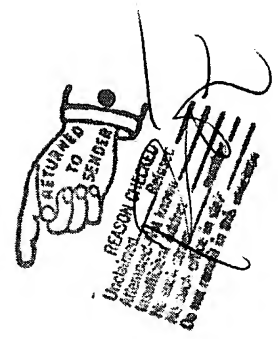
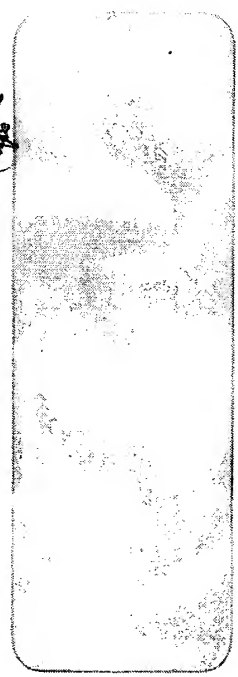
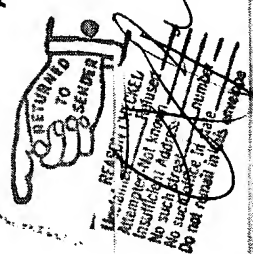
P.O. BOX 1450

ALEXANDRIA, VA 22313-1450

IF UNDELIVERABLE RETURN IN TEN DAYS

OFFICIAL BUSINESS

AN EQUAL OPPORTUNITY E



RECEIVED  
MAR 22 2004  
TECH CENTER 1600/2900



# UNITED STATES PATENT AND TRADEMARK OFFICE

UNITED STATES DEPARTMENT OF COMMERCE  
United States Patent and Trademark Office  
Address: COMMISSIONER FOR PATENTS  
P.O. Box 1450  
Alexandria, Virginia 22313-1450  
www.uspto.gov

APPLICATION NO.	FILING DATE	FIRST NAMED INVENTOR	ATTORNEY DOCKET NO.	CONFIRMATION NO.
10/005,220	12/04/2001	Keith D. Allen	R-741	6858
7590 03/08/2004				
DELTAGEN, INC. 740 Bay Road Redwood City, CA 94603				
			EXAMINER PARAS JR, PETER	
			ART UNIT 1632	PAPER NUMBER

DATE MAILED: 03/08/2004

Please find below and/or attached an Office communication concerning this application or proceeding.

**Office Action Summary**

Application No.

10/005,220

Applicant(s)

ALLEN, KEITH D.

Examiner

Peter Paras, Jr.

Art Unit

1632

-- The MAILING DATE of this communication appears on the cover sheet with the correspondence address --  
Period for Reply

A SHORTENED STATUTORY PERIOD FOR REPLY IS SET TO EXPIRE 3 MONTH(S) FROM THE MAILING DATE OF THIS COMMUNICATION.

- Extensions of time may be available under the provisions of 37 CFR 1.136(a). In no event, however, may a reply be timely filed after SIX (6) MONTHS from the mailing date of this communication.
- If the period for reply specified above is less than thirty (30) days, a reply within the statutory minimum of thirty (30) days will be considered timely.
- If NO period for reply is specified above, the maximum statutory period will apply and will expire SIX (6) MONTHS from the mailing date of this communication.
- Failure to reply within the set or extended period for reply will, by statute, cause the application to become ABANDONED (35 U.S.C. § 133). Any reply received by the Office later than three months after the mailing date of this communication, even if timely filed, may reduce any earned patent term adjustment. See 37 CFR 1.704(b).

**Status**

- 1) ☐ Responsive to communication(s) filed on \_\_\_\_.
- 2a) ☐ This action is **FINAL**. 2b) ☒ This action is non-final.
- 3) ☐ Since this application is in condition for allowance except for formal matters, prosecution as to the merits is closed in accordance with the practice under *Ex parte Quayle*, 1935 C.D. 11, 453 O.G. 213.

**Disposition of Claims**

- 4) ☒ Claim(s) 14 and 25-41 is/are pending in the application.
- 4a) Of the above claim(s) 39 is/are withdrawn from consideration.
- 5) ☐ Claim(s) \_\_\_\_ is/are allowed.
- 6) ☒ Claim(s) 14 and 25-41 is/are rejected.
- 7) ☐ Claim(s) \_\_\_\_ is/are objected to.
- 8) ☐ Claim(s) \_\_\_\_ are subject to restriction and/or election requirement.

**Application Papers**

- 9) ☐ The specification is objected to by the Examiner.
- 10) ☒ The drawing(s) filed on 04 December 2001 is/are: a) ☒ accepted or b) ☐ objected to by the Examiner.  
Applicant may not request that any objection to the drawing(s) be held in abeyance. See 37 CFR 1.85(a).  
Replacement drawing sheet(s) including the correction is required if the drawing(s) is objected to. See 37 CFR 1.121(d).
- 11) ☐ The oath or declaration is objected to by the Examiner. Note the attached Office Action or form PTO-152.

**Priority under 35 U.S.C. § 119**

- 12) ☐ Acknowledgment is made of a claim for foreign priority under 35 U.S.C. § 119(a)-(d) or (f).
- a) ☐ All b) ☐ Some \* c) ☐ None of:
1. ☐ Certified copies of the priority documents have been received.
  2. ☐ Certified copies of the priority documents have been received in Application No. \_\_\_\_.
  3. ☐ Copies of the certified copies of the priority documents have been received in this National Stage application from the International Bureau (PCT Rule 17.2(a)).

\* See the attached detailed Office action for a list of the certified copies not received.

**Attachment(s)**

- |   |   |
|---|---|
| 1) <input checked="" type="checkbox"/> Notice of References Cited (PTO-892)   | 4) <input type="checkbox"/> Interview Summary (PTO-413)<br>Paper No(s)/Mail Date. ____. |
| 2) <input type="checkbox"/> Notice of Draftsperson's Patent Drawing Review (PTO-948)  | 5) <input type="checkbox"/> Notice of Informal Patent Application (PTO-152)             |
| 3) <input checked="" type="checkbox"/> Information Disclosure Statement(s) (PTO-1449 or PTO/SB/08)<br>Paper No(s)/Mail Date <u>1003</u> . | 6) <input type="checkbox"/> Other: ____.  |

### **DETAILED ACTION**

Applicant's preliminary amendment received on 12/3/02 has been entered.

Claims 1-13 and 15-24 have been cancelled. Claim 14 has been amended. New claims 25-41 have been added. Claims 14 and 25-41 are pending.

### ***Election/Restrictions***

Restriction to one of the following inventions is required under 35 U.S.C. 121:

- I. Claims 14, 25-38 and 40-41, drawn to a transgenic mouse comprising a disruption in an endogenous RPTPB gene, a method of producing the same mouse, and cells comprising a disruption in an endogenous RPTPB, classified in classes 800, 800, and 435, subclasses 18, 21 and 325.
- II. Claim 39, drawn to a targeting construct for an RPTPB gene, classified in class 435, subclass 320.1.

Inventions I and II are unrelated. Inventions are unrelated if it can be shown that they are not disclosed as capable of use together and they have different modes of operation, different functions, or different effects (MPEP § 806.04, MPEP § 808.01). In the instant case the different inventions are materially different products having different functions. For example the transgenic mouse of Group I can be used as a disease model while the targeting construct of Group II can be used for disrupting an RPTPB gene in a cell *in vitro*. Because these inventions are distinct for the reasons given above and have acquired a separate status in the art because of their recognized



divergent subject matter, different classification, and separate search requirement, restriction for examination purposes as indicated is proper.

During a telephone conversation with Robert Driscoll on 2/10/04 a provisional election was made without traverse to prosecute the invention of Group I, claims 14, 25-38, and 40-41. Affirmation of this election must be made by applicant in replying to this Office action. Claim 39 is withdrawn from further consideration by the examiner, 37 CFR 1.142(b), as being drawn to a non-elected invention.

#### ***Sequence Compliance***

This application contains sequence disclosures that are encompassed by the definitions for nucleotide and/or amino acid sequences set forth in 37CFR 1.821(a)(1) and (a)(2). However, this application fails to comply with the requirements of 37 CFR 1.821 through 1.825 for the reason(s) set forth on the attached Notice To Comply With Requirements For Patent Applications Containing Nucleotide Sequence And/Or Amino Acid Sequence Disclosures.

Applicants are required to comply with all of the requirements of 37 C.F.R. §§ 1.821 through 1.825. Any response to this Office Action, which fails to meet all of these requirements, will be considered non-responsive. The nature of the noncompliance with the requirements of 37 C.F.R. §§ 1.821 through 1.825 did not preclude the examination of the application on the merits, the results of which are communicated below.

***Drawings***

The drawings filed on 12/4/01 are accepted.

***Claim Objections***

Claim 40 is objected to as it depends from a non-elected claim.

***Claim Rejections - 35 USC § 101***

35 U.S.C. 101 reads as follows:

Whoever invents or discovers any new and useful process, machine, manufacture, or composition of matter, or any new and useful improvement thereof, may obtain a patent therefor, subject to the conditions and requirements of this title.

Claim 40 is rejected under 35 U.S.C. 101 because the claimed invention is directed to non-statutory subject matter. The claim is directed to a murine embryonic stem cell comprising a disruption in a RPTPB gene the scope of which is interpreted to read on a murine embryonic stem cell *in vivo*, which embraces a mouse or rat comprising a naturally occurring disruption in an RPTPB gene. Amending the claim to read on an isolated murine stem cell may be sufficient to overcome the instant rejection.

Claims 14, 25-38, and 40-41 are rejected under 35 U.S.C. 101 because the claimed invention is not supported by either a substantial and specific asserted utility or a well-established utility.

The claims are directed to a transgenic mouse comprising a disruption in an endogenous RPTPB gene wherein the mouse exhibits embryonic lethality, wherein lethality occurs at E9.5-10.5 and the embryo exhibits reduced vascular development

The instant specification has contemplated that the nucleotide sequence set forth in SEQ ID NO: 1 encodes a RPTPB gene. The instant specification has further contemplated that disruption of the nucleotide sequence set forth in SEQ ID NO: 1 in a mouse will produce a phenotype related to RPTPB. The instant specification has purported that such mice may be used to identify agents that modulate or ameliorate a phenotype associated with a disruption in SEQ ID NO: 1.

The instant specification has disclosed a heterozygous transgenic mouse whose genome comprises a disruption in SEQ ID NO: 1 [that does not exhibit a phenotype], wherein a mouse embryo whose genome comprises a homozygous disruption in SEQ ID NO: 1 exhibits embryonic lethality, wherein lethality occurs at E9.5-10.5 and the embryo exhibits reduced vascular development. The claims embrace such a mouse and a method of making the mouse. The instant specification has discussed that phenotype, such as embryonic lethality exhibited by such a transgenic mouse could correlate to a disease or disorder. However, the evidence of record does not provide a correlation between the observed embryonic lethality and any disease or disorder. Moreover, while the specification has purported that the nucleotide sequence set forth in SEQ ID NO: 1 encodes a RPTPB, the evidence of record has failed to provide a correlation between any RPTPB related disease/disorder and embryonic lethality. The specification has provided general assertions that the claimed transgenic mice may be used to identify agents that affect a phenotype related to the mice.

As such, the asserted utility, for the transgenic mouse embraced by the claims, of screening agents that may affect a phenotype of said mouse as provided by the instant

Art Unit: 1632

specification and encompassed by the claims, does not appear to be specific and substantial. The asserted utility does not appear specific and substantial to the skilled artisan since the evidence of record has not provided any suggestion of a correlation between any RPTPB, embryonic lethality, and any disease or disorder. Since the evidence of record has not provided a correlation between embryonic lethality and any disease or disorder, the utility of identifying agents that affect embryonic lethality is not apparent. The evidence of record has not provided any other utilities for the transgenic mouse embraced by the claims that are specific, substantial, and credible.

The asserted utility of the transgenic mouse embraced by the claims is based on the expectation that disrupting the nucleotide sequence set forth in SEQ ID NO: 1 would result in a detectable phenotype in the mouse. The phenotype observed in the transgenic mice embraced by the claims is embryonic lethality. While the phenotypes exhibited by the claimed transgenic mouse are contemplated to be associated with a disease, the association of embryonic lethality with any disease has yet to be elucidated. In fact the art suggests that phenotypes, such as embryonic lethality, are greatly influenced by the genetic background of the transgenic knockout mouse. For example, Casademunt et al report (EMBO, 1999, 18(21): 6050-6061) *nrif* <sup>-/-</sup> mice exhibit differences in embryonic lethality that appear dependent on the genetic background of the mouse. In short, transgenic *nrif* <sup>-/-</sup> mice in a BL6 background cannot survive past E12 while in an Sv129 background such transgenic mice are viable and healthy to adulthood. See the abstract and throughout the entire document. Furthermore, LeCouter et al (Development, 1998, 125: 4669-4679) observe that a null

mutation in a p130 is lethal at E11-13 on a Balb/cJ background but when such a mutation is crossed onto a C57BL/6 background the resulting mice are viable and fertile. See the abstract and throughout the entire document. More to the point, Harroch et al (Molecular and Cellular Biology, 2000, 20(20): 7706-7715; IDS) discuss that an RPTPB null mutation crossed into a Swiss Webster genetic background result in mice having no obvious abnormalities. See the abstract and throughout the entire document. The instant specification has taught use of ES cells from a 129/OlaHSD genetic background to generate chimeric mice, which were then bred onto a C57BL6 genetic background to produce the instantly claimed mice exhibiting embryonic lethality as homozygous embryos. See pages 50-51 of the instant specification.

Therefore, the references suggest a need to provide independent evidence of an association of embryonic lethality with a disease or disorder. However, neither the specification nor any art of record provides evidence of the existence of a correlation between embryonic lethality and a disease or disorder, leaving the skilled artisan to speculate and investigate the uses of the transgenic mouse embraced by the claims. The specification essentially gives an invitation to experiment wherein the artisan is invited to elaborate a functional use for the transgenic mouse embraced by the claims. In light of the above, the skilled artisan would not find the asserted utility of the transgenic mouse embraced by the claims to be specific and substantial.

***Claim Rejections - 35 USC § 112, 1<sup>st</sup> paragraph***

The following is a quotation of the first paragraph of 35 U.S.C. 112:

The specification shall contain a written description of the invention, and of the manner and process of making and using it, in such full, clear, concise, and exact terms as to enable any person skilled in the art to which it pertains, or with which it is most nearly connected, to make and use the same and shall set forth the best mode contemplated by the inventor of carrying out his invention.

Claims 14, 25-38, and 40-41 are also rejected under 35 U.S.C. 112, first paragraph. Specifically, since the claimed invention is not supported by either a substantial and specific asserted utility or a well established utility for the reasons set forth above, one skilled in the art clearly would not know how to use the claimed invention.

In addition the following additional rejections are necessitated under 35 U.S.C. 112, first paragraph:

Both the specification and the state of the art have taught that the transgenic knockout technology requires the use of embryonic stem cells that have been genetically manipulated to comprise a disruption in a nucleotide sequence of interest. The specification has not taught creation of a transgenic knockout mouse by methods that do not require embryonic stem cells. Presently, the transgenic knockout technology is limited to the mouse system. See below.

With regard to the claim breadth, claims 38 and 40 embrace murine embryonic stem cells, which encompass species other than mice, such as rats and gerbils. The specification fails to teach use of embryonic stems from species other than mice. It is well known in the knockout art that the production of knockout animals other than mice is undeveloped. This is because ES cell technology is generally limited to the mouse

Art Unit: 1632

system, at present, and that only "putative" ES cells exist for other species. See Moreadith et al. at page 214, Summary. Seamark (Reproductive Fertility and Development, 1994) supports this observation by reporting that totipotency for ES cell technology in many livestock species has not been demonstrated (page 6, Abstract). Likewise, Mullins et al (Journal of Clinical Investigation, 1996) state, "although to date chimeric animals have been generated from several species including the pig, in no species other than the mouse has germline transmission of an ES cell been successfully demonstrated." (page S38, column 1, first paragraph). Furthermore, claims 25-38 as written do not appear to require germline transmission of the disrupted nucleotide sequence. These claims may be broadly interpreted to read on a single cell comprising a disrupted nucleotide sequence. Since the claims do not require germline transmission of the disrupted nucleotide sequence it would be unpredictable if an ES cell comprises the disrupted nucleotide sequence. The evidence of record does not support germline transmission of non-ES cells. Also, it would be unpredictable if a disruption of a nucleotide sequence in a single cell would result in a phenotype; the instant specification has not provided any uses for a transgenic mouse that does not exhibit a phenotype resulting from disruption of a nucleotide sequence (see below). Amending the claims to read on a "transgenic mouse whose genome comprises" would be sufficient to suggest germline transmission. Given the unpredictable state of the art it would have required undue experimentation for the skilled artisan to create transgenic knockout non-human animals of species other than the mouse.

Claims 14 and 25-27 encompasses transgenic mice that comprise a disruption in a RPTPB gene, particularly the nucleotide sequence set forth in SEQ ID NO: 1, that do not exhibit any particular phenotype. Claims 14 and 28-38 embrace transgenic mice exhibiting a particular phenotype, wherein a broad interpretation of the claimed animals could read on disruption of a RPTPB gene in a single cell. Claims 14, 25 and 27-38 embrace transgenic mice comprising a heterozygous disruption of an RPTPB gene. The specification has taught that transgenic mouse embryos whose genomes comprise a homozygous disruption of the RPTPB gene exhibit a phenotype of embryonic lethality. The specification has not provided guidance correlating to a phenotype in the other transgenic mice embraced by the claims. The state of the art at the time of filing was such that one of skill could not predict the phenotype of a knockout mouse (Moreadith et al., 1997, J. Mol. Med., Vol. 75, pages 208-216; see page 208, column 2, last full paragraph). Also see Leonard et al (Immunological Reviews, 1995, pages 97-114) who discuss that inactivation of the gene encoding cytokine receptor  $\gamma$  chain in transgenic mice results in a phenotype different from that expected. Finally, Moens et al. (Development, Vol. 119, pages 485-499, 1993) disclose that two mutations produced by homologous recombination in two different locations of the N-myc gene produce two different phenotypes in mouse embryonic stem cells, one leaky and one null (see abstract). The specification has asserted that the nucleotide sequence set forth in SEQ ID NO: 1 encodes a RPTPB. However, it would be difficult to predict any phenotype resulting from disruption of the sequence of SEQ ID NO: 1 in light of the above. Moreover, as the claims read on disruption of a RPTPB gene in a single cell, it would be



unpredictable if such a disruption would result in any phenotype. The specification discloses a phenotype exhibited by transgenic mouse embryos whose genome comprises a homozygous disruption in the nucleotide sequence set forth in SEQ ID NO: 1 is embryonic lethality. See pages 50-52 of the specification. Claims 14 and 25-27 as written, do not include a phenotype that differs from the wild-type mouse. One of skill in the art would not know how to use a transgenic knockout non-human animal that lacks a phenotype, particularly because the instant specification has not provided uses for such; the transgenic mice that have a phenotype may be used for drug testing according to the instant specification. The claims (14, 25 and 27-38) embracing heterozygous mice are not enabled as the specification has not disclosed a phenotype for such and because as previously stated, the skilled artisan would not know how to use a transgenic mouse lacking a phenotype. Accordingly, the claims are not commensurate in scope with the phenotype disclosed in the specification. Given the unpredictable nature of a phenotype that results from disruption of a nucleotide sequence it would have required undue experimentation for the skilled artisan to make and use the invention as claimed.

It is noted that the claims, which embrace a homozygous disruption of the RPTPB gene, are directed to a transgenic mouse. However, use of transgenic mouse language implies a full term mouse was created. This language appears inconsistent with the teachings of the specification because it appears that the homozygous mouse embryos did not mature to term given the phenotype of embryonic lethality.

***Claim Rejections - 35 USC § 102***

The following is a quotation of the appropriate paragraphs of 35 U.S.C. 102 that form the basis for the rejections under this section made in this Office action:

A person shall be entitled to a patent unless –

(a) the invention was known or used by others in this country, or patented or described in a printed publication in this or a foreign country, before the invention thereof by the applicant for a patent.

Claims 14 and 25-27 are rejected under 35 U.S.C. 102(a) as being anticipated by Harroch (IDS).

The claims are directed to a transgenic mouse comprising a disruption in an RPTPB gene.

Harroch et al teach transgenic mice comprising a homozygous disruption in the RPTPB gene.

Accordingly, Harroch et al anticipate all of the instant claim limitations.

**Conclusion**

**No claim is allowed.**

Art Unit: 1632

Any inquiry concerning this communication or earlier communications from the examiner(s) should be directed to Peter Paras, Jr., whose telephone number is (571) 272-0732. The examiner can normally be reached Monday-Friday from 8:30 to 4:30 (Eastern time).

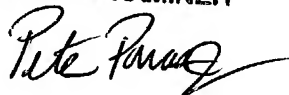
If attempts to reach the examiner by telephone are unsuccessful, the examiner's supervisor, Amy Nelson, can be reached at 571-272-0804. Papers related to this application may be submitted by facsimile transmission. Papers should be faxed via the PTO Fax Center located in Crystal Mall 1. The faxing of such papers must conform with the notice published in the Official Gazette, 1096 OG 30 (November 15, 1989). The CM1 Official Fax Center number is (703) 872-9306.

Inquiries of a general nature or relating to the status of the application should be directed to Dianiece Jacobs whose telephone number is (571) 272-0532.

Peter Paras, Jr.

Art Unit 1632

**PETER PARAS, JR.**  
**PRIMARY EXAMINER**



**NOTICE TO COMPLY WITH REQUIREMENTS FOR PATENT APPLICATIONS CONTAINING  
NUCLEOTIDE SEQUENCE AND/OR AMINO ACID SEQUENCE DISCLOSURES**

The nucleotide and/or amino acid sequence disclosure contained in this application does not comply with the requirements for such a disclosure as set forth in 37 C.F.R. 1.821 - 1.825 for the following reason(s):

- ☒ 1. This application clearly fails to comply with the requirements of 37 C.F.R. 1.821-1.825. Applicant's attention is directed to these regulations, published at 1114 OG 29, May 15, 1990 and at 55 FR 18230, May 1, 1990.
- ☐ 2. This application does not contain, as a separate part of the disclosure on paper copy, a "Sequence Listing" as required by 37 C.F.R. 1.821(c).
- ☐ 3. A copy of the "Sequence Listing" in computer readable form has not been submitted as required by 37 C.F.R. 1.821(e).
- ☐ 4. A copy of the "Sequence Listing" in computer readable form has been submitted. However, the content of the computer readable form does not comply with the requirements of 37 C.F.R. 1.822 and/or 1.823, as indicated on the attached copy of the marked -up "Raw Sequence Listing."
- ☐ 5. The computer readable form that has been filed with this application has been found to be damaged and/or unreadable as indicated on the attached CRF Diskette Problem Report. A Substitute computer readable form must be submitted as required by 37 C.F.R. 1.825(d).
- ☐ 6. The paper copy of the "Sequence Listing" is not the same as the computer readable form of the "Sequence Listing" as required by 37 C.F.R. 1.821(e).
- ☒ 7. Other: Figure 2A contains an unidentified sequence.

**Applicant Must Provide:**

- ☒ Either a substitute Figure 2A that identifies the sequence or an amendment to the specification in the Drawings section that identifies the sequence in Figure 2A.
- ☐ An initial or substitute paper copy of the "Sequence Listing", as well as an amendment directing its entry into the specification.
- ☐ A statement that the content of the paper and computer readable copies are the same and, where applicable, include no new matter, as required by 37 C.F.R. 1.821(e) or 1.821(f) or 1.821(g) or 1.825(b) or 1.825(d).

For questions regarding compliance to these requirements, please contact:

For Rules Interpretation, call (703) 308-4216

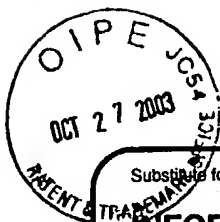
For CRF Submission Help, call (703) 308-4212

PatentIn Software Program Support (SIRA)

Technical Assistance.....703-287-0200

To Purchase PatentIn Software.....703-306-2600

**PLEASE RETURN A COPY OF THIS NOTICE WITH YOUR RESPONSE**



PTO/SB/08B (10-01)  
Approved for use through 10/31/2002. OMB 0651-0031  
U.S. Patent and Trademark Office: U.S. DEPARTMENT OF COMMERCE  
Under the Paperwork Reduction Act of 1995, no persons are required to respond to a collection of information unless it contains a valid OMB control number

Substitute for form 1449B/PTO <b>INFORMATION DISCLOSURE STATEMENT BY APPLICANT</b>  (use as many sheets as necessary)		<b>Complete If Known</b>	
		Applicati n Numb r	10/005,220
		Filing Date	December 4, 2001
		First Named Invent r	ALLEN
		Art Unit	Unassigned
		Examiner Name	Unassigned
Sheet	2	of	2
		Attorney Docket Number	R-741

OTHER PRIOR ART – NON PATENT LITERATURE DOCUMENTS			
Examiner Initials *	Cite No. <sup>1</sup>	Include name of the author (in CAPITAL LETTERS), title of the article (when appropriate), title of the item (book, magazine, journal, serial, symposium, catalog, etc.), date, page(s), volume-issue number(s), publisher, city and/or country where published.	T <sup>2</sup>
PP	AA	S. HARROCH, et al., "No Obvious Abnormality in Mice Deficient in Receptor Protein Tyrosine Phosphatase $\beta$ " <i>Molecular and Cellular Biology</i> , Vol. 20(20) October 2000, pp.7706-7715	
PP	AB	TAKAFUMI SHINTANI, et al., "Neurons and well as astrocytes express proteoglycan-type protein tyrosine phosphatase $\zeta$ RPTP $\beta$ : analysis of mice in which the <i>PTP<math>\zeta</math>RPTP<math>\beta</math></i> gene was replaced with the <i>LacZ</i> gene" Vol. 247, (1998) pp. 135-138	

Examiner Signature	<i>Pete Parus</i>	Date Considered	3/3/04
--------------------	-------------------	-----------------	--------

\*EXAMINER: Initial if reference considered, whether or not citation is in conformance with MPEP 609. Draw line through citation if not in conformance and not considered. Include copy of this form with next communication to applicant.

<sup>1</sup> Applicant's unique citation designation number (optional). <sup>2</sup> Applicant is to place a check mark here if English language Translation is attached.

Burden Hour Statement: This form is estimated to take 2.0 hours to complete. Time will vary depending upon the needs of the individual case. Any comments on the amount of time you are required to complete this form should be sent to the Chief Information Officer, U.S. Patent and Trademark Office, Washington, DC 20231. DO NOT SEND FEES OR COMPLETED FORMS TO THIS ADDRESS. SEND TO: Assistant Commissioner for Patents, Washington, DC 20231.  
Unsaved Document



Under the Paperwork Reduction Act of 1995, no persons are required to respond to a collection of information unless it contains a valid OMB control number

Approved for use through 10/31/2002. OMB 0651-0031

U.S. Patent and Trademark Office: U.S. DEPARTMENT OF COMMERCE

Substitute for form 1449B/PTO

## INFORMATION DISCLOSURE STATEMENT BY APPLICANT

(use as many sheets as necessary)

Sheet 2 of 2

### Complete if Known

Application Number	10/005,220
Filing Date	December 4, 2001
First Named Inventor	ALLEN
Art Unit	Unassigned
Examiner Name	Unassigned
Attorney Docket Number	R-741

### FOREIGN PATENT DOCUMENTS

Examiner Initials*	Cite No. <sup>1</sup>	Foreign Patent Document			Publication Date MM-DD-YYYY	Name of Patentee or Applicant of Cited Document	Pages, Columns, Lines, Where Relevant Passages or Relevant Figures Appear	T <sup>6</sup>
		Country Code <sup>3</sup>	Number <sup>4</sup>	Kind Code <sup>5</sup> (if known)				
PP	AC	WO	00/06712	A2	02/10/00	Merck Frosst Ca. Inc.		

Examiner Signature	<i>Pete Parag</i>	Date Considered	3/8/04
-----------------------	-------------------	--------------------	--------

\*EXAMINER: Initial if reference considered, whether or not citation is in conformance with MPEP 609. Draw line through citation if not in conformance and not considered. Include copy of this form with next communication to applicant.

<sup>1</sup> Applicant's unique citation designation number (optional). <sup>2</sup> Applicant is to place a check mark here if English language Translation is attached.

Burden Hour Statement: This form is estimated to take 2.0 hours to complete. Time will vary depending upon the needs of the individual case. Any comments on the amount of time you are required to complete this form should be sent to the Chief Information Officer, U.S. Patent and Trademark Office, Washington, DC 20231. DO NOT SEND FEES OR COMPLETED FORMS TO THIS ADDRESS. SEND TO: Assistant Commissioner for Patents, Washington, DC 20231.

Unsaved Document

<b>Notice of References Cited</b>	Application/Control No. 10/005,220	Applicant(s)/Patent Under Reexamination ALLEN, KEITH D.	
	Examiner Peter Paras, Jr.	Art Unit 1632	Page 1 of 2

**U.S. PATENT DOCUMENTS**

*		Document Number Country Code-Number-Kind Code	Date MM-YYYY	Name	Classification
	A	US-			
	B	US-			
	C	US-			
	D	US-			
	E	US-			
	F	US-			
	G	US-			
	H	US-			
	I	US-			
	J	US-			
	K	US-			
	L	US-			
	M	US-			

**FOREIGN PATENT DOCUMENTS**

*		Document Number Country Code-Number-Kind Code	Date MM-YYYY	Country	Name	Classification
	N					
	O					
	P					
	Q					
	R					
	S					
	T					

**NON-PATENT DOCUMENTS**

*		Include as applicable: Author, Title Date, Publisher, Edition or Volume, Pertinent Pages)
	(u)	Casademunt et al. EMBO, 1999, 18(21): 6050-6061.
	(v)	LeCouter et al. Development, 1998, 125: 4669-4679.
	(w)	Leonard et al. Immunological Reviews. 1995, 97-114.
	(x)	Moens et al. Development. 1993, 119: 485-499.

\*A copy of this reference is not being furnished with this Office action. (See MPEP § 707.05(a).)  
Dates in MM-YYYY format are publication dates. Classifications may be US or foreign.

<b>Notice of References Cited</b>	Application/Control No. 10/005,220	Applicant(s)/Patent Under Reexamination ALLEN, KEITH D.	
	Examiner Peter Paras, Jr.	Art Unit 1632	Page 2 of 2

**U.S. PATENT DOCUMENTS**

*		Document Number Country Code-Number-Kind Code	Date MM-YYYY	Name	Classification
	A	US-			
	B	US-			
	C	US-			
	D	US-			
	E	US-			
	F	US-			
	G	US-			
	H	US-			
	I	US-			
	J	US-			
	K	US-			
	L	US-			
	M	US-			

**FOREIGN PATENT DOCUMENTS**

*		Document Number Country Code-Number-Kind Code	Date MM-YYYY	Country	Name	Classification
	N					
	O					
	P					
	Q					
	R					
	S					
	T					

**NON-PATENT DOCUMENTS**

*		Include as applicable: Author, Title Date, Publisher, Edition or Volume, Pertinent Pages)
	U	Moreadith et al. J. Mol. Med., 1997, 75: 208-216.
	V	Mullins et al. J. Clin. Invest., 1996, 98(11): S37-40.
	W	Seamark et al. Reprod. Fertil Dev., 1994, 6(5): 653-657
	X	

\*A copy of this reference is not being furnished with this Office action. (See MPEP § 707.05(a).)  
Dates in MM-YYYY format are publication dates. Classifications may be US or foreign.



## The zinc finger protein NRIF interacts with the neurotrophin receptor p75<sup>NTR</sup> and participates in programmed cell death

Elisabeth Casademunt, Bruce D.Carter<sup>1</sup>,  
Isabel Benzel, José M.Frade<sup>2</sup>,  
Georg Dechant and Yves-Alain Barde<sup>3</sup>

Department of Neurobiochemistry, Max Planck Institute of Neurobiology, D-82152 Martinsried, Germany and <sup>1</sup>Center for Molecular Neuroscience, Vanderbilt University Medical School, Nashville, TN 37232, USA

<sup>2</sup>Present address: Instituto Cajal de Neurobiología, CSIC, Avda. Dr. Arce 37, E-28002 Madrid, Spain

<sup>3</sup>Corresponding author  
e-mail: yves\_barde@neuro.mpg.de

E.Casademunt and B.D.Carter contributed equally to this work

NRIF (neurotrophin receptor interacting factor) is a ubiquitously expressed zinc finger protein of the Krüppel family which interacts with the neurotrophin receptor p75<sup>NTR</sup>. The interaction was first detected in yeast and then biochemically confirmed using recombinant GST–NRIF fusions and p75<sup>NTR</sup> expressed by eukaryotic cells. Transgenic mice carrying a deletion in the exon encoding the p75<sup>NTR</sup>-binding domain of NRIF display a phenotype which is strongly dependent upon genetic background. While at the F<sub>2</sub> generation there is only limited (20%) embryonic lethality, in a congenic BL6 strain *nrif*<sup>−/−</sup> mice cannot survive beyond E12, but are viable and healthy to adulthood in the Sv129 background. The involvement of NRIF in p75<sup>NTR</sup>/NGF-mediated developmental cell death was examined in the mouse embryonic neural retina. Disruption of the *nrif* gene leads to a reduction in cell death which is quantitatively indistinguishable from that observed in *p75<sup>NTR</sup>−/−* and *ngf*<sup>−/−</sup> mice. These results indicate that NRIF is an intracellular p75<sup>NTR</sup>-binding protein transducing cell death signals during development.

**Keywords:** apoptosis/embryonic lethality/genetic background/p75<sup>NTR</sup>/zinc finger protein

### Introduction

The neurotrophins, including nerve growth factor (NGF), brain-derived neurotrophic factor (BDNF), neurotrophin-3 and neurotrophin-4/5 have a well-established and essential role as agents preventing programmed cell death during the development of the mammalian nervous system (Snider, 1994). This function is mediated through the binding of neurotrophins to a family of tyrosine kinases, the trk receptors. In addition, there is a considerable body of evidence to suggest that the neurotrophins have a wider role in regulating neuronal function, including the modulation of synaptic plasticity (McAllister *et al.*, 1999), the regulation of dendritic arborization (Ruit *et al.*, 1990;

McAllister *et al.*, 1996) or the control of growth cone guidance *in vitro* (Zheng *et al.*, 1994; Gallo *et al.*, 1997). Recently, and somewhat surprisingly, the neurotrophins have also been shown to promote programmed cell death during normal development. In contrast to the survival activity mediated via the trk receptors, neurotrophin-induced apoptosis is a function mediated by a neurotrophin receptor unrelated to the trks, the p75<sup>NTR</sup> receptor (Dechant and Barde, 1997). A role for p75<sup>NTR</sup> in cell death has been documented (for a review, see Casaccia-Bonofil *et al.*, 1999) using cultured cells (Rabizadeh *et al.*, 1993; Casaccia-Bonofil *et al.*, 1996; Gu *et al.*, 1999; Soiliu-Hänninen *et al.*, 1999), including neurons (Barrett and Bartlett, 1994; Davey and Davies, 1998). *In vivo*, p75<sup>NTR</sup>-mediated cell death has been observed in the developing avian and murine retinae (Frade *et al.*, 1996; Frade and Barde, 1999) and in sympathetic neurons (Bamji *et al.*, 1998). However, the actual binding partners of p75<sup>NTR</sup> involved in pro-apoptotic signalling are not well characterized.

Initially, p75<sup>NTR</sup> was thought merely to modulate neurotrophin binding to the trks and the subsequent signal transduction through well-established tyrosine kinase receptor pathways (Segal and Greenberg, 1996). Indeed, substantial evidence supports such a co-receptor role for p75<sup>NTR</sup>, including an increase in binding affinity (Hempstead *et al.*, 1991; Battleman *et al.*, 1993) and selectivity (Benedetti *et al.*, 1993) of a given trk for its cognate neurotrophin. Also, p75<sup>NTR</sup> associates with all three trk receptors and can be co-immunoprecipitated with them (Bibel *et al.*, 1999). In addition, trk signalling is enhanced in the presence of p75<sup>NTR</sup> (Davies *et al.*, 1993; Lee *et al.*, 1994; Verdi *et al.*, 1994). However, the widespread expression of p75<sup>NTR</sup>, including in a variety of cells not expressing catalytic forms of trks, suggested that p75<sup>NTR</sup> also has an independent function. The first indication that p75<sup>NTR</sup> could initiate a signal transduction pathway independently of the trks was the observation that neurotrophin binding to p75<sup>NTR</sup> stimulated the hydrolysis of sphingomyelin to produce the intracellular mediator ceramide (Dobrowsky *et al.*, 1995), although the function of this lipid second messenger is still not fully understood. Further, NGF was reported to activate the transcription factor NF- $\kappa$ B in neuroblastoma cells (Korner *et al.*, 1994) as well as in primary cultures of sensory (Wood, 1995) and sympathetic neurons (Maggirwar *et al.*, 1998), and in both Schwann cells (Carter *et al.*, 1996; Khursigara *et al.*, 1999) and oligodendrocytes (Ladiwala *et al.*, 1998; Yoon *et al.*, 1998). This activation of NF- $\kappa$ B was shown to occur through binding to the p75<sup>NTR</sup> receptor (Carter *et al.*, 1996; Khursigara *et al.*, 1999). Neurotrophin binding to p75<sup>NTR</sup> has also been observed to stimulate the stress-activated kinase, c-jun kinase, which has been implicated in mediating p75<sup>NTR</sup>-induced apoptosis

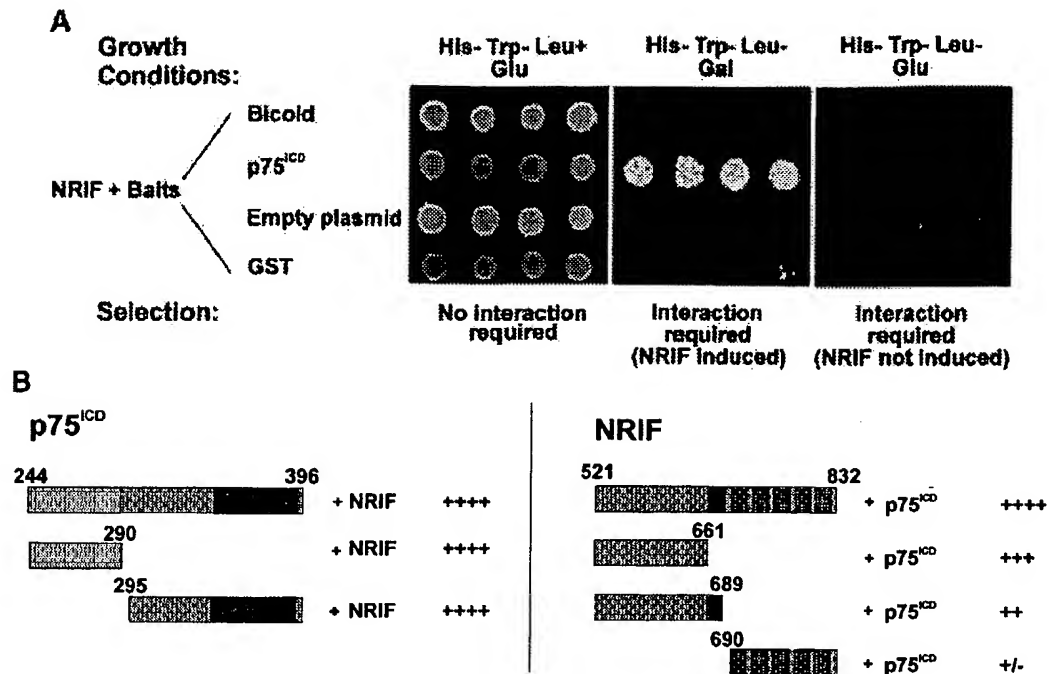


Fig. 1. (A) Isolation of NRIF as a p75<sup>NTR</sup> interactor from a yeast two-hybrid screen. Screening of a human fetal library for p75<sup>NTR</sup>-interacting proteins resulted in the isolation of several candidate cDNAs. Yeast clones capable of growing under selective conditions (His<sup>-</sup> Trp<sup>-</sup> Leu<sup>+</sup> on galactose plates) were tested further against other baits (bicoid, GST) and empty plasmid to confirm the specificity of the interaction. Only yeast expressing both p75<sup>ICD</sup> and NRIF grew under selective conditions. (B) Mapping of the interacting regions. Deletion constructs expressing the indicated fragments of p75<sup>ICD</sup> (left) and mouse NRIF (right) were co-transfected in yeast and their ability to support growth on selective media was compared with yeast co-expressing p75<sup>ICD</sup> and NRIF (residues 521–832). Whereas the three p75<sup>ICD</sup> fragments supported growth at comparable rates (left), the NRIF region N-terminal to the zinc fingers was clearly the most important for the interaction (right).

(Casaccia-Bonnett *et al.*, 1996; Bamji *et al.*, 1998; Yoon *et al.*, 1998).

The p75<sup>NTR</sup> receptor belongs to a large family of transmembrane proteins including the tumour necrosis factor (TNF) receptors R1 and R2, Fas, CD40, CD30, OX40, lymphotoxin- $\beta$  receptor, CD27 and DR3, 4 and 5 (for a review, see Casaccia-Bonnett *et al.*, 1998). Cysteine repeats in the extracellular domains originally formed the basis for defining members of this family. In addition, the cytoplasmic domains of several of these receptors have features in common, suggesting their involvement in protein-protein interactions. At the structural level, the cytoplasmic domain of both FAS/Apo-1/CD95 and of p75<sup>NTR</sup> shows a similar motif consisting of a closely packed bundle of six short  $\alpha$ -helices (Huang *et al.*, 1996; Liepinsh *et al.*, 1997). Several of these protein-protein interaction domains are now known to initiate signalling cascades leading to cell death or to the activation of the transcription factor NF- $\kappa$ B. For receptors such as TNFR1 and R2, as well as Fas, CD40 or CD30, a number of cytoplasmic proteins have been identified which associate with these domains and appear to function as signal transducers (for a review, see Nagata, 1997). One such adaptor protein, TRAF6, initially identified on the basis of its interactions with CD40 and interleukin-1 (IL-1) (see Arch *et al.*, 1998), has been implicated as mediating p75<sup>NTR</sup> activation of NF- $\kappa$ B (Khursigara *et al.*, 1999).

We report here the identification of a novel protein which interacts with the intracellular domain of p75<sup>NTR</sup> which we term NRIF, for Neurotrophin Receptor Interacting Factor. NRIF appears to play a role in p75<sup>NTR</sup>-

mediated apoptosis since mice with the *nrif* gene deleted exhibit reduced cell death in early retinal cells, similar to p75<sup>-/-</sup> and the *ngf*<sup>-/-</sup> mice (Frade and Barde, 1999).

## Results

### Isolation of NRIF as an intracellular interactor of p75<sup>NTR</sup> in a yeast two-hybrid screen

To identify proteins interacting with p75<sup>NTR</sup>, the intracellular domain (ICD) of the rat p75<sup>NTR</sup> receptor (residues 244–396) was fused to the C-terminus of the lexA DNA-binding protein in a yeast expression vector (Gyuris *et al.*, 1993). This bait plasmid was co-transfected into a leucine-deficient yeast strain containing the lexA-binding domain upstream of the *LEU2* gene, along with a human fetal brain library fused to the B42 transcription activator under the control of a GAL1-inducible promoter in pJG4-5. We isolated 17 clones which demonstrated selective growth on galactose.

Upon sequence analysis, one of the clones, designated pJG-NRIF, was found to encode 1.3 kb of a novel sequence fused in the reading frame of B42 and having homology with a number of zinc finger proteins. This clone was also able to activate transcription of *lacZ* from the reporter plasmid pSH18-34 (which contains lexA-binding domains upstream of *lacZ*) when co-transfected with p75<sup>NTR</sup>ICD, as evidenced by  $\beta$ -galactosidase staining (data not shown). To assess further the specificity of the interaction with p75<sup>NTR</sup>, several 'false baits' were tested, including plasmids coding for the *Drosophila* protein bicoid, GST and the empty bait plasmid. Only co-transfection of

```

      ↓ ↓
1  MEDSMASTLP TTPHESVKF EDVSLTFTEE ENAQDLPQOK CIYREIMMEN
      KRAB A
51  YSNMISVEH FSKPNVISQL EKAEDCWPMQ REIPQDTLPE CSWSPDPGM
      KRAB B
101 NSFPSPKSLM KIEVVEVLTL NKDVAGPRNA LIQSLYPEDL NPGNLKPAQL
151 PSKRLTDTEA SRQKFRHFQY EESAGPQKAM SQLRKLCHQW LQPNTRSKKQ
201 ILELLVLEQF LNALPEKFRV MVESQHPEDC KAVVALLENN TSVSKODASL
251 ACSSEATDQL KEKRGVATIL PVTFAAEVPA EEPVTFQDVA VDFNEEERWL
301 LGPTQKTEYH DVMLETIGNL VSVGWEPTLG NRELTPDSPI PVVKPIHDPN
351 TKDLSRNGTQ STVFESILED GVKEMHTIES NQVGNLQKQG HPQKPFESS
401 KSQDQTSRHK SQGSLNEVLP RRYVKVKQKG TGRKRGRTNT ISMTRGLRIR
451 KQKQDSVENQ GRSGSTFVTH GSSIKKQQQG SEQGKPGTSR DPITLTVPAK
501 VYQKATGSKE SILMDSSDAM VSDVPPKIHQ KGEVWHKVG ESNNSMLQSS
551 VQNHQMESGA GRASDNLSTL HALPVKSHQK GYKEGNVQGN RNSMKHKPH
601 QKSGKGERVE ELSTSEKHVP YVKNHLTSE RGKDREINAS IKDPYIKTY
651 YRSDVGRLR RANNCRAKFS LRAQGISFIK INKGSQVCIC SECGKLFRNA
701 RYFSVHKKIH TGERPYMMA CGKAFVQSSS LTQRLRIEIS ERPFCESECG
751 RTFNDRSAIS QRLRTTGAK PYHCERCCKA FRQSSHLTRA ERTHTGERPY
801 VCIKCGKFT QSSHLIGHQK THGIKFKKQP KL*

```

**Fig. 2.** Amino acid sequence of the predicted NRIF protein. Predicted amino acid sequence as translated from the *nrif* 6.3 cDNA clone (see text). Large arrows indicate the two potential translation initiation sites. The positions of the two N-terminal KRAB boxes, KRAB A and KRAB B, the pseudo-finger and the five zinc finger domains, are indicated. A group of regularly spaced leucine residues clustered at the N-terminal part of the protein, downstream of the KRAB domains, indicated in bold (L), could function as a nucleocytoplasmic signal (Nigg, 1997). The underlined sequence (residues 329–374) shares relatively high homology with several other KRAB-containing zinc finger proteins. The small arrow at position 530 marks the N-terminal end of the partial, human *nrif* cDNA isolated from the yeast two-hybrid screen. A potential nuclear localization signal is underlined. The sequence contains consensus sites for amidation, cAMP phosphorylation, CK2 phosphorylation, PK-C phosphorylation, myristoylation and Asn glycosylation. Sequence data have been submitted to the DDBJ/EMBL/GenBank database under accession No. AJ242914.

pJG-NRIF with p75<sup>NTR</sup>ICD enabled the yeast to survive (Figure 1).

#### Cloning and sequence analysis of mouse NRIF

To obtain a full-length clone of mouse NRIF, a post-natal day 1 mouse cDNA library was screened with a 0.9 kb fragment from the human clone which contained the putative zinc finger domain. A 3.289 kb clone (clone 6.3) was isolated which contained a 2.645 kb uninterrupted, open reading frame with two consecutive, 5' Kozak consensus sequences (Kozak, 1995), two Krüppel-related boxes (KRAB) at the N-terminus (Bellefroid *et al.*, 1991; Rosati *et al.*, 1991; Constantinou-Deltas *et al.*, 1992), five zinc finger motifs followed by a potential nuclear localization signal (NLS) at the C-terminus and a 644 bp 3'-untranslated region (Figure 2). Primer extension analysis demonstrated that cDNA clone 6.3 corresponds to an NRIF full-length transcript (data not shown). Depending on whether the first or the second translation initiation codon is used, the predicted NRIF protein consists of 832 or 828 residues and has a mol. wt of 94 080.0 or 93 617.53 Da and a pI of 9.65 or 9.77, respectively.

Mouse NRIF clone 6.3 (Figure 2) is 56% identical overall to the partial human NRIF clone at the amino acid

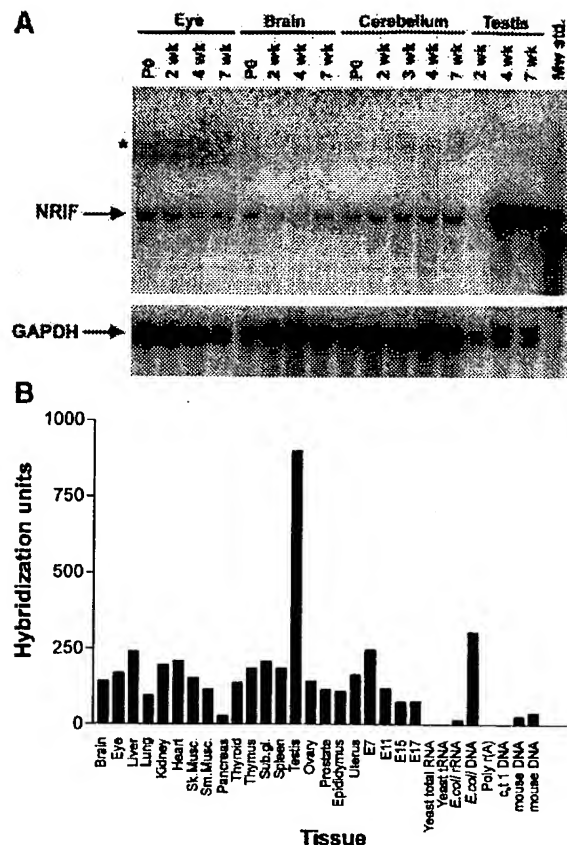


**Fig. 3.** Tissue distribution of the *nrif* mRNA. Northern blot analysis (A) and poly(A)<sup>+</sup> RNA dot blots (B) were used to characterize the RNA banding pattern and accumulation levels of the *nrif* mRNA. (A) The *nrif* cDNA probe detects a double band of ~3.7 kb (arrow) which is most abundant in adult testis, as well as a minor, larger transcript (asterisk). (B) The accumulation levels of the *nrif* mRNA were quantified with a dot blot (Clontech) where the loading was normalized to mRNA expression levels of eight housekeeping genes. The *nrif* mRNA is expressed ubiquitously and at relatively low levels in all tissues examined, except in testis. Sk. Musc, skeletal muscle; Sm. Musc, smooth muscle; Sub. gl., submaxillary gland; E7, E11, E15 and E17, whole embryos at the corresponding embryonic (E) stages. Note that the hybridization signal at E7 is 2-fold higher than at E11 and 3.7-fold higher than at E15. The signal detected in the negative control 'E.coli DNA' is likely to be due to the probe being prepared from an *E.coli* host.

level. Like human NRIF, it contains five predicted zinc fingers and a pseudo-finger which are 83% identical between human and mouse. The N-terminal half of the protein is much more divergent, sharing only 27% sequence identity. A search in the DNA and protein sequence databases while preparing this manuscript revealed that both the human and the mouse NRIF sequences have been identified independently. Human NRIF corresponds to the partial Zfp2 (DDBJ/EMBL/GenBank accession No. U71598) sequence submitted in 1996 by Petroni *et al.* (unpublished), who identified it as an up-regulated mRNA in an erythroleukaemia cell line. Similarly, a fragment of the mouse NRIF sequence is also present in the expressed sequence tag (EST) database as a 628 bp, Sugano mouse kidney mKia *Mus musculus* cDNA clone (EM\_NEW:AJ317700, submitted 18.12.98,

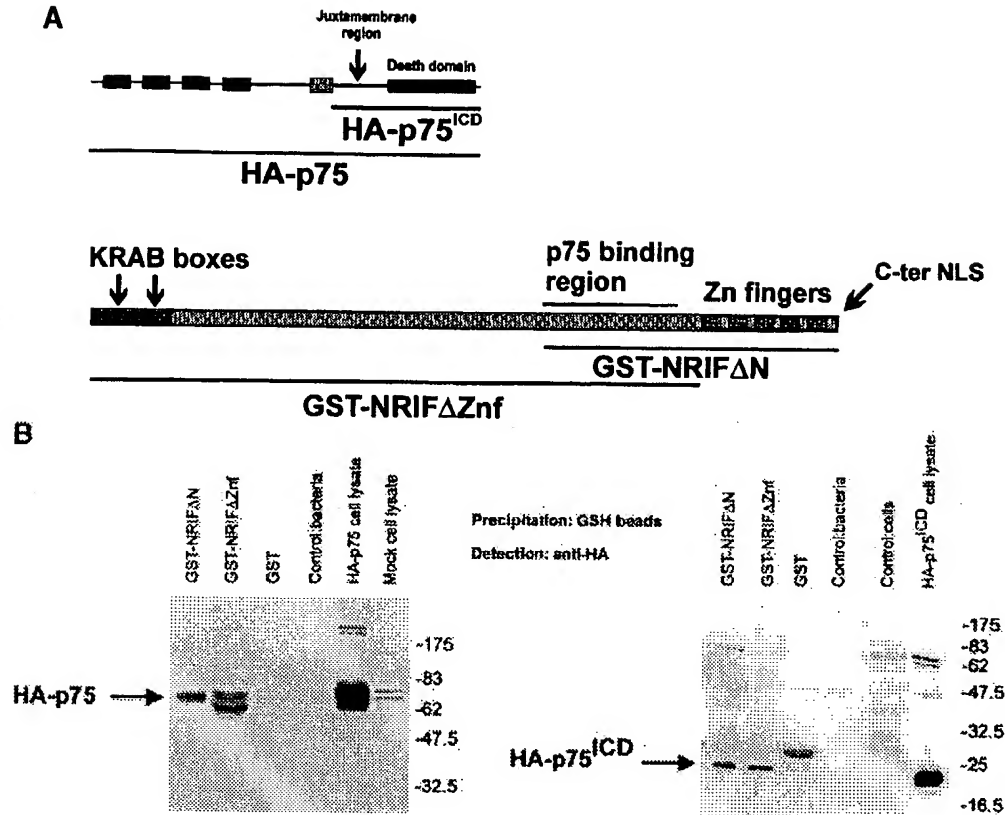


**Fig. 4.** Biochemical interaction between p75<sup>NTR</sup> and NRIF. To confirm the interaction observed in yeast, recombinant GST-NRIF fusion proteins (diagrammed in A) were expressed in *E. coli* and immobilized on beads. (B) Whole extracts from 293 cells expressing HA-tagged p75 (left panel) and HA-tagged p75ICD (right panel) were incubated with NRIF-loaded beads in a 'pull-down' assay. Co-precipitated p75<sup>NTR</sup>, visualized with an anti-HA antibody, was detected only when beads were loaded with GST-NRIF (lanes 1 and 2), but not when the beads contained only GST (lane 3). Negative controls included beads loaded with non-NRIF-expressing bacterial extracts (control bacteria), and cell extracts from mock transfections (control cells). Lanes 5 (left panel) and 6 (right panel) correspond to whole-cell lysates from cells expressing HA-p75 or HA-p75ICD, respectively. The unspecific band detected at ~26 kDa in the right panel is most likely due to an excess of GST protein as seen in Coomassie-stained gels (not shown).

WashU-HHMI Mouse EST Project; 99.4% identity in a 170 bp overlap with mouse NRIF).

The chromosomal locations of the mouse and the human NRIF genes have been determined. Mouse NRIF was mapped using a BSS DNA panel and two oligonucleotide primers which detected a single strand conformation polymorphism (SSCP) (Beier *et al.*, 1992; Beier, 1993) between the two parental strains (C57BL/6J × SPRET/Ei and SPRET/Ei) in the last intron of the *nrif* gene (see Figure 6A). The locus has been given the Zfp110 symbol and maps to chromosome 7, co-segregating with a large cluster of other loci at the most proximal position (see <http://www.jax.org/resources/documents/cmdata/bkmap/maps/7MapPage.html>). Given the presence of a zinc finger cluster on this chromosome which is conserved in human chromosome 19 (Stubbs *et al.*, 1996; Shannon and Stubbs, 1998), mapping of the human NRIF gene to the telomeric region of chromosome 19 further confirms that mouse NRIF (corresponding to cDNA clone 6.3) and the human NRIF sequence (originally isolated from the yeast two-hybrid screen) are indeed orthologues.

#### Mapping the interaction domains

The intracellular domain of p75<sup>NTR</sup> can be divided into two sub-domains: the juxta-membrane region (residues

244–290) is 95% conserved between chick (Heuer *et al.*, 1990) and human (Johnson *et al.*, 1986; Huang *et al.*, 1996), suggesting some important, conserved function, and the C-terminus (residues 300–399) has homology to other proteins of this receptor family (Feinstein *et al.*, 1995). This latter region can be further subdivided into two segments showing a low degree of homology with the *Drosophila* death protein *Reaper* (residues 300–350 and 366–399). To determine which regions are important for the interaction between NRIF and p75<sup>NTR</sup>, deletion mutants were tested in the yeast system (Figure 1B). The juxta-membrane sequence was sufficient for interaction with human NRIF and supported growth of the yeast on Leu<sup>-</sup> plates to a similar extent as the full-length p75ICD. Interestingly, the so-called death domain (Liepinsh *et al.*, 1997) in the remaining C-terminus also interacted with NRIF, suggesting that these two regions may regulate the interaction co-operatively or that NRIF may bind as a dimer to both domains. The first *Reaper*-like region could not be tested alone for interaction because it auto-activated *LEU2* transcription in the absence of NRIF.

To determine which regions of mouse NRIF are responsible for association with p75<sup>NTR</sup>, deletion constructs of the mouse clone were prepared from an initial construct containing only the last third of the cDNA

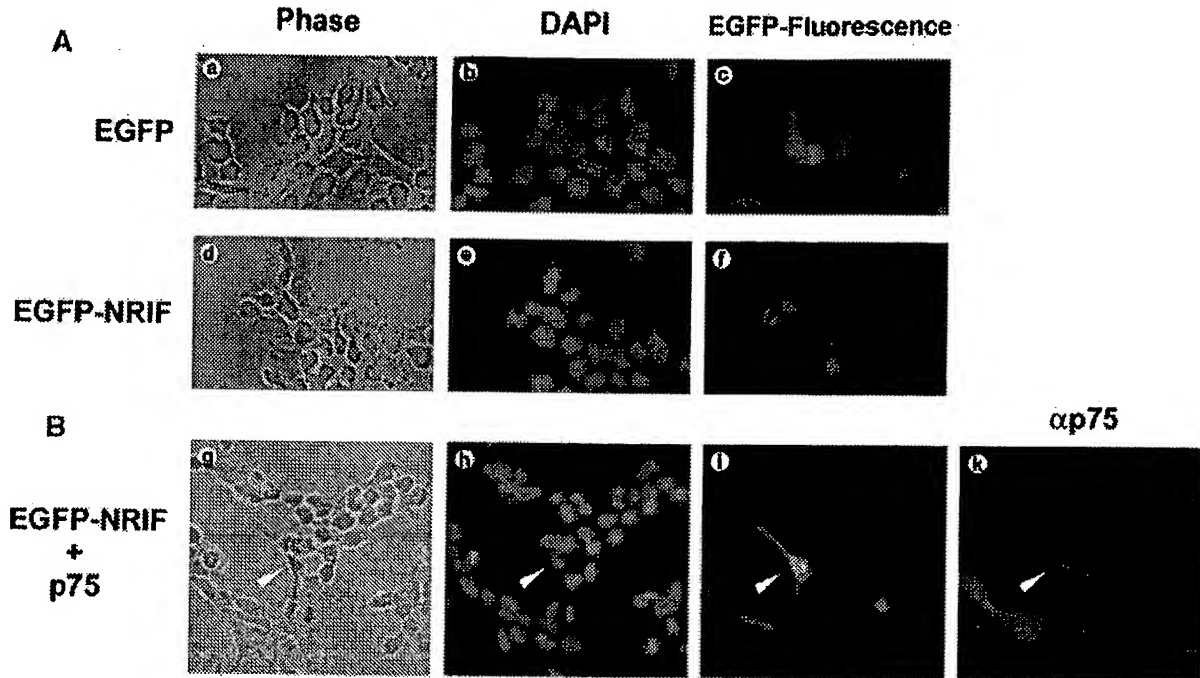


Fig. 5. Subcellular localization of NRIF in transfected 293 cells. (A) 293 cells were transiently transfected with EGFP (a-c) or EGFP-NRIF (d-f). Surviving cells (since EGFP-NRIF expression kills many cells that are removed as floaters) were fixed and stained with DAPI to visualize nuclei (b and e). In contrast to EGFP (c), EGFP-NRIF shows mainly nuclear localization, sometimes with a punctuate appearance (f). (B) 293 cells were transiently co-transfected with EGFP-NRIF and p75<sup>NTR</sup>, fixed, stained with DAPI (h) and immunostained for p75 (k). Note the difference in efficiency of p75 expression (k) compared with EGFP-NRIF-expressing cells (i). While most cells still show nuclear localization of EGFP-NRIF, co-expression of the p75<sup>NTR</sup> receptor causes three times as many cells to also express EGFP-NRIF in the cytoplasm (arrowhead), compared with EGFP-NRIF alone.

(region corresponding to the human NRIF fragment originally isolated from the yeast screen). Three mouse NRIF deletion constructs were generated (Figure 1B, right), deleting the pseudo-finger and the zinc fingers, only the zinc finger domain, or the N-terminal region. No significant interaction was observed between p75<sup>NTR</sup> and the zinc fingers, as would be predicted if this region is a DNA- (or RNA-) binding domain. In contrast, the yeast co-transfected with the NRIF construct lacking the pseudo-finger grew best, suggesting that this remaining region is responsible for the association of NRIF with p75<sup>NTR</sup>.

#### NRIF is expressed ubiquitously in mouse tissues

Northern blots probed with the mouse cDNA clone indicated a major double band of ~3.7 kb for the mRNA encoding NRIF, as well as a minor transcript of higher molecular weight, which most likely corresponds to a highly related transcript encoded by a homologous gene (Figure 3A; see Discussion). The NRIF mRNA appears to be ubiquitously expressed albeit at relatively low levels, except in testis (Figure 3A and B). Intact sciatic nerve shows no or very low transcript levels, as indicated by RT-PCR analysis, but NRIF is strongly expressed in dissociated Schwann cells (data not shown). RT-PCR analysis performed in mouse embryonic tissues prepared at E15 indicated that NRIF is also ubiquitously expressed during development, and at higher levels than in the adult. The NRIF mRNA is also expressed in all cell lines analysed (data not shown).

#### Biochemical interaction of NRIF and p75<sup>NTR</sup> *in vitro*

The physical interaction between NRIF and p75<sup>NTR</sup> was verified biochemically by co-precipitation of the p75 protein expressed in transfected 293 cells with recombinant mouse NRIF protein immobilized on Sepharose beads. Two different portions of the mouse NRIF cDNA were fused to GST: GST-NRIFΔN contains only the last third of the NRIF protein, and GST-NRIFΔZnf expresses full-length NRIF without its zinc fingers (Figure 4A). The levels of recombinant NRIF protein produced and their binding to the Sepharose beads vary depending on the portion of the protein expressed: GST-NRIFΔZnf is induced and bound to the beads at levels comparable to those of the GST moiety alone, while GST-NRIFΔN, containing the five zinc fingers, is poorly expressed, difficult to solubilize under a variety of conditions, and binds inefficiently to the beads. To test the interaction of these two proteins with p75<sup>NTR</sup>, 293 cells were transfected with rat p75<sup>NTR</sup> cDNA clones (Figure 4A) expressing either haemagglutinin (HA)-tagged p75<sup>NTR</sup>ICD (HA-p75ICD) or HA-tagged full p75<sup>NTR</sup> (HA-p75). As detected by immunoblot, GST-NRIF fusions immobilized on Sepharose beads were capable of binding both the intracellular domain of p75 (HA-p75ICD; Figure 4B right) and the full-length receptor (HA-p75; Figure 4B left) from transfected cells even under high salt conditions, whereas GST alone could not. This confirms the biochemical interaction of NRIF with p75<sup>NTR</sup>. Curiously, GST-NRIFΔZnf pulls down a slightly different form of p75<sup>NTR</sup> (Figure 4B, left, lane 2).

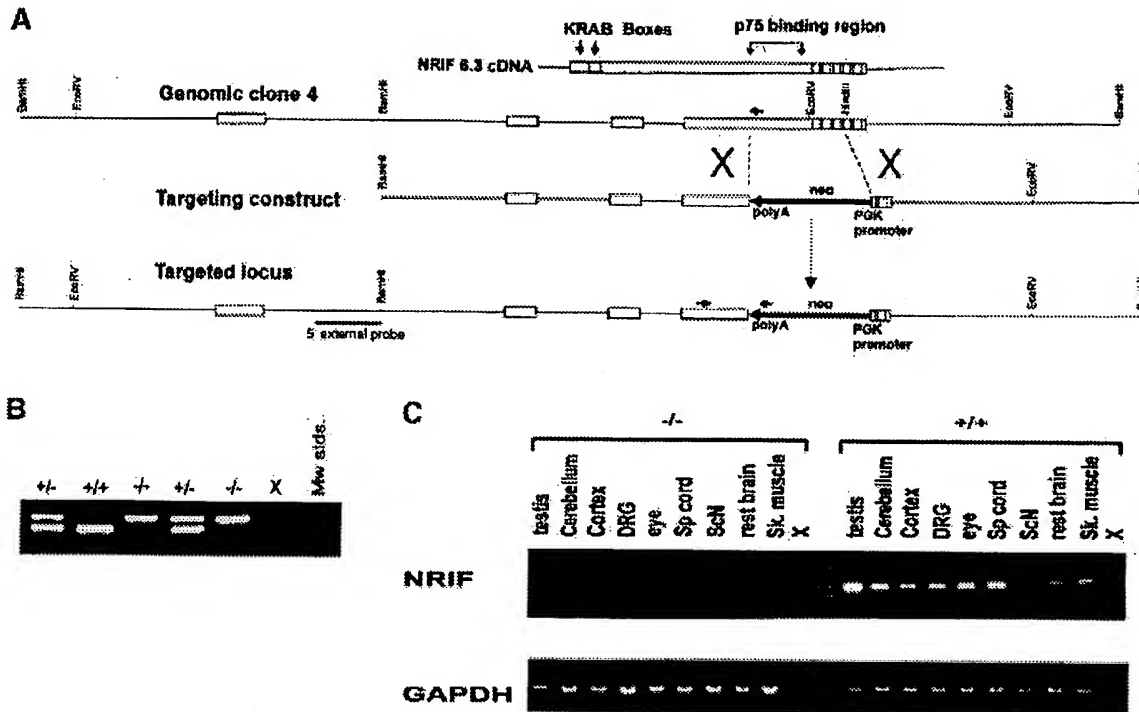


Fig. 6. Genomic targeting of the mouse *nrif* gene. (A) Deletion of the *nrif* exon encoding the p75<sup>NTR</sup>-binding region. Shown are the mouse *nrif* cDNA clone 6.3 (predicted amino acid sequence shown in Figure 2), mouse genomic clone 4 isolated from a 129Sv genomic library, and the targeting construct, where the region encoding the p75-interacting portion was replaced by a pGKneo cassette in the antisense orientation. Following homologous recombination in ES cells, the targeted allele can be detected by Southern analysis of genomic *EcoRV* digests probed with the depicted 5' external probe. (B) Genotype analysis. Each PCR (performed on genomic DNA from tail biopsies) contains three primers capable of amplifying the wild-type 521 bp allele (+/+ lanes) and the 572 bp targeted allele (-/- lanes). Heterozygous mice amplify both bands (+/- lanes). Annealing positions for the three primers are indicated by arrows in (A). (C) RT-PCR analysis of *nrif* +/+ and -/- littermates. The absence of transcript from the *nrif* targeted region was confirmed by RT-PCR from RNA prepared from the listed tissues/organs. Wild-type samples contain the *nrif* transcript (upper panel, right), whereas mutant littermates (left) do not express any detectable levels of the targeted region, even after 40 PCR cycles. Equal cDNA levels were used in all PCRs as shown by comparable GAPDH amplification products (lower panel). DRG, dorsal root ganglia; Sp. cord, spinal cord; ScN, sciatic nerve; Sk. muscle, skeletal muscle.

#### Subcellular localization of the NRIF protein

In order to visualize the subcellular distribution of the NRIF protein in eukaryotic cells, we constructed an enhanced green fluorescent protein (EGFP)-NRIF protein fusion and monitored its expression by fluorescence microscopy. Already at this level, it became clear that overexpression of NRIF can kill transfected cells. Induction of apoptosis was quantified using an enzyme-linked immunosorbent assay (ELISA) method (see Frade and Barde, 1999). Between 20 and 28 h after transfection, NRIF-transfected cells accumulate 86% more free nucleosomes in their cytoplasm than do mock-transfected cells.

Despite the very low rate of successful transfection and expression, the few viable cells that express EGFP-NRIF show primarily nuclear localization of the protein (Figure 5A). Fluorescence levels are variable, ranging from diffuse to strong, with a granulate pattern which does not co-localize with nucleoli (Figure 5A, panel f, and data not shown). Co-transfection of p75<sup>NTR</sup> substantially changes this exclusively nuclear localization: in some co-transfected cells, EGFP-NRIF can be seen both in the nucleus and in the cytoplasm (Figure 5B, panels i and k), or even only in the periphery, co-localizing with p75<sup>NTR</sup>. This indicates that the physical interaction between NRIF and p75<sup>NTR</sup> can also take place in living cells. Whether the mostly nuclear localization of NRIF is

an artefact of overexpression in transfected cells due to the cytomegalovirus (CMV) promoter is a possibility that cannot be excluded, but expression of NRIF under the control of weaker promoters does not yield detectable levels of expression.

#### Genomic targeting of the mouse *nrif* gene

In order to evaluate the functional significance of the interaction between NRIF and p75<sup>NTR</sup>, we generated a mouse line with a targeted deletion in the *nrif* gene. The targeting strategy was designed so that the resulting mice would lack the NRIF fragment demonstrated to bind p75<sup>NTR</sup> (as mapped in the yeast assay, see Figure 1B). A 6.5 kb *Bam*HI genomic clone (clone 4) isolated from a 129Sv library was identified and selected for genomic targeting of *nrif*. Subcloning of this phage fragment into a pBluescript vector and sequencing revealed the presence of two intronic regions interrupting the spacer region of NRIF (Figure 6A) and confirmed the identity of this clone as the genomic counterpart of the NRIF 6.3 cDNA described above. The 1.2 kb genomic fragment that encodes the p75<sup>NTR</sup>-binding domain and four of the five zinc fingers were replaced by a pGK-neo selection cassette, and the resulting targeting construct (Figure 6A) was electroporated into R1 cells. Correct homologous recombination events were identified by Southern analysis



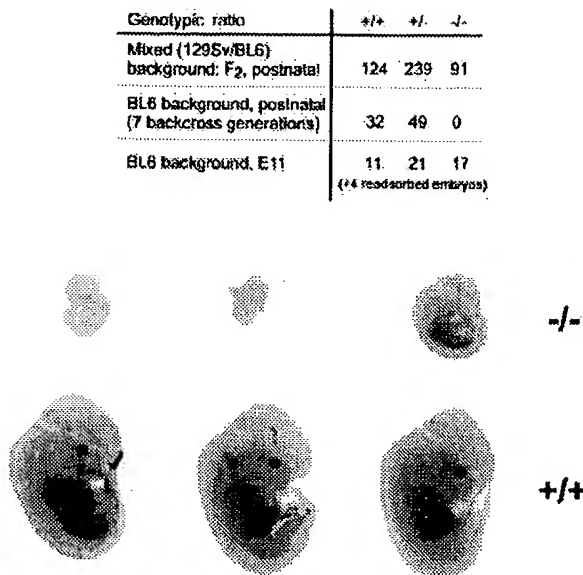


Fig. 7. The *nrif* mutation is viable in mixed (BL6/129Sv) and 129Sv backgrounds, but embryonically lethal in congenic BL6 strains. Table: genotypic ratios obtained for the *nrif* mutation at the F<sub>2</sub> generation (mixed 129Sv/BL6 background) and at the N<sub>7</sub> F<sub>1</sub> generation (seven BL6 backcross generations followed by one intercross), after birth ('postnatal') and at E11. While at the F<sub>2</sub> generation there is only a 20% reduction in the proportion of *nrif*<sup>-/-</sup> mice, in a BL6 background the *nrif* mutation is embryonically lethal, and no *nrif*<sup>-/-</sup> mice survive beyond E12. Photo: severe growth retardation observed at E12 in *nrif*<sup>-/-</sup> embryos in the BL6 background. The photograph shows six members of one litter analysed at E12. Note the difference between the three embryos of the upper row (*nrif*<sup>-/-</sup>) as compared with their three wild-type littermates shown below. At E12, *nrif*<sup>-/-</sup> embryos are severely growth retarded or in different stages of reabsorption. By E15, all *nrif*<sup>-/-</sup> embryos presumably have been resorbed.

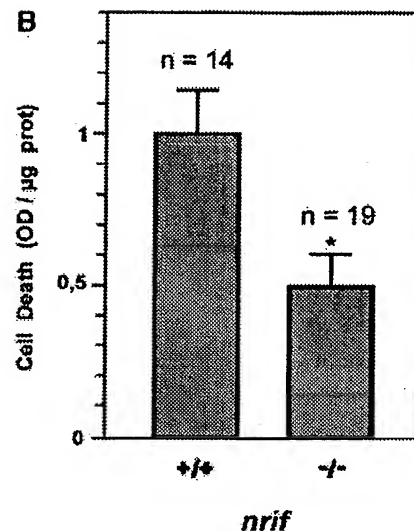
using an external 5' probe (Figure 6A). We identified 13 potential candidates amongst 650 isolated G418-resistant clones and, after confirming correct integration with an internal probe, four clones were further selected for injection into BL6 blastocysts. Chimeric mice generated from two of these ES clones (2/4 and 4/39) transmitted the mutation through their germline, and the progeny resulting from the two lines showed the same phenotypic traits at the following generations. A PCR-based assay was developed to show that only the genomic copy corresponding to the 6.3 cDNA was targeted and to screen for the mutant allele (Figure 6B). Complete absence of the targeted region was demonstrated by the lack of RT-PCR product in *nrif*<sup>-/-</sup> tissues (Figure 6C).

#### The effect of the *nrif* mutation is strongly dependent on the genomic background

At the F<sub>2</sub> generation, *nrif*<sup>-/-</sup> mice appear to be viable and fertile, with no obvious gross anatomical defect. Homozygous mutant males appear to be more docile and show an age-dependent, large reduction (up to 70% in young animals) in testis weight, although histological sections through testes show no obvious morphological alterations (data not shown). Genotypic segregation at the F<sub>2</sub> generation slightly deviates from Mendelian: ~20% of the *nrif*<sup>-/-</sup> progeny die before or shortly after birth (Figure 7).



n(+/+)=4  
n(-/-)=7



\* p<0.05

Fig. 8. Reduction of apoptosis in the retina of *nrif*<sup>-/-</sup> embryos. Quantification of apoptotic levels in E15.5 retina was done from *nrif*<sup>+/+</sup> and *nrif*<sup>-/-</sup> littermates. (A) RT-PCR analysis performed on *nrif*<sup>+/+</sup> (n = 4) and *nrif*<sup>-/-</sup> (n = 7) retinæ demonstrating the presence of p75<sup>NTR</sup> and NGF in *nrif*<sup>-/-</sup> embryos (B: blank control). (B) Levels of soluble nucleosomes in *nrif*<sup>-/-</sup> embryos were normalized to the amount of protein and then to the mean obtained for *+/+* embryos. In *nrif*<sup>-/-</sup>, there is a 50% decrease in the levels of cell death, compared with 48% observed in *p75*<sup>-/-</sup> and 56% in *ngf*<sup>-/-</sup> embryos (Frade and Barde, 1999).

In order to generate congenic mouse strains harbouring the *nrif* mutation, F<sub>1</sub> heterozygous males were mated to BL6 females and founder F<sub>0</sub> chimeric males were mated to 129Sv females. In each case, this initial mating was followed by nine consecutive backcrosses of heterozygous males to BL6 or to 129Sv females, respectively. Surprisingly, to date, interbreeding of heterozygous animals at the N<sub>6</sub>(BL6) backcross generation could never produce viable *nrif*<sup>-/-</sup> progeny (Figure 7), whereas the 129Sv lineage produces *nrif*<sup>-/-</sup> pups even after 10 generations of consecutive backcrosses. Embryonic death in the BL6 background seems to occur around E12, since no living *nrif*<sup>-/-</sup> embryos were found at E13, E14 or E15, whereas several litters examined at E11 contained living homozygous mutants in Mendelian proportions (Figure 7). With wide variability, E12 *nrif*<sup>-/-</sup> embryos showed very

different degrees of growth retardation in comparison with their wild-type littermates (Figure 7). Such a lethal phenotype could be rescued easily by interbreeding of heterozygous mice in the two congenic strains [*nrif*<sup>+/-</sup>-N<sub>10</sub>(BL6)×*nrif*<sup>+/-</sup>-N<sub>10</sub>(Sv129)], indicating that only the BL6 context cannot support the *nrif* mutation in homozygosis.

#### **NRIF plays a role in developmental cell death in the mouse retina**

In order to evaluate the possible involvement of NRIF in the pro-apoptotic pathway of p75<sup>NTR</sup> *in vivo*, we quantified cell death levels in the retina of wild-type and *nrif*<sup>+/-</sup> E15.5 F<sub>2</sub> littermates. Nine litters with both <sup>+/+</sup> and <sup>-/-</sup> embryos were analysed, and the amounts of free nucleosomes in retinal extracts quantified as described before (Frade and Barde, 1999). Despite variability, as previously observed with both the *ngf* and the p75<sup>NTR</sup> mutations (see Frade and Barde, 1999), we observed a significant reduction in the levels of cell death in the *nrif*<sup>+/-</sup> group when compared with their wild-type littermates (Figure 8). This reduction is quantitatively indistinguishable from what has been observed in p75<sup>-/-</sup> and *ngf*<sup>-/-</sup> mutants (Frade and Barde, 1999).

#### **Discussion**

Accumulating evidence suggests that p75<sup>NTR</sup> can initiate programmed cell death in a number of specific cell types (Casaccia-Bonnel et al., 1998). However, unlike the well-characterized signal transduction pathways used by the trk receptors (Kaplan and Miller, 1997), the signalling molecules recruited by p75<sup>NTR</sup> in its pro-apoptotic function are still unknown. To date, only TRAF6 has been reported as a p75<sup>NTR</sup>-interacting molecule mediating p75<sup>NTR</sup> effects, and it seems to be involved in the activation of NF-κB (Khursigara et al., 1999). To gain more insight into the underlying mechanisms of p75<sup>NTR</sup> signalling, we used the yeast two-hybrid system and identified NRIF. This novel protein associates with the cytoplasmic domain of p75<sup>NTR</sup>. Together with TRAF6, NRIF represents the first adaptor molecule found to interact directly with p75<sup>NTR</sup> to transduce signals elicited by neurotrophin binding at the cell membrane.

The mouse *nrif* gene encodes a 94 kDa zinc finger protein of the Krüppel family. Although originally isolated on the basis of its interaction with the intracellular domain of p75<sup>NTR</sup> in yeast cells (Figure 1), our pull-down assays demonstrated that full-length p75<sup>NTR</sup> from mammalian cells also interacts with NRIF (Figure 4B, left). Further, the ICD of p75<sup>NTR</sup> alone was precipitated by NRIF (Figure 4B, right), suggesting that the extracellular portion of the receptor is not required for the interaction. As mapped in yeast cells, NRIF and p75<sup>NTR</sup> appear to interact between the region immediately N-terminal to the zinc fingers of NRIF, and two discrete portions of the p75<sup>NTR</sup> (Figure 1): the highly conserved juxta-membrane sequence of p75<sup>NTR</sup>, shown to be the TRAF6-binding domain (Khursigara et al., 1999), and the death domain (Liepinsh et al., 1997). Deletion of either region of p75<sup>NTR</sup> did not prevent interaction with NRIF (Figure 1), indicating that NRIF can bind to both regions, possibly as a dimer. In yeast cells, the zinc fingers alone do not participate in the

binding of NRIF to p75<sup>NTR</sup> (Figure 1), indicating that they are potentially free and capable of binding DNA or RNA.

The primary structure of NRIF (Figure 2), including its five zinc fingers, two N-terminal KRAB domains and a putative NLS, suggest that it may translocate to the nucleus and regulate gene expression. Indeed, several zinc finger proteins containing KRAB domains have been shown to be transcriptional repressors (Witzgall et al., 1994). The subcellular distribution of NRIF supports such a role also for this interactor: when expressed in 293 cells, EGFP-NRIF is primarily nuclear, but upon co-expression of p75<sup>NTR</sup> both proteins can be seen co-localizing outside the nucleus (Figure 5B). This raises the possibility that the p75<sup>NTR</sup>-NRIF signalling system may function in a manner similar to other receptor-transcription factor associations, such as Notch and Su(H) (Weinmaster, 1997) or the transforming growth factor-β (TGF-β) receptors and SMADs (Heldin et al., 1997). Upon activation of these receptors, their associated factors are released and translocate to the nucleus where they mediate their respective functions.

The *nrif* mRNA is expressed ubiquitously, but at higher and constant levels in the embryo, while in the adult mouse accumulation levels of the *nrif* mRNA vary among tissues and organs (Figure 3). The presence of a human *nrif* homologous and syntenic gene in the human genome further supports an evolutionarily conserved, important function. Furthermore, both the mouse and the human genome contain a second, highly related *nrif* gene which most likely arose as a result of a gene duplication. Zinc finger gene clusters in mouse chromosome 7 and human chromosome 19 are currently being fully sequenced (Lawrence Livermore Laboratories), so it will be interesting to see whether more members of the *nrif* family are described in the future.

In support of an essential role for NRIF, all cell lines examined express the *nrif* mRNA, as determined by RT-PCR studies (data not shown). However, the cellular function of NRIF has proven difficult to assess due to the very low levels of detectable expression upon transfection of the cDNA in a variety of cell lines, e.g. COS7, BHK, CV1, NIH-3T3 and HN10. Even 293 cells, known and widely used for their high efficiency of transfection, only rarely express transfected *nrif*, indicating that there may be a very narrow range of accumulation of the NRIF protein still allowing cell viability and/or proliferation. Overexpression of the NRIF protein seems to be toxic for transfected cells, and the proportion of successfully transfected cells that can express tagged *nrif* cDNAs is very low. It is possible that only cells in a particular stage of their cell cycle allow overexpression of NRIF.

To evaluate more directly the physiological significance of the NRIF-p75<sup>NTR</sup> interaction *in vivo*, we generated *nrif*<sup>-/-</sup> mice by homologous recombination. Based on our mapping studies in yeast (Figure 1) and with recombinant NRIF protein (Figure 4), we replaced the p75<sup>NTR</sup>-binding region of NRIF with a pGKneo selection cassette (Figure 6). The resulting *nrif*<sup>-/-</sup> mice express a truncated NRIF transcript lacking the p75<sup>NTR</sup>-binding region and four of its five zinc fingers. These mice show a reduction in cell death in embryonic retina (Figure 8) which is virtually identical in its extent to what is observed in the p75 and *ngf* mutants (Frade and Barde,



1999), pointing to these three genes being operative in the same pathway. Our results are compatible with the hypothesis that during the period of naturally occurring cell death in the developing retina, NRIF actively participates in the apoptotic process mediated by p75<sup>NTR</sup>. Several zinc finger proteins of the C2H2 type have already been shown to participate in programmed cell death. For example, TIEG, a TGF- $\beta$ -inducible gene in pancreatic epithelial cells, has been shown to induce apoptosis when overexpressed (Cook *et al.*, 1998). Similarly, *Zac1* is a tumour suppressor gene expressed only in brain and pituitary gland and, like p53, it can regulate apoptosis and cell cycle arrest (Spengler *et al.*, 1997). Krox-20, originally identified as a serum response immediate early gene (IEG) (Chavrier *et al.*, 1988), activates transcription from a specific DNA recognition element (Swirnoff and Milbrandt, 1995), controls segmentation during hindbrain development (Schneider-Maunoury *et al.*, 1993) but also regulates susceptibility to apoptosis in developing Schwann cells (Zorick *et al.*, 1999). Like Krox-20 and Nurr77 (Watson and Milbrandt, 1990), *nrif* is also induced in cultured cells by NGF; yet a direct interaction of a KRAB-containing zinc finger protein with a neurotrophin receptor has so far only been shown for NRIF. Presumably, binding of NGF to p75<sup>NTR</sup> induces a conformational change in the receptor which then releases NRIF. NRIF, in turn, could translocate to the cell nucleus where its zinc fingers would bind specific DNA sequences, while its KRAB domains could silence basal and inducible transcription. Future work will attempt to identify downstream targets of the NRIF protein, the p75<sup>NTR</sup> gene itself being a candidate. Indeed, p75<sup>NTR</sup> mRNA levels are up-regulated in *nrif*<sup>-/-</sup> mice (E.Casademunt, unpublished data, and Figure 8).

Unexpectedly, the phenotype of the *nrif* mutation appears to be masked in the mixed BL6/Sv129 background. Although at the F<sub>2</sub> generation (BL6:Sv129 50:50 hybrids) the mutation causes only limited lethality, after seven backcross generations to the BL6 strain *nrif*<sup>-/-</sup> mice are no longer viable beyond E12 (Figure 7). The fact that the lethal phenotype can be rescued by only one generation of mating to *nrif*<sup>+/+</sup> mice of Sv129 background strongly indicates that the BL6 genome cannot support the homozygous mutation. This situation is in principle analogous, but exactly opposite in the details to that described for the *Pax-2* (Schwarz *et al.*, 1997), *Egfr* (Threadgill *et al.*, 1995) and *Tgfb1* mutations (Bonyadi *et al.*, 1997), all of which have lethal consequences in a congenic Sv129 background. Our results are a further illustration of the need to evaluate the effect of targeted mutations in different congenic backgrounds (see e.g. Banbury Conference on Genetic Background in Mice, 1997; Frankel, 1998).

In conclusion, NRIF is the first zinc finger protein described to interact with the p75<sup>NTR</sup> receptor and to play an active role in developmental programmed cell death. NRIF may therefore represent a new class of receptor-associated transcription factors important for regulating cell viability.

## Materials and methods

### Interaction trap

Plasmid vectors and yeast strain EGY48 required for the interaction trap were all generously provided by R.Brent (Gyuris *et al.*, 1993). The bait

p75<sup>NTR</sup> construct was generated by PCR amplification from a full-length rat p75<sup>NTR</sup> cDNA clone (provided by E.Shooter) using the following primers: 5'-ATC GAA TTC TTC AAG AGG TGG AAC AG and 5'-GAG GGA TCC GTG AGT TCA CAC TGG GG, and in-frame cloning into the *EcoRI*-*BamHI* sites of the yeast bait *lexA* fusion pEG202 vector. The interaction trap was performed as previously described (Gyuris *et al.*, 1993), using a human, 22-week-old, fetal, frontal cortex cDNA library cloned into the pJG4-5 plasmid (provided by D.Kraic). Out of  $1.3 \times 10^6$  colonies plated, 200 grew under selective conditions and 17 of them showed galactose-dependent growth (conditions for induction of the library). Yeast DNA was isolated and retested for specific interaction with the p75<sup>NTR</sup>ICD bait and with additional baits, e.g. bicoid and GST. Deletion constructs of rat p75<sup>NTR</sup> were generated by PCR amplification of the cDNA encoding residues 244-290 and 295-396, and subcloned into pEG202. Deletion constructs of mouse *nrif* were PCR amplified from the cDNA encoding residues 521-661, 521-689 and 690-832, and subcloned into pJG4-5.

### Cloning of the mouse *nrif* cDNA and genomic clones

Approximately  $7.5 \times 10^5$  p.f.u. of a P1 mouse brain cDNA library in  $\lambda$ ZAPII (Stratagene) were plated and transferred to nylon membranes (Hybond N, Amersham). The filters were screened with a 0.9 kb, *EcoRI*-*XhoI* human *nrif* cDNA probe including the zinc finger domain, radiolabelled by random priming (Amersham). Hybridization was carried out with  $5\times$  SSC,  $5\times$  Denhardt's, 50 mM Tris-HCl pH 7.4, 1% SDS, 40% formamide and 100  $\mu$ g/ml salmon sperm DNA at 42°C overnight. The filters were washed at 65°C in  $1\times$  SSC, 0.1% SDS. Positive clones were *in vivo* excised using Exassist phage and SOLR recipient cells (Stratagene), and recovered as pBluescript SK plasmids. Sequence analyses were done with the MacMolloy or the Wisconsin Genetics Computer Group software.

Approximately  $2 \times 10^6$  genomic clones from a mouse (129/Sv) genomic library made in the  $\lambda$ FIXII vector (Stratagene) and plated in LE392 host cells were screened using two radioactively labelled, overlapping fragments of the mouse NRIF 6.3 cDNA (*NcoI*-*EcoRI*, 1582 bp and *NcoI*-*BamHI*, 653 bp). Hybridization and washing were done according to Church and Gilbert (1984). Six out of 14 independent clones which hybridized with both probes appeared to be independent isolates of the same gene, and all further work was with genomic clone 4 (Figure 6A).

### Northern and RT-PCR analysis

Total RNA was extracted following a modified RNAzol B method (P.Chomczynski, Wak-Chemie Medical GmbH) from mouse embryonic (E15.5) and adult (1-2 months old) tissues. For Northern analysis, 20  $\mu$ g of total RNA was glyoxylated, electrophoresed on 1.2% agarose gels in 10 mM NaH<sub>2</sub>PO<sub>4</sub>/Na<sub>2</sub>HPO<sub>4</sub> pH 6.5 and vacuum-transferred to Hybond N membranes. *nrif* mRNA levels were quantified using an RNA Master Blot (Clontech) following the manufacturer's instructions and a Molecular Dynamics phosphorimager. Northern blots were probed with a 1.1 kb *SpeI*-*EcoRV* fragment of the *nrif* cDNA which excludes the zinc finger region. RT-PCRs were done from 500 ng of total RNA essentially as described (Friedel *et al.*, 1997), using the following PCR primers: 5'-GTG ATG CTA GAG ACC TTG GG; 5'-CAC CAT GGC ATC GCT ACT GTC C. Because of the low levels of expression of the *nrif* mRNA, the PCR requires 5-fold higher levels of starting cDNA than those required to amplify the GAPDH transcript. Cycle parameters were 94°C 4 min; 94°C 30 s, 58°C 30 s, 72°C 40 s, 35 cycles.

### Recombinant NRIF protein expression

Production of recombinant NRIF proteins in *E.coli* JM109 was induced for 4 h at room temperature by 0.5 mM isopropyl- $\beta$ -D-thiogalactopyranoside (IPTG) with 0.1 mM ZnCl<sub>2</sub>. Bacterial pellets were resuspended in lysis buffer [50 mM HEPES pH 7.9, 1% Triton X-100, 5 mM dithiothreitol (DTT), 0.5 M NaCl, 0.1 mM ZnCl<sub>2</sub>, 1 mM phenylmethylsulfonyl fluoride (PMSF), 5  $\mu$ g/ml aprotinin, 5  $\mu$ g/ml leupeptin] and lysed by sonification. Soluble protein obtained by centrifugation was bound to glutathione-Sepharose 4B beads (Pharmacia Biotech) for 4 h at 4°C. Control beads were prepared by using the same host bacteria lacking any plasmid. Bound beads were washed extensively with  $1\times$  phosphate-buffered saline (PBS), 0.3 M NaCl, 0.1 mM ZnCl<sub>2</sub>. Protein binding to the beads was assessed by SDS-PAGE analysis of a small aliquot eluted with Laemmli sample buffer.

### Cell culture and transfection

293 cells (Graham *et al.*, 1977) were cultured in Dulbecco's modified Eagle's medium (DMEM, Gibco-BRL) supplemented with 10% fetal

calf serum (Sigma) and 1% penicillin/streptomycin (Gibco-BRL) at 37°C and 5% CO<sub>2</sub>. Transient transfection was by the calcium phosphate precipitation method according to Chen and Okayama (1987), seeding  $2.5 \times 10^6$  cells onto 10 cm plates the day preceding transfection. Transfection efficiency was estimated by parallel transfection with a pCMV-GFP vector (pEGFP-N1, Clontech).

#### Pull-down assays/Western blot

Two days after transfection, cells were washed with ice-cold PBS and lysed in 1 ml of lysis buffer/plate [25 mM HEPES pH 7.5, 150 mM NaCl, 10% glycerol, 0.8 % NP-40, 4 mM Pefabloc (Boehringer Mannheim), 5 µg/ml aprotinin, 5 µg/ml leupeptin] followed by centrifugation at 15 000 g, 4°C for 20 min. The supernatant (300 µl) was mixed with binding buffer (900 µl; 25 mM HEPES pH 7.5, 150 mM KCl, 5 mM MgCl<sub>2</sub>, 0.13 mM ZnCl<sub>2</sub>, 5 mM DTT, 4 mM Pefabloc, 5 µg/ml aprotinin, 5 µg/ml leupeptin), and incubated overnight with a 50 µl bed volume of protein-loaded glutathione-Sepharose 4B beads (see above). After washing the beads once with washing buffer 1 (WB1: 40 mM HEPES pH 7.5, 300 mM NaCl, 5 mM MgCl<sub>2</sub>, 0.1 mM ZnCl<sub>2</sub>, 1 mM DTT) and twice with WB2 (150 mM NaCl, otherwise like WB1), the proteins were eluted by boiling with 50 µl of 2× Laemmli buffer for 8 min, separated on a 10 or 12% SDS-polyacrylamide gel and transferred to PVDF membranes (Immobilon-P, Millipore). Protein blots were blocked with 5% non-fat milk powder in TBST (25 mM Tris pH 7.5, 150 mM NaCl, 0.1% Tween-20), incubated overnight at 4°C with 0.5 µg/ml anti-HA monoclonal antibody (Boehringer Mannheim) in blocking buffer, washed five times with TBST, incubated with goat anti-mouse IgG-POD (Pierce, 1:10 000 in blocking buffer) for 1 h at room temperature, washed again and finally developed using the ECL detection system (Amersham).

#### Construction of p75<sup>NTR</sup> and NRIF expression plasmids

The intracellular domain of p75<sup>NTR</sup> (starting with Lys251) used for pull-down experiments was amplified by PCR from rat p75<sup>NTR</sup> cloned into pcDNA3 (Invitrogen) with the following primers: 5'-GTC AAG CTT GCC ACC ATG TAT CCT TAT GAC GTG CCT GAC TAT GCC GGG GGA AAG AGG TGG AAC AGC TG (which introduces a Kozak consensus sequence followed by a HA tag and a glycine linker), and 5'-GTC GCG GCC GCT CAC ACT GGG GAT GTG GCA G (primer 'p75end'), and then subcloned into *Hind*III-*NorI*-digested pRC/CMV (Invitrogen), creating HA-p75ICD. Full-length -p75 was amplified by PCR from the same template with primers 5'-GTC GCT AGC TTA TCC TTA TGA CGT GCC TGA CTA TGC CGG GGG AAA GGA GAC ATG TTC CAC AGC and 'p75end' and subcloned into pRC/CMV AC7 (Bibel *et al.*, 1999).

The full-length NRIF coding sequence (residues 2–832) was amplified by PCR with primers 5'-GAGGACAGTATGGCTTCC and 5'-CTAC-AATTTGGGCTGCTTC, and subcloned into pEGFP-C1, fusing EGFP at the N-terminus of NRIF to produce pEGFP-NRIF, or into pFLAG-CMV-2 creating N-terminally flagged NRIF (pFLAG-NRIF). The GST-NRIFΔZnF construct was made by subcloning the NRIF cDNA sequence excluding the zinc fingers from pFLAG-NRIF into pGEX-2T (Pharmacia). GST-NRIFAN was generated by PCR amplification from cDNA clone 6.3 (Figure 6A) and subcloning into pGEX-4T-1 (Pharmacia).

#### Immunocytochemistry

Transiently transfected 293 cells grown on 13 mm glass coverslips (coated with poly-L-lysine, Sigma, 0.01%) were fixed with 2–4% paraformaldehyde in PBS for 15 min at room temperature, permeabilized with 0.2% Triton X-100/PBS, blocked in 10% bovine serum albumin, 10% normal goat serum (NGS)/PBS for at least 1 h at room temperature, and incubated overnight at 4°C with a polyclonal antibody against the intracellular domain of p75<sup>NTR</sup> in PBS/5% NGS. After three 10 min washes with PBS, cells were incubated for 1 h at room temperature with LRSC-conjugated goat anti-rabbit IgG (Jackson ImmunoResearch Laboratories) and 4',6-diamidino-2-phenylindole (DAPI) at 0.5 µg/ml in PBS/5% NGS. Following five 10 min washes with PBS, cells were mounted in 'Immunofluore Mounting Medium' (ICN Biochemicals) and analysed using fluorescence microscopy.

#### NrIF gene targeting. Breeding scheme

To target the *nrif* gene, the genomic region corresponding to the region between residues 520 and 777 (Figures 2 and 6A) was replaced by the neo cassette from the pGKneoA vector (from Soriano *et al.*, 1991), resulting in a targeting construct where the 5' arm was 3.2 kb, the 3' arm was 2.3 kb and the transcription orientation of the neo cassette was

opposite to that of the *nrif* gene. R1 ES cells (Nagy *et al.*, 1993) were electroporated, selected with G418 and screened by Southern blot with an external 5' probe (Figure 6A) which recognizes a 6.5 kb wild-type band and a 9 kb mutant band in a genomic *EcoRV* digest.

BL6 mice were of the C57BL/6NJCrl (Charles River Laboratories) strain; Sv129 mice of the 129SvPas substrain. Chimeric mice were generated by transfer of BL6 blastocysts injected with targeted ES cells into pseudopregnant females. After generation of F<sub>2</sub> viable homozygous offspring, an intensive programme of backcrossing to BL6 and 129Sv was started by mating F<sub>1</sub> heterozygous females to BL6 males and founding chimeric mice to 129Sv females. In each case, heterozygous females were mated to BL6 and 129Sv males, respectively, for 10 consecutive generations in order to obtain congenic strains of each background. Mice were genotyped by Southern and PCR analysis from tail or yolk sac DNA extracted as described before (Laird *et al.*, 1991; Hogan *et al.*, 1994). PCR primers for *nrif* genotyping were as follows: 5'-TCC ATG ACA CGA GGT TTA CG, 5'-CAG AAG TGC TAA GTT CCT CG and 5'-GAT TCG CAG CGC ATC GCC TTC, and cycle parameters: 94°C 4 min; 94°C 30 s, 57°C 30 s, 72°C 1 min, 35 cycles. The two first primers amplify the 521 bp wild-type band, whereas the first and third primer amplify the 572 bp targeted band.

#### Quantification of cell death in E15.5 retina

Heterozygous F<sub>1</sub> mice were mated until a vaginal plug (E0.5) was observed. Fifteen days later (E15.5), embryonic retinas were prepared and processed as described in Frade and Barde (1999), with duplicate measurements from each retina. The results are based on the analysis of nine litters (78 embryos). Six litters generated by homozygous +/+ and -/- parents were also analysed to evaluate the degree of variability between littermates of the same litter.

#### Acknowledgements

We are indebted to O.Momoh and B.Kunkel for outstanding technical assistance, D.v.Schack and W.Wendler for help at the initial stages of this work, M.Meyer for invaluable help with gene targeting, D.Beier for advice with the SSCP, L.Rowe and L.Maltais (Jackson Laboratories) for help with the chromosomal mapping of the *nrif* gene, L.Stubbs (Lawrence Livermore Labs) for sharing unpublished data, and J.Chalcraft for photographic work. Supported in part by grants from the National Institutes of Health (ROINS38220) and the National Alliance for Research on Schizophrenia and Depression (B.D.C.), and by the European Union, Biotechnology Programme PL960024 (Y.A.B.).

#### References

- Arch,R.H., Gedrich,R.W. and Thompson,C.B. (1998) Turnor necrosis factor receptor-associated factors (TRAFs)—a family of adaptor proteins that regulates life and death. *Genes Dev.*, **12**, 2821–2830.
- Bamji,S.X., Majdan,M., Poznaniak,C.D., Belliveau,D.J., Aloyz,R., Kohn,J., Causing,C.G. and Miller,F.D. (1998) The p75 neurotrophin receptor mediates neuronal apoptosis and is essential for naturally occurring sympathetic neuron death. *J. Cell. Biol.*, **140**, 911–923.
- Banbury Conference on Genetic Background in Mice (1997) Mutant mice and neuroscience: recommendations concerning genetic background. *Neuron*, **19**, 755–759.
- Barrett,G.L. and Bartlett,P.F. (1994) The p75 nerve growth factor receptor mediates survival or death depending on the stage of sensory neuron development. *Proc. Natl Acad. Sci. USA*, **91**, 6501–6505.
- Battleman,D.S., Geller,A.I. and Chao,M.V. (1993) HSV-1 vector-mediated gene transfer of the human nerve growth factor receptor p75<sup>NGFR</sup> defines high-affinity NGF binding. *J. Neurosci.*, **13**, 941–951.
- Beier,D.R. (1993) Single-strand conformation polymorphism (SSCP) analysis as a tool for genetic mapping. *Mamm. Genome*, **4**, 627–631.
- Beier,D.R., Dushkin,H. and Sussman,D.J. (1992) Mapping genes in the mouse using single-strand conformation polymorphism analysis of recombinant inbred strains and interspecific crosses. *Proc. Natl Acad. Sci. USA*, **89**, 9102–9106.
- Bellefroid,E.J., Poncelet,D.A., Lecocq,P.J., Revelant,O. and Martial,J.A. (1991) The evolutionarily conserved Krüppel-associated box domain defines a subfamily of eukaryotic multifingered proteins. *Proc. Natl Acad. Sci. USA*, **88**, 3608–3612.
- Benedetti,M., Levi,A. and Chao,M.V. (1993) Differential expression of nerve growth factor receptors leads to altered binding affinity and neurotrophin responsiveness. *Proc. Natl Acad. Sci. USA*, **90**, 7859–7863.

- linked zinc-finger gene families in human and mouse: evidence for orthologous genes. *Genomics*, **49**, 112–121.
- Snider, W.D. (1994) Functions of the neurotrophins during nervous system development: what the knockouts are teaching us. *Cell*, **77**, 627–638.
- Soiliu-Hänninen, M., Ekert, P., Bucci, T., Syroid, D., Bartlett, P.F. and Kilpatrick, T.J. (1999) Nerve growth factor signaling through p75 induces apoptosis in Schwann cells via a Bcl-2-independent pathway. *J. Neurosci.*, **19**, 4828–4838.
- Soriano, P., Montgomery, C., Geske, R. and Bradley, A. (1991) Targeted disruption of the *c-src* proto-oncogene leads to osteopetrosis in mice. *Cell*, **64**, 693–702.
- Spengler, D., Villalba, M., Hoffmann, A., Pantaloni, C., Houssami, S., Bockaert, J. and Journot, L. (1997) Regulation of apoptosis and cell cycle arrest by Zacl, a novel zinc finger protein expressed in the pituitary gland and the brain. *EMBO J.*, **16**, 2814–2825.
- Stubbs, L. *et al.* (1996) Detailed comparative map of human chromosome 19q and related regions of the mouse genome. *Genomics*, **35**, 499–508.
- Swimoff, A. and Milbrandt, J. (1995) DNA-binding specificity of NGFI-A and related zinc finger transcription factors. *Mol. Cell. Biol.*, **15**, 2275–2287.
- Threadgill, D.W. *et al.* (1995) Targeted disruption of mouse EGF receptor: effect of genetic background on mutant phenotype. *Science*, **269**, 230–234.
- Verdi, J.M., Birren, S.J., Ibáñez, C.F., Persson, H., Kaplan, D.R., Benedetti, M., Chao, M.V. and Anderson, D.J. (1994) p75<sup>LNGFR</sup> regulates Trk signal transduction and NGF-induced neuronal differentiation in MAH cells. *Neuron*, **12**, 733–745.
- Watson, M.A. and Milbrandt, J. (1990) Expression of the nerve growth factor-regulated NGFI-A and NGF-IB genes in the developing rat. *Development*, **110**, 173–183.
- Weinmaster, G. (1997) The ins and outs of Notch signaling. *Mol. Cell. Neurosci.*, **9**, 91–102.
- Witzgall, R., O'Leary, E., Leaf, A., Onaldi, D. and Bonventre, J.V. (1994) The Krüppel-associated box-A (KRAB-A) domain of zinc finger proteins mediates transcriptional repression. *Proc. Natl Acad. Sci. USA*, **91**, 4514–4518.
- Wood, J.N. (1995) Regulation of NF-kappaB activity in rat dorsal root ganglia and PC12 cells by tumour necrosis factor and nerve growth factor. *Neurosci. Lett.*, **192**, 41–44.
- Yoon, S.O., Casaccia-Bonnel, P., Carter, B. and Chao, M.V. (1998) Competitive signaling between TrkA and p75 nerve growth factor receptors determines cell survival. *J. Neurosci.*, **18**, 3273–3281.
- Zheng, J.Q., Felder, M., Connor, J.A. and Poo, M. (1994) Turning of nerve growth cones induced by neurotransmitters. *Nature*, **368**, 140–144.
- Zorick, T.S., Syroid, D.E., Brown, A., Gridley, T. and Lemke, G. (1999) Krox-20 controls SCIP expression, cell cycle exit and susceptibility to apoptosis in developing myelinating Schwann cells. *Development*, **126**, 1397–1406.

Received July 2, 1999; revised and accepted September 7, 1999

## Strain-dependent embryonic lethality in mice lacking the retinoblastoma-related p130 gene

Jennifer E. LeCouter, Boris Kablar, Peter F. M. Whyte, Chuyan Ying and Michael A. Rudnicki\*

Institute for Molecular Biology and Biotechnology, McMaster University, 1280 Main Street West, Hamilton, Ontario, Canada L8S 4K1

\*Author for correspondence (e-mail: rudnicki@mcmaster.ca)

Accepted 21 September; published on WWW 9 November 1998

### SUMMARY

The retinoblastoma-related p130 protein is a member of a conserved family, consisting of Rb, p107 and p130, which are believed to play important roles in cell-cycle control and cellular differentiation. We have generated a null mutation in *p130* by gene targeting and crossed the null allele into Balb/cJ and C57BL/6J strains of mice. In an enriched Balb/cJ genetic background, *p130*<sup>-/-</sup> embryos displayed arrested growth and died between embryonic days 11 and 13. Histological analysis revealed varying degrees of disorganization in neural and dermamyotomal structures. Immunohistochemistry with antibody reactive with Islet-1 indicated markedly reduced numbers of neurons in the spinal cord and dorsal root ganglia. Immunohistochemistry with antibody reactive with desmin indicated a similar reduction in the number of differentiated myocytes in the myotome. The myocardium of mutant embryos was abnormally thin and resembled an earlier staged two-chambered heart consisting of the bulbus cordis and the ventricular chamber. TUNEL

analysis indicated the presence of extensive apoptosis in various tissues including the neural tube, the brain, the dermomyotome, but not the heart. Immunohistochemistry with antibody reactive with PCNA revealed increased cellular proliferation in the neural tube and the brain, and decreased proliferation in the heart. The placentas of *p130*<sup>-/-</sup> embryos did not display elevated apoptosis and were indistinguishable from wild type suggesting that the phenotype was not due to placental failure. Following a single cross with the C57BL/6 mice, *p130*<sup>-/-</sup> animals were derived that were viable and fertile. These results indicate that *p130* in a Balb/cJ genetic background plays an essential role that is required for normal development. Moreover, our experiments establish that second-site modifier genes exist that have an epistatic relationship with *p130*.

Key words: p130, Balb/C, Embryonic lethality, Mouse, Retinoblastoma

### INTRODUCTION

In the developing embryo, combinatorial signals elicit appropriate patterning and morphogenesis via regulatory networks that control stem-cell determination, proliferation, differentiation and programmed death (Slack, 1992). The retinoblastoma (Rb) family, including *Rb*, *p107* and *p130*, plays an integral role in these regulatory pathways, in part by negatively regulating E2F-dependent transcription (Weinberg, 1995). Moreover, an important role for p130 in repressing cell cycle progression during differentiation is supported by the observation that p130:E2F complexes are predominant in differentiated cells (Muller, 1995; Nevins et al., 1997). Different members of the Rb-family also regulate the activity of other transcription factors including the developmentally important paired homeodomain-containing proteins MHOX, Chx10 and Pax-3 (Wiggin et al., 1997), as well as the transcriptional control proteins C/EBP and c-Myc (Chen et al., 1996; Weinberg, 1995; Whyte, 1995).

Rb-family members differentially bind cyclins and their associated kinases (cyclin-dependent kinases or Cdk) resulting in the differential phosphorylation of Rb-members

during progression through the cell cycle. Consequently, Rb, p107 and p130 are hypophosphorylated during different phases of the cell cycle allowing the formation of complexes that contain different E2F transcription factors (Nevins et al., 1997). The multimember E2F-family of transcription factors regulates the transcription of many genes, for example, thymidylate synthase, ribonucleotide reductase M2, DHFR, B-myb and cdc2 that are involved in DNA synthesis and cell-cycle progression. Complexes containing hypophosphorylated Rb-family members are believed to bind promoters at E2F sites and inhibit transcription by recruiting HDAC1, a histone deacetylase, to repress gene expression via chromatin remodeling (Brehm et al., 1998; Luo et al., 1998; Magnaghi-Jaulin et al., 1998). Presumably, the cyclic activation and repression of E2F-regulated genes facilitates appropriate gene expression and hence progression through the cell cycle (Muller, 1995).

Mice carrying targeted mutations in *Rb* display phenotypes supportive of a role for Rb in cellular differentiation. Homozygous mutant embryos die in utero between day 13.5 and day 15.5 of gestation and exhibit defects in erythropoiesis and extensive cell death in the central nervous system (Clarke

et al., 1992; Jacks et al., 1992; Lee et al., 1992, 1994; Macleod et al., 1996). Chimeras containing both wild-type and *Rb*-deficient cells are viable, but exhibit adrenal medulla hyperplasias, pituitary tumors and lens cataracts (Maandag et al., 1994; Williams et al., 1994). Unlike *Rb*-deficient embryos, *Rb*<sup>-/-</sup> wild-type chimeras contain mature *Rb*-deficient erythrocytes suggesting that erythroid differentiation is delayed rather than blocked in the absence of *Rb*.

Mice lacking either *p107* or *p130* in a mixed 129/Sv:C57BL/6J genetic background exhibit no overt phenotype, are viable and fertile, and embryonic fibroblasts derived from the mutants display normal cell-cycle kinetics (Cobrinik et al., 1996; Herrera et al., 1996; Hurford et al., 1997; Lee et al., 1996). Embryos lacking both *Rb* and *p107* die in utero 2 days earlier than *Rb*-deficient embryos and exhibit apoptosis in the liver and central nervous system suggesting some redundancy in function. Compound mutant mice lacking both *p130* and *p107* die soon after birth and exhibit defective endochondral bone development likely due to a deficiency in osteoblast differentiation. Taken together, these data suggested that *p107* and *p130* have relatively subtle roles in regulating the cell cycle and that a significant degree of overlap in function exists between the proteins (Cobrinik et al., 1996; Lee et al., 1996).

We have independently derived a targeted null mutation in *p130* into the germline of mice. In our experiments, we bred chimeras with mice from the Balb/cJ strain. Surprisingly, we observed that mice lacking *p130* displayed an embryonic lethal phenotype associated with reduced cellular differentiation and increased apoptosis. These data strongly support the assertion that *p130* in a Balb/cJ genetic background plays an essential role that is required for normal development. Moreover, the observed strain-dependence of the phenotype suggests that second-site modifier genes exist that have an epistatic relationship with *p130*.

## MATERIALS AND METHODS

### Generation of *p130* mutant mice

A 13 kb fragment of the *p130* locus was cloned from a J1 genomic library and was used to construct a targeting vector containing 3 kb of 5'- and 7.2 kb of 3'-homologous sequence. The PGK-neo expression cassette was inserted in the opposite transcriptional orientation to *p130* immediately downstream of the codon encoding aa 106 (Fig. 1). The *p130* targeting vector was linearized with *NorI* and gene targeting performed with the J1 line of ES cells as described previously (Rudnicki et al., 1992). Targeting events were detected by Southern analysis of *EcoRV*-digested genomic DNA using a 5' flanking probe. Two independent targeted lines were injected into Balb/cJ blastocyst stage embryos to generate chimeras. Chimeras were subsequently mated to Balb/cJ females and the resulting heterozygous mice were bred to produce homozygous mutant mice. Care of animals was in accordance with institutional guidelines.

### Northern and immunoblot analysis

Northern analysis of total RNA (10 µg) was performed using standard techniques with the full-length mouse *p130* cDNA as probe (LeCouter et al., 1996). Immunoblot analysis was performed as follows. Protein lysates were prepared by lysing in modified TNE (1 mM NaV and 10 µg/ml PMSF, aprotinin, pepstatin and leupeptin) or EBC lysis buffer (50 mM Tris HCl, pH 7.5, 0.5% NP40, 150 mM NaCl and protease inhibitors). Protein (30 µg) was electrophoresed on 7.5% SDS-

polyacrylamide gels and transferred to PVDF membranes. Membranes blocked with 5% skim milk powder in TBST were incubated for 1 hour at room temperature with anti-*p130* antibody C-20 (Santa Cruz) diluted 1:500. Following five washes in TBST, secondary antibody (diluted 1:2000) was incubated at RT for 1 hour. After five TBST washes, proteins were visualized by ECL detection (Amersham).

### Histopathology and immunohistochemistry

Preparation, fixation, sectioning and staining of tissue samples for light microscopy of histological preparations were performed as described previously (Kablar et al., 1997). Following timed matings, embryos were isolated at different stages of gestation and fixed in 4% paraformaldehyde in PBS for 12-20 hours. Processing and staining with antibodies reactive with Isl-1 (Developmental Hybridoma Bank), desmin (Dako) and PCNA (Dakopatts) was performed as previously described (Kablar et al., 1997). TUNEL analysis was performed with the ApopTag Kit (Oncor). All sections were lightly counterstained with hematoxylin.

## RESULTS

### Targeted inactivation of *p130* in mice

The *p130* gene was disrupted by homologous recombination in J1 embryonic stem (ES) cells using standard techniques (Rudnicki et al., 1992). The *p130* targeting vector was constructed by inserting the PGK-neo cassette (McBurney et al., 1991) into a 1 kb deletion originating from a *Bam*HI site introduced into an exon immediately downstream of the codon encoding aa 160 to a *Kpn*I site within the downstream intron. The PGK-neo cassette was inserted in the opposite transcriptional orientation to *p130* (Fig. 1A). Approximately 1% of G418-resistant clones contained the targeted *p130* allele as revealed by Southern analysis. A probe upstream of the targeting vector detected an 18.5 kb *EcoRV* fragment from the wild-type *p130* allele, whereas a 7.5 kb *EcoRV* fragment was detected following homologous recombination (Fig. 1B).

Chimeras were generated following microinjection of two independently derived targeted ES lines into Balb/cJ blastocysts. Southern analysis of tail DNA in *p130*<sup>+/-</sup> germline progeny revealed the predicted restriction fragment length polymorphism (not shown). Two independent *p130* mutant mouse lines were derived into the germline and the observed homozygous embryonic lethal phenotype was completely identical in all experiments and are hereafter discussed together (see below).

To confirm that the engineered disruption of *p130* by PGK-neo had generated a null mutation, we examined expression of *p130* at the level of mRNA and protein by northern and immunoblot analysis. RNA and protein was isolated from E14 embryos from an enriched C57BL/6 genetic background as previously described (LeCouter et al., 1998). Northern analysis was performed on total RNA using the full-length mouse *p130* cDNA as probe (Fig. 1C). The mature 4.9 kb *p130* mRNA was readily detected in wild-type total RNA (Fig. 1C, lane 1) and the level of *p130* mRNA was reduced by about half in *p130*<sup>+/-</sup> total RNA (Fig. 1C, lane 2). However, no *p130* mRNA was detected in RNA isolated from *p130*<sup>-/-</sup> samples (Fig. 1C, lane 3).

Immunoblot analysis was performed with antiserum C20 (Santa Cruz) reactive with the carboxyl-terminal 20 aa of *p130*. The *p130* protein was readily detected in wild-type extracts and

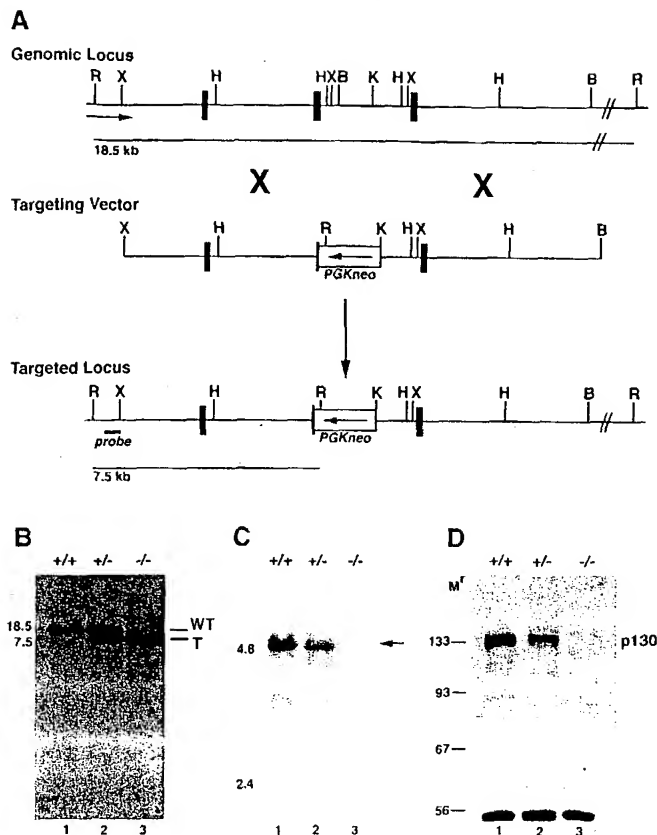


**Fig. 1.** Targeted disruption of the  $p130$  gene. (A) Genomic locus, targeting vector and structure of the disrupted  $p130$  locus with exons depicted as filled boxes. The targeting vector contained 3 kb of 5'- and 7.2 kb of 3'-homologous sequence. The PGK-neo expression cassette was inserted in the opposite transcriptional orientation to  $p130$  immediately downstream of the aa 106 codon. (B) Southern analysis of  $EcoRV$ -digested DNA isolated from E11.5 embryos derived from a heterozygous intercross resulted in the predicted restriction length polymorphism. (C) Northern blot analysis of total RNA probed with the full-length mouse cDNA revealed a complete absence of a transcript from the targeted  $p130$  allele. (D) Immunoblot analysis with antibody C20 reactive with  $p130$  (Santa Cruz) against tissue lysates indicated that no protein was expressed from the targeted allele. Abbreviations: E,  $EcoRV$ ; X,  $XbaI$ ; H,  $HindIII$ ; B,  $BamHI$ ; Mr, relative mobility in kD.

reduced levels were observed in  $p130^{+/-}$  extracts (Fig. 1D, lanes 1 and 2). No detectable product was detected in  $p130^{-/-}$  lysates (Fig. 1D, lane 3). Moreover, no smaller molecular weight species were apparent in  $p130^{-/-}$  extracts. Therefore we conclude that disruption of  $p130$  with PGK-neo generated a null allele.

### Embryonic lethality in the absence of $p130$

Genotyping of the weaned 3-week-old progeny derived from interbreeding of  $p130^{+/-}$  mice revealed an absence of  $p130^{-/-}$  animals. Moreover, inspection of newly delivered litters revealed no increased incidence of non-viable newborn pups. Together, this suggested that  $p130^{-/-}$  embryos were not being delivered and indicated that  $p130^{-/-}$  embryos were dying in utero.

**Table 1.** Viability of embryos derived from  $p130^{+/-}$  interbreeding

Genotype	Days post coitum					
	9.5	10.5	11.5	12.5	13.5	14.5
Wild type	6	17	15	13	9	5
$p130^{+/-}$	15	31	23	23	13	14
$p130^{-/-}$	4	14	9	2	0	0

The  $F_1$   $p130^{+/-}$  offspring of chimeras bred with Balb/cJ mice were interbred and Cesarean sections performed at different gestational ages. Note, the morning following mating is considered 0.5 days post coitum.

To delineate the gestational stage that  $p130^{-/-}$  embryos were being lost, Cesarean sections were performed at successive days postcoitum (dpc) following timed matings (Table 1). DNA was isolated from the fetal portion of the placenta and the conceptuses genotyped by Southern analysis. At 9.5 dpc and 10.5 dpc, we observed an approximate Mendelian frequency of 1:2:1 of wild-type,  $p130^{+/-}$  and  $p130^{-/-}$  genotypes. However, about 50% of the expected numbers of  $p130^{-/-}$  embryos were observed on 11.5 dpc, whereas only about 10% of the expected numbers of  $p130^{-/-}$  embryos were observed on 12.5 dpc. On and after 13.5 dpc, no viable  $p130^{-/-}$  embryos were detected (Table 1). In addition, we observed that approximately 25% of the conceptuses were non-viable and were undergoing absorption on and after 12.5 dpc. Therefore, we conclude that a null mutation in  $p130$  in a Balb/cJ genetic background resulted in an embryonic lethal phenotype with embryos dying between embryonic day 11 and 13.

### Embryos lacking $p130$ display abnormal growth

Inspection of  $p130^{-/-}$  embryos revealed a disparity in growth that increased with gestational age until 11.5 dpc when the mutant embryo reached approximately 25% of the normal size (Fig. 2A). Mutant embryos at 10.5 dpc exhibited beating hearts with seemingly normal vascularization and distribution of blood. However, mutant hearts displayed an abnormal dilated morphology and appeared to resemble the two-chambered hearts of earlier-stage embryo. More anterior structures appeared normal, for example, 10.5 dpc  $p130^{-/-}$  embryos exhibited normal brain segmentation, normal elaboration of branchial arches and normal morphology of forelimbs. Posterior structures were reduced and mutant 10.5 dpc embryos failed to form hind limb buds. By 11.5 dpc, the remaining viable mutant embryos had progressed little in development and appeared similar in size to 10.5 dpc  $p130^{-/-}$  embryos (Fig. 2A).

One possible explanation for the observed growth arrest of  $p130^{-/-}$  embryos was that function of the placenta was compromised due to abnormal placental development. Importantly, dissection of the placentas from  $p130^{-/-}$  embryos revealed a normal anatomy and arrangement of extraembryonic blood vessels and membranes. Histological analysis of hematoxylin-stained sections indicated a normal cytomorphology including that of giant cells and placental labyrinth. To assess the extent of apoptosis in  $p130^{-/-}$  placentas, TUNEL analysis was performed to detect the presence of fragmented DNA in apoptotic bodies (Gavrieli et al., 1992). Importantly, no evidence of apoptosis was detected by TUNEL staining (Fig. 3). Taken together, these data support



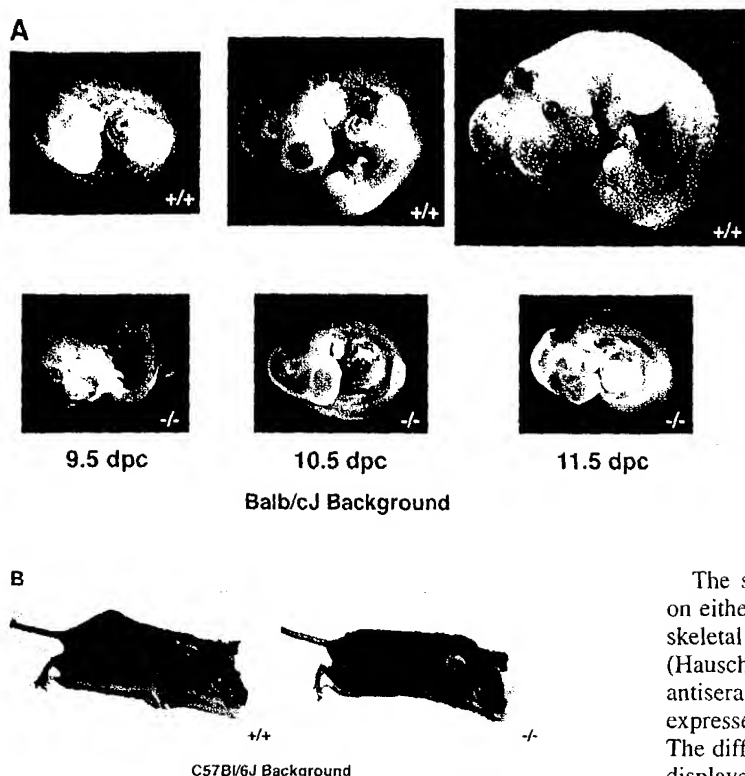


Fig. 2. Embryonic growth deficiency in the absence of *p130* is strain-dependent. (A) Wild-type embryos at 9.5 dpc have turned whereas *p130*<sup>-/-</sup> embryos were typically observed in the lordotic position and displayed reduced numbers of somites. By 10.5 dpc, *p130*<sup>-/-</sup> embryos are about half the normal size of wild-type embryos and displayed normal development of brain structures, however more posterior structures, including the heart and the hind limb region, were underdeveloped. The mutant embryo at 11.5 dpc was strikingly smaller than wild type and appeared arrested at the E10.5 stage. (B) In the C57Bl/6J genetic background, *p130*<sup>-/-</sup> mice were viable, fertile and displayed no overt phenotype (see Table 2). Note, 9.5 dpc and 10.5 dpc embryos were photographed before fixation, whereas 11.5 dpc embryos were photographed postfixation.

the conclusion that the growth deficit of *p130*<sup>-/-</sup> embryos was not due to placental failure.

#### Impaired neurogenesis and myogenesis in *p130*<sup>-/-</sup> embryos

Histological examination of sections of 10.5 dpc *p130*<sup>-/-</sup> embryos revealed some variability in the histological appearance of embryos presumably reflecting their overall viability. A typical 10.5 dpc *p130*<sup>-/-</sup> embryo that exhibited a beating heart when delivered is described below. Histological analysis revealed varying degrees of disorganization in neural and dermamyotomal structures, a poorly formed notochord and, in addition, a thin myocardium (Figs 4, 5).

Neuroepithelial cells within the neural tube are the progenitors of motor neurons that differentiate in response to signals from the floor plate of the neural tube (Yamada et al., 1991, 1993). To assess neuronal differentiation, immunohistochemistry was performed with antibody reactive against the LIM-domain transcription factors *Isl-1* and *Isl-2*, expressed in newly born motor and sensory neurons (Ericson et al., 1992; Tsuchida et al., 1994). We observed severely decreased numbers of *Isl-1/2*-expressing motor neurons within the ventral horn of a somewhat disorganized neural tube and similarly decreased numbers of sensory neurons within a poorly demarcated dorsal root ganglia (compare Fig. 4A and B). Moreover, the neural epithelium in the neural tube entirely failed to elaborate a basement membrane and cells were not organized into layers as in the wild-type neural tube (Figs 4B,D, 5). The floorplate of the neural tube was observed to have undergone marked apoptotic loss at thoracic and lumbar levels (compare Figs 4A and B, 5A and B). However, reduced numbers of neurons were noted at all levels.

The somite-derived dermamyotome, segmentally arranged on either side of the neural tube, forms the first differentiated skeletal muscle of the embryo known as the myotome (Hauschka, 1994). Myogenic differentiation was assessed with antisera reactive to desmin, an intermediate filament protein expressed in skeletal and cardiac muscle (Kablar et al., 1997). The differentiated myotome of wild-type embryos at 10.5 dpc displayed the typical pattern of desmin-expressing myocytes (Fig. 4C). By contrast, the differentiated myotome of *p130*<sup>-/-</sup> embryos was composed of very few desmin-expressing skeletal myocytes (compare Fig. 4C and D). The observed reduction in numbers of myotomal myocytes was also found at all levels.

Inspection of 10.5 dpc *p130*<sup>-/-</sup> embryos revealed a somewhat dilated myocardium and abnormal cardiac morphology suggestive of a defect in chamber formation (Fig. 2A). To characterize cardiac structure of *p130*<sup>-/-</sup> embryos, serial sections were performed through the hearts and

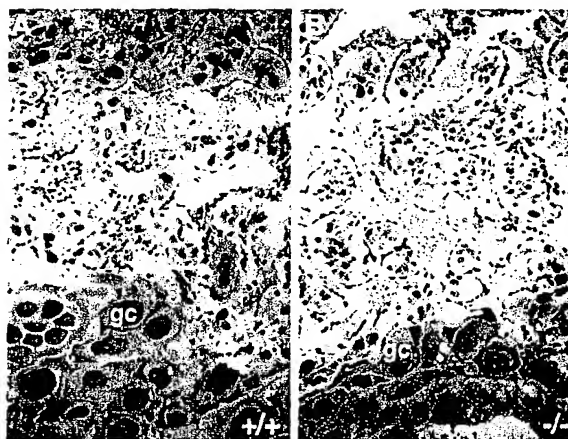
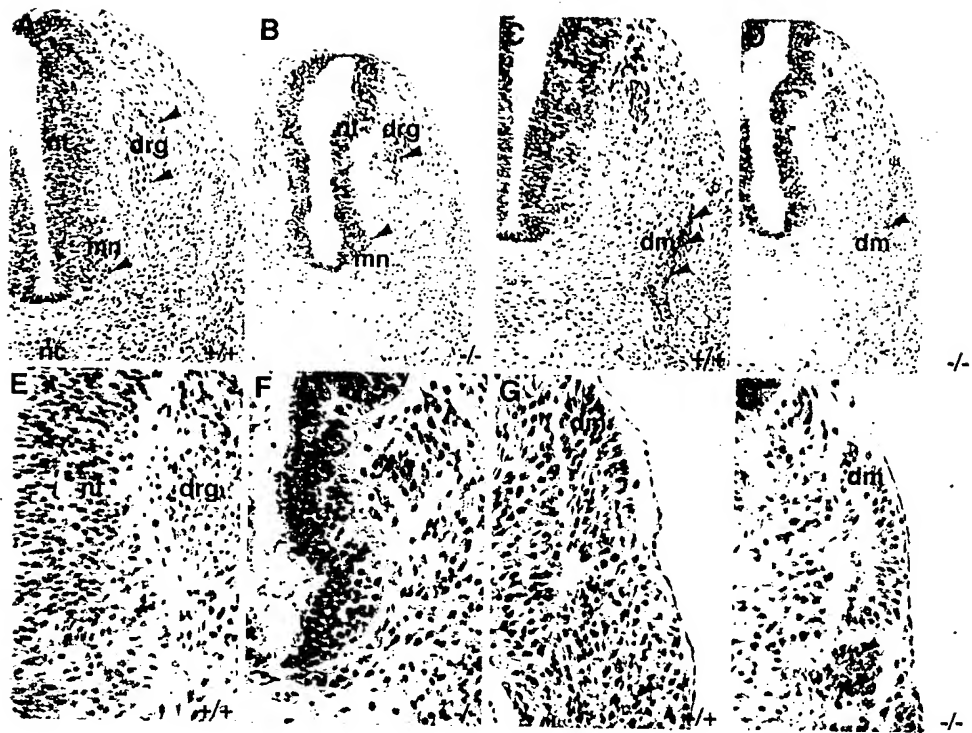


Fig. 3. Normal placental cytomorphology and absence of apoptosis of *p130*-deficient placentas. The placentas of wild-type (A) and *p130*<sup>-/-</sup> (B) embryos were identical in appearance and both contained very few apoptotic bodies. Abbreviations: gc, giant cells; la, labyrinth. Panels were photographed at a magnification of 400x.

**Fig. 4.** Deficient myogenesis and neurogenesis and associated apoptosis in E10.5 *p130*<sup>-/-</sup> embryos. Wild-type embryos (A) contained numerous motor and sensory neurons in the neural tube and dorsal root ganglia as detected with antibody reactive to Isl-1/2. Embryos lacking *p130* (B) were reduced in size, displayed a disorganized morphology and contained severely reduced numbers of Isl-1/2-expressing motor and sensory neurons. The normal myotome of wild-type embryos (C) was reduced to a small rudiment in *p130*<sup>-/-</sup> embryos (D) as revealed by staining with antibody reactive to desmin. TUNEL analysis revealed low levels of apoptosis in wild-type embryos (E,G) and markedly increased numbers of apoptotic bodies (arrowheads) in the neural tube, dorsal root ganglia and dermamyotome of *p130*<sup>-/-</sup> embryos (F,H). Note the absence of the notochord, the disorganized neural floor plate and absence of a basement membrane in the neural tubes of *p130*<sup>-/-</sup> embryos (B,F). Abbreviations: nt, neural tube; nc, notochord; mn, motor neurons; drg, dorsal root ganglia; dm, dermamyotome. Panels were photographed at magnification of 200 $\times$  (A-D), 400 $\times$  (E-H).



immunohistochemistry was performed with antibody reactive with desmin. The myocardium of *p130*<sup>-/-</sup> embryos was poorly developed with a thin wall usually only a single cell in thickness. However, the pericardium and endocardium appeared normal. Examination of serial sections revealed a failure to properly loop and form the four-chambered heart (compare Fig. 6A and B, C and D). Instead, the mutant heart somewhat resembled the two chambered E8.5 heart consisting of the bulbus cordis and the ventricular chamber (Fig. 6).

#### Increased apoptosis and cellular proliferation in *p130*<sup>-/-</sup> embryos

The observed deficiency in neurogenic and myogenic development and presence of numerous subcellular bodies suggested that many cells in *p130*<sup>-/-</sup> embryos had undergone programmed death. Therefore, to assess the levels of apoptosis in *p130*-deficient embryos, we performed TUNEL analysis on sectioned material. Wild-type embryos typically contained few apoptotic cells disseminated through the neural tube and dermamyotome (Figs 4E,G, 5A). By contrast, *p130*<sup>-/-</sup> embryos contained numerous apoptotic bodies throughout the neural tube and floor plate, and within the epithelial and delaminating portions of the dermamyotome (Figs 4F,H, 5B). In addition,

extensive apoptosis was also observed in the midgut and urogenital ridge, but not the mesonephros (Fig. 6). Moreover, little or no apoptosis was detected in the *p130*<sup>-/-</sup> lung bud,



**Fig. 5.** Loss of floor plate in E10.5 *p130*<sup>-/-</sup> embryos. TUNEL analysis revealed low levels of apoptosis in wild-type neural tube (A) and markedly increased numbers of apoptotic bodies (arrowheads) in the neural tube of *p130*<sup>-/-</sup> embryos (B). Note the almost complete absence of a floor plate in the *p130*<sup>-/-</sup> neural tube. Abbreviations: fp, floor plate; nc, notochord. Panels were photographed at magnification of 400 $\times$ .



foregut and hepatic primordia (Fig. 7). Note that the morphological development of the midgut, urogenital ridge, mesonephros, lung bud, foregut and liver primordia were at an appropriate stage for 10.5 dpc embryos but appeared abnormal due to markedly reduced cellularity in surrounding structures and poorly elaborated basement membranes. Interestingly, the myocardium of *p130*<sup>-/-</sup> embryos, like the wild-type myocardium, contained very few apoptotic nuclei (Fig. 8E,F). Taken together, these data suggest that the absence of *p130* differentially affects the differentiation or survival of myotomal and neuronal cells versus cardiac myocytes.

Examination of neural structures in the heads of *p130*<sup>-/-</sup> embryos suggested that cell survival within the developing central nervous system was severely perturbed in the absence of *p130*. TUNEL analysis of 10.5 dpc *p130*<sup>-/-</sup> embryos revealed reduced size and extensive apoptosis in the optic vesicle (Fig. 9E), optic stalk (Fig. 9G), facial acoustic neural crest complex (Fig. 9I) and otic vesicle (Fig. 9K). By contrast, wild-type embryos displayed only moderate numbers of apoptotic bodies in head neural structures (Fig. 9A,D,F,H,J). Interestingly, *Rb*-deficient embryos display elevated apoptosis and inappropriate proliferation in brain and retinal neurons

(Clarke et al., 1992; Jacks et al., 1992; Lee et al., 1992, 1994; Maandag et al., 1994). Therefore, taken together these data suggest that *Rb* and *p130* play important functions in coupling cellular differentiation to cell-cycle control, particularly in the context of neural cell development.

To investigate whether *p130*<sup>-/-</sup> embryos exhibited inappropriate proliferation, we performed immunohistochemistry with antibody PC10 reactive with proliferating cell nuclear antigen (PCNA). Replicating cells



Fig. 6. Increased apoptosis in the urogenital ridge and midgut in *p130*<sup>-/-</sup> 10.5 dpc embryos. TUNEL analysis revealed low levels of apoptosis in wild-type embryos (A,C,E) and markedly increased numbers of apoptotic bodies (arrowheads) in the urogenital ridge (B,D) and midgut (B,F) of *p130*<sup>-/-</sup> embryos. Abbreviations: a, midline dorsal aorta; dm, dermamyotome; g, midgut; m, mesonephric duct/vesicle; nt, neural tube; u, urogenital ridge. Panels were photographed at magnification of 200 $\times$  (A-D) and 400 $\times$  (C-F).

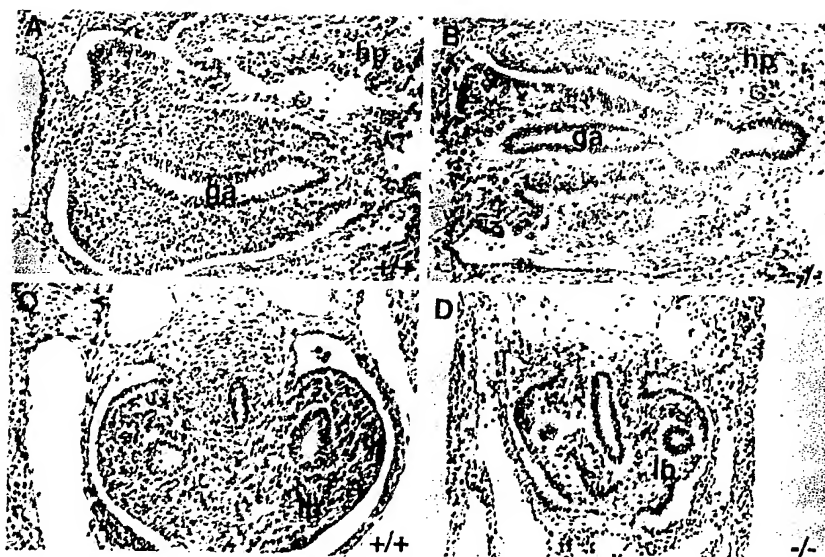
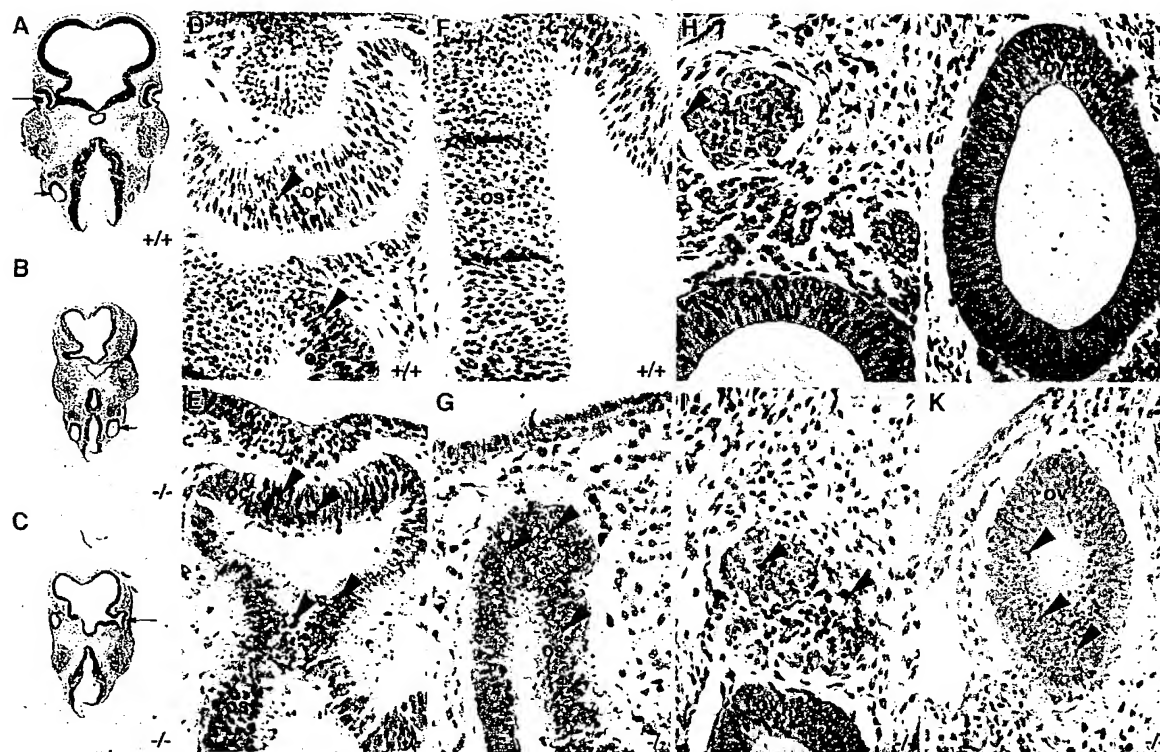


Fig. 7. Absence of apoptosis in lung bud, foregut and hepatic primordia in E10.5 *p130*<sup>-/-</sup> embryos. TUNEL analysis revealed negligible levels of apoptosis in both wild-type (A,C) and *p130*<sup>-/-</sup> (B,D) lung bud, foregut and hepatic primordia. Abbreviations: lb, lung bud; ga, gastric dilatation of foregut; hp, hepatic/biliary primordia. Panels were photographed at magnification of 400 $\times$ .

**Fig. 8.** Abnormal cardiogenesis in  $p130^{-/-}$  embryos. Immunohistochemistry with antibody reactive with desmin revealed the four-chambered myocardium of wild-type embryos (A,C). By contrast, the myocardium of  $p130^{-/-}$  embryos (B,D) was poorly developed and serial sections indicated the presence of two-chambers, the bulbus cordis and the ventricular chamber. TUNEL analysis did not reveal any significant apoptosis in wild-type (E) or mutant (F) hearts. Abbreviations: m, myocardium; pc, pericardium; ra, right atria; la, left atria; rv, right ventricle; lv, left ventricle. Panels were photographed at magnification of 100 $\times$  (A,D) and 400 $\times$  (B,C,E,F).



**Fig. 9.** Increased apoptosis and poor differentiation of head neural structures in the absence of  $p130$ . TUNEL analysis of 10.5 dpc wild-type embryos (A) revealed moderate numbers of apoptotic bodies in the optic vesicles (D), optic stalks (F), facial acoustic neural crest complexes (H) and otic vesicles (J). The head neural structures of  $p130^{-/-}$  embryos (B, C) displayed reduced size and extensive apoptosis in the optic vesicles (E), optic stalks (G), facial acoustic neural crest complexes (I) and otic vesicles (K). Note the absence of a basement membrane lining the neural structures of  $p130^{-/-}$  embryos. In A-C, long arrow denotes optic vesicle and stalk, and short arrow denotes otic vesicle. In the remainder of the panels, arrowheads indicate TUNEL-positive cells. Abbreviations: oc, optic cup; os, optic stalk; fa, facio-auditory preganglion complex; ov, otic vesicle. Panels were photographed at 400 $\times$  magnification with the exception of A-C, at 25 $\times$ .

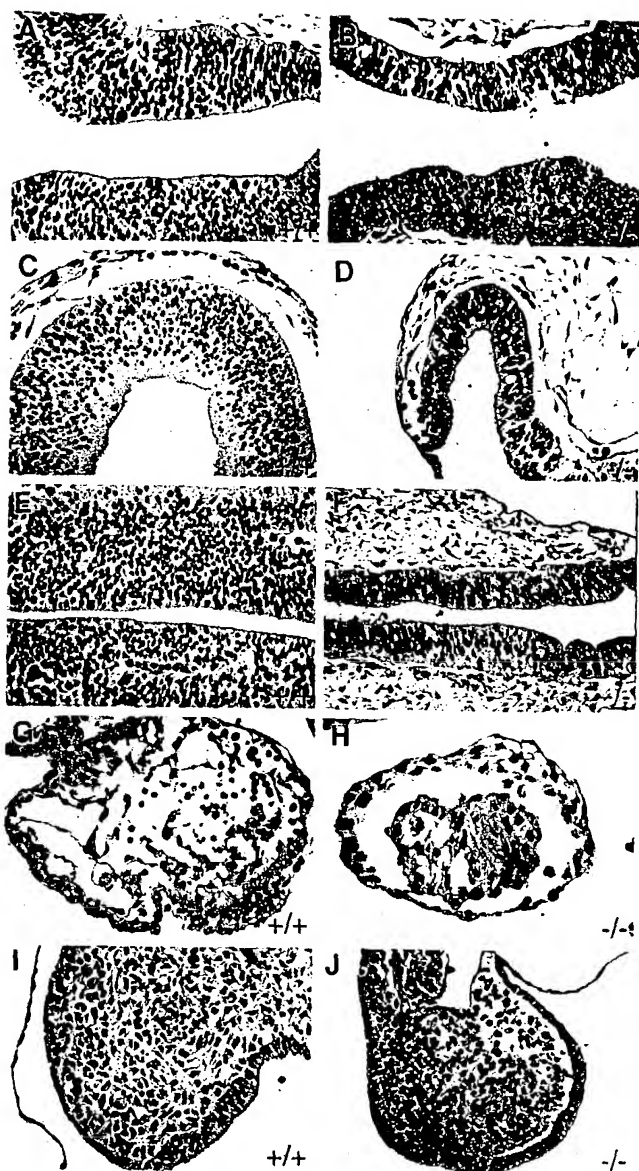


Fig. 10. Detection of increased cellular proliferation by PCNA-expression. Immunohistochemistry of sectioned E10.5  $p130^{-/-}$  embryos with antibody PC10 revealed over a 2-fold increase in numbers of PCNA-expressing cells as revealed by nuclear staining in the telencephalon (A,B), diencephalon (C,D) and the neural tube (E,F). By contrast,  $p130^{-/-}$  cardiac muscle contained 1.6-fold fewer proliferative cells (G,H) and no difference in the proportion of PCNA-expressing cells was observed between mutant and wild-type branchial arches (I,J). Panels were photographed at 400 $\times$  magnification.

express PCNA at high levels during S-phase thus immunodetection of PCNA in tissues allows a determination of relative mitotic activity (Megeney et al., 1996). In 10.5 dpc  $p130^{-/-}$  embryos, the numbers of PCNA-expressing cells were increased 2.1-fold in the telencephalon (Fig. 10A,B), 2.6-fold in the diencephalon (Fig. 10C,D) and 2.1-fold in the neural tube (Fig. 10E,F). By contrast  $p130^{-/-}$  cardiac muscle contained 1.6-fold fewer PCNA-expressing cells (Fig. 10G,H), and no difference in the proportion of PCNA-expressing cells

Table 2. Genetic background specifies the penetrance of the  $p130^{-/-}$  phenotype

Genotype	Intercross		
	Chimera $\times$ Balb/cJ $\downarrow$ $F_1^{+/-} \times F_1^{+/-}$ *	$F_1^{+/-} \times$ Balb/cJ $\downarrow$ $B_1^{+/-} \times B_1^{+/-}$ †	$F_1^{+/-} \times$ C57BL/6J $\downarrow$ $B_1^{+/-} \times B_1^{+/-}$ §
Wild type	42	12	21
$p130^{+/-}$	78	28	39
$p130^{-/-}$	0	0	24

\*The  $F_1$   $p130^{+/-}$  progeny of the founding chimeras bred with Balb/cJ mice when interbred yielded no viable  $p130^{-/-}$  pups.

†The  $B_1$   $p130^{+/-}$  mice derived from an  $F_1$   $p130^{+/-} \times$  Balb/cJ mating when interbred also failed to produce  $p130^{-/-}$  mice.

§The  $B_1$   $p130^{+/-}$  mice, derived from a  $F_1$   $p130^{+/-} \times$  C57BL/6J mating, when interbred generated litters that contained viable and fertile  $p130^{-/-}$  mice that displayed an apparently normal phenotype (see Fig. 2B).

was observed between mutant and wild-type branchial arches (Fig. 10I,J). Therefore, a tissue-specific correlation between the presence of inappropriate proliferation and increased apoptosis was evident in  $p130^{-/-}$  embryos.

#### The $p130$ mutant phenotype is strain dependent

The relatively normal phenotype of the  $p130^{-/-}$  mice previously described in a mixed 129/Sv:C57BL/6J genetic background (Cobrinik et al., 1996) and the embryonic lethal phenotype of  $p130^{-/-}$  mice in an enriched Balb/cJ background suggested that the penetrance of the  $p130^{-/-}$  phenotype was dependent on second site modifier genes. To test this hypothesis, we bred  $F_1$   $p130^{+/-}$  mice, the progeny of the founding chimeras and Balb/cJ mice, with either C57BL/6J or Balb/cJ mice. The resulting  $B_1$   $p130^{+/-}$  mice were then interbred to generate  $p130^{-/-}$  mice. The  $B_1$   $p130^{+/-}$  mice derived from the  $F_1$   $p130^{+/-} \times$  C57BL/6J cross have one set of C57BL/6J chromosomes and a second set composed of a mixture of Balb/cJ and 129/Sv chromosomes. The 129/Sv chromosomes are derived from the embryonic stem cells. The  $B_1$   $p130^{+/-}$  mice derived from the  $F_1$   $p130^{+/-} \times$  Balb/cJ cross have one set of Balb/cJ chromosomes and a second set composed of an undefined mixture of Balb/cJ and 129/Sv chromosomes. Thus, such crosses allow an assessment of the contribution of Balb/cJ and C57BL/6J genetic backgrounds to the penetrance of the phenotype. However, these experiments do not directly assess the contribution of the 129/Sv genetic background to the penetrance of the phenotype.

As described above,  $p130^{-/-}$  animals derived from an  $F_1$   $p130^{+/-} \times F_1$   $p130^{+/-}$  mating displayed 100% penetrance of the lethal phenotype (see Table 2, 1st column). In a small proportion of  $F_2$   $p130^{-/-} \times F_2$   $p130^{-/-}$  matings, we observed litters that contained a mixture of runted and normal-sized  $F_3$   $p130^{-/-}$  mice suggesting that multiple recessive second-site modifier genes were segregating in the population. Interbreeding of  $B_1$   $p130^{+/-}$  mice derived from a  $F_1$   $p130^{+/-} \times$  Balb/cJ mating gave rise to  $p130^{-/-}$  mice that also exhibited a 100% penetrance of the phenotype (Table 2, 2nd column). By contrast, interbreeding of  $B_1$   $p130^{+/-}$  mice derived from a  $F_1$   $p130^{+/-} \times$  C57BL/6J mating gave rise to  $p130^{-/-}$  mice that were viable and fertile, and displayed no detectable phenotype (Fig. 2B). Taken together, these data suggest that the C57BL/6J genetic background suppressed the  $p130^{-/-}$  embryonic lethal phenotype apparent on a Balb/cJ genetic background (Table 2,

3rd column). Therefore, we conclude that multiple second-site modifier genes exist that have an epistatic relationship with *p130*.

## DISCUSSION

We have generated a null allele of *p130* by gene targeting in mice and crossed the mutant allele into Balb/cJ and C57BL/6J strains of mice. Embryos lacking *p130* in a genetic background enriched for Balb/cJ were reduced in size and died between embryonic stages E11 and E13. Immunohistochemistry with Isl-1 antibody revealed profoundly reduced numbers of motor neurons in the spinal cord and sensory neurons in the dorsal root ganglia. In addition, immunohistochemistry with antibody reactive to desmin similarly indicated markedly reduced numbers of differentiated myocytes within the myotome. The hearts of mutant embryos displayed unusually thin walls and appeared delayed in development. TUNEL analysis indicated the presence of numerous apoptotic bodies in many tissues including the neural tube, dermamyotome and brain, but not in the heart or the histologically normal placenta. Immunohistochemistry with antibody reactive with PCNA revealed increased cellular proliferation in the neural tube and the brain, and decreased proliferation in the heart. Importantly, following a backcross to C57BL/6J mice, *p130*<sup>-/-</sup> animals were derived that were phenotypically normal. These data clearly indicate that *p130* plays an essential role in development, but in a strain-dependent manner.

Embryos deficient for *p130* contained low numbers of Isl-1, expressing neurons in the neural tube and low numbers of desmin-expressing myocytes in the dermamyotome. This deficiency was correlated with the presence of reduced notochord and floor plate structures in the trunk, together with increased levels of apoptosis. Several contributing mechanisms can be proposed to functionally explain the embryonic lethal phenotype in the absence of *p130* in a genetic background enriched for Balb/cJ. For example, patterning and morphogenesis may be perturbed following loss of key structures during development and cellular differentiation. Alternatively, cell survival may be detrimentally affected because of a unique function of *p130* in withdrawal from the cell cycle or in enforcing terminal differentiation.

Apoptotic loss of structures like the notochord during the development of *p130*<sup>-/-</sup> embryos could contribute significantly to the embryonic phenotype. For example, the determination of progenitors of motor neurons is regulated in part by signals from the notochord and floor plate of the neural tube (Yamada et al., 1991, 1993). Sonic hedgehog (Shh) is expressed in the notochord and the floor plate in the trunk where it functions to induce the progenitors of motor neurons. These progenitors, situated in the ventricular epithelium of the ventral neural tube, are induced to migrate laterally and to differentiate and settle in a single continuous primary motor column (Tanabe et al., 1995). Additionally, Shh, expressed in the floor plate and the notochord, and Wnt family members, expressed in the dorsal neural tube, have been suggested to combinatorially activate myogenesis in the somite (Munsterberg et al., 1995). Wnts positively stimulate myogenesis in the somite whereas Shh is believed to activate Noggin expression in the dorsal somite, inhibiting the repression of myogenesis by lateral-plate-

derived BMP4 (Hirsinger et al., 1997; Marcelle et al., 1997; Reshef et al., 1998). Therefore, it is interesting to speculate that loss of structures such as the floorplate in *p130*<sup>-/-</sup> embryos may contribute to the severity *p130*-mutant phenotype.

A loss-of-function mutation in *p130* may also result in cell-autonomous deficits in cellular differentiation. For example, the reduced neurogenesis and myogenesis observed in *p130*<sup>-/-</sup> embryos may reflect a global perturbation of patterning due to specific requirements for *p130* in directly negatively regulating proteins with paired-like homeodomains that play key developmental roles (Wiggan et al., 1997). Alternatively, appropriate withdrawal from the cell cycle and terminal differentiation may be detrimentally affected due to an important regulatory role played by the formation of specific E2F/*p130* complexes (Muller, 1995; Whyte, 1995). For example, myoblasts contain free E2F as well as E2F complexed with *p107* and to a lesser degree *p130*, but not *Rb*, whereas differentiated myocytes primarily contain E2F complexed with *p130*, but not *p107* or *Rb* (Corbeil et al., 1995; Shin et al., 1995). In differentiated myocytes, E2F complexes are primarily composed of E2F-4/*p130* and formation of this complex has been suggested to be a necessary event in terminal differentiation (Puri et al., 1997; Shin et al., 1995). Similarly, formation of analogous E2F/*p130* complexes has been observed during both neuronal and cardiomyocyte differentiation (Flink et al., 1998; Raschella et al., 1997). Therefore, the low numbers of cells expressing Isl-1 or desmin in *p130*<sup>-/-</sup> embryos may reflect an important and unique role for *p130* in withdrawing from the cell cycle or enforcing terminal differentiation. Clearly, the presence of markedly increased numbers of PCNA-expressing cells in tissues containing increased numbers of apoptotic cells supports this later hypothesis.

In *Rb*-deficient embryos, cells continue to replicate in regions of the central and peripheral nervous system that normally contain only postmitotic cells with many of the neurons undergoing apoptosis shortly after entering an ectopic S-phase (Lee et al., 1994). Apoptosis in the nervous system of *Rb*<sup>-/-</sup> embryos is p53-dependent and correlates with increased levels of E2F, cyclin E and p21 (Macleod et al., 1996). In muscle, lack of *Rb* similarly results in apoptotic loss of inappropriately proliferating cells that fail to undergo terminal differentiation (Wang et al., 1997; Zacksenhaus et al., 1996). Heterozygous *Rb* mice develop lens cataracts due to loss-of-homozygosity in *Rb*, in which cells are poorly differentiated, are highly proliferative and undergo very high rates of apoptosis. By contrast, heterozygous *Rb* mice bred into a p53-homozygous mutant background exhibit overt lens hyperplasias with no associated apoptosis (Morgenbesser et al., 1994). Similarly, transgenic mice expressing human papilloma virus type 16 (HPV-16) E7 in retinal cells exhibit very high rates of retinal cell apoptosis. However, expression of both E7 and E6 transgenes, or the E7 transgene in p53-mutant mice induces retinal tumors with a reduction or absence of associated apoptosis (Howes et al., 1994; Pan and Griep, 1994). HPV-16 E7-protein binds all *Rb*-family members suggesting that the failure of retinoblastomas to form in targeted *Rb*-mutant mice is a consequence of functional redundancy amongst the *Rb*-family.

Inappropriate activation of E2F in a wide variety of cell types leads to p53-enhanced apoptosis (Hiebert et al., 1995;



Phillips et al., 1997; Qin et al., 1994; Shan and Lee, 1994). Moreover, Rb and p130 appear to induce G<sub>1</sub> arrest via biochemically distinct mechanisms involving either E2F-1 or E2F-4 (Vairo et al., 1995). Therefore, generation of compound *p130<sup>-/-</sup>p53<sup>-/-</sup>* embryos in a Balb/cJ genetic background may elucidate whether the observed widespread apoptosis is p53-dependent as well as potentially allow partial rescue of the phenotype.

We have also derived a targeted null mutation in *p107* and have bred the mutant allele into either Balb/cJ or C57BL/6J genetic backgrounds. We observed that *p107<sup>-/-</sup>* embryos in an enriched Balb/cJ background are viable and fertile but exhibit diathetic myeloid metaplasia, a severe postnatal growth deficiency and an accelerated cell cycle (LeCouter et al., 1998). By contrast, *p107<sup>-/-</sup>* mice in a C57BL/6J background display no apparent phenotype (LeCouter et al., 1998; Lee et al., 1996). These data strongly support our interpretation that second-site modifier genes exist that effect the penetrance of null mutations in both *p130* and *p107*.

Mice carrying targeted null mutations (for example in *IGF-1*, *fibronectin*, *EGFR*, *CFTR*, *TGFβ1*, *TGFβ3* and *β1-adrenergic receptor*) can display highly variable penetrance of phenotype on different genetic backgrounds (Bonyadi et al., 1997; George et al., 1993; Liu et al., 1993; Proetzel et al., 1995; Rohrer et al., 1996; Rozmahel et al., 1996; Sibilia and Wagner, 1995; Threadgill et al., 1995). Clearly, these observations underscore the significance of second-site modifier genes when characterizing null mutations. The molecular basis for the penetrance of the *p130<sup>-/-</sup>* phenotype on C57BL/6J versus Balb/cJ backgrounds remains to be established. Nevertheless, the breeding data is consistent with the existence of multiple modifier alleles representing either recessive loss-of-function mutations in the C57BL/6J background, dominant gain-of-function mutations in the Balb/cJ background, or a mixture of both (Table 2). Alternatively, our data does not rule out the possibility that heterozygosity at some modifier alleles contributes to the observed phenotype. In addition, our experiments do not directly assess the role played by the ES-derived 129/Sv chromosomes segregating in the different offspring. However, genetic analysis should allow a resolution of this issue. Currently, we are performing microsatellite analysis to accurately determine the number of modifying genes and to map their approximate locations. Clearly, the molecular identification of genes epistatically interacting with p130 and p107 will further our understanding of the regulatory pathways within which Rb-family members operate.

M. A. R. is a Research Scientist of the National Cancer Institute of Canada and a member of the Canadian Genetic Disease Network of Excellence. We thank Dr John Hassell for critical reading of the manuscript and Linda May for expert technical assistance. This work was supported by a grants from the National Cancer Institute of Canada to M. A. R. and P. F. M. W.

## REFERENCES

Bonyadi, M., Rusholme, S. A., Cousins, F. M., Su, H. C., Biron, C. A., Farrell, M. and Akhurst, R. J. (1997). Mapping of a major genetic modifier of embryonic lethality in TGF beta 1 knockout mice. *Nat. Genet.* **15**, 207-11.

- Brehm, A., Miska, E. A., McCance, D. J., Reid, J. L., Bannister, A. J. and Kouzarides, T. (1998). Retinoblastoma protein recruits histone deacetylase to repress transcription. *Nature* **391**, 597-601.
- Chen, P. L., Riley, D. J., Chen-Kiang, S. and Lee, W. H. (1996). Retinoblastoma protein directly interacts with and activates the transcription factor NF-IL6. *Proc. Natl. Acad. Sci. USA* **93**, 465-9.
- Clarke, A. R., Maandag, E. R., van Roon, M., van der Lugt, N. M., van der Valk, M., Hooper, M. L., Berns, A. and te Riele, H. (1992). Requirement for a functional Rb-1 gene in murine development. *Nature* **359**, 328-30.
- Cobrinik, D., Lee, M. H., Hannon, G., Mulligan, G., Bronson, R. T., Dyson, N., Harlow, E., Beach, D., Weinberg, R. A. and Jacks, T. (1996). Shared role of the pRB-related p130 and p107 proteins in limb development. *Genes Dev.* **10**, 1633-44.
- Corbeil, H. B., Whyte, P. and Branton, P. E. (1995). Characterization of transcription factor E2F complexes during muscle and neuronal differentiation. *Oncogene* **11**, 909-20.
- Ericson, J., Thor, S., Edlund, T., Jessell, T. M. and Yamada, T. (1992). Early stages of motor neuron differentiation revealed by expression of homeobox gene *Islet-1*. *Science* **256**, 1555-60.
- Flink, I. L., Oana, S., Maitra, N., Bahl, J. J. and Morkin, E. (1998). Changes in E2F complexes containing retinoblastoma protein family members and increased cyclin-dependent kinase inhibitor activities during terminal differentiation of cardiomyocytes. *J. Mol. Cell Cardiol.* **30**, 563-78.
- Gavrieli, Y., Sherman, Y. and Ben-Sasson, S. A. (1992). Identification of programmed cell death in situ via specific labelling of nuclear DNA fragmentation. *J. Cell Biol.* **119**, 493-501.
- George, E. L., Georges-Labouesse, E. N., Patel-King, R. S., Rayburn, H. and Hynes, R. O. (1993). Defects in mesoderm, neural tube and vascular development in mouse embryos lacking fibronectin. *Development* **119**, 1079-91.
- Hauschka, S. D. (1994). The embryonic origin of muscle. In *Myology* (ed. A. G. Engel and C. Franzini-Armstrong). Vol. 1. pp. 3-73. New York: McGraw-Hill.
- Herrera, R. E., Sah, V. P., Williams, B. O., Makela, T. P., Weinberg, R. A. and Jacks, T. (1996). Altered cell cycle kinetics, gene expression, and G1 restriction point regulation in Rb-deficient fibroblasts. *Mol. Cell Biol.* **16**, 2402-7.
- Hiebert, S. W., Packham, G., Strom, D. K., Haffner, R., Oren, M., Zambetti, G. and Cleveland, J. L. (1995). E2F-1:DP-1 induces p53 and overrides survival factors to trigger apoptosis. *Mol. Cell Biol.* **15**, 6864-6874.
- Hirsinger, E., Duprez, D., Jouve, C., Malapert, P., Cooke, J. and Pourquie, O. (1997). Noggin acts downstream of Wnt and Sonic Hedgehog to antagonize avian somite patterning. *Development* **124**, 4605-4614.
- Howes, K. A., Ransom, N., Papermaster, D. S., Lasudry, J. G. H., Albert, D. M. and Windle, J. J. (1994). Apoptosis or retinoblastoma: alternative fates of photoreceptors expressing the HPV-16 E7 gene in the presence or absence of p53. *Genes Dev.* **8**, 1300-1310.
- Hurford, R. K., Jr., Cobrinik, D., Lee, M. H. and Dyson, N. (1997). pRB and p107/p130 are required for the regulated expression of different sets of E2F responsive genes. *Genes Dev.* **11**, 1447-63.
- Jacks, T., Fazeli, A., Schmitt, E. M., Bronson, R. T., Goodell, M. A. and Weinberg, R. A. (1992). Effects of an Rb mutation in the mouse. *Nature* **359**, 295-300.
- Kablar, B., Krastel, K., Ying, C., Asakura, A., Tapscott, S. J. and Rudnicki, M. A. (1997). MyoD and Myf-5 differentially regulate the development of limb versus trunk skeletal muscle. *Development* **124**, 4729-38.
- LeCouter, J. E., B., K., Hardy, W. R., Ying, C., Megeney, L. A., May, L. L. and Rudnicki, M. A. (1998). Strain-dependent myeloid metaplasia, growth deficiency, and shortened cell-cycle in mice lacking p107. *Mol. Cell Biol.* (in press).
- LeCouter, J. E., Whyte, P. F. and Rudnicki, M. A. (1996). Cloning and expression of the Rb-related mouse p130 mRNA. *Oncogene* **12**, 1433-40.
- Lee, E. Y., Chang, C. Y., Hu, N., Wang, Y. C., Lai, C. C., Herrup, K., Lee, W. H. and Bradley, A. (1992). Mice deficient for Rb are nonviable and show defects in neurogenesis and haematopoiesis. *Nature* **359**, 288-94.
- Lee, E. Y., Hu, N., Yuan, S. S., Cox, L. A., Bradley, A., Lee, W. H. and Herrup, K. (1994). Dual roles of the retinoblastoma protein in cell cycle regulation and neuron differentiation. *Genes Dev.* **8**, 2008-21.

- Lee, M. H., Williams, B. O., Mulligan, G., Mukai, S., Bronson, R. T., Dyson, N., Harlow, E. and Jacks, T. (1996). Targeted disruption of p107: functional overlap between p107 and Rb. *Genes Dev.* **10**, 1621-32.
- Liu, J. P., Baker, J., Perkins, A. S., Robertson, E. J. and Efstratiadis, A. (1993). Mice carrying null mutations of the genes encoding insulin-like growth factor I (Igf-I) and type I IGF receptor (Igf1r). *Cell* **75**, 59-72.
- Luo, R. X., Postigo, A. A. and Dean, D. C. (1998). Rb interacts with histone deacetylase to repress transcription. *Cell* **92**, 463-73.
- Maandag, E. C., van der Valk, M., Vlaar, M., Feltkamp, C., O'Brien, J., van Roon, M., van der Lugt, N., Berns, A. and te Riele, H. (1994). Developmental rescue of an embryonic-lethal mutation in the retinoblastoma gene in chimeric mice. *EMBO J.* **13**, 4260-8.
- Macleod, K. F., Hu, Y. and Jacks, T. (1996). Loss of Rb activates both p53-dependent and independent cell death pathways in the developing mouse nervous system. *EMBO J.* **15**, 6178-88.
- Magnaghi-Jaulin, L., Groisman, R., Naguibneva, I., Robin, P., Lorain, S., Le Villain, J. P., Troulen, F., Trouche, D. and Harel-Bellan, A. (1998). Retinoblastoma protein represses transcription by recruiting a histone deacetylase. *Nature* **391**, 601-5.
- Marcelle, C., Stark, M. R. and Bronner-Fraser, M. (1997). Coordinate actions of BMPs, Wnts, Shh and noggin mediate patterning of the dorsal somite. *Development* **124**, 3955-3963.
- McBurney, M. W., Sutherland, L. C., Adra, C. N., Leclair, B., Rudnicki, M. A. and Jardine, K. (1991). The mouse Pkg-1 gene promoter contains an upstream activator sequence. *Nucleic Acids Res.* **19**, 5755-61.
- Megeney, L. A., Kablar, B., Garrett, K., Anderson, J. E. and Rudnicki, M. A. (1996). MyoD is required for myogenic stem cell function in adult skeletal muscle. *Genes Dev.* **10**, 1173-83.
- Morgenbesser, S. D., Williams, B. O., Jacks, T. and DePinho, R. A. (1994). p53-dependent apoptosis produced by Rb-deficiency in the developing mouse lens. *Nature* **371**, 72-4.
- Muller, R. (1995). Transcriptional regulation during the mammalian cell cycle. *Trends Genet.* **11**, 173-8.
- Munsterberg, A. E., Kitajewski, J., Bumcrot, D. A., McMahon, A. P. and Lassar, A. B. (1995). Combinatorial signaling by Sonic hedgehog and Wnt family members induces myogenic bHLH gene expression in the somite. *Genes Dev.* **9**, 2911-22.
- Nevins, J. R., Leone, G., DeGregori, J. and Jakoi, L. (1997). Role of the Rb/E2F pathway in cell growth control. *J. Cell Physiol.* **173**, 233-6.
- Pan, H. and Griep, A. E. (1994). Altered cell cycle regulation in the lens of HPV-16 E6 or E7 transgenic mice: implications for tumor suppressor gene function in development. *Genes Dev.* **8**, 1285-1299.
- Phillips, A. C., Bates, S., Ryan, K. M., Helin, K. and Vousden, K. H. (1997). Induction of DNA synthesis and apoptosis are separable functions of E2F-1. *Genes Dev.* **11**, 1853-1863.
- Proetzel, G., Pawlowski, S. A., Wiles, M. V., Yin, M., Boivin, G. P., Howles, P. N., Ding, J., Ferguson, M. W. and Doetschman, T. (1995). Transforming growth factor-beta 3 is required for secondary palate fusion. *Nat. Genet.* **11**, 409-14.
- Puri, P. L., Balsano, C., Burgio, V. L., Chirillo, P., Natoli, G., Ricci, L., Mattei, E., Graessmann, A. and Levrero, M. (1997). MyoD prevents cyclinA/cdk2 containing E2F complexes formation in terminally differentiated myocytes. *Oncogene* **14**, 1171-84.
- Qin, X. Q., Livingston, D. M., Kaelin, W. G., Jr. and Adams, P. D. (1994). Deregulated transcription factor E2F-1 expression leads to S-phase entry and p53-mediated apoptosis. *Proc. Natl. Acad. Sci. USA* **91**, 10918-10922.
- Raschella, G., Tanno, B., Bonetto, F., Amendola, R., Battista, T., De Luca, A., Giordano, A. and Paggi, M. G. (1997). Retinoblastoma-related protein pRb2/p130 and its binding to the B-myb promoter increase during human neuroblastoma differentiation. *J. Cell Biochem.* **67**, 297-303.
- Reshef, R., Maroto, M. and Lassar, A. B. (1998). Regulation of dorsal somitic cell fates: BMPs and Noggin control the timing and pattern of myogenic factor expression. *Genes Dev.* **12**, 290-303.
- Rohrer, D. K., Desai, K. H., Jasper, J. R., Stevens, M. E., Regula, D. P., Jr., Barsh, G. S., Bernstein, D. and Kobilka, B. K. (1996). Targeted disruption of the mouse beta1-adrenergic receptor gene: developmental and cardiovascular effects. *Proc. Natl. Acad. Sci. USA* **93**, 7375-80.
- Rozmahel, R., Wilschanski, M., Matin, A., Plyte, S., Oliver, M., Auerbach, W., Moore, A., Forstner, J., Durie, P., Nadeau, J., et al. (1996). Modulation of disease severity in cystic fibrosis transmembrane conductance regulator deficient mice by a secondary genetic factor. *Nat. Genet.* **12**, 280-7.
- Rudnicki, M. A., Braun, T., Hinuma, S. and Jaenisch, R. (1992). Inactivation of MyoD in mice leads to up-regulation of the myogenic HLH gene Myf-5 and results in apparently normal muscle development. *Cell* **71**, 383-90.
- Shan, B. and Lee, W. H. (1994). Deregulated expression of E2F-1 induces S-phase entry and leads to apoptosis. *Mol. Cell Biol.* **14**, 8166-73.
- Shin, E. K., Shin, A., Paulding, C., Schaffhausen, B. and Yee, A. S. (1995). Multiple change in E2F function and regulation occur upon muscle differentiation. *Mol. Cell Biol.* **15**, 2252-62.
- Sibilia, M. and Wagner, E. F. (1995). Strain-dependent epithelial defects in mice lacking the EGF receptor. *Science* **269**, 234-8.
- Slack, J. M. W. (1992). Models for man: the mouse and the chick. In *From Egg to Embryo*, pp. 171-277. Cambridge: Cambridge University Press.
- Tanabe, Y., Roelink, H. and Jessell, T. M. (1995). Induction of motor neurons by Sonic hedgehog is independent of floor plate differentiation. *Current Biol.* **5**, 651-8.
- Threadgill, D. W., Dlugosz, A. A., Hansen, L. A., Tennenbaum, T., Lichti, U., Yee, D., LaMantia, C., Mourtou, T., Herrup, K., Harris, R. C., et al. (1995). Targeted disruption of mouse EGF receptor: effect of genetic background on mutant phenotype. *Science* **269**, 230-4.
- Tsuchida, T., Ensini, M., Morton, S. B., Baldassare, M., Edlund, T., Jessell, T. M. and Pfaff, S. L. (1994). Topographic organization of embryonic motor neurons defined by expression of LIM homeobox genes. *Cell* **79**, 957-970.
- Vairo, G., Livingston, D. M. and Ginsberg, D. (1995). Functional interaction between E2F-4 and p130: evidence for distinct mechanisms underlying growth suppression by different retinoblastoma protein family members. *Genes Dev.* **9**, 869-81.
- Wang, J., Guo, K., Wills, K. N. and Walsh, K. (1997). Rb functions to inhibit apoptosis during myocyte differentiation. *Cancer Res.* **57**, 351-4.
- Weinberg, R. A. (1995). The retinoblastoma protein and cell cycle control. *Cell* **81**, 323-30.
- Whyte, P. (1995). The retinoblastoma protein and its relatives. *Semin. Cancer Biol.* **6**, 83-90.
- Wiggan, O., Taniguchi-Sidle, A. and Hamel, P. A. (1997). Interaction of the pRb-family proteins with factors containing paired-like homeodomains. *Oncogene* **16**, 227-236.
- Williams, B. O., Schmitt, E. M., Remington, L., Bronson, R. T., Albert, D. M., Weinberg, R. A. and Jacks, T. (1994). Extensive contribution of Rb-deficient cells to adult chimeric mice with limited histopathological consequences. *EMBO J.* **13**, 4251-9.
- Yamada, T., Pfaff, S. L., Edlund, T. and Jessell, T. M. (1993). Control of cell pattern in the neural tube: motor neuron induction by diffusible factors from notochord and floor plate. *Cell* **73**, 673-86.
- Yamada, T., Placzek, M., Tanaka, H., Dodd, J. and Jessell, T. M. (1991). Control of cell pattern in the developing nervous system: polarizing activity of the floor plate and notochord. *Cell* **64**, 635-47.
- Zacksenhaus, E., Jiang, Z., Chung, D., Marth, J. D., Phillips, R. A. and Gallie, B. L. (1996). pRb controls proliferation, differentiation, and death of skeletal muscle cells and other lineages during embryogenesis. *Genes Dev.* **10**, 3051-3064.

# Role of the Common Cytokine Receptor $\gamma$ Chain in Cytokine Signaling and Lymphoid Development

WARREN J. LEONARD<sup>1</sup>, ELIZABETH W. SHORES<sup>2</sup> & PAUL E. LOVE

## INTRODUCTION

X-linked severe combined immunodeficiency (XSCID) is an inherited disease in which patients exhibit profoundly diminished cell-mediated and humoral immunity. This disease results from mutations in the common cytokine receptor  $\gamma$  chain,  $\gamma_c$ . In order to understand more about the role of  $\gamma_c$  in lymphoid development, we have analyzed mice in which the  $\gamma_c$  gene was specifically inactivated by homologous recombination. These mice exhibit a wide range of interesting immunological abnormalities, some shared by humans with XSCID and some that are different. The differences are indicative of variations in lymphoid development between humans and mice, and potentially will allow new insights into the roles of  $\gamma_c$ -dependent cytokines in both species. Moreover, the mutant ( $\gamma_c^{-/-}$ ) mice provide a valuable animal model of  $\gamma_c$  deficiency and therefore represent potential targets for reconstitution by gene therapeutic approaches.

## X-LINKED SEVERE COMBINED IMMUNODEFICIENCY: IDENTIFICATION OF THE MOLECULAR DEFECT

Severe combined immunodeficiency diseases represent a spectrum of disorders (reviewed in Leonard et al. 1994, Leonard, in press), with XSCID accounting for ap-

<sup>1</sup>Laboratory of Molecular Immunology, National Heart, Lung, and Blood Institute, NIH, Bethesda, MD 20892, U.S.A.; <sup>2</sup>Division of Hematologic Products, Center for Biologics Evaluation and Research, FDA, Bethesda, MD 20892, U.S.A.; <sup>3</sup>Laboratory of Mammalian Genes and Development, National Institute of Child Health and Human Development, NIH, Bethesda, MD 20892, U.S.A.

Correspondence to: Dr. Warren J. Leonard, Bldg. 10, Rm. 7N244, NHLBI, Bethesda, MD 20892-1674

proximately half of all cases of SCID (Conley 1992). Affected males exhibit profoundly diminished numbers of T cells, explaining the lack of cell-mediated immunity. B-cell numbers are normal or even increased, but are nonfunctional. The lack of B-cell function has been assumed to result in part from a lack of T-cell help since the addition of normal T cells *in vitro* can promote at least some B-cell responses (Conley 1992). However, an intrinsic B-cell defect is also indicated by the non-random X-inactivation patterns observed in the mature B cells of XSCID carrier females (Conley 1992). XSCID patients also lack natural killer (NK) cells. In contrast to these lymphoid abnormalities, other blood cells are represented in normal numbers and exhibit normal function.

The discovery of the molecular defect in XSCID came not from studies targeted to that end, but rather from basic studies on the IL-2 receptor. This receptor is known to contain at least three subunits, the  $\alpha$  (Leonard et al. 1982, Leonard et al. 1984, Nikaido et al. 1984, Cosman et al. 1984),  $\beta$  (Sharon et al. 1986, Tsudo et al. 1986, Teshigawara et al. 1987, Hatakeyama et al. 1989) and  $\gamma$  (Takeshita et al. 1992) chains. These three chains together are responsible for forming three classes of IL-2 receptors. Whereas intermediate affinity receptors ( $\beta + \gamma$  chains) are expressed on resting lymphocytes, high affinity ( $\alpha + \beta + \gamma$  chains) and low affinity ( $\alpha$  chains without  $\beta$  or  $\gamma$ ) receptors are found on activated T cells (Leonard et al. 1994, Taniguchi 1995, Leonard, in press). The high and intermediate affinity receptors are capable of transducing IL-2 signals, whereas low affinity receptors cannot. Corresponding to this observation, it is interesting that both  $\beta$  and  $\gamma$  chains (the shared components of high and intermediate affinity receptors) are members of the cytokine receptor superfamily (Bazan 1990), whereas  $\alpha$  is not. Experiments using chimeric receptor constructs indicate that heterodimerization of the cytoplasmic domains of  $\beta$  and  $\gamma$  is necessary and sufficient for signaling (Nakamura et al. 1994, Nelson et al. 1994).

Analysis of the  $\gamma$  chain gene revealed that it was located on the X chromosome at position Xq13 (Noguchi et al. 1993c) previously established to be the locus of XSCID (the SCIDX1 locus) (de Saint Basile et al. 1987). Sequencing of DNA prepared from EBV infected cell lines from XSCID patients subsequently established that the  $\gamma$  chain gene was defective in XSCID (Noguchi et al. 1993c). A large number of patients with XSCID have now been studied (reviewed in Leonard, in press). The range of identified mutations include a number of premature stop codons, insertions, deletions and splice junction defects of such a nature that even if the  $\gamma$  chain mRNA and protein product were stably produced, functional alterations would be expected in the protein. In addition, a number of point mutations have been found that result in single amino acid changes (Puck et al. 1993, DiSanto et al. 1994a, 1994b, Ishii et al. 1994, Russell et al. 1994, Clark et al. 1995). In some cases, amino acid alterations in the extracellular domain have been demonstrated to inhibit IL-2 binding, whereas mutations in the cytoplasmic domain interfere with signal transduction. Thus, a number of naturally occurring mutations have helped to clarify the functional domains of the  $\gamma$  chain protein.



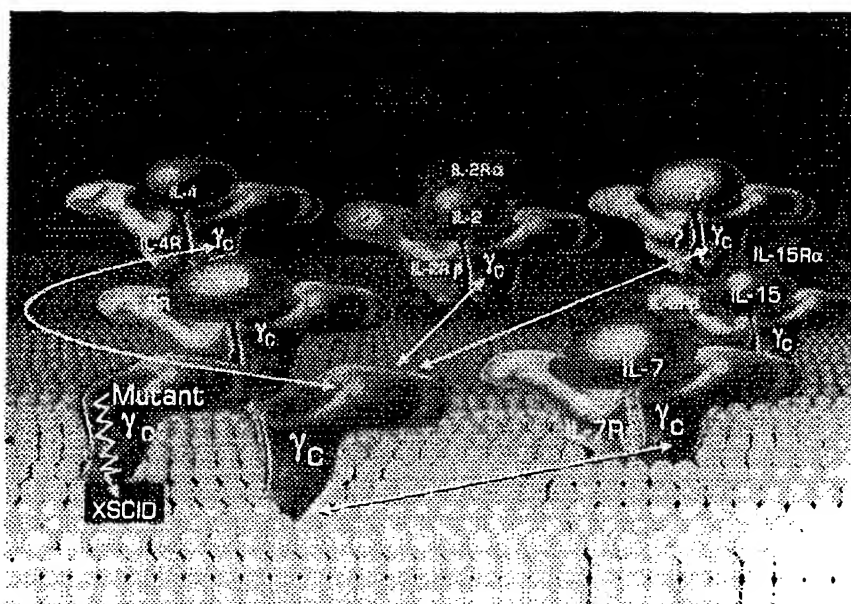


Figure 1. Schematic of the common cytokine receptor  $\gamma$  chain ( $\gamma_c$ ) as a component of the IL-2, IL-4, IL-7, IL-9 and IL-15 receptors. In males, XSCID results from mutations in  $\gamma_c$ .

#### A COMMON CYTOKINE RECEPTOR SUBUNIT

One of the puzzling features of the discovery that defects in  $\gamma$  chain caused XSCID in humans was that, in contrast to the profound block in T-cell development observed in XSCID patients, mice (Schorle et al. 1991) and humans (Pahwa et al. 1989, Weinberg & Parkman 1990) lacking IL-2 expression exhibit normal T-cell development. In other words, mutations in a component of the IL-2 receptor yielded defects more severe than those found associated with IL-2 deficiency. This observation led to the hypothesis that the  $\gamma$  chain was a component of other cytokine receptors as well (Noguchi et al. 1993), consistent with the precedents that the hematopoietic cytokines IL-3, IL-5 and GM-CSF all share a common  $\beta$  chain,  $\beta_c$  (Miyajima et al. 1992), and that another set of cytokines all share the IL-6 receptor signal transducer gp130 (Taga & Kishimoto 1995). Although the  $\gamma$  chain was initially hypothesized (see Leonard et al. 1994 for the rationale underlying this hypothesis) and confirmed (Kondo et al. 1993, Russell et al. 1993, Noguchi et al. 1993b, Kondo et al. 1994) to be a component of the IL-4 and IL-7 receptors, it is now also known to be a component of the IL-9 (Russell et al. 1994, Kimura et al. 1995) and IL-15 (Giri et al. 1994) receptors as well. Since the  $\gamma$  chain is shared by multiple cytokine receptors (Figure 1), it is now denoted as the common cytokine receptor  $\gamma$  chain,  $\gamma_c$ , in keeping with the nomenclature adopted for the hematopoi-

etic cytokines (Miyajima et al. 1992). The overall clinical features of XSCID can ostensibly be accounted for by the simultaneous inactivation of five cytokine systems in patients with this disease. In all likelihood, inactivation of IL-7 signaling is primarily responsible for the lack of T-cell development in this disease (Leonard 1994, Leonard, in press), particularly in view of the phenotype of IL-7 deficient mice (von Freeden-Jeffry et al. 1995).

#### JANUS FAMILY TYROSINE KINASES JAK1 AND JAK3

As noted above, heterodimerization of IL-2R $\beta$  and  $\gamma_c$  is sufficient to trigger cell proliferation. To understand this phenomenon, it was necessary to identify the essential signaling molecule(s) that associate with each chain. It was striking that stimulation of activated T cells or NK cells by IL-2 rapidly induced the tyrosine phosphorylation of Jak1 and Jak3, two different Janus family tyrosine kinases (Johnston et al. 1994, Witthuhn et al. 1994). An analysis of protein-protein interactions revealed that Jak1 associates with IL2R $\beta$  and Jak3 associates with  $\gamma_c$  (Boussiotis et al. 1994, Russell et al. 1994, Miyazaki et al. 1994). Moreover, Jak3 can also interact with IL-2R $\beta$  following IL-2 stimulation (Russell et al. 1994). The importance of the  $\gamma_c$ -Jak3 interaction was established by the identification of a family pedigree with an X-linked immunodeficiency in which there was a single amino acid change in  $\gamma_c$  (Leu 271 mutated to Gln) (Schmalstieg et al. 1995, Russell et al. 1994). This mutation was shown to greatly diminish the ability of  $\gamma_c$  to interact with Jak3 (Russell et al. 1994). A particularly exciting aspect of this finding was that affected individuals in this family have a moderate rather than severe form of immunodeficiency; therefore, the partial loss of Jak3 association corresponded to the partial loss of immune function. These data suggest that XSCID may result from mutations of  $\gamma_c$  that directly or indirectly prevent the activation of Jak3 (i.e. either by inhibiting cytokine binding or by preventing  $\gamma_c$ -Jak3 association). Moreover, some autosomal recessive cases of SCID that are clinically and immunologically indistinguishable from XSCID have been found to result from mutations in Jak3 (Macchi et al. 1995, Russell et al. 1995).

#### DEVELOPMENT OF A MURINE MODEL OF $\gamma_c$ -DEFICIENCY

Given the profound abnormalities in humans with XSCID, we wished to develop a murine model of  $\gamma_c$  deficiency on the assumption that such animals would (1) allow more detailed analysis of the role of  $\gamma_c$  in lymphoid development, (2) clarify the similarities and differences in  $\gamma_c$  function in humans and mice, (3) serve as a murine model for potential reconstitution of  $\gamma_c$  in distinct lineages, (4) allow structure-function relationships for  $\gamma_c$ , and (5) serve as an animal model of XSCID, thereby facilitating the evaluation of gene therapeutic approaches. Successful gene therapy of mice using already established  $\gamma_c$ -expressing viruses (Qazilbash et al. 1995) could increase the rationale for progressing to gene therapy in humans. A

naturally occurring form of XSCID in dogs (Henthorn et al. 1994, Somberg et al. 1994) may also be valuable in this regard.

#### CHARACTERIZATION OF THE MURINE $\gamma_c$ GENE, PREPARATION OF A TARGETING VECTOR, AND GENERATION OF $\gamma_c$ -DEFICIENT MICE

The murine  $\gamma_c$  gene, like the human gene, is located on the X chromosome; in mice,  $\gamma_c$  maps between *Zfx* and *Plp* (Cao et al. 1993). The murine cDNA has 80% amino acid identity to human  $\gamma_c$  (Cao et al. 1993). The entire gene was cloned and sequenced (Cao et al. 1995). As expected, like the human  $\gamma_c$  gene (Noguchi et al. 1993a), the murine gene is divided into eight exons. A sequence-replacement targeting vector was prepared by standard methodology (Tybulewicz et al. 1991), the vector was transfected into embryonic stem (ES) cells, and homologous recombination achieved (Cao et al. 1995). Because  $\gamma_c$  is located on the X chromosome and the ES cells are of male lineage, a single recombination event was sufficient to create a  $\gamma_c$ -null cell line. The ES cells were injected into C57BL/6 blastocysts, chimeric mice were generated, and germline transmission was achieved. Mating of heterozygous ( $\gamma_c^{+/-}$ ) females with wild-type males or of heterozygous females with  $\gamma_c^{-/Y}$  males yielded progeny with the expected ratios based on Mendelian genetics (Cao et al. 1995). In an independent study,  $\gamma_c^{-/Y}$  mice were also generated by DiSanto et al. (1995) using a cre-loxP recombination approach.

#### GROSS AND MICROSCOPIC ANALYSIS OF $\gamma_c^{-/Y}$ MICE

$\gamma_c^{-/-}$  females,  $\gamma_c^{+/-}$  females, and  $\gamma_c^{-/Y}$  males were indistinguishable in gross appearance from wild-type littermates. Housed under SPF conditions,  $\gamma_c$ -deficient mice that have been followed for up to 7 months appear healthy (our unpublished observations). However, three mice have developed a wasting syndrome characterized by runted appearance, matted hair, and failure to thrive (see below).

At necropsy, heterozygous females were indistinguishable from wild-type males and females, consistent with the normal phenotype of human XSCID carrier females. In XSCID carrier females, strictly nonrandom X-inactivation patterns are observed in T cells, NK cells, and mature B cells (reviewed in Conley 1992, Puck 1993, Leonard et al. 1994); indicating that only those cells in which the mutant X was inactivated could mature and terminally differentiate. Thus, the levels of  $\gamma_c$  in cells of carrier females are normal, equivalent to individuals who have wild-type  $\gamma_c$  at both alleles. Presumably, the same conditions operate in  $\gamma_c^{+/-}$  female mice.

The  $\gamma_c^{-/Y}$  males examined were all abnormal, but the phenotype differed to some extent, depending on the age of the mice. These data are largely from Cao et al. (1995) and are summarized in Table I. The youngest mice analyzed (3-week-old mice) had small thymuses and small spleens, but otherwise had grossly

TABLE I  
*Properties of  $\gamma_c$  knockout mice*

1. Small hypoplastic thymuses with increased CD4:CD8 ratio.
2. Small hypoplastic spleens at 3 weeks of age but then increasing in cellularity and size. Increased CD4:CD8 ratio.
3. Greatly diminished conventional B cells in bone marrow and spleen but detectable peritoneal B-1 cells.
4. Absent peripheral lymph nodes. Inactive follicles in mesenteric nodes.
5. No gut-associated lymphoid tissue.
6. No  $\gamma\delta$  cells in skin, gut, or thymus.
7. No NK cells.
8. Striking  $\gamma_c$ -independent proliferation in thymus.
9. Readily detectable IgM levels; other Ig levels severely diminished.

normal chest and abdominal cavity organs. The slightly older animals that have been examined, ranging in age from 4 to 9 weeks of age, also had small thymuses, but surprisingly, the spleens in these animals were increased in size. Microscopic examination of  $\gamma_c^{-/-}$  thymuses revealed marked lymphoid hypoplasia with an indistinct corticomedullary junction (Cao et al. 1995). Hassall's corpuscles and a cortical rim of lymphocytes could be identified and basic thymic architecture was retained, in contrast to what is seen in SCID/NCR mice. At 3 weeks of age, the spleens were remarkable for their diminished white pulp and lymphocyte hypoplasia. In contrast, the red pulp was indistinguishable from that of normal littermates. However, with increasing age, the spleens increased in size and cellularity.

Although lymph nodes were not grossly observed in  $\gamma_c^{-/-}$  mice, at necropsy, a mesenteric node was identified in a  $\gamma_c^{-/-}$  mouse (Cao et al. 1995). The node was much smaller than mesenteric nodes in normal sibling mice; moreover, the single lymphoid follicle identified lacked a germinal center.

Remarkably, no gut-associated lymphoid tissue could be identified in either the small or large intestine of  $\gamma_c^{-/-}$  mice. Significantly, all of the  $\gamma_c^{-/-}$  and  $\gamma_c^{-/-}$  mice necropsied to date (n=13) exhibited enlarged spleens and thickening of the large bowel. Histological examination of the bowel revealed proliferative typhlitis (inflammation of the cecum) and colitis, with an increase in crypt depth. Intestinal intraepithelial lymphocytes (IELs) were notably absent, but abundant mononuclear infiltrates were observed in the lamina propria. Inflammatory bowel disease (IBD) has also been reported in several other immunodeficient lines of mice generated by gene targeting, including mice lacking IL-2 (Sadlack et al. 1993), IL-10 (Kuhn et al. 1993), MHC class II, or the T cell receptor  $\alpha$  or  $\beta$  chains (Mombaerts et al. 1993). Although none of these mice exhibit disease identical to human IBD (ulcerative colitis or Crohn's disease), many characteristic features are present including crypt abscesses, mucosal ulcerations and granulomas. Absence

of these features in  $\gamma_c$ -deficient mice could reflect a different etiology of IBD; however, further analysis is required, particularly with older mice. Interestingly, large numbers of *Helicobacter hepaticus* were observed in the crypts and lumens of the cecum and colon of  $\gamma_c^{-/-}$  males (Cao et al. 1995). While these findings are consistent with speculation that an immune response to gut bacterial flora (either antigen specific or mitogen driven) may contribute to the development of IBD in gene-targeted (Strober & Ehrhardt 1993, MacDonald 1994) and SCID (Russell et al. 1995) mice, a causal relationship between *H. hepaticus* and the inflammatory changes in the  $\gamma_c^{-/-}$  mice has not been established.

#### PHENOTYPIC ANALYSIS OF T AND B CELLS IN $\gamma_c^{-/-}$ MICE

Although thymocytes were greatly diminished in total numbers, flow cytometric analysis of thymocytes revealed that CD4<sup>-</sup>CD8<sup>-</sup> double negative (DN), CD4<sup>+</sup>CD8<sup>-</sup> and CD4<sup>-</sup>CD8<sup>+</sup> single positive (SP), and CD4<sup>+</sup>CD8<sup>+</sup> double positive (DP) cells were all represented (Cao et al. 1995). The  $\gamma_c^{-/-}$  thymocytes appeared to include a relatively high proportion of mature cells, with a relative increase in the number of cells bright for TCR $\beta$ , CD3 $\epsilon$ , and CD5, and a corresponding decrease in the number of cells expressing high levels of HSA. Interestingly, there was a significant increase in the CD4<sup>+</sup>CD8<sup>-</sup>:CD4<sup>-</sup>CD8<sup>+</sup> ratio in the thymus. Although a role for specific cytokines and their receptors has not been established in positive selection, the increased percentage of CD4<sup>+</sup> thymocytes suggests this possibility. Splenocytes also exhibited an increase in the CD4<sup>+</sup>CD8<sup>-</sup>:CD4<sup>-</sup>CD8<sup>+</sup> ratio (Cao et al. 1995), consistent with the skewing observed in the thymus. These appeared to be conventional CD4<sup>+</sup> T cells and not the population of class I MHC educated CD4<sup>+</sup> T cells (Bendelac et al. 1994, Coles & Raulet 1994, Lantz & Bendelac 1994) since few cells were TCR V $\beta$ 8 positive and they did not stain with antibody to NK1.1 (Cao et al. 1995). In fact, no NK1.1<sup>+</sup> cells were identified, consistent with the lack of natural killer cytolytic activity in  $\gamma_c^{-/-}$  mice (Cao et al. 1995). In contrast, granulocytes (Gr1<sup>+</sup> cells) and monocytes/macrophages (Mac1<sup>+</sup> cells) were increased.

Analysis of B cells in both spleen and bone marrow by staining for B220 and  $\mu$  revealed a significant decrease in the number of conventional B cells. There was also a decrease in the number of B220<sup>+</sup> CD43<sup>-</sup> cells in the bone marrow of  $\gamma_c$ -deficient mice (unpublished data; DiSanto et al. 1995), consistent with a requirement for IL-7R in B cell development (Peschon et al. 1994). In contrast, "self replenishing" peritoneal B-1 cells (Kantor & Herzenberg 1993) were less affected. Both CD5<sup>+</sup> and CD5<sup>-</sup> B-1 cells were identified in  $\gamma_c$ -deficient mice. The presence of these cells may explain the detectable levels of serum IgM expressed in the  $\gamma_c^{-/-}$  mice; the other classes of immunoglobulin were greatly diminished (Cao et al. 1995). This finding was expected for IgG1 and IgE, given that in the absence of  $\gamma_c$ , IL-4 signaling should be defective, and is also consistent with the phenotype of IL-4<sup>-/-</sup> mice (Kuhn et al. 1991).

As mentioned above, humans with XSCID generally lack T cells, so it was surprising that significant numbers of T cells were found in  $\gamma_c^{-/Y}$  mice (Cao et al. 1995). The T cells appeared to be strictly  $\alpha\beta$  TCR<sup>+</sup> as  $\gamma\delta$  T cells were not identified in the thymus or spleen. Moreover, examination of the skin revealed that although Langerhans cells were normal in number and distribution,  $\gamma\delta$  TCR<sup>+</sup> dendritic epidermal T cells were absent. iIELs were also absent, and specific staining for  $\gamma\delta$  TCR<sup>+</sup> cells in the intestine was negative. Thus, it appears that  $\gamma_c^{-/Y}$  mice exhibit a total absence of all populations of  $\gamma\delta$  T cells, whereas at least a subset of  $\alpha\beta$  T cells are able to mature and populate the peripheral lymphoid tissue (Cao et al. 1995). The lack of  $\gamma\delta$  T cells could be responsible in part for the relative paucity of  $\alpha\beta$  TCR<sup>+</sup> thymocytes and T cells in  $\gamma_c^{-/Y}$  mice as previous studies have suggested that  $\gamma\delta$  TCR<sup>+</sup> thymocytes can contribute to the development of  $\alpha\beta$  T cells (Shores et al. 1990, Ferrick et al. 1990, Iwashima et al. 1991).

The presence of T cells in the spleen but almost complete absence of lymph nodes in  $\gamma_c^{-/Y}$  mice was unexpected. One possible explanation for these findings is that  $\gamma_c$ -dependent cytokine signals might participate in T cell homing to lymph nodes. Alternatively, in the absence of appropriately activated lymphocytes (and the factors they secrete), endothelial cells may not be induced to a state capable of supporting lymphocyte homing. While these remain intriguing possibilities, additional studies are required to clarify the basis for the decreased lymph node mass.

One of the most interesting findings in  $\gamma_c^{-/Y}$  mice was the increase in numbers of CD4<sup>+</sup> T cells, particularly with advancing age. This is unlikely to be a result of expansion as peripheral T cells from these mice failed to proliferate in culture (Cao et al. 1995). The marked accumulation of T cells in  $\gamma_c^{-/Y}$  mice with advancing age is also consistent with the proposed role of  $\gamma_c$ -mediated signals in peripheral negative selection. Whereas T cells stimulated through the TCR in the absence of co-stimulation usually enter a state of anergy, it has been shown that induction of anergy could be prevented if concomitant signals were delivered through  $\gamma_c$  (Boussiotis et al. 1994). Results from another study suggest that IL-2 is important for the induction of cell death. High doses of antigen in combination with IL-2 have been shown to induce cell death both in antigen-specific cell lines and in a transgenic model of EAE (Critchfield et al. 1994). Hence, it is possible that the T cells that accumulate in  $\gamma_c^{-/Y}$  mice represent "anergized" T cells with potentially autoreactive TCR specificities.

#### COMPARISON OF T- AND B-CELL ABNORMALITIES IN HUMANS WITH XSCID AND $\gamma_c^{-/Y}$ MICE

As noted above, in human XSCID, T cells are absent or profoundly diminished in numbers. In contrast, in  $\gamma_c^{-/Y}$  mice, though diminished, T cells are present and with

time can increase to essentially normal numbers in the spleen (Cao et al. 1995). Although peripheral T cells from  $\gamma_c^{-/-}$  mice did not respond to stimulation with either concanavalin A or to PMA + IL-4, stimuli strictly dependent on  $\gamma_c$ , there was modest proliferation to anti-CD3 + anti-CD28 and to PMA + ionomycin (Cao et al. 1995). Splenocyte proliferation was approximately 10 to 20% of wild-type control levels with PMA + ionomycin and approximately 5% of control levels with anti-CD3 + anti-CD28 (Cao et al. 1995). However, quite unexpectedly, thymocytes from  $\gamma_c$ -deficient mice proliferated as well as control thymocytes in response to stimulation with anti-CD3 + anti-CD28 (Figure 2; Cao et al. 1995).

These findings were surprising for at least two reasons. First, they indicated that T-cell development could proceed in the absence of  $\gamma_c$  in mice. Second, they revealed that T cells, but more strikingly thymocytes, can be stimulated to proliferate independently of  $\gamma_c$ -mediated signals. Both of these findings could be explained by the actions of cytokine(s) whose receptors do not contain  $\gamma_c$ . Although it is unclear which cytokine(s) might be responsible, it may be relevant that IL-7R $^{-/-}$  mice exhibit a more severe phenotype (Peschon et al. 1994) than do  $\gamma_c^{-/-}$  mice (Cao et al. 1995). This finding initially seems remarkable given that the absence of  $\gamma_c$  should inactivate IL-2, IL-4, IL-7, IL-9, and IL-15 signaling. Thus, one might assume that IL-7R $^{-/-}$  mice would respond to all cytokines except IL-7. However, this may not in fact be the case. Loss of IL-7R would also inactivate signaling in response to another cytokine, thymic stromal derived lymphopoietin (TSLP) (Peschon et al. 1994). The TSLP receptor contains IL-7R but it has not been determined whether it contains  $\gamma_c$ . Thus, we speculate that TSLP action contributes to T-cell development in the  $\gamma_c^{-/-}$  mice (Cao et al. 1995). Since no human homologue of TSLP has been identified, it is conceivable that humans with XSCID lack this cytokine to compensate for the loss of IL-7 action and therefore exhibit more severe defects than do  $\gamma_c^{-/-}$  mice.

Regarding B-cell development, it is notable that IL-7R $^{-/-}$  mice, IL-7R $^{-/-}$  mice and mice treated with anti-IL-7 antibodies both exhibit a block in B-cell development (von Freeden-Jeffry et al. 1995, Peschon et al. 1994, Grabstein et al. 1993). Thus, in  $\gamma_c^{-/-}$  mice, it seems likely that the block in development of conventional B cells (Cao et al. 1995) results from inactivation of IL-7 signaling, consistent with the action of IL-7 as a pre-B-cell growth factor. These findings also support the contention that B-1 peritoneal B cells, whose development is less affected in  $\gamma_c^{-/-}$  mice, are derived from a separate lineage from conventional B cells (Kantor & Herzenberg 1993). It is striking that in human XSCID, B cells are normal or even increased in number, albeit nonfunctional. This observation suggests either that IL-7 is a major pre-B cell growth factor in mice, but not in humans, or that alternative  $\gamma_c$ -independent pathway(s) exist to support B-cell development in humans. Although this hypothesis is attractive, it should be emphasized that other explanations could exist to explain the observed differences between XSCID patients and  $\gamma_c^{-/-}$  mice. For example, the degree to which maternal factors (eg., cytokines) influence fetal development may not be identical in both species.

# THYMOCYTES FROM $\gamma_c$ -KNOCKOUT MICE RESPOND TO $\gamma_c$ -INDEPENDENT BUT NOT $\gamma_c$ -DEPENDENT STIMULI

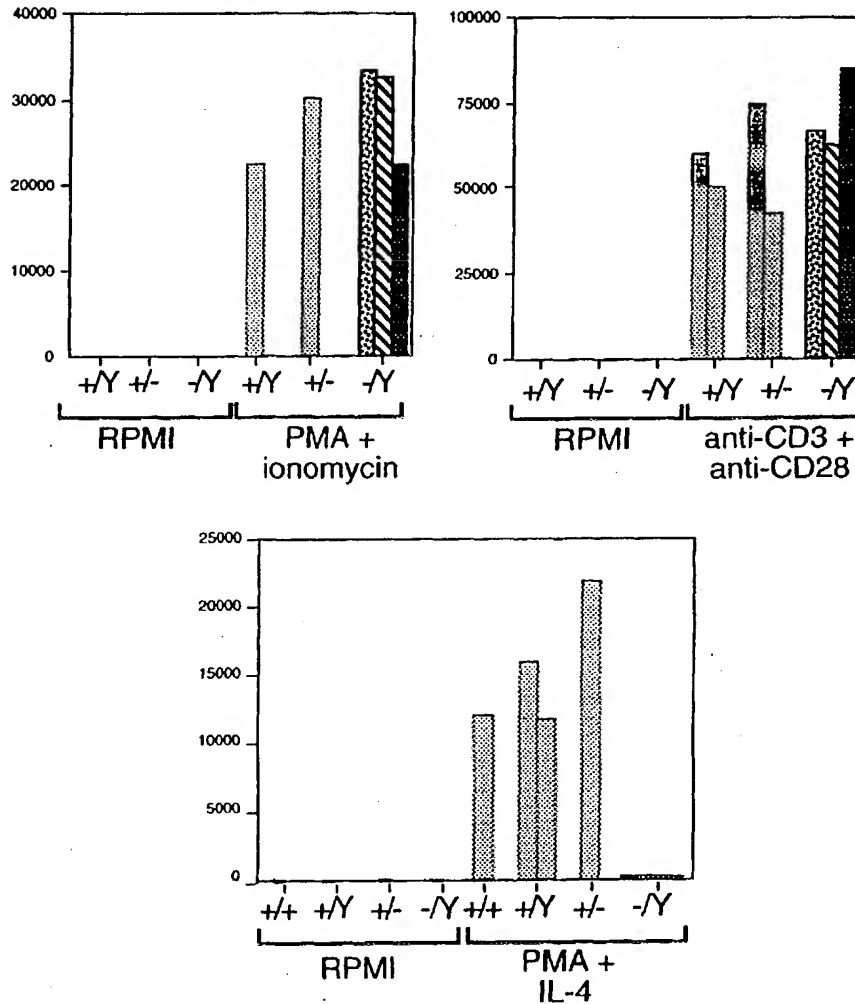


Figure 2. Thymocytes from  $\gamma_c^{-/-}$  mice respond to PMA + ionomycin and to anti-CD3 + anti-CD28 ( $\gamma_c$ -independent stimuli), but not to PMA + IL-4 (a  $\gamma_c$ -dependent stimulus).



# COMPARISON OF IMMUNOLOGICAL DEFECTS ASSOCIATED WITH MUTATION OF THE GENES ENCODING IL-2, IL-2R $\alpha$ , IL-2R $\beta$ , AND $\gamma_c$

The first component of the IL-2/IL-2 receptor system to be analyzed in a murine system was IL-2 (Schorle et al. 1991). These mice develop normally during the first 3–4 weeks of life and exhibit normal thymocyte and peripheral T-cell subset composition. Some mice subsequently develop splenomegaly, lymphadenopathy, and severe anemia and die between 4 and 9 weeks of age (Sadlack et al. 1993). Of those that survive, 100% develop a form of IBD that resembles ulcerative colitis in humans (Sadlack et al. 1993). This syndrome is characterized by chronic diarrhea, intestinal bleeding, and rectal prolapse, as well as by the microscopic detection of crypt abscesses and mucosal ulcerations. Interestingly, the IL-2<sup>-/-</sup> mice not only exhibit splenomegaly and lymphadenopathy, but have a high number of activated T and B cells in the colonic mucosa and drastically elevated IgG1 and autoantibody production.

Mice lacking IL-2R $\beta$  expression would be expected to manifest a simultaneous loss of IL-2 and IL-15 signaling. The IL-15 receptor is analogous to the IL-2 receptor in that they both share IL-2R $\beta$  and  $\gamma_c$  (Grabstein et al. 1994, Bamford et al. 1994, Giri et al. 1994). They differ only in the expression of different  $\alpha$  chains, each of which has a relatively short cytoplasmic domain. So far, it appears that IL-2 and IL-15 induce identical signals when cells can respond to both cytokines (Grabstein et al. 1994, Bamford et al. 1994, Giri et al. 1994, Lin et al. 1995). Thus, if IL-2R $\beta$  were restricted solely to IL-2 and IL-15 signaling, the phenotype might be expected to be quite similar to that found in IL-2 deficient mice. In IL-2R $\beta$ <sup>-/-</sup> mice, thymic development was normal between 1 and 3 weeks of age, suggesting that IL-2R $\beta$  is not required for T-cell development in the thymus (Suzuki et al. 1995). Interestingly, however, by 6 weeks of age, absolute numbers of thymocytes were only approximately 15% of normal levels. Since there was an increase in single positive and decrease in double positive thymocytes, this could potentially reflect general stress-induced changes. By 3 weeks of age, homozygous mice exhibited splenomegaly and lymphadenopathy, with large lymphoblastoid T cells, albeit in a normal CD4<sup>+</sup>CD8<sup>-</sup> to CD4<sup>+</sup>CD8<sup>+</sup> ratio. The activated CD4 cells collectively synthesized both T<sub>H</sub>1 ( $\gamma$ -interferon) and T<sub>H</sub>2 (IL-4) cytokines and stimulated synthesis of high levels of serum immunoglobulin by B cells, including autoantibodies. These included anti-erythrocyte antibodies that likely mediate the autoimmune hemolytic anemia found in IL-2R $\beta$ <sup>-/-</sup> mice. Although the T cells were activated, there was no response to specific antigen nor to polyclonal activators. B- to T-cell ratios in lymph nodes were normal at three weeks of age, but by 8 weeks of age, B cells had essentially disappeared; this could be prevented by blocking the increase in CD4<sup>+</sup> T cells by treatment with anti-CD4 antibodies. Thus, in the absence of IL-2R $\beta$ , there is a disruption of normal lymphoid homeostasis.

Mice lacking IL-2R $\alpha$  expression initially have normal development of T and B

cells, but as adults, they exhibit marked lymphoid expansion with polyclonal T- and B-cell activation (Willerford et al. 1995). With time, autoimmune disorders, including inflammatory bowel disease and hemolytic anemia develop. Mice lacking IL-2R $\alpha$  expression are most similar to the IL-2 knockout mice, but nevertheless some differences exist (Willerford et al. 1995). Among the possible explanations for the differences would be the known ability of IL-2 to trigger certain responses via intermediate affinity IL-2 receptors (Siegel et al. 1987), which contain IL-2R $\beta$  and  $\gamma_c$ , but not IL-2R $\alpha$ .

In the IL-2, IL-2R $\alpha$ , IL-2R $\beta$ , and  $\gamma_c$  knockout mice, it is interesting that there is a transition point at approximately 3 weeks of age. In  $\gamma_c$  knockout mice, this represents the point at which the spleen enlarges and CD4<sup>+</sup> T-cell expansion occurs, whereas for the IL-2R $\beta$  deficient mice, this represents the point at which thymic involution occurs, and for the IL-2 knockout mice, it is at approximately 4 weeks of life that splenomegaly, lymphadenopathy, and severe anemia develop.

The fact that the phenotypes of IL-2<sup>-/-</sup>, IL-2R $\alpha$ <sup>-/-</sup>, IL-2R $\beta$ <sup>-/-</sup>, and  $\gamma_c$ <sup>-/-</sup> mice are all different emphasizes the complexity of cytokine-cytokine receptor systems. The principles of "cytokine pleiotropy" and "cytokine redundancy" have been reviewed in detail (Paul 1989, Leonard 1994). In addition, however, one also needs to consider the principles of "cytokine receptor subunit pleiotropy", and "cytokine receptor subunit redundancy". Cytokine pleiotropy refers to multiple actions by a single cytokine, often on multiple cell types, whereas cytokine redundancy refers to the settings where several cytokines exert overlapping actions, making it difficult to know *a priori* how severe the loss of any single cytokine will be. In effect, if a biological "function" is important, it may be subserved by more than one cytokine. Cytokine receptor pleiotropy refers to the rather well established principle that individual receptor components may act in multiple different cytokine systems. Although this has been discussed above for  $\beta_c$ ,  $\gamma_c$ , and gp130, there are an ever increasing number of receptor molecules that have been recognized to be shared by multiple cytokines (see Table II). Finally, there is the interesting phenomenon of cytokine receptor redundancy, a principle perhaps best illustrated in the murine IL-3 system, wherein IL-3 signaling requires a functional IL-3R $\alpha$  and either the common  $\beta$  chain ( $\beta_c$ ) or an IL-3 receptor specific  $\beta$  chain that shares 91% amino acid identity to  $\beta_c$  (Miyajima et al 1992). IL-3R $\beta$  cannot work with IL-5 or GM-CSF and does not exist in humans. For the mouse, however, IL-3R $\beta$  can fully replace  $\beta_c$  in mediating IL-3 action. A more confusing example appears to exist for IL-4. In this setting, it is clear that IL-4R is required for IL-4 actions, but depending on the cell type, either  $\gamma_c$  or an alternate additional chain (operationally denoted  $\gamma^1$  and hypothesized to potentially be the IL-13R [Lin et al. 1995]) can transduce IL-4 signals. It appears that T-cell responses to IL-4 are strictly dependent on  $\gamma_c$ , whereas IL-4 responses on certain other cells can be mediated in the absence of  $\gamma_c$  and presumably require the alternate chain. It is also possible that the specific signals induced by IL-4 may depend in part on the type of receptor expressed on a given cell. If so, then

TABLE II

*Cytokine receptor pleiotropy: involvement of receptor subunits as components of multiple cytokine receptors*

Shared Chain	Cytokines whose receptors contain the shared chain
$\gamma_c$	IL-2, IL-4, IL-7, IL-9, IL-15
gp130	IL-6, leukemia inhibitory factor (LIF), oncostatin M (OSM), ciliary neurotrophic factor (CNTF), IL-11, cardiotrophin-1
$\beta_c$	IL-3, IL-5, and GM-CSF
LIF receptor	LIF, OSM, and CNTF
IL-2R $\beta$	IL-2, IL-15
IL-4R	IL-4, IL-13
IL-7R	IL-7, TSLP

in this instance the principle of cytokine receptor subunit redundancy would not truly establish a redundant situation but rather would explain the basis for pleiotropic actions by IL-4. In any case, the complicated network of cytokines and cytokine receptor chains makes it difficult to predict with certainty the outcome of inactivation of any individual cytokine or receptor chain. In fact, the creation of mice defective in individual chains has allowed a greater understanding of the roles that various proteins may play.

#### SUMMARY

To examine the role of  $\gamma_c$  in lymphoid development, we have analyzed mice in which the  $\gamma_c$  gene was specifically inactivated by homologous recombination. These mice also serve as an animal model of human X-linked severe combined immunodeficiency (XSCID). Interestingly,  $\gamma_c$  knockout mice exhibited a somewhat different phenotype than humans with XSCID. Absolute T-cell numbers are greatly diminished in young  $\gamma_c^{-/-}$  mice, but accumulate with age.  $\gamma\delta$  T cells and NK cells are absent in  $\gamma_c^{-/-}$  mice and conventional B cells are greatly diminished, yet substantial numbers of peritoneal B-1 cells are present. Since humans with XSCID have essentially no mature T cells, it is especially striking that T cells are readily apparent in  $\gamma_c^{-/-}$  mice. This observation indicates that in these mice, the  $\gamma_c$ -dependent block in T cell development is less severe than it is in humans. It is possible but unproven that thymic stromal derived lymphopoietin, TSLP, contributes to thymocyte development in these mice. Since B-cell numbers are normal in humans with XSCID, it is also striking that  $\gamma_c^{-/-}$  mice paradoxically exhibit greatly diminished numbers of B cells. This likely indicates that IL-7 signaling plays a critical role in pre-B cell maturation in mice but is less important in humans. Thus, the abnormalities observed in  $\gamma_c^{-/-}$  mice have provided clues to assist in dissecting the

role of cytokines and their receptors in lymphoid development and have also identified interesting differences in the regulation of this process in mice and humans.

#### ACKNOWLEDGMENTS

We thank Dr. Sarah M. Russell, NHLBI for preparing Figure 2.

#### REFERENCES

- Bamford, T. N., Grant, A. J., Burton, J. D., Peters, C., Kurys, G., Goldman, C. K., Brennan, J., Roessler, E. & Waldmann, T. A. (1994) The interleukin (IL)-2 receptor beta chain is shared by IL-2 and a cytokine, provisionally designated IL-T, that stimulates T cell proliferation and the induction of lymphokine activated killer cells. *Proc. Natl. Acad. Sci. USA* **91**, 4940.
- Bazan, J. F. (1990) Structural design and molecular evolution of a cytokine receptor superfamily. *Proc. Natl. Acad. Sci. USA* **87**, 6934.
- Bendelac, A., Kileen, N., Littman, D. R. & Schwartz, R. H. (1994) A subset of CD4<sup>+</sup> thymocytes selected by MHC class I molecules. *Science* **263**, 1774.
- Boussiotis, V. A., Barber, D. L., Nakarai, T., Freeman, G. J., Gribben, J. G., Bernstein, G. M., d'Andrea, A. D., Ritz, J. & Nadler, L. M. (1994) Prevention of T cell anergy by signaling through the  $\gamma_c$  chain of the IL-2 receptor. *Science* **266**, 1039.
- Cao, X., Kozak, C. A., Liu, Y.-J., Noguchi, M., O'Connell, E. & Leonard, W. J. (1993) Characterization of cDNAs encoding the murine interleukin 2 receptor (IL-2R)  $\gamma$  chain: chromosomal mapping and tissue specificity of IL-2R  $\gamma$  chain expression. *Proc. Natl. Acad. Sci. USA* **90**, 8464.
- Cao, X., Shores, E. W., Hu-Li, J., Anver, M. R., Kelsall, B. L., Russell, S. M., Drago, J., Noguchi, M., Grinberg, A., Bloom, E. T., Paul, W. E., Katz, S. I., Love, P. E., & Leonard, W. J. (1995). Defective lymphoid development in mice lacking expression of the common cytokine receptor  $\gamma$  chain. *Immunity* **2**, 223.
- Clark, P. A., Lester, T., de Alwis, M., Jones, A. & Kinnon, C. (1995). Unambiguous assignment of carrier status for females in X-linked severe combined immunodeficiency families based on direct mutational analysis. In *Progress in Immune Deficiency V* (Edited by I. Caragol, T. Espanol, G. Fontan & N. Matamoros. Springer-Verlag, Barcelona), p. 139.
- Coles, M. C. & Raulet, D. R. (1994) Class I dependence of the development of CD4<sup>+</sup>CD8<sup>+</sup> NK1.1<sup>+</sup> thymocytes. *J. Exp. Med.* **180**, 395.
- Conley, M. E. (1992) Molecular approaches to analysis of X-linked immunodeficiencies. *Annu. Rev. Immunol.* **10**, 215.
- Cosman, D., Ceretti, D. P., Larsen, A., Park, L., March, C., Dower, S., Gillis, S. & Urdal, D. (1984) Cloning, sequence and expression of human interleukin 2 receptor. *Nature* **321**, 768.
- Critchfield, J. M., Racke, M. K., Zuniga-Pflucker, J. C., Cannella, B., Raine, C. S., Goverman, J. & Lenardo, M. J. (1994) T cell deletion in high antigen dose therapy of autoimmune encephalomyelitis. *Science* **263**, 1139.
- de Saint Basile, G. D., Arveiler, B., Oberle, I., Malcolm, S., Levinsky, R. J., Lau, Y. L., Hofker, M., Debre, M., Fischer, A., Griscelli, C. & Mandel, J. L. (1987) Close linkage of the locus for X chromosome-linked severe combined immunodeficiency to polymorphic DNA markers in Xq11-Xq13. *Proc. Natl. Acad. Sci. USA* **84**, 7576.
- DiSanto, J. P., Dautry-Varsat, A., Certain, S., Fischer, A. & de Saint Basile, G. (1994a) Inter-

- leukin-2 receptor  $\gamma$  chain mutations in X-linked severe combined immunodeficiency disease result in the loss of high-affinity IL-2 receptor binding. *Eur. J. Immunol.* **24**, 475.
- DiSanto, J. P., Rieux-Laucat, F., Dautry-Varsat, A., Fischer, A. & de Saint Basile, G. (1994b) Defective human interleukin 2 receptor  $\gamma$  chain in an atypical X chromosome-linked severe combined immunodeficiency with peripheral T cells. *Proc. Natl. Acad. Sci. USA* **91**, 9466.
- DiSanto, J. P., Muller, W., Guy-Grand, D., Fischer, A. & Rajewsky, K. (1995) Lymphoid development in mice with a targeted deletion of the interleukin 2 receptor gamma chain. *Proc. Natl. Acad. Sci. USA* **92**, 377.
- Ferrick, D. A., Chan, A., Rabemtulla, A., Widacki, S., Xia, M., Broughton, H., Gajewski, D. A., Ballhausen, W., Allison, J. P., Bluestone, J. A., Burke, K., Van Ewijk, W., & Mak, T. (1990). Expression of a T cell receptor  $\gamma$  chain (V $\gamma$ 1.1J $\gamma$ 4C $\gamma$ 4) transgene in mice influences T cell receptor ontogeny and thymic architecture during development. *J. Immunol.* **145**, 200.
- Giri, J. G., Ahdieh, M., Eisenman, J., Shanebeck, K., Grabstein, K., Kumaki, S., Namen, A., Park, L. S., Cosman, D. & Anderson, D. (1994) Utilization of the  $\beta$  and  $\gamma$  chains of the IL-2 receptor by the novel cytokine IL-15. *EMBO J.* **13**, 2822.
- Grabstein, K. H., Waldschmidt, T. G., Finkelman, F. D., Hess, B. W., Alpert, A. R., Boyani, N. E., Namen, A. E. & Morrissey, P. (1993) Inhibition of murine B and T cell lymphopoiesis *in vivo* by anti-IL-7 monoclonal antibody. *J. Exp. Med.* **17**, 257.
- Grabstein, K. H., Eisenman, J., Shanebeck, K., Rauch, C., Srinivasan, S., Fung, V., Beers, C., Richardson, J., Schoeber, M. A., Ahdieh, M., Johnson, L., Alderson, M. R., Watson, J. D., Anderson, D. M. & Giri, J. G. (1994). Cloning of a T cell growth factor that interacts with the  $\beta$  chain of the interleukin-2 receptor. *Science* **264**, 965.
- Hatakeyama, M., Tsudo, M., Minamoto, S., Kono, T., Doi, T., Miyata, T., Miyasaka, M. & Taniguchi, T. (1989) Interleukin-2 receptor  $\beta$  chain gene; generation of three receptor forms by cloned human  $\alpha$  and  $\beta$  cDNAs. *Science* **244**, 551.
- Henthorn, P. S., Somberg, R. L., Fimiana, V. M., Puck, J. M., Patterson, D. F. & Felsburg, P. J. (1994) IL-2R $\gamma$  gene microdeletion demonstrates that canine X-linked severe combined immunodeficiency is a homologue of the human disease. *Genomics* **23**, 69.
- Ishii, N., Asao, H., Kimura, Y., Takeshita, T., Nakamura, M., Tsuchiya, S., Konno, T., Maeda, M., Uchiyama, T. & Sugamura, K. (1994) Impairment of ligand binding and growth signaling of mutant IL-2 receptor  $\gamma$ -chains in patients with X-linked severe combined immunodeficiency. *J. Immunol.* **153**, 1310.
- Iwashima, M., Davis, M. M., & Chen, Y. -H. (1991). A  $\gamma\delta$  T cell receptor heterodimer induces the expression of CD4 and CD8 in thymocytes. *J. Exp. Med.* **174**, 293.
- Johnston, J. A., Kuwamura, M., Kirken, R. A., Chen, Y. Q., Blake, T. B., Shibuya, K., Ortaldo, J. R., McVicar, D. W. & O'Shea, J. J. (1994) Phosphorylation and activation of the Jak-3 Janus kinase in response to interleukin-2. *Nature* **370**, 151.
- Kantor, A. B. & Herzenberg, L. A. (1993) Origin of murine B cell lineages. *Annu. Rev. Immunol.* **11**, 501.
- Kimura, Y., Takeshita, T., Kondo, M., Ishii, N., Nakamura, M., van Snick, J. & Sugamura, K. (1995). Sharing of the IL-2 receptor  $\gamma$  chain with the functional IL-9 receptor complex. *Internat. Immunol.* **7**, 115.
- Kondo, M., Takeshita, T., Ishii, N., Nakamura, M., Watanabe, S., Arai, K. & Sugamura, K. (1993) Sharing of the interleukin-2 (IL-2) receptor  $\gamma$  chain between receptors for IL-2 and IL-4. *Science* **26**, 1874.
- Kondo, M., Takeshita, T., Higuchi, M., Nakamura, M., Sudo, T., Nishikawa, S. & Sugamura, K. (1994) Functional participation of the IL-2 receptor  $\gamma$  chain in IL-7 receptor complexes. *Science* **263**, 1453.

- Kuhn, R., Rajewsky, K. & Muller, W. (1991) Generation and analysis of interleukin-4 deficient mice. *Science* **254**, 707.
- Kuhn, R., Lohler, J., Rennick, D., Rajewsky, K. & Muller, W. (1993) Interleukin-10-deficient mice develop chronic enterocolitis. *Cell* **75**, 263.
- Lantz, O. & Bendelac, A. (1994) An invariant T cell receptor  $\alpha$  chain is used by a unique subset of major histocompatibility complex Class I-specific CD4<sup>+</sup> and CD4<sup>-</sup>CD8<sup>-</sup> T cells in mice and humans. *J. Exp. Med.* **180**, 1097.
- Leonard, W. J., Depper, J. M., Uchiyama, T., Smith, K. A., Waldmann, T. A. & Greene, W. C. (1982) A monoclonal antibody that appears to recognize the receptor for human T-cell growth factor; partial characterization of the receptor. *Nature* **300**, 267.
- Leonard, W. J., Depper, J. M., Crabtree, G. R., Rudikoff, S., Pumphrey, J., Robb, R. J., Kronke, M., Svetlik, P. B., Pfeffer, N. J., Waldmann, T. A. & Greene, W. C. (1984) Molecular cloning and expression of cDNAs for the human interleukin-2 receptor. *Nature* **311**, 626.
- Leonard, W. J. (1994) The defective gene in X-linked severe combined immunodeficiency encodes a shared interleukin receptor subunit: implications for cytokine pleiotropy and redundancy. *Curr. Opin. Immunol.* **6**, 631.
- Leonard, W. J., Noguchi, M., Russell, S. M. & McBride, O. W. (1994) The molecular basis of X-linked severe combined immunodeficiency: the role of the interleukin-2 receptor  $\gamma$  chain as a common  $\gamma$  chain,  $\gamma_c$ . *Immunol. Rev.* **138**, 61.
- Leonard, W. J. (1996) The molecular basis of X-linked combined immunodeficiency: defective cytokine receptor signaling. *Annu. Rev. Med.* **47**, 229.
- Lin J. -X., Migone T. -S., Tsang M., Friedmann, M., Weatherbee, J. A., Zhou, L., Yamauchi, A., Bloom, E. T., Mietz, J., John, S. & Leonard, W. J. (1995) The role of shared receptor motifs and common Stat proteins in the generation of cytokine pleiotropy and redundancy by IL-2, IL-4, IL-7, IL-13, and IL-15. *Immunity* **2**, 331.
- Macchi, P., Villa, A., Giliani, S., Sacco, M. G., Frattini, A., Porta, F., Ugazio, A. G., Johnston, J. A., Candotti, F., O'Shea, J. J., Vezzoni, P. & Notarangelo, L. D. (1995) Mutations of Jak-3 gene in patients with autosomal severe combined immune deficiency (SCID). *Nature* **377**, 65.
- MacDonald, T. T. (1994) Inflammatory bowel disease in knockout mice. *Current Biol.* **4**, 261.
- Miyajima, A., Kitamura, T., Harada, N. et al. (1992) Cytokine receptors and signal transduction. *Annu. Rev. Immunol.* **10**, 295.
- Miyazaki, T., Kawahara, A., Fujii, H., Nakagawa, Y., Minami, Y., Liu, Z. -J., Oishi, I., Silvennoinen, O., Witthuhn, B. A., Ihle, J. N. & Taniguchi, T. (1994) Functional activation of Jak1 and Jak3 by selective association with IL-2 receptor subunits. *Science* **266**, 1045.
- Mombaerts, P., Mizaguchi, F., Grusby, M. J., Glimcher, L. H., Bhan, A. K., Tonegawa, S. (1993) Spontaneous development of inflammatory bowel disease in T cell receptor mutant mice. *Cell* **75**, 275.
- Nakamura, Y., Russell, S. M., Mess, S. A., Friedmann, M., Erdos, M., Francois, C., Jacques, Y., Adelstein, S. & Leonard, W. J. (1994) Heterodimerization of the IL-2 receptor  $\beta$  and  $\gamma$ -chain cytoplasmic domains is required for signalling. *Nature* **369**, 330.
- Nelson, B. H., Lord, J. D. & Greenberg, P. D. (1994) Cytoplasmic domains of the interleukin-2 receptor  $\beta$  and  $\gamma$  chains mediate the signal for T-cell proliferation. *Nature* **369**, 333.
- Nikaido, T., Shimizu, A., Ishida, N., Sabe, H., Teshigawara, K., Maeda, M., Uchiyama, T., Yodoi, J. & Honjo, T. (1984) Molecular cloning of cDNA encoding human interleukin-2 receptor. *Nature* **311**, 631.
- Noguchi, M., Adelstein, S., Cao, X. & Leonard, W. J. (1993a) Characterization of the human interleukin-2 receptor  $\gamma$  gene. *J. Biol. Chem.* **268**, 13601.

- Noguchi, M., Nakamura, Y., Russell, S. M., Ziegler, S. F., Tsang, M., Cao, X. & Leonard, W. J. (1993b) Interleukin-2 receptor  $\gamma$  chain: a functional component of the interleukin-7 receptor. *Science* **262**, 1877.
- Noguchi, M., Yi, H., Rosenblatt, H. M., Filipovich, A. H., Adelstein, S., Modi, W. S., McBride, O. W. & Leonard, W. J. (1993c) Interleukin-2 receptor  $\gamma$  chain mutation results in X-linked severe combined immunodeficiency in humans. *Cell* **73**, 147.
- Pahwa, R., Chatila, T., Pahwa, S., Paradise, C., Day, N. K., Geha, R., Schwartz, S. A., Slade, H., Oyaizu, N. & Good, R. A. (1989) Recombinant interleukin 2 therapy in severe combined immunodeficiency disease. *Proc. Natl. Acad. Sci. USA* **86**, 5069.
- Paul, W. E. (1989) Pleiotropy and redundancy: T cell-derived lymphokines in the immune response. *Cell* **57**, 521.
- Peschon, J. J., Morrissey, P. J., Grabstein, K. H., Ramsdell, F. J., Maraskovsky, E., Gliniak, B. C., Park, L. S., Ziegler, S. F., Williams, D. E., Ware, C. B., Meyer, J. D. & Davison, B. L. (1994) Early lymphocyte expansion is severely impaired in interleukin-7 receptor-deficient mice. *J. Exp. Med.* **180**, 1955.
- Puck, J. M. (1993) X-linked immunodeficiencies. *Adv. Human Genetics* **21**, 104.
- Puck, J. M., Deschenes, S. M., Porter, J. C., Dutra, A. S., Brown, C. J., Willard, H. F. & Henthorn, P. S. (1993) The interleukin-2 receptor  $\gamma$  chain maps to Xq13.1 and is mutated in X-linked severe combined immunodeficiency, SCIDX1. *Hum. Molec. Genet.* **2**, 1099.
- Qazilbash, M. H., Walsh, C. E., Russell, S. M., Noguchi, M., Mann, M. M., Leonard, W. J. & Liu, J. M. (1995) Retroviral vector for gene therapy of X-linked severe combined immunodeficiency syndrome. *J. Hematotherapy* **4**, 91.
- Russell, R. J., Haines, D. C., Anver, M. R., Battles, J. K., Gorelick, P. L., Blumenauer, L. L., Gonda, M. A. & Ward, J. M. (1995) Use of antibiotics to prevent hepatitis and typhlitis in male SCID mice spontaneously infected with *Helicobacter hepaticus*. *Lab. Ani. Sci.*, in press.
- Russell, S. M., Keegan, A. D., Harada, N., Nakamura, Y., Noguchi, M., Leland, P., Friedmann, M. C., Miyajima, A., Puri, R. K., Paul, W. E. & Leonard, W. J. (1993) Interleukin-2 receptor  $\gamma$  chain: a functional component of the interleukin-4 receptor. *Science* **262**, 1880.
- Russell, S. M., Johnston, J. A., Noguchi, M., Kawamura, M., Bacon, C. M., Friedmann, M., Berg, M., McVicar, D. W., Withuhn, B. A., Silvennoinen, O., Goldman, A. S., Schmalstieg, F. C., Ihle, J. N., O'Shea, J. J. & Leonard, W. J. (1994) Interaction of IL-2R $\beta$  and  $\gamma_c$  chains with Jak1 and Jak3: Implications for XSCID and XCID. *Science* **266**, 1042.
- Russell, S. M., Tayebi, N., Nakajima, H., Riedy, M. C., Roberts, J. L., Aman, M. J., Migone, T.-S., Noguchi, M., Market, M. L., Buckley, R. H., O'Shea, J. J. & Leonard, W. J. (1995) Mutation of Jak3 in a patient with SCID: essential role of Jak3 in lymphoid development. *Science* **270**, 797.
- Sadlack, B., Merz, H., Schorle, H., Schimpl, A., Feller, A. C. & Horak, I. (1993) Ulcerative colitis-like disease in mice with a disrupted interleukin-2 gene. *Cell* **75**, 253.
- Schmalstieg, F. C., Leonard, W. J., Noguchi, M., Berg, M., Rudloff, H. E., Denney, R. M., Dave, S. K., Brooks, E. G. & Goldman, A. S. (1995) Missense mutation in exon 7 of the common  $\gamma$  chain gene causes a moderate form of X-linked combined immunodeficiency. *J. Clin. Invest.* **95**, 1169.
- Schorle, H., Holtzschke, T., Hunig, T., Schimpl, A. & Horak, I. (1991) Development and function of T cells in mice rendered interleukin-2 deficient by gene targeting. *Nature* **352**, 621.
- Sharon, M., Klausner, R. D., Cullen, B. R., Chizzonite, R. & Leonard, W. J. (1986) Novel interleukin-2 receptor subunit detected by cross-linking under high affinity conditions. *Science* **234**, 859.

- Shores, E. W., Sharrow, S. O., Uppenkamp, I. & Singer, A. (1990) T cell receptor negative thymocytes from SCID mice can be induced to enter the CD4/CD8 differentiation pathway. *Eur. J. Immunol.* **20**, 69.
- Siegel, J. P., Sharon, M., Smith, P. L. & Leonard, W. J. (1987) The IL-2 receptor  $\beta$  chain (p70): role in mediating signals for LAK, NK, and proliferative activities. *Science* **238**, 75.
- Somberg, R. L., Robinson, J. P. & Felsburg, P. J. (1994) T lymphocyte depletion and function in dogs with X-linked severe combined immunodeficiency. *J. Immunol.* **153**, 4006.
- Strober, W. & Ehrhardt, R. O. (1993) Chronic intestinal inflammation: An unexpected outcome in cytokine or T cell receptor mutant mice. *Cell* **75**, 203.
- Suzuki, H., Kundig, T. M., Furlonger, C., Wakeham, A., Timms, E., Matsuyama, T., Schmits, R., Simard, J. J. L., Ohashi, P. S., Griesser, H., Taniguchi, T., Paige, C. J. & Mak, T. W. (1995) Deregulated T cell activation and autoimmunity in mice lacking interleukin-2 receptor  $\beta$ . *Science* **268**, 1472.
- Taga, T. & Kishimoto, T. (1995). Signaling mechanisms through cytokine receptors that share signal transducing receptor components. *Curr. Opin. Immunol.* **7**, 17.
- Takeshita, T., Asao, H., Ohtani, K., Ishii, N., Kumaki, S., Tanaka, N., Munakata, H., Nakamura, M. & Sugamura, K. (1992) Cloning of the  $\gamma$  chain of the human IL-2 receptor. *Science* **257**, 379.
- Taniguchi, T. (1995) Cytokine signaling through nonreceptor protein tyrosine kinases. *Science* **268**, 251.
- Teshigawara, K., Wang, H. M., Kata, K. & Smith, K. A. (1987) Interleukin-2 high affinity receptor expression requires two distinct binding proteins. *J. Exp. Med.* **165**, 223.
- Tsuda, M., Kozak, R. W., Goldman, C. K. & Waldmann, T. A. (1986) Demonstration of a non-Tac peptide that binds interleukin-2: a potential participant in a multichain interleukin-2 receptor complex. *Proc. Natl. Acad. Sci. USA* **83**, 9694.
- Tybulewicz, V. L. J., Crawford, C. E., Jackson, P. K., Bronson, R. T. & Mulligan, R. C. (1991) Neonatal lethality and lymphopenia in mice with a homozygous disruption of the *c-abl* proto-oncogene. *Cell* **65**, 1153.
- von Freeden-Jeffry, U., Vieira, P., Lucian, L. A., McNeil, T., Burdach, S. E. & Murray, R. (1995) Lymphopenia in interleukin (IL)-7 gene-deleted mice identifies IL-7 as a nonredundant cytokine. *J. Exp. Med.* **181**, 1519.
- Weinberg, K. & Parkman, R. (1990) Severe combined immunodeficiency due to a specific defect in the production of interleukin-2. *N. Eng. J. Med.* **322**, 1718.
- Willerford, D. M., Chen, J., Ferry, J. A., Davidson, L., Ma, A. & Alt, F. W. (1995). Interleukin-2 receptor  $\alpha$  chain regulates the size and content of the peripheral lymphoid compartment. *Immunity* **3**, 521.
- Witthuhn, B. A., Silvennoinen, O., Miura, O., Lai, K. S., Cwik, C., Liu, E. T. & Ihle, J. N. (1994) Involvement of the Jak-3 Janus kinase in signalling by interleukins 2 and 4 in lymphoid and myeloid cells. *Nature* **370**, 153.



## Defects in heart and lung development in compound heterozygotes for two different targeted mutations at the *N-myc* locus

Cecilia B. Moens<sup>1,3</sup>, Brian R. Stanton<sup>2</sup>, Luis F. Parada<sup>2</sup> and Janet Rossant<sup>1,3,\*</sup>

<sup>1</sup>Division of Molecular and Developmental Biology, Samuel Lunenfeld Research Institute, 600 University Ave, Toronto, Ontario, M5G 1X5, Canada

<sup>2</sup>Molecular Embryology Section, ABL-Basic Research Program, National Cancer Institute - Frederick Cancer Research and Development Center, Frederick, Maryland 21702-1201, USA

<sup>3</sup>Department of Molecular and Medical Genetics, University of Toronto

\*Author for correspondence

### SUMMARY

Two types of mutant allele, one leaky and one null, have been generated by gene targeting at the *N-myc* locus in embryonic stem cells and the phenotypes of mice homozygous for these mutations have been described. These mutations have shown that *N-myc* has a number of functions during development, including a role in branching morphogenesis in the lung, which manifests itself at birth in mice homozygous for the leaky allele, and roles in the development of the mesonephric tubules, the neuroepithelium, the sensory ganglia, the gut and the heart, which become evident at midgestation in embryos homozygous for the null allele. In an attempt to define roles for *N-myc* at other stages of development, we have combined the two types of *N-myc* mutant allele in a compound heterozygote that as a result contains approximately 15% of normal levels of N-Myc protein. Compound heterozygotes died during gestation at a time

intermediate to the times of death of embryos homozygous for either mutation individually, and their death appeared to result from cardiac failure stemming from hypoplasia of the compact subepicardial layer of the myocardium. Investigation of the expression pattern of *N-myc* and various markers of differentiation in wild-type and compound heterozygote mutant hearts has suggested that *N-myc* may function in maintaining the proliferation and/or preventing the differentiation of compact layer myocytes. This study illustrates the importance of generating different mutations at a given locus to elucidate fully the function of a particular gene during development.

Key words: *N-myc*, heart development, targeted mutagenesis, mouse mutant

### INTRODUCTION

*N-myc* is a member of the *myc* family of proto-oncogenes, which includes *N-myc*, *c-myc*, and *L-myc*. Myc proteins are site-specific DNA-binding proteins (Blackwell et al., 1990; Prendergast and Ziff, 1991; Alex et al., 1992), belonging to the basic-helix-loop-helix class of transcription factors, which includes genes that control cell fate determination in such diverse processes as myogenesis, neurogenesis and sex determination (reviewed in Garrell and Campuzano, 1991).

Deregulated expression of *myc* genes has been implicated in the genesis or progression of a number of naturally occurring tumours, in the transformation of cells in culture and in the formation of tumours in transgenic mice (reviewed in DePinho et al., 1991). In general, the sites of expression of a given *myc* gene in vivo reflect the types of tumours associated with its elevated expression. Thus *N-myc* is expressed predominantly in the embryo where it is restricted to undifferentiated subsets of cells in the central and peripheral nervous system, lung, kidney and eye

(Mugrauer et al., 1988; Hirning et al., 1991; Zimmerman et al., 1986) and overexpression of *N-myc* has been associated with tumours of embryonic origin such as neuroblastoma (Kohl et al., 1983; Schwab et al., 1983), small-cell lung cancer (Nau et al., 1986; Wong et al., 1986), Wilm's tumour (Nisen et al., 1986) and retinoblastoma (Lee et al., 1984). *N-myc* is also expressed in the skin (Mugrauer et al., 1988), in the epithelial layer of the intestine (Hirning et al., 1991) and, earlier in development, in the heart, sclerotome and visceral arches (Kato et al., 1991).

The functioning of a Myc protein in vivo should depend not only on its own level of expression, but also on the levels of Max, a protein which, like the Myc proteins, possesses a basic-helix loop helix-leucine zipper (bHLH-LZ) domain (Blackwood and Eisenman, 1991), and which associates with N-Myc, L-Myc and c-Myc proteins in vivo (Blackwood et al., 1992; Wenzel et al., 1991; Mukherjee et al., 1992). Max is required for specific DNA binding by Myc proteins (Blackwood and Eisenman, 1991; Prendergast and Ziff, 1991; Kato et al., 1992; Barrett et al., 1992), and has

been shown to be required for transcriptional activation (Amati et al., 1992) and transformation (Amati et al., 1993) by *c-myc*. Unlike Myc proteins, Max is able to form homodimers in vitro and thereby to bind the *myc*-binding site (Prendergast and Ziff, 1991; Kato et al., 1992). However Max does not transactivate downstream genes on its own (Amati et al., 1992; Kretzner et al., 1992) because it lacks a transactivation domain (Kato et al., 1992) which Myc proteins possess (Kato et al., 1990). Both transformation of fibroblasts by *c-myc* and *N-myc* (Mukherjee et al., 1992; Makela et al., 1992; Prendergast et al., 1992) and transcriptional transactivation by *c-myc* (Amati et al., 1992; Kretzner et al., 1992) have been shown to be enhanced by low levels of Max and inhibited by excess Max, suggesting that Myc function is indeed influenced by levels of Max. Recently, bHLH-LZ proteins have been isolated which also bind the Myc recognition site and which suppress transcription as heterodimers with Max (Ayer et al., 1993; Zervos et al., 1993). One of these, Mad (Ayer et al., 1993), has been shown to compete with Myc for Max in vitro and in transfected cells. Thus high levels of expression of Max dimerization partners may indirectly affect Myc function in vivo by competing for available Max protein and for DNA-recognition sites. Finally, Myc function in vivo may be affected by the levels of other Myc proteins (Mukherjee et al., 1992; Resar et al., 1993).

In an effort to understand the function of *myc* genes in embryogenesis, leaky and null mutations were made in *N-myc* in embryonic stem cells by homologous recombination (Charron et al., 1990; Stanton et al., 1990; Sawai et al., 1991; Moens et al., 1992). These mutations have allowed a description of the function of *N-myc* at different stages of development. Mice homozygous for the null mutations die at midgestation (Stanton et al., 1992; Charron et al., 1992) while mice homozygous for the leaky mutation survive until birth, when they die due to a defect in lung branching morphogenesis (Moens et al., 1992). The latter phenotype is consistent with the normal expression of *N-myc* in the developing lung epithelium, and has led us to postulate that *N-myc* plays a role in the response of the lung epithelium to the signals from the lung mesenchyme that induce epithelial branching.

There have been two detailed reports of the phenotype of mice carrying null mutations in *N-myc* (Stanton et al., 1992; Charron et al., 1992). In the homozygous condition, these mutations cause embryonic death at around 11.5 days p.c. and cause hypoplasia in a number of components of the embryo, different aspects of which have been emphasized by the two groups. The developing genitourinary system shows a reduced number of mesonephric tubules in mutant embryos, which is consistent with *N-myc*'s normal expression in the newly induced epithelium of the meso- and metanephric tubules (Kato et al., 1991; Mugrauer et al., 1988). The genital ridge is also hypoplastic. Stanton et al. (1992) also describe a defect in the development of the stomach and intestine, consistent with *N-myc*'s expression in the epithelium of these tissues (Hirning et al., 1991). Homozygotes also have reduced cranial and spinal ganglia and a thin neuroepithelium in the telencephalon; both of these are sites of *N-myc* expression in the embryo. Finally, homozygotes have a defect in heart development in which

the heart appears to cease development at 9.5 days p.c. (Charron et al., 1992) and as a result is poorly compartmentalized and appears not to have undergone the normal epithelial-to-mesenchymal transitions that result in the formation of the septa and valves. This is again consistent with a previous description of *N-myc* expression in the myocardium of the 9.5 day embryo (Kato et al., 1991).

By combining leaky and null alleles of *N-myc* in a compound heterozygote, we hoped to investigate *N-myc* function in the mouse embryo at a stage intermediate to those identified by the null and leaky alleles individually. We find that compound heterozygotes indeed survive longer than null homozygotes, but that they die before birth. The mutant phenotype includes a more severe defect in branching morphogenesis of the lung, as well as a cardiac myocyte hypoplasia in the compact subepicardial layer of the ventricular myocardium. We show that, consistent with this phenotype, *N-myc* expression in the developing myocardium is restricted to the compact layer. A role for *myc* genes in the control of myocyte differentiation in the heart is discussed.

## MATERIALS AND METHODS

### PCR genotyping of embryos

Yolk sacs from dissected embryos were washed several times in fresh PBS and placed in 100–200 µl of proteinase K buffer with non-ionic detergents (50 mM KCl, 10 mM Tris pH 8.3, 2.0 mM MgCl<sub>2</sub>, 0.1 mg/ml gelatin, 0.45% Nonidet P-40, 0.45% Tween-20). 10 µg of proK was added to each tube and samples were incubated at 55°C overnight. 10 µl of the mixture was placed in a PCR tube with 30 µl sterile water and heated to 94°C for 10 minutes before cooling to 62°C. 0.1 µg of each primer, 200 µM dNTPs, 10x reaction buffer and Taq polymerase (Promega) were added and PCR was run with an annealing temperature of 62°C (1 minute), an extension temperature of 72°C (2 minutes), and a denaturing temperature of 94°C (1 minute). Each consecutive cycle was extended by 2 seconds. The oligonucleotide primers used for the PCR detection of 9a, BRP and wild-type alleles of *N-myc* are shown in Fig. 1. Their sequences are as follows: primer a (*N-myc* intron 1): 5'-GGTAGTCGCGCTAGT AAGAG-3'; primer b (*N-myc* exon 2): 5'-GGCGTGGGCA GCAGCTCAAAC-3'; primer c (*N-myc* intron 2): 5'-CCGAGCATCTGTGCGCAAGTC-3'; primer d (neo): 5'-GACCGCTATCAGGACATAGCG-3'.

### Western blotting

An anti-human *N-myc* monoclonal antibody, NCM1100 (Ikegaki et al., 1986), was generously provided by Dr R. Kennett. 11.5 days p.c. embryos from 9a/+xBRP/+ crosses were dissected and homogenized in several volumes of 1x sample buffer without bromophenol blue (60 mM Tris, pH 6.8, 2% SDS, 0.1 M DTT, 0.32% pharmalyte 3–10 (Pharmacia)). Samples were boiled for 5 minutes and chromosomal DNA was sheared by repeated passage through a 26-gauge needle before freezing at –20°C for future use. Yolk sacs were washed several times in PBS and were prepared for and typed by PCR as described above. After typing, extracts of embryos of each genotype were pooled and the concentration of protein in each sample was determined by the Bradford assay (protein assay reagent from Biorad). Approximately 20 µg of protein from each genotype in 2x loading buffer (0.1 M Tris pH 6.8, 20% glycerol, 4% SDS, 0.2% bromophenol blue, 0.2 M DTT) was run in a 10% SDS-PAGE. Protein was transferred onto PVDF membrane (Immobilon-P, Millipore). Application of primary antibody and fixation of the primary antibody to the blot with 0.2%

glutaraldehyde was performed as described (Ikegaki and Kennett, 1989). Horseradish peroxidase-conjugated goat anti-mouse secondary antibody and reagents for the chemiluminescent detection of HRP activity were obtained in the ECL western blotting kit (Amersham) and were used as suggested by the manufacturer.

### Histology

Dissected embryos were fixed in 10% buffered formalin overnight at room temperature, then were dehydrated and cleared by soaking sequentially in 70%, 80%, 90% and 95% ethanol, 1:1 ethanol:xylene, xylene, 1:1 xylene:paraffin wax, (TissuePrep 2, Fisher Scientific) each for 1 hour. Embryos were then oriented and embedded in paraffin wax. Mutant embryos and control littermates were oriented either for sagittal or frontal sections. 5  $\mu$ m sections were placed on slides, which were dried overnight at 37°C. Slides were dewaxed, rehydrated, and stained with hematoxylin and eosin. To analyse mutant phenotypes, sections throughout wild-type and mutant embryos were carefully examined in order to find those sections that passed through corresponding regions of the different embryos. Mutant embryos were always compared to non-mutant littermates rather than to non-mutant embryos from other litters, in order to rule out differences due to age.

### RNA in situ hybridizations

Probes for in situ were as follows. *N-myc*: a 541 bp *Pst*I-*Sca*I fragment of the *N-myc* genomic clone N7.7 (DePinho et al., 1986), including largely 3'-untranslated sequence; *c-myc*: a 351 bp *Hae*III fragment including the untranslated first exon (Bossone et al., 1992); *flk-1*: an 800 bp fragment spanning the transmembrane domain and part of the extracellular ligand-binding domain (Yamaguchi et al., 1993) and  $\alpha$ -cardiac actin, a 130 bp *Bam*HI fragment including the first untranslated exon of the mouse  $\alpha$ -cardiac actin gene (Sassoon et al., 1988). In situ hybridization was carried out essentially as described (Frohman et al., 1990) with the following modifications: in vitro-transcribed,  $\alpha$ -<sup>35</sup>S-labeled RNA probes were used at  $5 \times 10^4$  disintegrations/minute per 1  $\mu$ l of hybridization solution for the  $\alpha$ -cardiac actin probe, and at  $1 \times 10^5$  disintegrations/minute per 1  $\mu$ l of hybridization solution for *c-myc*, *N-myc* and *flk-1* probes. Slides were hybridized at 53°C overnight, and were washed in the presence of 0.1%  $\beta$ -mercaptoethanol as a reducing agent. High stringency washes were in 50% formamide, 0.1%  $\beta$ -mercaptoethanol, and  $1 \times$  SSC at 65°C. Final rinses in  $2 \times$  and  $0.1 \times$  SSC were at 65°C for 15 minutes. Slides were exposed for either 6 days (for  $\alpha$ -cardiac actin probe) or for 14 days (for *N-myc*, *flk-1* and *c-myc* probes). After developing and photographing with dark-field illumination, slides were stained with hematoxylin and eosin and were rephotographed with bright-field illumination.

## RESULTS

### Time of death of N-myc compound heterozygotes

The leaky mutation that was generated in *N-myc* (Moens et al., 1992) was termed *N-myc*<sup>9a</sup> and the null allele of *N-myc* used in this study was named *N-myc*<sup>BRP</sup> (Stanton et al., 1992). Both the *N-myc*<sup>9a</sup> mutation and the *N-myc*<sup>BRP</sup> mutation are lethal in the homozygous condition. Therefore, *N-myc*<sup>9a/BRP</sup> embryos were generated by crossing *N-myc*<sup>9a/+</sup> females to *N-myc*<sup>BRP/+</sup> males, with the expected ratio of embryos being 1 *N-myc*<sup>+/+</sup>: 1 *N-myc*<sup>9a/+</sup>: 1 *N-myc*<sup>BRP/+</sup>: 1 *N-myc*<sup>9a/BRP</sup>. The reciprocal cross was also performed: no differences in mutant phenotypes were observed.

In order to expedite the genotypic analysis of offspring from this cross, a PCR strategy was designed that used four

oligonucleotide primers to distinguish 9a, BRP, and wild-type alleles of *N-myc* (Fig. 1). 161 live offspring from *N-myc*<sup>9a/+</sup>  $\times$  *N-myc*<sup>BRP/+</sup> crosses were typed by PCR between 1 day and 3 weeks after birth. Among these pups, 59 were *N-myc*<sup>+/+</sup>, 53 were *N-myc*<sup>9a/+</sup> and 49 were *N-myc*<sup>BRP/+</sup>. No live animals were *N-myc*<sup>9a/BRP</sup>. No pups were observed to die postnatally as occurred in the case of *N-myc*<sup>9a/9a</sup> newborns, suggesting that the *N-myc*<sup>9a/BRP</sup> phenotype was indeed more severe than the *N-myc*<sup>9a/9a</sup> phenotype.

We dissected embryos from *N-myc*<sup>9a/+</sup>  $\times$  *N-myc*<sup>BRP/+</sup> crosses at various stages of gestation in order to determine the time during gestation when *N-myc*<sup>9a/BRP</sup> embryos died. Between 8.5 and 11.5 days p.c., *N-myc*<sup>9a/BRP</sup> embryos were phenotypically normal and constituted approximately 25% of the total number of embryos, by PCR analysis. Of 268 embryos dissected between 8.5 and 11.5 days p.c., 61 (23%) were *N-myc*<sup>9a/BRP</sup> embryos. This is clearly different from the situation in *N-myc*<sup>BRP/BRP</sup> embryos, which were all found to be dead by 11.5 days p.c. (Stanton et al., 1992). The observed differences in phenotype among the various mutants were unlikely to be due to different genetic background effects, since all mutant phenotypes were analysed in outbred mice.

Occasionally, *N-myc*<sup>9a/BRP</sup> embryos at 11.5 days were slightly smaller than their littermates but were otherwise indistinguishable from their wild-type or single heterozygote littermates. However, by 12.5 days, most *N-myc*<sup>9a/BRP</sup> embryos were distinguishable from their littermates either because they were dead and necrotic, or because they were alive but had a characteristic edema of the body wall in the neck area (Fig. 2). Subsequent histological analysis identified this swelling as likely being the result of extravasation of fluid from the vascular compartment into the connective tissue, since the jugular veins are dilated in these embryos (Fig. 7g,h). Of 230 embryos dissected at 12.5 days p.c., 42 (18%) were *N-myc*<sup>9a/BRP</sup>, but among these, 12 were dead and necrotic, 23 had the characteristic edema described above, two were smaller than normal and five were phenotypically normal. After 12.5 days p.c., live *N-myc*<sup>9a/BRP</sup> embryos were progressively less frequent and all were phenotypically abnormal. *N-myc*<sup>9a/BRP</sup> embryos that survived until 14.5 days p.c. were always smaller than normal and had a large edema in the neck area. Live *N-myc*<sup>9a/BRP</sup> embryos were not observed after 14.5 days p.c. Coincident with the loss of *N-myc*<sup>9a/BRP</sup> embryos there was an increase in the number of resorptions visible in the uterus. These resorptions were not typed, but presumably were derived from *N-myc*<sup>9a/BRP</sup> embryos, since the sum of the number of *N-myc*<sup>9a/BRP</sup> embryos and the number of resorptions added up to approximately 25% of the total number of embryos and resorptions at each stage of gestation. These data are shown graphically in Fig. 3.

### N-Myc protein levels in mutant embryos

Although we have previously shown reduced *N-myc* mRNA levels in *N-myc*<sup>9a/9a</sup> embryos (Moens et al., 1992), N-Myc protein levels have not been determined in mice bearing either the leaky or the null *N-myc* alleles. In the present study, we have used western blot analysis to assess N-Myc protein levels in embryos with the various *N-myc* genotypes. Fig. 4 shows a western blot performed on

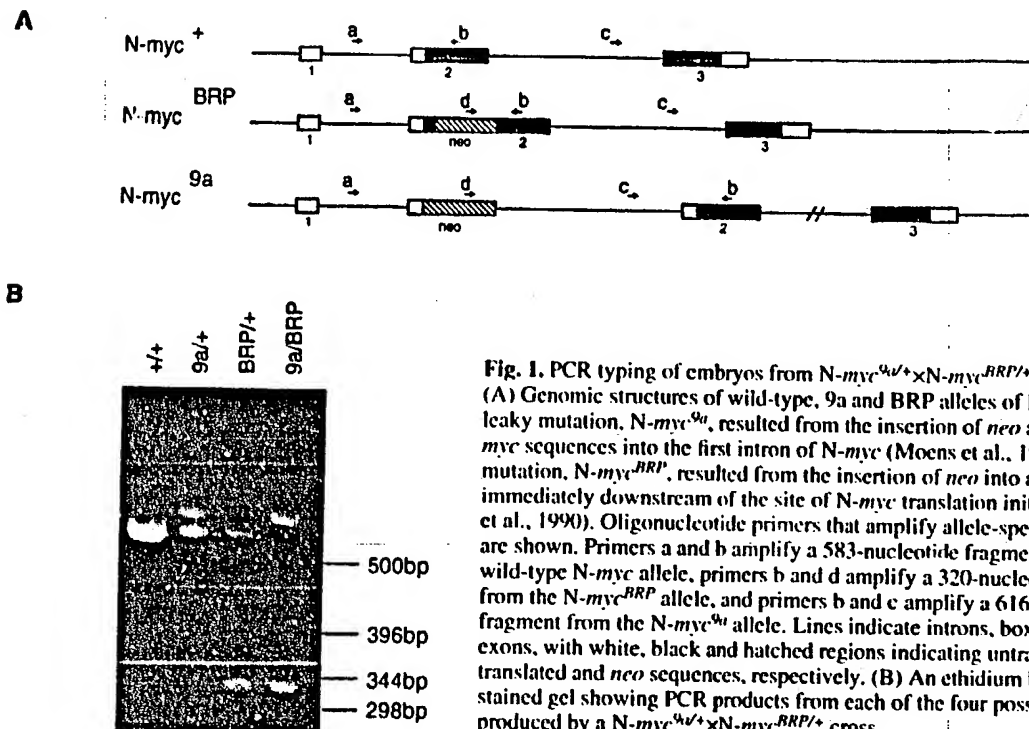


Fig. 1. PCR typing of embryos from *N-myc*<sup>9a/+</sup> × *N-myc*<sup>BRP/+</sup> crosses. (A) Genomic structures of wild-type, 9a and BRP alleles of *N-myc*. The leaky mutation, *N-myc*<sup>9a</sup>, resulted from the insertion of *neo* and flanking *N-myc* sequences into the first intron of *N-myc* (Moens et al., 1992). The null mutation, *N-myc*<sup>BRP</sup>, resulted from the insertion of *neo* into a *Xho* site immediately downstream of the site of *N-myc* translation initiation (Stanton et al., 1990). Oligonucleotide primers that amplify allele-specific fragments are shown. Primers a and b amplify a 583-nucleotide fragment from the wild-type *N-myc* allele, primers b and d amplify a 320-nucleotide fragment from the *N-myc*<sup>BRP</sup> allele, and primers b and c amplify a 616-nucleotide fragment from the *N-myc*<sup>9a</sup> allele. Lines indicate introns, boxes indicate exons, with white, black and hatched regions indicating untranslated, translated and *neo* sequences, respectively. (B) An ethidium bromide-stained gel showing PCR products from each of the four possible genotypes produced by a *N-myc*<sup>9a/+</sup> × *N-myc*<sup>BRP/+</sup> cross.

extracts of whole 11.5 days p.c. embryos from a *N-myc*<sup>9a/+</sup> × *N-myc*<sup>BRP/+</sup> cross, using a monoclonal antibody that was raised against human N-Myc protein (Ikegaki et al., 1986), but which also recognizes mouse N-Myc protein. N-Myc protein runs at approximately  $65 \times 10^3 M_r$ . This N-Myc antibody also showed binding to a protein of approximately  $100 \times 10^3 M_r$ . The relative intensities of this cross-reacting band between lanes matched the relative intensities of a ubiquitously expressed protein phosphatase, *syp* (not shown), so this band was used as a loading control in scanning densitometry. The amount of N-Myc protein in *N-myc*<sup>9a/BRP</sup> embryos was considerably lower than in their wild-type or singly heterozygous littermates. While *N-myc*<sup>9a/9a</sup> embryos had approximately 25% of wild-type levels of N-Myc protein (not shown), *N-myc*<sup>9a/BRP</sup> embryos had approximately 15% of wild-type levels, as determined by scanning densitometry of this and several other, similar Western blots. This is consistent with the more severe phenotype of *N-myc*<sup>9a/BRP</sup> embryos. *N-myc*<sup>BRP/+</sup> embryos had approximately 50% of wild-type levels of N-Myc protein, consistent with the *N-myc*<sup>BRP</sup> mutation being a null mutation.

#### Histological analysis of *N-myc*<sup>9a/BRP</sup> embryos

In order to determine more precisely the phenotype of *N-myc*<sup>9a/BRP</sup> embryos, histological analysis of hematoxylin and eosin-stained, sectioned embryos was performed at various stages of development. We examined a total of 42 *N-myc*<sup>9a/BRP</sup> embryos and 50 *N-myc*<sup>+/+</sup> littermates in this manner (5 *N-myc*<sup>9a/BRP</sup> embryos at 14.5 days p.c., 28 at 12.5 days p.c., 3 at 11.5 days p.c., and 6 at 10.5 days p.c.). Younger embryos were analyzed without sectioning, after whole-mount RNA in situ hybridization with various

probes (data not shown). Occasionally, *N-myc*<sup>9a/+</sup> embryos were used as controls since we have previously shown that the *N-myc*<sup>9a</sup> mutation has no phenotypic effect in the heterozygous condition. *N-myc*<sup>9a/BRP</sup> embryos not used for histology were used for N-Myc protein analysis and RNA in situ analysis.

Before 12.5 days p.c., *N-myc*<sup>9a/BRP</sup> embryos were apparently normal and could not generally be distinguished from their littermates either by gross morphology or by histological examination of sectioned embryos. The first signs of lethality occurred at 12.5 days, when 12 out of 42 *N-myc*<sup>9a/BRP</sup> were clearly in the process of resorption. Aside from the edema in the neck area, described above, and their slightly smaller size, live *N-myc*<sup>9a/BRP</sup> embryos at 12.5 days were still not grossly abnormal. However careful examination of specific organ systems did reveal particular defects.

#### Lung development

*N-myc*<sup>9a/9a</sup> mice die at birth due to a defect in lung branching morphogenesis, consistent with the observation that N-myc is expressed in the lung epithelium at early stages of lung development (Moens et al., 1992). Specifically, at 12.5 days p.c., when wild-type lungs have tertiary and quaternary branches, *N-myc*<sup>9a/9a</sup> lungs had only the beginnings of tertiary branches. The further reduction in the amount of N-Myc protein in *N-myc*<sup>9a/BRP</sup> embryos led to an enhancement of this phenotype, as predicted. Branching morphogenesis in *N-myc*<sup>9a/BRP</sup> lungs was all but blocked (Fig. 5A,B), *N-myc*<sup>9a/BRP</sup> embryos having only the beginnings of secondary branches. Interestingly, the pattern of branching was normal, as can be observed by the presence of a rudimentary right postcaval lobe extending to the left



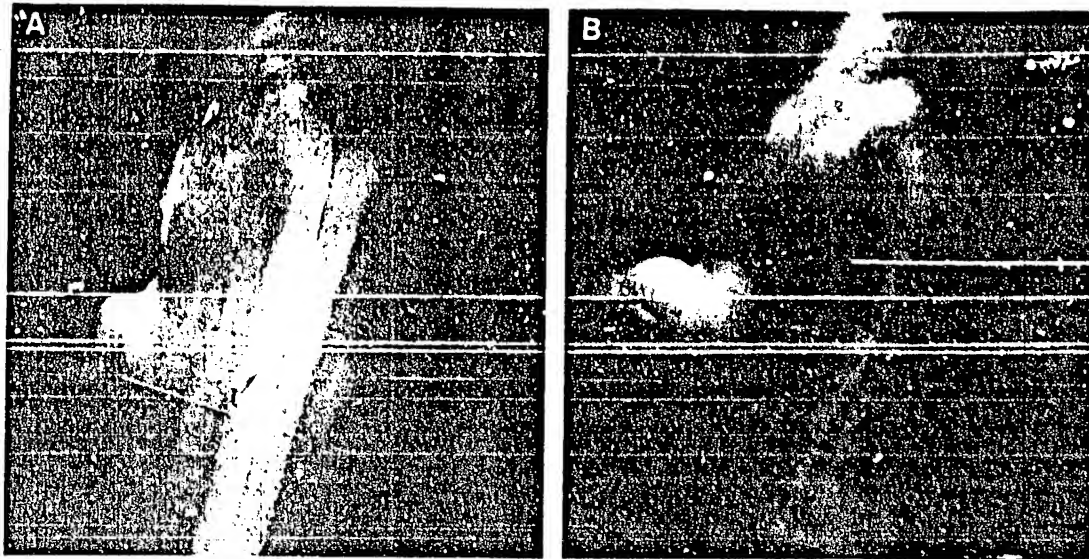


Fig. 2. *N-myc*<sup>9a/BRP</sup> embryos are edematous in the region of the neck. (A) Wild-type 12.5 days p.c. embryo, dorsal view. (B) *N-myc*<sup>9a/BRP</sup> embryo, showing swelling of the tissue and expanded, blood-filled jugular veins.

side of the *N-myc*<sup>9a/BRP</sup> embryo (Fig. 5B). The lungs begin their development by budding from the trachea into the surrounding mesenchyme and are visible as two pouches at 10.5 days of development. This early phase of lung development occurred normally in *N-myc*<sup>9a/BRP</sup> embryos (not shown).

In order to determine whether aspects of lung development other than the branching of the lung epithelium were affected by the reduction in N-Myc protein levels, we performed RNA in situ hybridizations on wild-type and *N-myc*<sup>9a/BRP</sup> lungs at 12.5 days p.c. (Fig. 6). *Flk-1*, which encodes a tyrosine kinase receptor for vascular endothelial

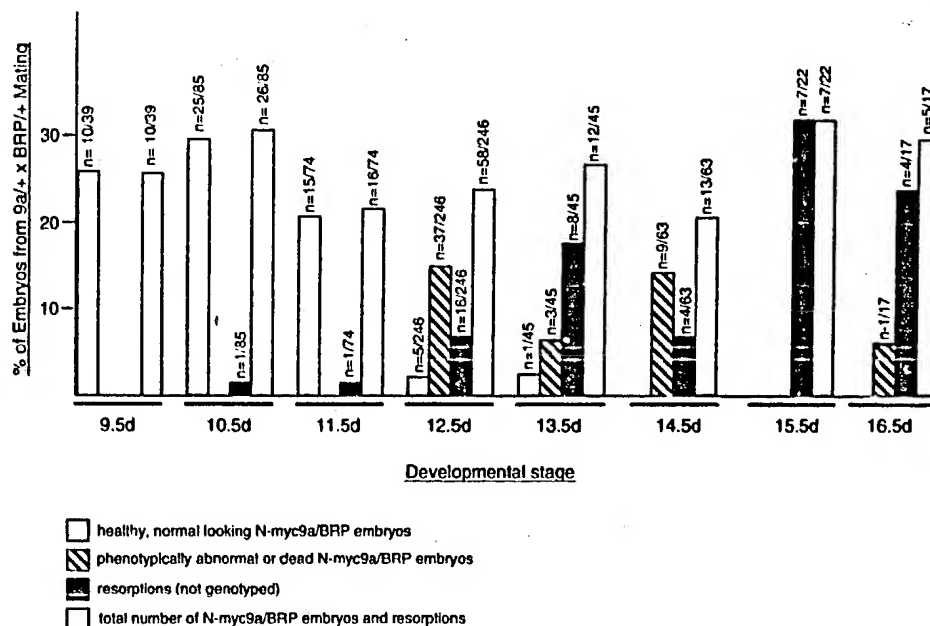


Fig. 3. Percentage of embryos in a *N-myc*<sup>9a/+</sup> × *N-myc*<sup>BRP/+</sup> litter that are *N-myc*<sup>9a/BRP</sup>, as a function of developmental stage. *N-myc*<sup>9a/BRP</sup> embryos are separated into two groups: (1) healthy, phenotypically normal embryos (stippled bars), and (2) phenotypically abnormal or dead embryos (hatched bars). Resorption sites visible in the uterus but not typed with respect to *N-myc* are included as a separate category (black bars). Note that the total of resorptions, abnormal *N-myc*<sup>9a/BRP</sup> embryos and normal *N-myc*<sup>9a/BRP</sup> embryos adds up to approximately 25% of the offspring at each time point (white bars). Numbers are given as a fraction of the total number of embryos dissected from *N-myc*<sup>9a/+</sup> × *N-myc*<sup>BRP/+</sup> crosses at that developmental stage.

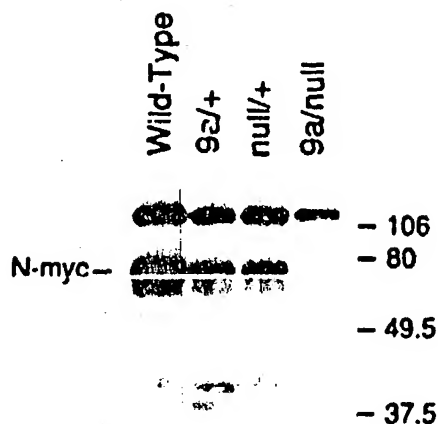


Fig. 4. Western analysis of N-Myc protein levels in extracts of 11.5 days p.c. embryos of the four possible types of offspring from an  $N\text{-myc}^{9a/+} \times N\text{-myc}^{BRP/+}$  cross. Each lane contains approximately 20  $\mu\text{g}$  of protein. The N-Myc protein runs at approximately  $65 \times 10^3 M_r$ . A cross-reacting band appears at approximately  $100 \times 10^3 M_r$ .

growth factor, marks endothelial cells in the developing capillaries and blood vessels in the mouse (Yamaguchi et al., 1993; Millauer et al., 1993), and as such is expressed in a punctate manner throughout the lung mesenchyme where the lung vasculature is developing (Fig. 6C). The pattern and intensity of *flk-1* expression was not affected in  $N\text{-myc}^{9a/BRP}$  lungs (Fig. 6G), indicating that the development of the lung vasculature is not affected by the reduction in N-Myc protein observed in  $N\text{-myc}^{9a/BRP}$  embryos. Fig. 6B,F shows the pattern of expression of N-myc in wild-type and  $N\text{-myc}^{9a/BRP}$  lungs, respectively, at 12.5 days p.c., reconfirming that expression is restricted to the lung epithelium and showing that the reduced N-Myc protein levels in  $N\text{-myc}^{9a/BRP}$  embryos did not lead to a complete loss of N-myc-expressing cells in the lung epithelium.  $N\text{-myc}^{9a/BRP}$  lungs appeared to express more than 15% of normal levels of N-

myc RNA (Fig. 6F). This is because the  $N\text{-myc}^{BRP}$  allele encodes a transcript that includes the entire N-myc open reading frame, but which contains stop codons that prevent translation of any part of the N-myc protein (Stanton et al., 1990). Fig. 6D,H demonstrate that levels of c-myc mRNA at the cellular level were not affected by the reduction in N-Myc protein in the lungs of  $N\text{-myc}^{9a/BRP}$  embryos. C-myc is normally expressed in the lung mesenchyme (Fig. 6D, Hirning et al., 1991) and the pattern and level of c-myc expression was not altered in the  $N\text{-myc}^{9a/BRP}$  lung, despite its reduced size (Fig. 6H).

#### Heart development

The other clearly visible defect in  $N\text{-myc}^{9a/BRP}$  embryos examined at 12.5 days p.c. was in the morphology of the heart. While  $N\text{-myc}^{9a/BRP}$  hearts had the normal four-chamber structure, normal endocardial cushions, valves and septa, the heart was small and the myocardium was abnormally thin (Fig. 7A-D). The latter defect was particularly apparent in the 'compact', or subepicardial layer of the ventricular myocardium while the atrial myocardium and the inner trabecular layer of the ventricles were less severely affected. In mammals, trabeculation occurs early during heart development and, at later stages, growth occurs largely in the compact layer (Rumyantsev, 1991). In  $N\text{-myc}^{9a/BRP}$  embryos, this growth of the compact layer appeared not to occur, so that the  $N\text{-myc}^{9a/BRP}$  myocardium at 12.5 days p.c. was no thicker than it had been at 10.5 days p.c.

Occasionally,  $N\text{-myc}^{9a/BRP}$  embryos survived until 14.5 days p.c. These embryos were always grossly abnormal, with large edemas in the neck area, and were smaller than their littermates. Fig. 7E and F compares wild-type and  $N\text{-myc}^{9a/BRP}$  hearts at this stage, showing that the compact layer of the myocardium of the compound heterozygote was still no more developed than it had been at 10.5 days.

It seems likely that this failure in the proliferation of the ventricular myocardium leads to a failure of the circulatory system and ultimately in fetal death. The inefficient function of the heart was demonstrated by the hugely expanded



Fig. 5. Comparison of lung development in wild-type (A) and compound heterozygote  $N\text{-myc}^{9a/BRP}$  (B) embryos at 12.5 days p.c. Comparable frontal sections were taken at the level of the right postcaval lobe. E, esophagus; L, left lung; RP, right lung, postcaval lobe. Bar, 200  $\mu\text{m}$ .

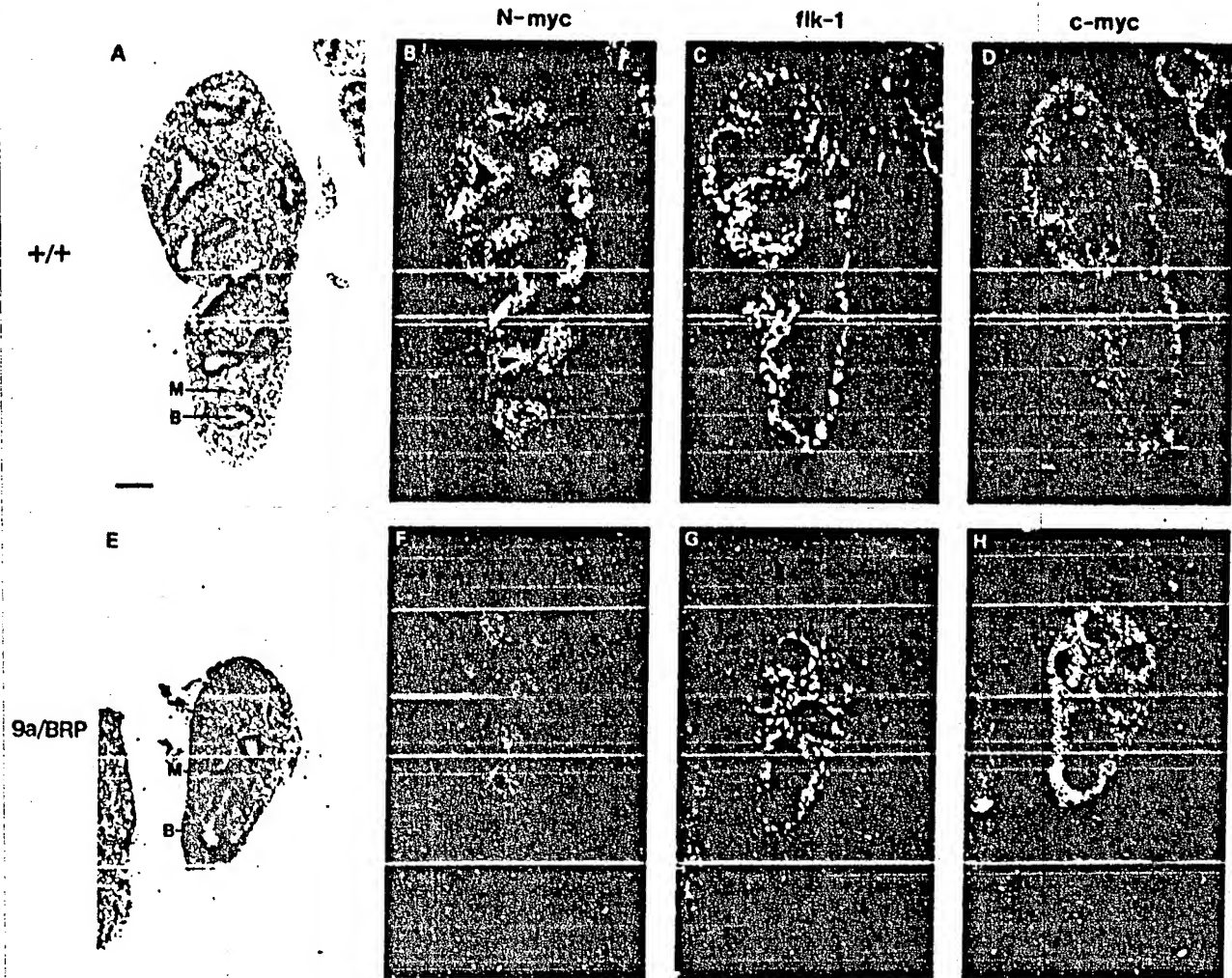


Fig. 6. Expression of *N-myc*, *flk-1*, and *c-myc* in wild-type and *N-myc*<sup>9a/BRP</sup> lungs at 12.5 days p.c. (A,E) Bright-field photomicrographs of sagittal sections of the left lung of +/+ (A) and compound heterozygote *N-myc*<sup>9a/BRP</sup> (E) embryos. Wild-type (B-D) and *N-myc*<sup>9a/BRP</sup> (F-H) serial sections hybridized to the RNA probes shown, were photographed in dark field. B, bronchiole; M, lung mesenchyme. Bar, 100  $\mu$ m.

jugular veins of *N-myc*<sup>9a/BRP</sup> embryos (Fig. 7G,H), since the lack of a highly muscularized ventricular myocardium pumping blood from the heart could lead to a back-up of blood in the major veins. However, it should be noted that we did not see this marked distension in the other major veins that lead into the heart.

We wished to determine whether the observed defect in the development of the compact layer of the ventricular myocardium correlated with *N-myc* expression in the heart. Expression of *N-myc* in the heart at 9.5 days p.c. has been described (Kato et al., 1991), and we have confirmed this by whole-mount RNA in situ hybridization (data not shown). However the differentiation of trabecular and compact layers has only just begun at this stage, and *N-myc* expression was not shown to be restricted to one specific layer. Our experiments indicate that, by 10.5 days p.c., *N-myc* expression in the heart is largely confined to the compact layer and not to the trabecular layer of the devel-

oping ventricular myocardium (Fig. 8B). For comparison,  $\alpha$ -cardiac actin, a marker of differentiated myocytes in the developing heart (Sassoon et al., 1988), is expressed in both the trabeculae and the compact layer (Fig. 8C). We observed continued *N-myc* expression in the compact layer at the time when a mutant phenotype was first observed in the heart (12.5 days p.c., Fig. 9B,G). This higher level of *N-myc* expression in the compact layer compared to the trabecular layer is consistent with a direct role in the development of the mutant phenotype we have observed in *N-myc*<sup>9a/BRP</sup> embryos.

Considerable *N-myc* expression was detected in the compact layer of 12.5 days p.c. *N-myc*<sup>9a/BRP</sup> hearts (Fig. 9B,G) because the *N-myc*<sup>BRP</sup> mutation prevents translation but not transcription of *N-myc*, as noted above. However, as expected, the layer of *N-myc*-expressing cells was narrower in the ventricular myocardium of compound heterozygotes than in the wild-type myocardium (compare Figs 9B and



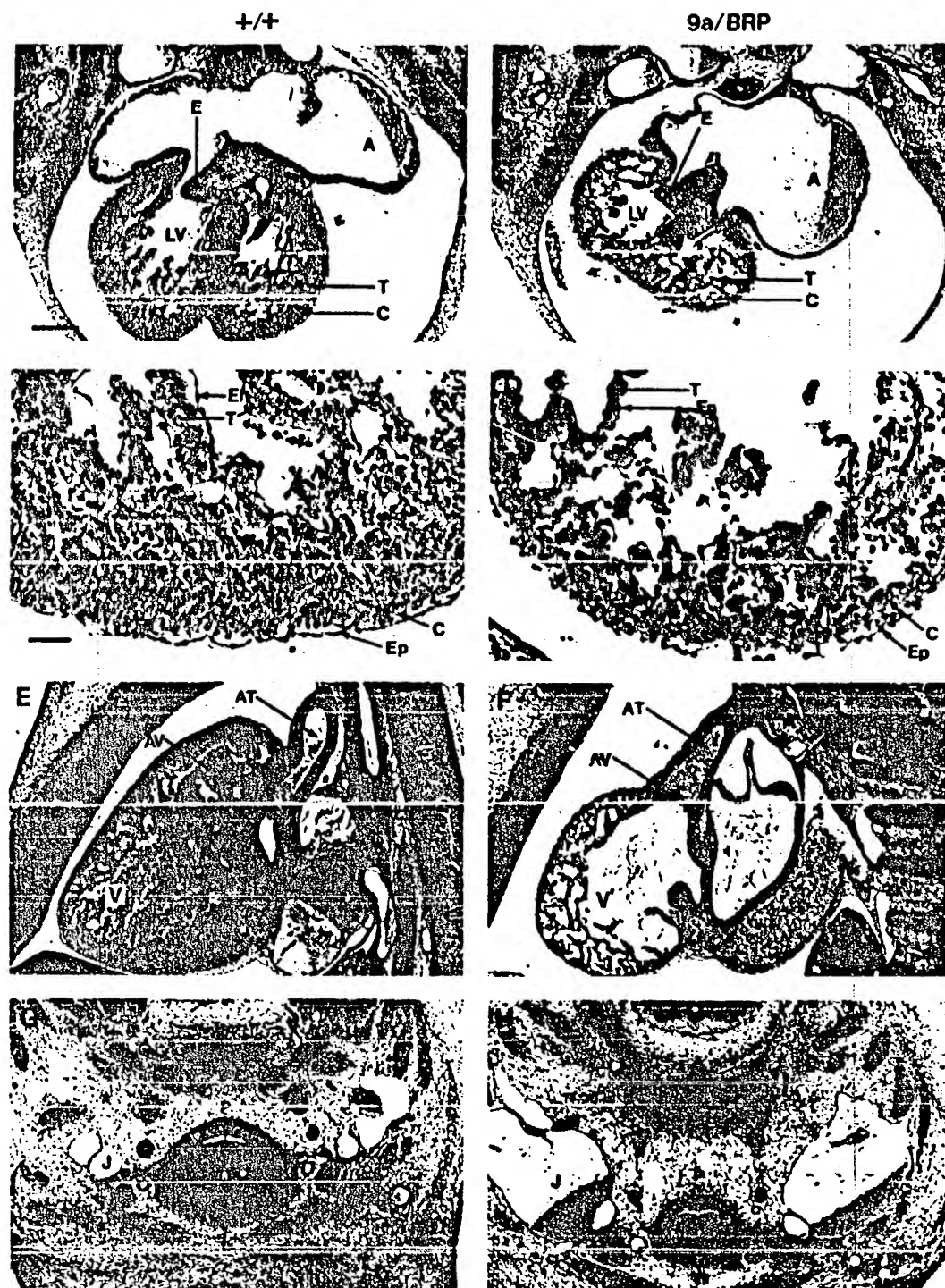


Fig. 7. Comparison of heart development in wild-type and compound heterozygote *N-myc*<sup>9a/BRP</sup> embryos at 12.5 and 14.5 days p.c. Left-hand photographs show wild-type embryos, and right-hand photographs show *N-myc*<sup>9a/BRP</sup> embryos. (A,B) Low-power magnification photomicrographs of frontal sections of 12.5 days p.c. hearts taken at the level of the left atrioventricular canal. (C,D) High-power magnification of the ventricle of 12.5 day hearts. (E,F) Sagittal sections of 14.5-day hearts. (G,H) Frontal sections through the jugular veins at 12.5 days. A, atrium; AT, aortic trunk; AV, aortic valve; C, compact layer; E, endocardial cushion; En, endocardium; Ep, epicardium; J, jugular veins; LV, left ventricle; P, pharynx; V, ventricle; T, trabeculae; Tr, trachea. For A,B,E,F,G,H: bar, 250 µm; for C,D: bar, 50 µm.



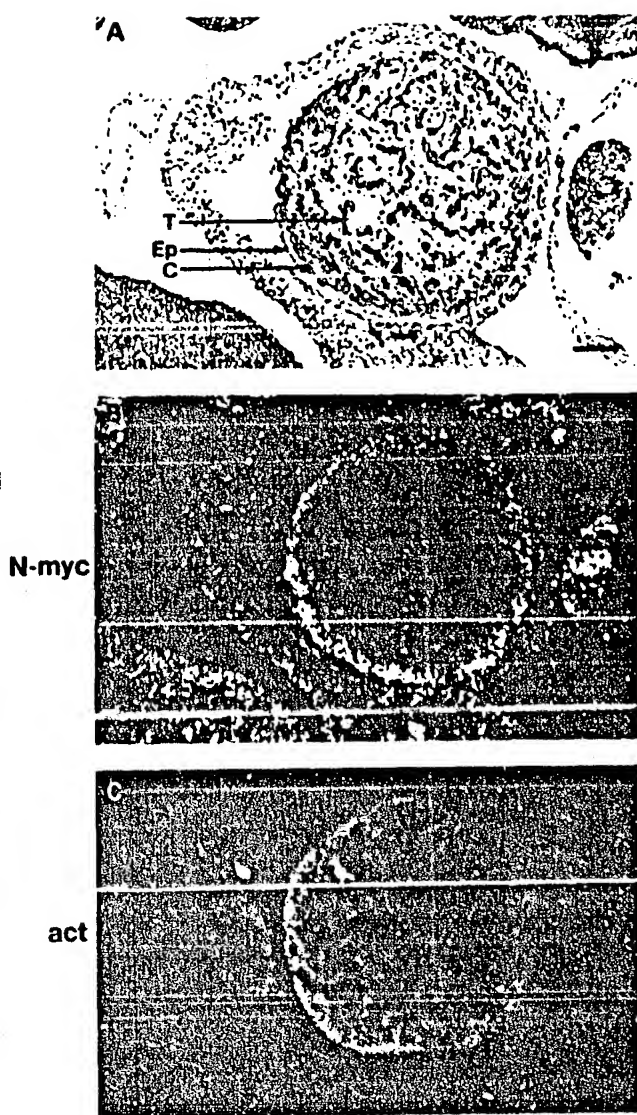


Fig. 8. Expression patterns of *N-myc* and  $\alpha$ -cardiac actin in the heart at 10.5 days p.c. (A) Bright-field photomicrograph of a hematoxylin and eosin-stained parasagittal section of a wild-type ventricle. (B,C) Dark-field photomicrographs of serial sections showing *N-myc* (B) and  $\alpha$ -cardiac actin (C) expression by RNA in situ hybridization. C, compact subepicardial layer; T, trabeculae; Ep, epicardium. Bar, 100  $\mu$ m.

8B). The observation that the mutant alleles continue to be transcribed in the *N-myc*<sup>9a/BRP</sup> myocardium suggests that cells that normally express *N-myc* are present but in reduced numbers.

*Flk-1*, the endothelial cell marker described above, is expressed in the endocardium (Yamaguchi et al., 1993), which is the mesodermally derived inner lining of the heart that later contributes to the endocardial cushion and heart valves through an epithelial-to-mesenchymal transition (Fig. 9D,I; Markwald et al., 1990). The differentiation of the endocardium was not affected in *N-myc*<sup>9a/BRP</sup> embryos, as

demonstrated by the continued expression of *flk-1* in the endocardium (compare Figs 10D,I and 8D,I). The *N-myc*<sup>9a/BRP</sup> genotype also did not prevent the differentiation of cardiac myocytes in the myocardium, as indicated by the strong expression of  $\alpha$ -cardiac actin in both the compact and trabecular layers of the mutant myocardium (compare Figs 10C,H and 9C,H).

The finding that reduction in *N-myc* expression in the compact layer of the heart caused a myocyte hypoplasia evident at 12.5 days p.c. was interesting, in that overexpression of the closely related *c-myc* proto-oncogene in the heart of transgenic mice has been described to cause a hyperplasia of the myocytes which is also evident during development (Jackson et al., 1990). The normal expression pattern of *c-myc* in the heart has not been described, so the relative roles of these two genes in myocyte proliferation in vivo was not clear. Fig. 9E,J demonstrates that *c-myc* is expressed at low levels in the heart, and that its pattern of expression is different, and to some extent complementary to that of *N-myc*. While *N-myc* is expressed in the compact layer of the ventricular myocardium, *c-myc* expression is largely restricted to cells adjacent to and on the outside of the compact layer, and to isolated cells or clusters of cells adjacent to and on the inside of the compact layer. The expression on the outer surface of the heart is similar to that of *flk-1* (Fig. 8D,I) and probably represents expression in the capillaries that run between the myocardium and epicardium (Viragh and Challice, 1981). The small foci of grains on the inner surface of the myocardium also appears to represent *c-myc* expression in endocardial cells, as they are found specifically in the vicinity of red-blood-cell-containing capillaries. *c-myc* mRNA was also observed in endothelial cells lining the endocardial cushion. *c-myc* is only expressed at low levels in the myocardium itself, in spite of the fact that when it is expressed ectopically in the myocardium it causes myocytic hyperplasia (Jackson et al., 1990). In *N-myc*<sup>9a/BRP</sup> hearts, the expression of *c-myc* did not appear to be affected (Fig. 10E,J).

#### Other tissues

Careful examination of *N-myc*<sup>9a/BRP</sup> embryos between 10.5 and 14.5 days p.c. gave no evidence of defects in the kidney or brain, both of which are major sites of *N-myc* expression in the embryo, and both of which are affected in *N-myc*<sup>BRP/BRP</sup> embryos (Stanton et al., 1992; Charron et al., 1992). In four *N-myc*<sup>9a/BRP</sup> embryos that survived until 14.5 days p.c., the kidneys were small but were structurally normal (not shown). *N-myc*<sup>BRP/BRP</sup> mice have also been described as having reduced genital ridges (Stanton et al., 1992) and cranial and spinal ganglia. However, these structures were indistinguishable in *N-myc*<sup>9a/BRP</sup> embryos from those of their wild-type littermates (not shown).

#### DISCUSSION

We have generated mice that carry two different mutant alleles of the *N-myc* proto-oncogene in order to identify functions for *N-myc* that were not revealed in mice homozygous for each mutation individually. The *N-myc*<sup>9a</sup> allele is a leaky mutation which in the homozygous condition causes perinatal lethality due to a defect early in lung branching

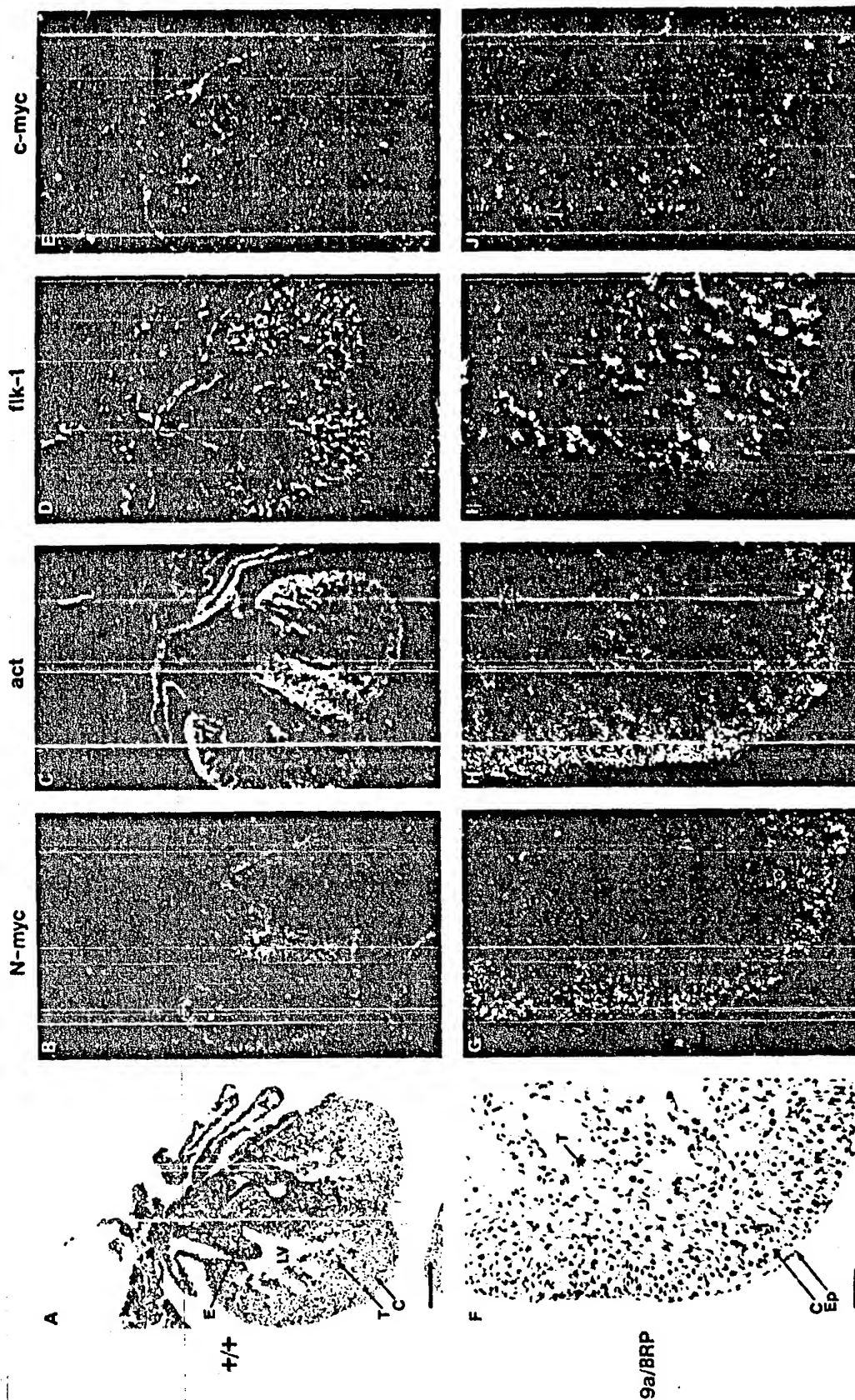


Fig. 9. Expression of N-myc, *flk-1* and c-myc in the wild-type heart at 12.5 days p.c. (A) Bright-field photomicrograph of a hematoxylin and eosin-stained frontal section in the region of the left atrioventricular canal. (F) High power magnification of the section shown in A, through the ventricle. (B-E) Dark-field photomicrographs of serial sections hybridized to the RNA probes shown above. (G-I) High power detail of the sections shown in B-E. Act,  $\alpha$ -cardiac actin; A, atrium; C, compact layer; E, endocardial cushion; Ep, epicardium; LV, left ventricle; T, trabeculae. For A-E, bar, 200  $\mu$ m; for F-I, bar, 50  $\mu$ m.

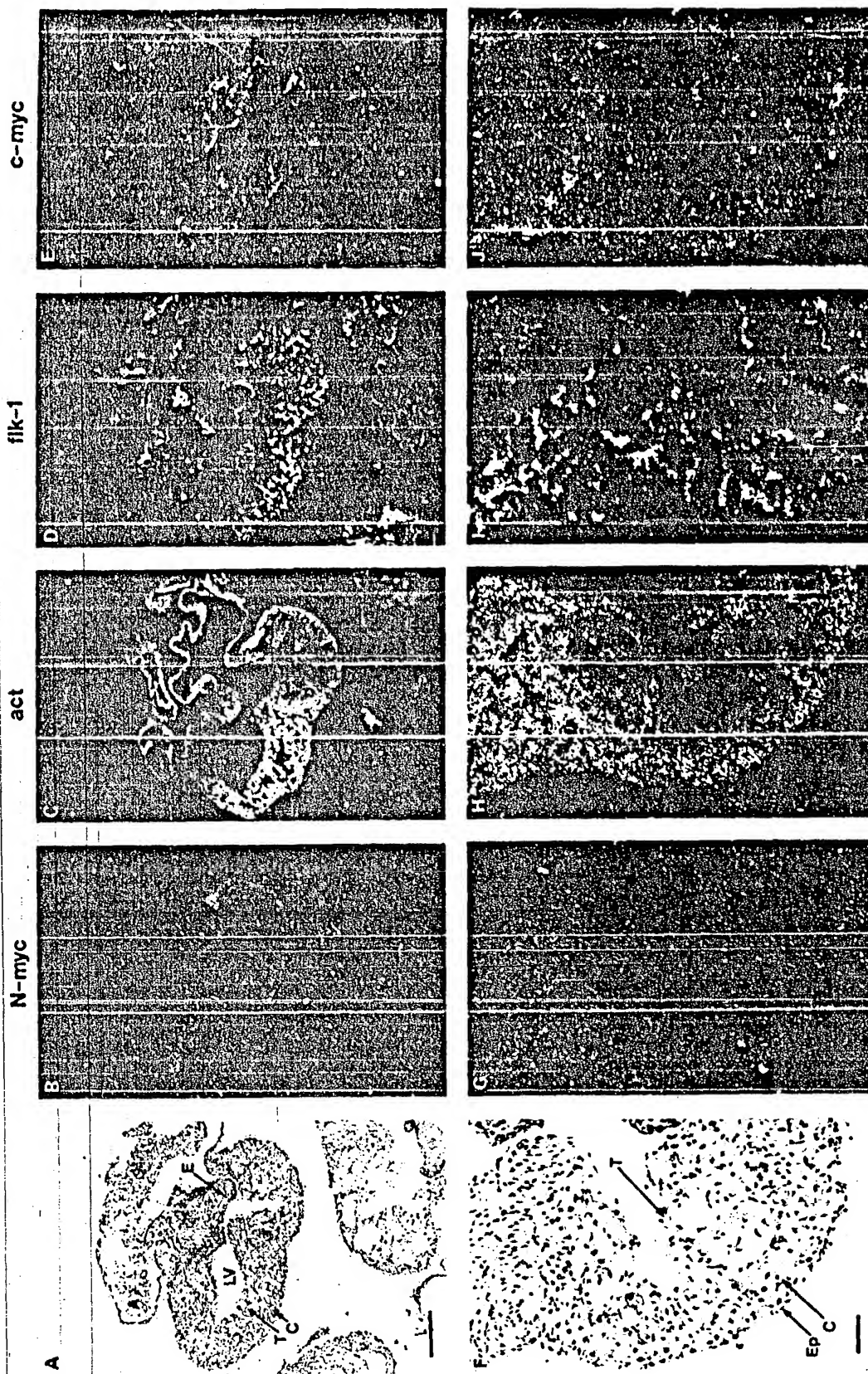


Fig. 10. Expression of N-myc,  $\alpha$ -cardiac actin, *flk-1* and *c-myc* in compound heterozygote N-myc<sup>0/0B6</sup> heart at 12.5 days p.c. (A) Bright-field photomicrograph of a hematoxylin and eosin-stained frontal section in a region comparable to that shown in Fig. 9. (F) High power magnification of the section shown in A, through the ventricle. (B-E) Dark-field

photomicrographs of serial sections hybridized to the RNA probes shown. (G-J) High power detail of the sections shown in B-E. Act,  $\alpha$ -cardiac actin; A, atrium; C, compact layer; E, endocardial cushion; Ep, epicardium; LV, left ventricle; T, trabeculae. For A-E, bar, 200  $\mu$ m, for F-J, bar, 50  $\mu$ m



morphogenesis. The levels of residual N-Myc protein (approximately 25% of normal levels) are presumably sufficient to support the normal development of other tissues in which N-myc normally functions. The N-myc<sup>BRP</sup> allele is likely to be a mutation, which, in the homozygous condition, results in embryonic lethality at approximately 11.5 days p.c., at which point the epithelial component of the mesonephros, brain, lung, stomach and intestine are all hypoplastic (Stanton et al., 1992). The phenotype of N-myc<sup>9a/BRP</sup> compound heterozygotes is intermediate to the two homozygous mutant phenotypes, consistent with the observation that the N-myc<sup>9a/BRP</sup> heterozygotes contain lower levels of N-Myc protein than are present in N-myc<sup>9a/9a</sup> embryos. N-myc<sup>9a/BRP</sup> embryos die between 12 and 15 days p.c., and a number of tissues that are affected in N-myc<sup>BRP/BRP</sup> homozygotes, such as the kidney, brain and cranial and spinal sensory ganglia, appear to be normal. The lungs, which are the main organ affected in N-myc<sup>9a/9a</sup> homozygotes, are even more severely affected in N-myc<sup>9a/BRP</sup> embryos. Compound heterozygotes also showed a defect in the development of the compact subepicardial layer of the heart, and appeared to die from a failure of heart function caused by a hypoplasia of ventricular myocytes in the compact layer. These results indicate a critical role for N-myc in the development of the heart.

#### N-myc in heart development

The reduced levels of N-Myc protein found in N-myc<sup>9a/BRP</sup> embryos result in a considerable thinning of the subepicardial compact layer of the myocardium by 12.5 days of development. Consistent with this phenotype, N-myc expression is expressed much more strongly in the compact layer of the heart at 10.5 and 12.5 days p.c. than in the trabecular layer of the myocardium or in the endothelium. Trabeculation, or formation of the myocardial projections that form a lattice of contractile cells throughout much of the ventricles of the embryonic heart, occurs early during heart development in the mouse, beginning around day 9.5 of gestation (Chalice and Viragh, 1973). By a number of ultrastructural and cytochemical criteria, the myocytes within the trabeculae are more highly differentiated than the myocytes in the compact layer (Rumyantsev, 1991). Thus compact layer myocytes are more basophilic and richer in RNA, while trabecular myocytes contain more mitochondria, ribosomes and granular endoplasmic reticulum. Myofibrils in trabecular myocytes are thicker and more highly organized than in compact layer myocytes, where myofibrils are present but are scattered randomly relative to one another in the cytoplasm. Consistent with this picture is the observation that the rate of cell proliferation in the compact layer is 2- to 3-fold higher than in the trabeculae (Rumyantsev, 1977; Tokuyasu, 1990). The highly differentiated myocytes in the trabecular layer have been postulated to be responsible for the early beating of the heart while, at later stages, the thickened compact layer becomes the major contractile force. The cardiac hypoplasia that we observe in N-myc<sup>9a/BRP</sup> embryos is more apparent in the compact layer. This may explain our observation that embryonic lethality does not occur until later during heart development, when heart function may depend more on the compact layer than on the trabecular layer.

Our observation of N-myc expression in the compact layer and the absence of development in the compact layer in N-myc<sup>9a/BRP</sup> mice suggests that N-myc is required either for the proliferation of myocytes in the compact layer, and/or for preventing the differentiation of these cells, although there are other possible explanations, such as that they are dying prematurely. The simplest explanation is the former. However, the second hypothesis, in which N-myc expression prevents the terminal differentiation of compact layer myocytes into trabecular-type myocytes, is consistent with previous descriptions of N-myc expression in the embryo, in which N-myc expression is correlated with cells in an undifferentiated state in the kidney, brain and skin, regardless of their proliferative state, and the further differentiation of these cells is correlated with down-regulation of N-myc (Mugrauer et al., 1988).

In their description of embryos homozygous for a null mutation in N-myc, Charron et al. (1992) noted a defect in the development in the heart, visible as early as 9.5 days p.c., in which development was apparently slowed as evidenced by the absence of endocardial cushion tissue and of interatrial and interventricular septa. It was postulated that N-myc is involved in the generation of the inductive signal sent by the myocardium to the endocardium to induce the epithelial-to-mesenchymal transition of the endocardium, which forms these anlagen of the cardiac valves and septa. Our results confirm a function for N-myc in the development in the heart, but tend to support a role for N-myc within the myocardium itself, although this could presumably have a secondary impact on endocardial differentiation in more severe mutants. We have not observed defects in the formation of septal or endocardial cushion tissue in N-myc<sup>9a/BRP</sup> embryos.

#### c-myc in heart development

When c-myc is overexpressed in the heart of RSV/c-myc transgenic mice, these mice develop a fetal cardiac myocyte hyperplasia and at birth have more than twice the normal number of cardiac myocytes (Jackson et al., 1990). This has suggested that endogenous c-myc may play a role in cardiac myocyte proliferation in vivo. However, we have demonstrated that c-myc is only expressed at low levels in the heart at 12.5 days p.c. and that this expression is largely in endothelial cells and not in the myocardium. Background levels of c-myc expression in the heart were also observed in mouse embryos at 13.5 days p.c. (Stanton et al., 1992) and in first trimester human embryos (Pfeifer-Ohlsson et al., 1985). N-myc, in contrast, is expressed at high levels in the compact layer of the ventricular myocardium at 10.5 and 12.5 days. Combined with the hypoplasia of the myocardium that we have observed in N-myc<sup>9a/BRP</sup> embryos, these data suggest that N-myc rather than c-myc may play a primary role in the regulation of proliferation and/or differentiation of ventricular myocytes during heart development, and that the effect of c-myc in these transgenic mice may reflect the possibility that in this instance c-myc can mimic the normal effects of N-myc. It has previously been observed that different myc family genes can cause the same tumour types in transgenic mice when they are overexpressed using identical promoters, even though this expression may be ectopic (Rosenbaum et al., 1989; Dildrop

et al., 1989; Adams et al., 1985). Furthermore, high levels of expression of one *myc* gene in transgenic mice can repress transcription of itself and of other *myc* genes (Rosenbaum et al., 1989; Dildrop et al., 1989; Adams et al., 1985). These results have suggested that at high levels, the various *myc* genes may be able to mimic each other's effects on downstream targets. This hypothesis has been strengthened by the observations that N-Myc and c-Myc proteins bind the same core DNA sequence in vitro, and that N-, L- and c-myc all form heterodimers with Max in vivo (Blackwood et al., 1992; Wenzel et al., 1991; Mukherjee et al., 1992), and all transform cells in culture through their interaction with Max (Mukherjee et al., 1992). We are presently crossing RSV/c-myc mice with the N-myc mutant mice to generate N-myc<sup>9a/BRP</sup> embryos that also express this c-myc transgene in the heart. If c-myc in these transgenics truly mimicks the normal role of N-myc, the cardiac myocyte hypoplasia of compound heterozygous embryos is expected to be rescued by the transgene.

Recently, Davis et al. (1993) have described the phenotype of mice that bear a null mutation in c-myc. These embryos die before 10.5 days p.c. and exhibit, among other abnormalities, an enlargement of the heart and a dilated, fluid-filled pericardium. This is unexpected in light of the observation, described above, that mice with ectopic expression of c-myc in the heart have enlarged hearts. However, it is still unclear whether the heart abnormality in the c-myc null mutants is a direct result of the mutation or is secondary to other defects that are causing the embryo to die.

In spite of the possibility that c-myc expression may be able to replace N-myc function, we observe no up-regulation of c-myc in either the compact layer of the myocardium or in the lung epithelium of N-myc<sup>9a/BRP</sup> mice. This may be because cross-regulation of the *myc* family genes does not normally occur in these tissues as it does when they are overexpressed in transformed cells or in transgenic mice. Stanton et al. (1992) showed that c-myc is expressed in the telencephalon of N-myc<sup>BRP/BRP</sup> embryos, and this observation was interpreted to indicate cross regulation of N-myc and c-myc in the neuroepithelium.

### N-myc in lung development

Mice homozygous for the N-myc<sup>9a</sup> mutation die at birth due to a defect in lung morphogenesis which is visible as early as 12.5 days p.c. (Moens et al., 1992). We have postulated that N-myc is required for the lung epithelium to respond to local inductive signals emanating from the lung mesenchyme, which cause branching to occur. N-myc<sup>9a/BRP</sup> embryos have more severely affected lungs, with only a rudimentary branching pattern at 12.5 days. However, the earliest events of lung development, in which two buds are induced to grow from the trachea by surrounding mesenchyme (Spooner and Wessells, 1970), occur normally in N-myc<sup>9a/BRP</sup> and indeed in N-myc<sup>BRP/BRP</sup> embryos (Stanton et al., 1992). We and others (Hirning et al., 1991; Moens et al., 1992) have shown that N-myc is expressed in the lung epithelium and, further, that expression is largely restricted to bronchioles and is present at very low levels in the trachea and bronchi. These results suggest that N-myc is involved in branching morphogenesis in the lung but not in the initial

induction of budding of the tracheal epithelium. Experimental manipulations in vitro have suggested that there are different mechanisms for budding versus branching of the lung epithelium. A number of different stimuli, including salivary gland mesenchyme and bronchial mesenchyme, can induce supernumerary buds in tracheal epithelium, but only bronchial mesenchyme is able to induce those buds to branch (Wessells, 1970; Spooner and Wessells, 1970). The phenotypes of mice bearing mutations in N-myc provide genetic evidence for such a mechanism for lung development and provide a candidate gene that is involved in the control of one process (branching) and not the other (budding).

### Tissue-specific effects of N-myc mutant alleles

Only a subset of the tissues that normally express N-myc are visibly affected in N-myc<sup>9a/BRP</sup> embryos. N-myc<sup>9a/9a</sup> embryos have approximately 25% of wild-type levels of N-Myc protein and, in these embryos, the lungs and spleen are the only tissues affected (Moens et al., 1992). N-myc<sup>9a/BRP</sup> embryos have approximately 15% of wild-type levels of N-Myc protein and, in these embryos, the heart is also affected. However, 15% of normal levels of N-Myc protein appear to be sufficient for normal genitourinary and nervous system development. The molecular basis for this remains to be determined. It is possible that different tissues within the embryo make different amounts of normal protein relative to the amounts in wild-type embryos. We have previously attempted to correlate the relative levels of normal N-myc mRNA in different tissues of N-myc<sup>9a/9a</sup> embryos with the presence or absence of a mutant phenotype (Moens et al., 1992) and, although there were differences among the tissues examined, no strong correlation could be established. Another explanation for the tissue-specific effects of N-myc mutant alleles is that different tissues are affected differently by approximately the same reduction in N-Myc protein because of differences in the ratio of N-Myc protein to Max (Blackwood and Eisenman, 1991), to Max-associated proteins such as Mad and Mxi1 (Ayer et al., 1993; Zervos et al., 1993), or to other Myc proteins.

Myc proteins require dimerization with Max for DNA binding (Blackwood and Eisenman, 1991; Prendergast and Ziff, 1991; Kato et al., 1992). A number of lines of evidence have suggested that Max overexpression can inhibit transformation (Mukherjee et al., 1992; Makela et al., 1992; Prendergast et al., 1992) and transactivation (Kretzner et al., 1992; Amati et al., 1992) by *myc* genes. Mad, cloned by virtue of its ability to dimerize with Max, has been shown to compete with Myc for binding to Max, and to thereby inhibit transactivation by Myc (Ayer et al., 1993). Mxi1 (Zervos et al., 1993) and other, as yet unidentified, Max partners presumably act in a similar manner and are also likely thereby to inhibit N-myc function. Also, L-Myc, a poorly transforming member of the Myc family, has been shown to prevent transformation by other *myc* genes, presumably by competing for and forming less active DNA-bound complexes with Max (Mukherjee et al., 1992). In cell types where a number of Max-associated and Myc proteins compete with N-Myc protein for dimerization with Max and sites on DNA, an 85% reduction in N-Myc protein is expected to reduce the response of downstream targets of N-

Myc more strongly than in cells where there are no competitors for Max binding. Interestingly, L-myc is co-expressed with N-myc in the lung, perhaps in the same cell type (Zimmerman et al., 1986), but the two genes are not co-expressed in the lung (Mugrauer and Ekblom, 1991), where neither the N-myc<sup>+/+</sup> nor the N-myc<sup>+/HRP</sup> embryos have an abnormal phenotype. It will be interesting to compare the detailed expression patterns of the various interacting factors with the tissues affected by the N-myc mutations.

### Conclusions

We have generated a third N-myc mutant phenotype by combining leaky and null alleles in a compound heterozygote. These mice have allowed us to study the function of N-myc at a stage in development that is not reached in embryos homozygous for the null allele (Stanton et al., 1992) and that is not affected in embryos homozygous for the leaky allele (Moens et al., 1992). Classical genetic studies of development in a number of systems have demonstrated the importance of studying the phenotypic effects of different mutant alleles and combinations of mutant alleles in a given gene in order to determine its multiple roles in the course of development. Our results have shown that the technique of gene targeting by homologous recombination in the mouse can be used to the same ends. The clear delineation of a function for N-myc in both lung branching morphogenesis and myocardial development also provides target tissues in which to search for the elusive downstream genes in the N-myc signaling pathway.

### Note added after acceptance

Recently, a third description of embryos homozygous for a putative null allele of N-myc has been published (Sawai et al., 1993). The overall phenotype of these mutant embryos is very similar to those described by Stanton et al. (1992) and Charron et al. (1992), but the defect in heart development is shown to be primarily in the myocardium.

We wish to thank Dr R. Kennett for the anti-N-myc antibody, Dr M. Buckingham for the  $\alpha$ -cardiac actin probe, T. Yamaguchi for the *flk-1* probe, Dr C. Asselin for the c-myc probe and Dr R. DePinho for the N-myc genomic clone from which probes for RNA in situ hybridization were subcloned. Our gratitude also to Dr Arch Perkins for his help in the phenotypic analysis of N-myc<sup>+/HRP</sup> mutants, to Alexandra Joyner for her critical reading of the manuscript, and to Valerie Pridoux, Chi-Chong Hui, Benny Miro and Ester Ivanyi for their generous assistance in various aspects of this work. This work was supported by a Terry Fox program project grant from the National Cancer Institute of Canada. C. B. M. was supported by a Natural Sciences and Engineering Research Council of Canada 'Centennial' Scholarship and a Medical Research Council of Canada Studentship. J. R. is an International Scholar of the Howard Hughes Medical Institute and a Terry Fox Cancer Research Scientist of the National Cancer Institute of Canada. B. R. S. and L. F. P. are sponsored by the NCI-DHHS under contract NO1-CO-74101 with ABL.

### REFERENCES

Adams, J. M., Harris, A. W., Pinkert, C. A., Corenran, L. M., Alexander, W. S., Cory, S., Palmiter, R. D. and Brinster, R. L. (1985).

The c-myc oncogene driven by immunoglobulin enhancers induces lymphoid malignancy in transgenic mice. *Nature* 318, 533-538.

Alex, R., Swezari, O., Meyer, S. and Dildrop, R. (1992). Determination of the DNA sequence recognized by the bHLH-zip domain of the N-Myc protein. *Nucleic Acids Res.* 20, 2257-2263.

Amati, B., Dalton, S., Brooks, M. W., Littlewood, T. D., Evan, G. I. and Land, H. (1992). Transcriptional activation by the human c-Myc oncoprotein in yeast requires interaction with Max. *Nature* 359, 421-426.

Amati, B., Brooks, M. W., Levy, N., Littlewood, T. D., Evan, G. I. and Land, H. (1993). Oncogenic activity of the c-Myc protein requires dimerization with Max. *Cell* 72, 233-245.

Ayer, D. E., Kretzner, L. and Eisenman, R. N. (1993). Max: a heterodimeric partner for Myc that antagonizes Myc transcriptional activity. *Cell* 72, 211-222.

Barrett, J., Mirer, M. J., Kato, G. J., Dosaka-Akita, H. and Dang, C. V. (1992). Activation domains of L-Myc and c-Myc determine their transforming potencies in rat embryo cells. *Mol. Cell Biol.* 12, 3130-3137.

Blackwell, T. K., Kretzner, L., Blackwood, E. M., Eisenman, R. N. and Weintraub, H. (1990). Sequence-specific DNA binding by the c-Myc protein. *Science* 250, 1149-1151.

Blackwood, E. M., Laeschner, B. and Eisenman, R. N. (1992). Myc and Max associate in vivo. *Genes Dev.* 6, 71-80.

Blackwood, E. M. and Eisenman, R. N. (1991). Max: a helix-loop-helix zipper protein that forms a sequence-specific DNA-binding complex with Myc. *Science* 251, 1211-1217.

Bossone, S. A., Asselin, C., Patel, A. J. and Marcu, K. B. (1992). Max, a zinc finger protein, binds to c-MYC and C2 gene sequences regulating transcriptional initiation and termination. *Proc. Natl. Acad. Sci. USA* 89, 7452-7456.

Challice, C. E. and Viragh, S. (1973). The architectural development of the early mammalian heart. *Tissue Cell* 6, 447-462.

Charron, J., Malynn, B. A., Robertson, E. J., Goff, S. P. and Alt, F. W. (1990). High-frequency disruption of the N-myc gene in embryonic stem and pre-B cell lines by homologous recombination. *Mol. Cell Biol.* 10, 1799-1804.

Charron, J., Malynn, B. A., Fisher, P., Stewart, V., Jeannotte, L., Goff, S. P., Robertson, E. J. and Alt, F. W. (1992). Embryonic lethality in mice homozygous for a targeted disruption of the N-myc gene. *Genes Dev.* 6, 2248-2257.

Davis, A. C., Wims, M., Spotts, G. D., Hann, S. R. and Bradley, A. (1993). A null c-myc mutation causes lethality before 10.5 days of gestation in homozygotes and reduced fertility in heterozygous female mice. *Genes Dev.* 7, 671-682.

DePinho, R. A., Legoux, E., Feldman, J. B., Kohl, N. E., Yancopoulos, G. D. and Alt, F. W. (1986). Structure and expression of the murine N-myc gene. *Proc. Natl. Acad. Sci. USA* 83, 1827-1831.

DePinho, R. A., Schreiber-Agus, N. and Alt, F. W. (1991). myc family oncogenes in the development of normal and neoplastic cells. *Adv. Cancer Res.* 57, 1-46.

Dildrop, R., Ma, A., Zimmerman, K., Hsu, E., Tesfaye, A., DePinho, R. A. and Alt, F. W. (1989). IgH enhancer-mediated deregulation of N-myc gene expression in transgenic mice: generation of lymphoid neoplasias that lack c-myc expression. *EMBO J.* 8, 1121-1128.

Frohman, M. A., Boyle, M. and Martin, J. R. (1990). Isolation of the mouse Hox-2.9 gene: Analysis of embryonic expression suggests that positional information along the anterior-posterior axis is specified by mesoderm. *Development* 110, 589-607.

Garrell, J. and Campuzano, S. (1991). The helix-loop-helix domain: A common motif for bristles, muscles and sex. *BioEssays* 13, 493-498.

Hirning, U., Schmid, P., Schulz, W. A., Rettenberger, G. and Hamelster, H. (1991). A comparative analysis of N-myc and c-myc expression and cellular proliferation in mouse organogenesis. *Mech. Dev.* 33, 119-126.

Ikegaki, N., Bukovsky, J. and Kennett, R. H. (1986). Identification and characterization of the NMYC gene product in human neuroblastoma cells by monoclonal antibodies with defined specificities. *Proc. Natl. Acad. Sci. USA* 83, 5929-5933.

Ikegaki, N. and Kennett, R. H. (1989). Glutaraldehyde fixation of the primary antibody-antigen complex on nitrocellulose paper increases the overall sensitivity of immunoblot assay. *J. Immunol. Met.* 124, 205-210.

Jackson, T., Allard, M. F., Sreenan, C. M., Doss, L. K., Bishop, S. P. and Swain, J. L. (1990). The c-myc proto-oncogene regulates cardiac development in transgenic mice. *Mol. Cell Biol.* 10, 3709-3716.

Kato, G. J., Barrett, J., Villa-Garcia, M. and Dang, C. V. (1990). An

- amino-terminal c-Myc domain required for neoplastic transformation activates transcription. *Mol. Cell Biol.* 10, 5914-5920.
- Kato, G. J., Lee, W. M. F., Chen, L. and Dang, C. V. (1992). Max: Functional domains and interaction with c-Myc. *Genes Dev.* 6, 81-92.
- Kato, K., Kanamori, A., Wakamatsu, Y., Sawal, N. and Kondoh, H. (1991). Tissue distribution of N-myc expression in the early organogenesis period of the mouse embryo. *Dev. Growth Diff.* 33, 29-36.
- Kohl, N. E., Kanda, N., Schrenck, R. R., Bruns, G., Latt, S. A., Gilbert, F. and Alt, F. W. (1983). Transposition and amplification of oncogene-related sequences in human neuroblastomas. *Cell* 35, 359-367.
- Kretzner, L., Blackwood, E. M. and Eisenman, R. N. (1992). Myc and Max proteins possess distinct transcriptional activities. *Nature* 359, 426-429.
- Lee, W. H., Murphree, A. J. and Benedict, W. F. (1984). Expression and amplification of the N-myc gene in primary retinoblastoma. *Nature* 309, 458-460.
- Makela, T. P., Koskinen, P. J., Vastrik, I. and Allitalo, K. (1992). Alternative forms of Max as enhancers or suppressors of Myc-Ras cotransformation. *Science* 256, 373-377.
- Markwald, R. R., Mjaatvedt, C. H., Krug, E. L. and Sinning, A. R. (1990). Inductive interactions in heart development: role of cardiac adherens in cushion tissue formation. *Ann. NY Acad. Sci.* 588, 13-25.
- Millauer, B., Witzmann-Voss, S., Schenck, H., Martinez, R., Moller, N. P. H., Risau, W. and Ullrich, A. (1993). High affinity VEGF binding and developmental expression suggest Flk-1 as a major regulator of vasculogenesis and angiogenesis. *Cell* 72, 835-846.
- Moens, C., Bernicot, Auerbach, A. B., Conlon, R. A., Joyner, A. I. and Rossant, J. (1992). A targeted mutation reveals a role for N-myc in branching morphogenesis in the embryonic mouse lung. *Genes Dev.* 6, 691-704.
- Mugrauer, G., Alt, F. W. and Ekblom, P. (1988). N-myc proto-oncogene expression during organogenesis in the developing mouse as revealed by *in situ* hybridization. *J. Cell Biol.* 107, 1325-1335.
- Mugrauer, G. and Ekblom, P. (1991). Contrasting expression patterns of three members of the myc family of protooncogenes in the developing and adult mouse kidney. *J. Cell Biol.* 112, 13-25.
- Mukherjee, B., Murgens, S. D. and DePinho, R. A. (1992). Myc family oncoproteins function through a common pathway to transform normal cells in culture: cross-interference by Max and trans-acting dominant mutants. *Genes Dev.* 6, 1480-1492.
- Nau, M. M., Brooks, B. J., Jr., Carney, D. N., Gazdar, A. F., Battey, J. F., Sausville, E. A. and Minna, J. D. (1986). Human small-cell lung cancers show amplification and expression of the N-myc gene. *Proc. Natl. Acad. Sci. USA* 83, 1092-1096.
- Nisen, P. D., Zimmerman, K., Cotter, S. V., Gilbert, F. and Alt, F. W. (1986). Enhanced expression of the N-myc gene in Wilms' tumours. *Cancer Res.* 46, 6217-6222.
- Pfeifer-Ohlsson, S., Rydner, J., Goustin, A. S., Larsson, E., Betsholtz, C. and Ohlsson, R. (1985). Cell-type-specific pattern of myc protooncogene expression in developing human embryos. *Proc. Natl. Acad. Sci. USA* 82, 5030-5034.
- Prendergast, G. C., Lawe, D. and Ziff, E. B. (1991). Association of Myc, the murine homolog of Max, with c-Myc stimulates methylation-sensitive DNA binding and Ras cotransformation. *Cell* 65, 395-407.
- Prendergast, G. C., Hopewell, R., Gorham, B. J. and Ziff, E. B. (1992). Biphasic effect of Max on Myc cotransformation activity and dependence on amino- and carboxy-terminal Max functions. *Genes Dev.* 6, 2429-2439.
- Prendergast, G. C. and Ziff, E. B. (1991). Methylation-sensitive sequence-specific DNA binding by the c-myc basic region. *Science* 251, 186-189.
- Resar, L. M. S., Dolde, C., Barrett, J. F. and Dang, C. V. (1993). B-myc inhibits neoplastic transformation and transcriptional activation by c-myc. *Mol. Cell Biol.* 13, 1130-1136.
- Rosenbaum, H., Webb, E., Adams, J. M., Cory, S. and Harris, A. W. (1989). N-myc transgene promotes B lymphoid proliferation, elicits lymphomas and reveals cross-regulation with c-myc. *EMBO J.* 8, 749-755.
- Rumyantsev, P. P. (1977). Interrelations of the proliferation and differentiation processes during cardiac myogenesis and regeneration. *Int. Rev. Cytol.* 51, 187-273.
- Rumyantsev, P. P. (1991). *Growth and Hyperplasia of Cardiac Muscle Cells*. London: Harwood Academic Publishers.
- Sassoon, D. A., Garner, I. and Buckingham, M. (1988). Transcripts of  $\alpha$ -cardiac and  $\alpha$ -skeletal actins are early markers for myogenesis in the mouse embryo. *Development* 104, 155-164.
- Sawal, S., Shlimon, A., Hanaoka, K. and Kondoh, H. (1991). Embryonic lethality resulting from disruption of both N-myc alleles in mouse zygotes. *New Biologist* 3, 861-869.
- Sawal, S., Shlimon, A., Wakamatsu, Y., Palmer, C., Hanaoka, K. and Kondoh, H. (1993). Defects of embryonic organogenesis resulting from targeted disruption of the N-myc gene in the mouse. *Development* 117, 1445-1455.
- Schwab, M., Allitalo, K., Klempner, K., Varmus, H. E., Bishop, J. M., Gilbert, F., Brodeur, G. M., Boldstein, M. and Trent, J. (1983). Amplified DNA with limited homology to myc cellular oncogene is shared by human neuroblastoma cell lines and a neuroblastoma tumour. *Nature* 305, 245-248.
- Spooner, B. S. and Wessells, N. K. (1970). Mammalian lung development: interactions in primordium formation and bronchial morphogenesis. *J. Exp. Zool.* 175, 445-454.
- Stanton, B. R., Reid, S. W. and Parada, L. F. (1990). Germ line transmission of an inactive N-myc allele generated by homologous recombination in mouse embryonic stem cells. *Mol. Cell Biol.* 10, 6755-6756.
- Stanton, B. R., Perkins, A. S., Tessarollo, L., Sassoon, D. A. and Parada, L. F. (1992). Loss of N-myc function results in embryonic lethality and failure of the epithelial component of the embryo to develop. *Genes Dev.* 6, 2235-2247.
- Tokuyasu, K. T. (1990). Co-development of embryonic myocardium and myocardial circulation. In *Developmental Cardiology: Morphogenesis and Function* (ed. E. B. Clark and A. Takao), pp. 205-218. Mount Kisco, NY: Futura Publishing Co., Inc.
- Viragh, S. and Challice, C. E. (1981). The origin of the epicardium and the embryonic myocardial circulation in the mouse. *Anat. Rec.* 201, 157-168.
- Wenzel, A., Czepluch, C., Hamann, U., Schuermann, J. and Schwab, M. (1991). The N-myc oncoprotein is associated *in vivo* with the phosphoprotein Max(p2022) in human neuroblastoma cells. *EMBO J.* 10, 3703-3712.
- Wessells, N. K. (1970). Mammalian lung development: interactions in the formation and morphogenesis of tracheal buds. *J. Exp. Zool.* 175, 455-466.
- Wong, A. J., Ruppert, J. M., Eggleston, J., Hamilton, S. R., Baylin, S. B. and Vogelstein, B. (1986). Gene amplification of c-myc and N-myc in small cell carcinoma of the lung. *Science* 233, 461-464.
- Yamaguchi, T. P., Dumont, D. J., Conlon, R. A., Breitman, M. and Rossant, J. (1993). Flk-1, a flt-1-related receptor tyrosine kinase is an early marker for heart and blood for endothelial cell precursors. *Development* in press.
- Zervos, A. S., Gyuris, J. and Brent, R. (1993). Max, a protein that specifically interacts with Myc to bind Myc-Max recognition sites. *Cell* 72, 223-232.
- Zimmerman, K., Vancopoulos, G. D., Collum, R. G., Smith, R. K., Kohl, N. E., Denis, K. A., Nau, M. M., Witte, O. N., Toran-Allerand, D., Gee, C. E., Minna, J. D. and Alt, F. W. (1986). Differential expression of myc family genes during murine development. *Nature* 319, 780-783.

(Accepted 30 June 1992)

## REVIEW

AV

Randall Wade Moreadith · Nina Butwell Radford

**Gene targeting in embryonic stem cells:  
the new physiology and metabolism**

Received: 28 June 1996 / Accepted: 4 October 1996

**Abstract** The development of transgenic technology, whereby genes (or mutations) can be stably introduced into the germline of experimental mammals, now allows investigators to create mice of virtually any genotype and to assess the consequences of these mutations in the context of a developing and intact mammal. In contrast to traditional “gain-of-function” mutations, typically created by microinjection of the gene of interest into the one-celled zygote, gene targeting via homologous recombination in pluripotent embryonic stem cells allows one to modify *precisely* the gene of interest. The purpose of this review is to introduce the reader to the history of development of embryonic stem cell technology, the current methods employed to create “knock-out” mice, and the application of these methods to solve problems in biology. While the technology promises to provide enormous insight into mammalian development genetics, our desire is that this review will stimulate the application of gene targeting in embryonic stem cells to begin to unravel problems in complex regulatory pathways, specifically intermediary metabolism and physiology.

**Key words** Gene targeting · Transgenic animals · Molecular biology · Metabolism · Physiology

**Abbreviations** *EC cell* Embryonal carcinoma cell · *ES cell* Embryonic stem cell · *HPRT* Hypoxanthine phosphoribosyltransferase · *NMR* Nuclear magnetic resonance

**Introduction**

The development of techniques for introducing genes (or mutations) stably into the germline of experimental

mammals [1], referred to as “transgenic technology,” has provided unique insight into complex biologic phenomena. Although simplistic, this technology can now be broadly defined into two experimental categories: “gain-of-function” mutations, typically created by microinjection of the gene (transgene) of interest directly into the zygote stage of development (for example, to define the controlling elements for a muscle-specific gene), and “loss-of-function” mutations, which employ embryonic stem (ES) cells. The technique of DNA microinjection results in *random integration* of the transgene, giving rise to the founder animal(s). The founder animals are then bred individually to establish independent lines of transgenic animals that can undergo further characterization [e.g., pattern(s), levels and consequences of expression of the transgene]. However, many of these lines exhibit variable expression of the gene of interest since the transgene may integrate in a manner that alters its expression (for example, by integration near controlling elements that affect the pattern and level of expression), and this may confound the interpretation of results.

In contrast, the development of gene targeting via homologous recombination in pluripotent ES cells allows one to modify *precisely* the gene of interest. It is now possible to create mice of virtually any genotype, and to assess the consequences of these mutations in the context of a developing and intact mammal. This technology, which is typically used to create the null genotype (“knock-out” mice), has frequently provided the definitive experimental evidence regarding the functions of the encoded proteins. However, in many instances these mutations have changed the prevailing notions. For example, gene targeting at the endothelin loci subsequently led to the creation of mice with Hirschsprung’s disease (aganglionic megacolon [2]) instead of the anticipated phenotype (abnormal control of blood pressure). Indeed, if one had even predicted these mice would survive the absence of a cellular gene that is so widely expressed, one might have been in the minority!

The purpose of this review is to introduce the reader to the history of development of ES technology, the cur-

R.W. Moreadith (✉) · N.B. Radford  
Molecular Cardiology Laboratories, 5323 Harry Hines Boulevard,  
University of Texas Southwestern Medical Center, Dallas,  
TX 75235-8573, USA

*Present address:*

<sup>1</sup> Quintiles, Inc., 1007 Slater Road, Morrisville, NC 27707, USA



rent methods employed to create "knock-out" mice, and the application of these methods to solve problems in biology. While the technology promises to provide enormous insight into mammalian development genetics, our desire is that this review will stimulate the application of gene targeting in ES cells to begin to unravel problems in complex regulatory pathways, specifically intermediary metabolism and physiology.

## Historical development

### Derivation and characterization of pluripotent stem cells

The development of gene-targeting technology in ES cells is an example of the convergence of classical cell biology with molecular biology. One of the seminal papers was published in 1975 by Mintz and colleagues at the Fox Chase Cancer Center [3]. It was well established that explantation of normal mouse embryos into extrauterine sites (typically the kidney capsule) subsequently led to the development of tumors known as teratocarcinomas. Cell lines could be derived from the tumors, passaged indefinitely in tissue culture, and when reintroduced into recipient mice gave rise to tumors with cell types representative of all germ layers (ectoderm, mesoderm, and endoderm). These properties suggested that these embryonal carcinoma (EC) cells were pluripotent, that is, capable of differentiating into a host of cell types under the appropriate conditions. In many instances these tumors contained cell types indistinguishable from the normal cellular counterpart in biochemical or ultrastructural detail. Thus, although these cells were considered to be "highly" malignant, it was quite clear that not all tissues derived from them displayed the malignant properties of the parental cells. Mintz and colleagues reasoned that these EC cells might in fact be totipotent – capable of contributing to the development of all *normal* tissues under the appropriate environmental cues "For this to occur, the initially malignant cells would presumably have to be brought into association with early embryo cells so that the latter could provide an organizational framework appropriate for normal development [3]." This was an astounding leap of logic at the time. She and her colleagues subsequently demonstrated that malignant EC cells, grown as an ascites tumor for over 8 years, could give rise to apparently normal mosaic mice upon introduction into normal blastocysts. Furthermore, the mosaic mice were capable of transmitting the EC cell genotype through the germline, that is, mating of these mosaic mice with wild-type partners gave rise to mice that were genotypically derived from the EC cells! These results, and those from many other laboratories, established the experimental basis for subsequent developments in the field. Indeed, Mintz precisely predicted the emergence of stem cell technology. "Thus, EC cells ... offer new possibilities for studying mammalian regulatory systems: the carcinoma cells

could first be experimentally mutagenized and selected during a brief *in vitro* sojourn and then cycled through mice via blastocyst injections. Participation in differentiation of a mosaic individual would permit developmental and biochemical analyses of the mutations; conversion of some cells to gametes would enable genetic analysis and mapping of the mutated regions through recombination and segregation during meiosis [3]."

These observations, made prior to the large-scale development of classical molecular biology (note that the above experiments were published prior to the development of DNA sequencing!) were quickly verified by many laboratories. However, working with EC cells proved to be quite cumbersome due to their propensity for aneuploidy, and the attention turned to isolation of pluripotent cells from *normal* embryos. Early attempts failed until 1981, when Evans and Kaufman [4] and Martin [5] independently described the growth and maintenance of euploid cells, derived from normal mouse embryos explanted in culture, that displayed pluripotent properties (hereafter referred to as ES cells). This was quickly followed by the demonstration in 1984 these cells were capable of giving rise to germline chimeras upon introduction into normal blastocysts [6]. The stage was set – one could grow normal, diploid ES cells in culture for multiple passages without loss of the ability to contribute to normal development. Furthermore, the cells contributed to the development of gametes at a high frequency (germline competence), and the haploid genomes of these cells were transmitted to the next generation. Thus, introduction of mutations in these cells offered the possibility of producing mice with a predetermined genotype.

### Homologous recombination: introduction of precise mutations into resident genes

In an elegant series of papers using mammalian cell lines [7–10], based primarily on prior work in *Saccharomyces cerevisiae*, it became clear that cloned DNA could be precisely altered *in vitro*, and when introduced into cells via a number of methods (infection, transfection) would homologously recombine with the resident gene and introduce the desired mutation at that site in the genome. In lower eukaryotes (yeast and *Neurospora*) recombination at the homologous locus is the favored reaction and can occur essentially without selection, but in higher eukaryotes (mouse and *Drosophila*) the frequency of homologous recombination is rare. This necessitates the use of *positive* selection; typically, these rare events are selected for by introduction of genes conveying resistance to otherwise toxic metabolites (hygromycin, neomycin). Note that the introduction of a positive selection marker gene is also frequently used to disrupt (mutate) the gene of interest. In addition, one can enhance the frequency of these events by employing the additional strategy of *negative* selection – most commonly performed by use of the thymidine kinase (*TK*) gene flanking the targeting vector. ES

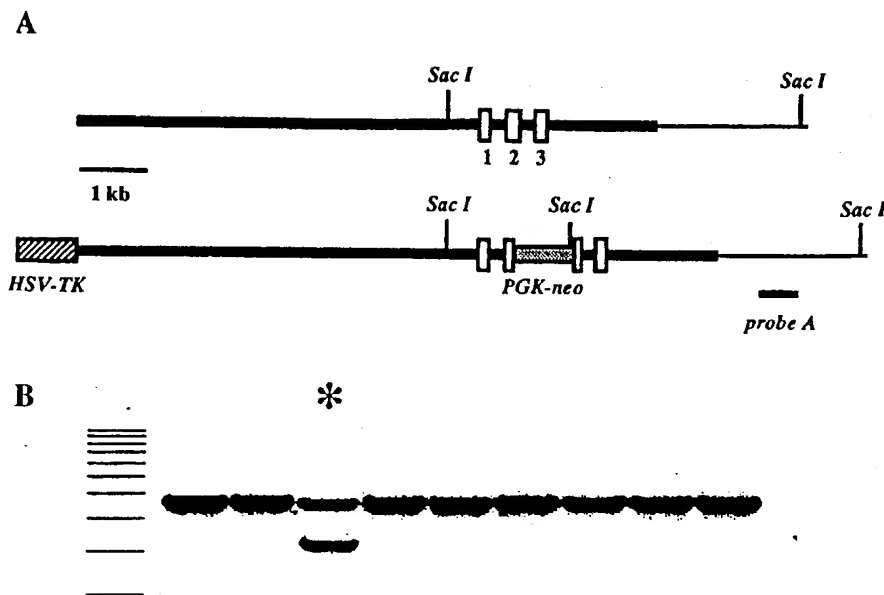


**Fig. 1A, B** Gene targeting at the murine cytochrome oxidase VIaH locus. **A** The structure of the gene, which has been reported elsewhere [12]. Briefly, the gene is comprised of three small exons (open rectangles). Exon 2 was disrupted with the expression cassette for neomycin phosphotransferase (*PGK-neo*), thus mutating the gene in its coding region and simultaneously providing positive selection. Heavy lines, the cloned vector used for transfection into J1 ES cells; note the targeting vector is flanked with the expression cassette for TK (*HSV-TK*) to allow for negative selection (see text). **B** Probe A was derived from a separate region of the gene (thin line) and was used to screen, by Southern analysis, DNA isolated from G418- and gancyclovir-resistant ES clones. Note the presence of the endogenous band at 5.7 kb in all clones, as well as the presence of the recombinant band at 4.2 kb (asterisk), in a *SacI* digest of genomic DNA. Clone 3 was then used for blastocyst injection as illustrated in Fig. 2 to generate germline chimeras. Bars (left), 1-kb-size markers

oment of all tissues and result in the production of chimeras (usually assessed at birth by acquisition of the dominant coat color phenotype Agouti). In subsequent matings of these chimeric mice, if the ES cells have contributed to formation of germ cells, the mutant gene is transmitted to their progeny. By mating heterozygotes, each harboring a mutated copy of the gene of interest (detected by analysis of the isolated DNA), one can derive embryos and mice which are homozygous for the mutation. These techniques are illustrated schematically in Fig. 2.

### "Knockout mice": the new genetics

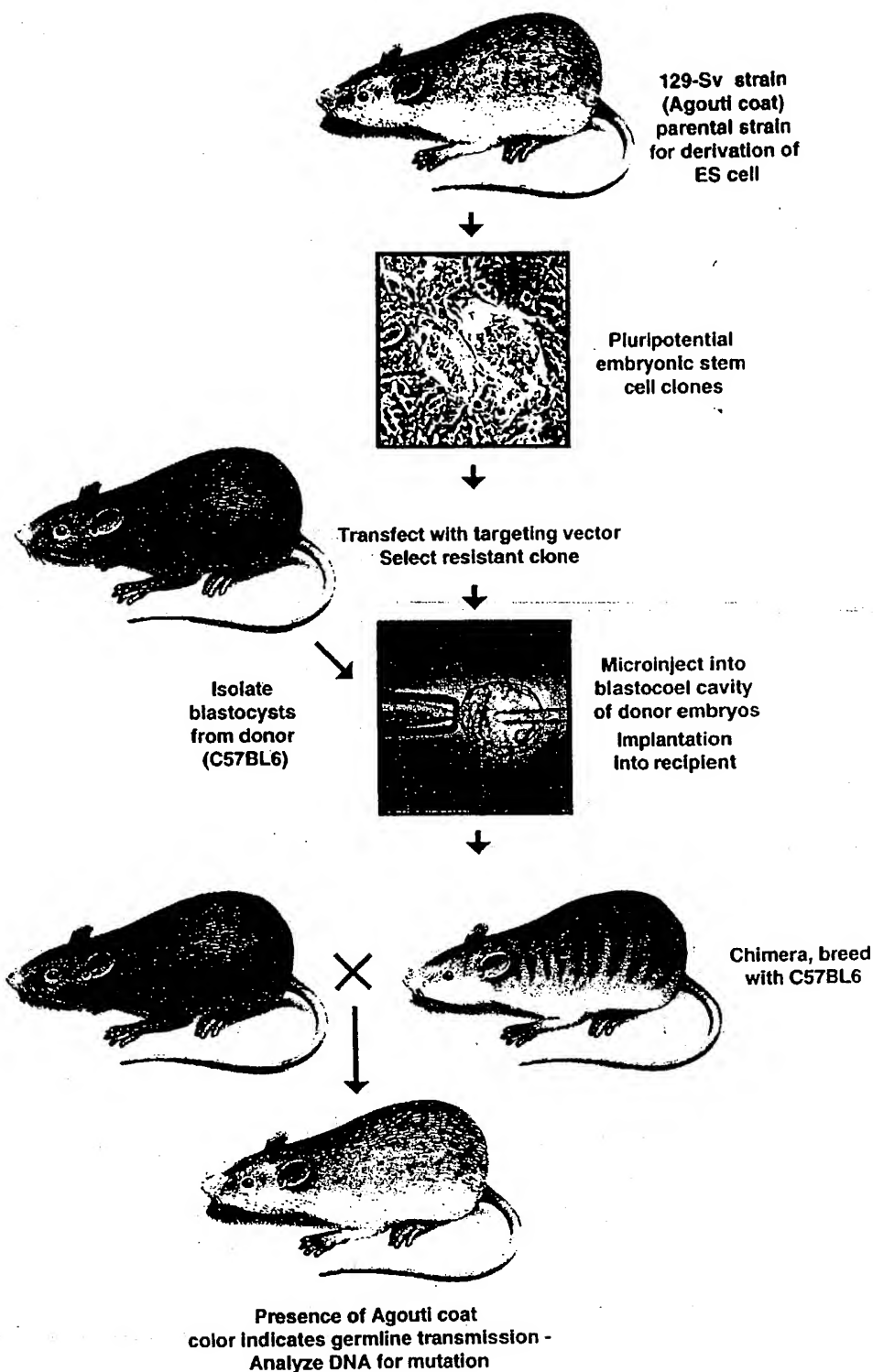
cell clones which retain the *TK* gene (nonhomologous recombination) do not survive the addition of gancyclovir (or homologues) to the media due to the accumulation of toxic nucleosides, whereas cell clones which have undergone an authentic recombination lose the *TK* gene. This combined strategy is known as *positive-negative* selection [11] and routinely increases the targeting frequency by an order of magnitude or more.

An example of gene targeting in ES cells is illustrated in Fig. 1. The gene of interest in this example is a muscle-specific subunit of cytochrome oxidase (VIaH). The structure and regulation of the gene have recently been defined in the author's laboratory [12], but the precise function of this subunit, postulated to regulate the steady-state activity of cytochrome oxidase, remains largely unknown in the context of an intact animal. It is anticipated that creation of mice which lack this subunit will provide more insight into the precise role this subunit may play in the bioenergetics of cardiac and skeletal muscle.

Once these mutated ES cells are isolated as a pure clone, they can be introduced into the blastocoele cavity of a normal embryo, where they participate in the devel-

The initial attempts at gene inactivation in murine ES cells took advantage of selection methods designed to reflect loss of an enzyme activity, hypoxanthine phosphoribosyltransferase (HPRT), following random integration of proviruses [13, 14]. Since the vast majority of ES cell lines used were male (male chimeric mice can be mated frequently, thus producing numerous offspring to assess germline competence), random integration of DNA (in this case retroviruses) would be expected to inactivate the single copy of the HPRT gene on the X chromosome at a low but detectable frequency and subsequently confer growth properties in a defined (hypoxanthine-aminopterin-thymidine) medium. These HPRT-minus cell lines were used to make mice deficient in HPRT, a potential mouse model of the human disorder Lesch-Nyhan syndrome [14, 15]. However, the absence of a neurologic phenotype in these mice was readily apparent, eventually precipitating a search for alternative explanations of why purine salvage might be different in the two species. This led to the elucidation that adenine phosphoribosyltransferase was the major enzyme involved in purine salvage in the mouse. Indeed, when HPRT-deficient mice were exposed to inhibitors of adenine phosphoribosyltransfer-

**Fig. 2** General strategy for creating "knock-out" mice



ase, they developed neurologic phenotypes more representative of the human disorder [16]. The HPRT locus continued to be the subject of intense investigation, however, defining many of the parameters routinely employed now to target genes – for example, length and degree of homology to mediate highly efficient gene targeting [17, 18].

The first description of gene targeting via homologous recombination in murine ES cells was published in 1987 [19]. To date, several hundred novel mouse mutants – “knockout” mice – have been created, with dozens being reported monthly. A synopsis of these mutations is obviously beyond the scope of this review, but it is readily apparent from a perusal of these mutations that the

**Table 1** Established methodologies for the study of murine physiology and metabolism

Methodology	Physiologic measure	References
<b>Cardiovascular system</b>		
Micromanometer catheter	LV hemodynamics	22-24
Indwelling arterial catheters	Blood pressure, heart rate	25-28
Reference microsphere and dilution	Cardiac output, regional blood flows, intravascular fluid volumes	26, 28
Echocardiography	LV mass, LV systolic function, wall motion abnormalities, heart rate	29-32
X-ray contrast microangiography	Ventricular volumes, ejection fraction	33
Swimming	Cardiac adaptations to chronic exercise	34
Langendorff perfusion	Intraventricular pressure, indices of LV contraction and relaxation, heart rate	35-37
Magnetic resonance imaging	Cardiac chamber sizes, coronary flow	38, 39
Magnetic resonance spectroscopy	pH, high energy phosphates	40
Tail-cuff sphygmomanometer	Blood pressure	27
<b>Pulmonary system</b>		
Plethysmography	Lung volumes, respiratory rate	41-44
Pulse oximetry	Arterial saturation	45
Pressure-volume curves	Elastic recoil	46
Forced oscillation	Pulmonary resistance	46
Methacholine challenge	Airway responsiveness	47
<b>Skeletal muscle</b>		
Skeletal muscle resection	Response to mechanical overload	48, 49
Magnetic resonance spectroscopy	pH, phosphocreatine, ATP, inorganic phosphate, creatine kinase flux	50, 51
Microvascular flow	Ischemia/reperfusion injury	49, 52, 53
Programmable treadmill	Fatiguability	54
Miscellaneous		55
Magnetic resonance imaging	Knee joint degeneration	56
	Polycystic kidneys	57
	Renal edema, hepatic iron deposition	58
Magnetic resonance spectroscopy	Hepatic ADP levels, creatine kinase flux	59
	Brain pH, free Mg, choline, N-acetylaspertate, creatine	60
Pathogen inoculation	Phagocyte oxidase function	61
Morris Water maze task, visible or hidden-platform tasks	Spatial learning	62, 63
Intruder test	Defensive aggression	64
Contextual and tone conditioning	Fear response	64
Swimming	Exercise-induced immunosuppression	65

technology has become one of the most powerful methods in the repertoire of approaches to gain insight into the functions of genes. To cite only a few applications, these include developmental biology, behavior and cognition, pharmaceutical research, and generation of models of human disease, such as cystic fibrosis and familial hypercholesterolemia [20, 21].

#### The new physiology and metabolism

Gene targeting in ES cells has only recently been applied to address problems in classical physiology and metabolism. Indeed, the creation of mutant animals, some of which have unpredictable and subtle phenotypes, has rekindled interest in developing techniques that allow one to characterize the animals precisely. This initiative, "molecular physiology," represents a new field of biology that addresses physiology and metabolism in the context of an intact animal harboring defined mutations in selected genes.

Established methodologies, such as light, immunofluorescence, and electron microscopy, are frequently used

in postmortem tissue to describe histologic and ultrastructural changes in organs of interest in particular transgenic models of disease. Functional studies in the isolated, intact organ have also been accomplished, but it is becoming increasingly clear that studies of physiology in the intact animal may yield the greatest insight. A summary of methodologies which have been adapted to study murine cardiovascular, respiratory, and skeletal muscle physiology in vitro and in vivo is presented in Table 1. The remainder of our discussion focuses on examples of methodologies which have been developed to interrogate primarily cardiovascular phenotypes. Although most of these examples represent gain-of-function mutations, it is clear the methods can be applied to loss-of-function mutations as well.

#### Cardiovascular "molecular physiology"

At the present time ES cell technology exists only in the mouse (although see discussion below); thus creation of animals with anticipated cardiac phenotypes requires that

techniques be developed to interrogate them (throughout development). Standard measures of cardiac function are well established in larger animals such as rabbits and dogs where invasive measurements can be made in anesthetized or chronically instrumented animals. Development of these same techniques in the mouse has only recently become available. In general this has necessitated the "miniaturization" of technology that allows investigators reproducibly to assess cardiovascular function, both in the isolated perfused heart and in the intact anesthetized mouse.

The isolated Langendorff preparation and the working heart model have been elegantly characterized in several native mouse strains under varied physiologic conditions [35]. Several laboratories, including our own, have used the Langendorff model to provide direct evidence linking overexpression of heat shock protein with enhanced myocardial recovery following global ischemia in transgenic mouse lines [36, 37, 40].

Our laboratory has combined isolated heart perfusions with nuclear magnetic resonance (NMR) to study the effect of overexpression of heat-shock proteins in the heart on changes in pH and high-energy phosphates at rest and following global ischemia [40]. We have found that NMR spectroscopy, which is routinely used to study perfused hearts from larger species such as the rat, rabbit, and guinea pig, can be adapted to suit a 100-mg mouse heart. Figure 3 shows  $^{23}\text{Na}$ -,  $^{31}\text{P}$ -, and  $^{13}\text{C}$ -NMR spectra obtained from three different perfused mouse heart protocols.

In panel A the  $^{23}\text{Na}$ -NMR spectra have been obtained in the presence of TmDOTP, a shift-reagent which shifts the extracellular sodium (Na) signal away from the intracellular Na signal [66]. Shown in the upper left is a single spectrum in which the extracellular Na and intracellular Na resonance peaks are labeled. Spectra, shown in a stacked plot format, were acquired every 3 min at baseline, during 15 min of ischemia, and during 24 min of recovery. In this heart there is sustained elevation of intracellular Na into recovery.

In panel B the  $^{31}\text{P}$ -NMR spectra were acquired every 5 min at baseline, during 15 min of ischemia, and then at 15 and 30 min of recovery. Shown are spectra at baseline, after 15 min of ischemia, and after 30 min of recovery. The phosphocreatine, inorganic phosphate, and three P resonances of adenosine triphosphate are labeled. Intracellular pH can be calculated from the chemical shift difference between the resonance peaks of phosphocreatine and inorganic phosphate [67]. These spectra show that there is incomplete recovery of adenosine triphosphate following this ischemic event.

In panel C there is a single  $^{13}\text{C}$ -NMR spectrum of the C4 carbon of glutamate from a mouse heart extract. The extract was prepared after the isolated heart was subjected to 25 min of ischemia and then reperfused with  $^{13}\text{C}$ -labeled acetate, octanoate (a short-chain fatty acid) and long-chain fatty acids. The resonance peaks marked with an asterisk arise from octanoate oxidation while the remainder arise from long-chain fatty acid oxidation. Analysis of this multiplet using  $^{13}\text{C}$ -NMR isotopomer methods yields information about the relative contribution of octanoate and long-chain fatty acids to the acetyl coenzyme A pool from which glutamate is synthesized

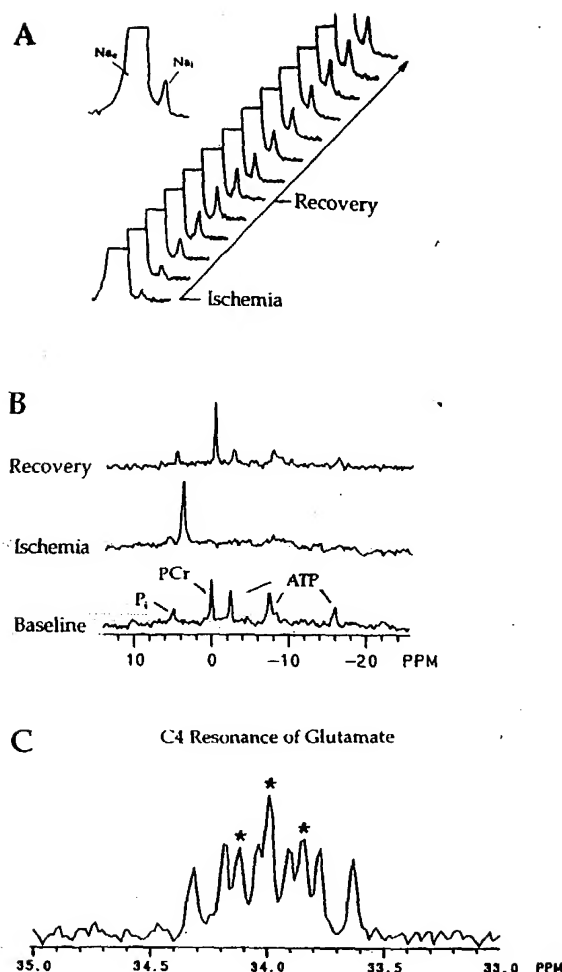


Fig. 3 A Upper left, a single  $^{23}\text{Na}$ -NMR spectrum obtained in the presence of TmDOTP in which the extracellular Na and intracellular Na resonance peaks are labeled. Right, spectra, shown in a stacked plot format, were acquired at baseline, during 15 min of ischemia and during 24 min of recovery. B  $^{31}\text{P}$ -NMR spectra acquired at baseline, after 15 min of ischemia and after 30 min of recovery. The phosphocreatine (PCr), inorganic phosphate ( $P_i$ ) and three P resonances of adenosine triphosphate (ATP) are labeled. C  $^{13}\text{C}$ -NMR spectrum of the C4 carbon of glutamate from a mouse heart extract which was prepared after the isolated heart was subjected to 25 min of ischemia and then reperfused with  $^{13}\text{C}$ -labeled acetate, octanoate (a short-chain fatty acid), and long-chain fatty acids. The resonance peaks marked with an asterisk arise from octanoate oxidation while the remainder arise from long-chain fatty acid oxidation. Analysis of this multiplet using  $^{13}\text{C}$ -NMR isotopomer methods yields information about the relative contribution of octanoate and long-chain fatty acids to the acetyl coenzyme A pool from which glutamate is synthesized

ysis of this multiplet using  $^{13}\text{C}$ -NMR isotopomer methods yields information about the relative contribution of octanoate and long-chain fatty acids to the acetyl coenzyme A pool from which glutamate is synthesized, in this case during reperfusion [68, 69]. This information may in turn provide insight into the postischemic activity of carnitine palmitoyl transferase (which is required for long-chain fatty acid metabolism).

Optimally of course cardiovascular phenotypes would be interrogated in the intact animal. A number of invasive, catheter-based methods have been successfully applied to the mouse to make hemodynamic measurements in both the conscious and unconscious animal. Exciting advances have also been made in the application of non-invasive techniques such as magnetic resonance imaging and echocardiography to interrogate murine cardiac function.

The importance of the application of these methodologies to murine models of disease cannot be understated. Using a number of techniques outlined in Table 1, investigators have been able to characterize the cardiovascular phenotypes of a number of transgenic mice including lines which overexpress atrial natriuretic factor [25, 28], heat-shock proteins [36, 37, 40], human tissue kallikrein [27],  $\beta$ -adrenergic receptors [24],  $\beta$ -adrenergic receptor kinase and  $\beta$ -adrenergic receptor kinase inhibitor [23] as well as phospholamban deficient lines [32].

## Summary

The advent of techniques to generate gain-of-function and loss-of-function mutations in laboratory animals represents one of the major accomplishments in cell and molecular biology in mammals over the past two decades. Although the technology is generally limited only to the mouse at present, substantial effort is underway to develop these techniques, and to refine existing techniques, in other species. Putative pluripotent ES cell lines have been derived in a number of other species including hamster [70], pig [71–75], sheep [73], cattle [76], rabbit [77], rat [78], mink [79], monkey [80], and even humans [81]. Thus it seems likely the technology will be advanced into these additional species over the next few years, and each one of these may lend itself uniquely to problems ranging from development to tissue and organ physiology. Additionally, techniques such as those illustrated here and in Table 1 will need to be refined and applied to address each new mutation.

**Acknowledgements** The authors apologize to uncited investigators in many areas of developmental biology for not being able to cite all of the relevant literature in this field due to page constraints. R.W.M. is supported by grants from the National Institutes of Health (NHLBI, RO1-51568), National Aeronautics and Space Administration (NSCORT, NAGW 3582), the Leuven Research and Development Institute (Leuven, Belgium) and is an Established Investigator of the American Heart Association. N.B.R. is supported by grants from the American Heart Association (95004180 and 95009510) and from the National Institutes of Health (P41-RR02584).

## References

- Gordon J, Seangos G, Plotkin D, Barbosa J, Ruddle F (1980) Genetic transformation of mouse embryos by microinjection of purified DNA. *Proc Natl Acad Sci USA* 77:7380–7384
- Hosoda K, Hammer R, Richardson J, Baynash A, Cheung J, Giard A, Yanigisawa M (1994) Targeted and natural (piebald-lethal) mutations of endothelin-B receptor gene produce megacolon associated with spotted coat color in mice. *Cell* 79:1267–1276
- Mintz B, Illmensee K (1975) Normal genetically mosaic mice produced from malignant teratocarcinoma cells. *Proc Natl Acad Sci USA* 72:3585–3589
- Evans M, Kaufman M (1981) Establishment in culture of pluripotent cells from mouse embryos. *Nature* 292:154–156
- Martin G (1981) Isolation of a pluripotent cell line from early embryos cultured in medium conditioned by teratocarcinoma stem cells. *Proc Natl Acad Sci USA* 78:7634–7638
- Bradley A, Evans M, Kaufman M, Robertson E (1984) Formation of germ-line chimaeras from embryo-derived teratocarcinoma cell lines. *Nature* 309:255–256
- Lin F, Sperle K, Sternberg N (1985) Recombination in mouse L cells between DNA introduced into cells and homologous chromosomal sequences. *Proc Natl Acad Sci USA* 82:1391–1395
- Smithies O, Gregg R, Boggs S, Koralewski M, Kucherlapati R (1985) Insertion of DNA sequences into the human chromosomal beta-globin locus by homologous recombination. *Nature* 317:230–234
- Thomas K, Folger K, Capecchi M (1986) High frequency targeting of genes to specific sites in the mammalian genome. *Cell* 44:419–428
- Thomas K, Capecchi M (1986) Introduction of homologous DNA sequences into mammalian cells induces mutations in the cognate gene. *Nature* 324:34–38
- Mansour S, Thomas K, Capecchi M (1988) Disruption of the proto-oncogene int-2 in mouse embryo-derived stem cells: a general strategy for targeting mutations to non-selectable genes. *Nature* 336:348–352
- Wan B, Moreadith R (1995) Structural characterization and regulatory element analysis of the heart isoform of cytochrome c oxidase VIa. *J Biol Chem* 270:26433–26440
- Robertson E, Bradley A, Kuehn M, Evans M (1986) Germ-line transmission of genes introduced into cultured pluripotent cells by retroviral vector. *Nature* 323:445–448
- Hooper M, Hardy K, Handyside A, Hunter S, Monk M (1987) HPRT-deficient (Lesch-Nyhan) mouse embryos derived from germline colonization by cultured cells. *Nature* 326:292–295
- Kuehn M, Bradley A, Robertson E, Evans M (1987) A potential animal model for Lesch-Nyhan syndrome through introduction of HPRT mutations into mice. *Nature* 326:295–298
- Wu C, Melton D (1993) Production of a model for Lesch-Nyhan syndrome in HPRT-deficient mice. *Nat Genet* 3:235–240
- Hasty P, Rivera-Pérez J, Chang C and Bradley A (1991) Target frequency and integration pattern for insertion and replacement vectors in embryonic stem cells. *Mol Cell Biol* 11:4509–4517
- Hasty P, Rivera-Pérez J and Bradley A (1991) The length of homology required for gene targeting in embryonic stem cells. *Mol Cell Biol* 11:5586–5591
- Thomas K, Capecchi M (1987) Site-directed mutagenesis by gene targeting in mouse embryo-derived stem cells. *Cell* 51:503–512
- Snouwaert J, Brigman K, Latour A, Malouf N, Boucher R, Smithies O, and Koller B (1992) An animal model for cystic fibrosis made by gene targeting. *Science* 257:1083–1088
- Ishibashi S, Brown MS, Goldstein JL, Gerard RD, Hammer RE and Herz J (1993) Hypercholesterolemia of low density lipoprotein receptor knockout mice and its reversal by adenovirus-mediated gene delivery. *Proc Natl Acad Sci USA* 89:7905–7909
- Hunter JJ, Tanaka N, Rockman HA, Ross J, Chien KR (1995) Ventricular expression of a MLC-2v-ras fusion gene induces cardiac hypertrophy and selective diastolic dysfunction in transgenic mice. *J Biol Chem* 270:23173–23178
- Koch WJ, Rockman HA, Samama P, Hamilton RA, Bond RA, Milano CA, Lefkowitz RJ (1995) Cardiac function in mice overexpressing the beta-adrenergic receptor kinase or a beta-ARK inhibitor. *Science* 268:1350–1353



24. Milano CA, Allen LF, Rockman HA, Dolber PC, McMinn TR, Chien KR, Johnson TD, Bond RA, Lefkowitz RJ (1994) Enhanced myocardial function in transgenic mice overexpressing the beta 2-adrenergic receptor. *Science* 264:582-586
25. Steinhilber ME, Cochrane KL, Field LJ (1990) Hypotension in transgenic mice expressing atrial natriuretic factor fusion genes. *Hypertension* 16:301-307
26. Barbee RW, Perry BD, Re RN, Murgo JP (1992) Microsphere and dilution techniques for the determination of blood flows and volumes in conscious mice. *Am J Physiol* 263:R728-R733
27. Wang J, Xiong W, Yang Z, Davis T, Dewey MJ, Chao J, Chao L (1994) Human tissue kallikrein induces hypotension in transgenic mice. *Hypertension* 23:236-243
28. Barbee RW, Perry BD, Re RN, Murgo JP, Field LJ (1994) Hemodynamics in transgenic mice with overexpression of atrial natriuretic factor. *Circ Res* 74:747-751
29. Manning MJ, Wei JY, Katz SE, Litwin SE, Douglas PS (1994) In vivo assessment of LV mass in mice using high-frequency cardiac ultrasound: necropsy validation. *Am J Physiol* 266:H1672-H1675
30. Gardin JM, Siri FM, Kitsis RN, Edwards JG, Leinwand LA (1995) Echocardiographic assessment of left ventricular mass and systolic function in mice. *Circ Res* 76:907-914
31. Manning MJ, Wei JY, Katz SE, Douglas PS, Gwathmey JK (1993) Echocardiographically detected myocardial infarction in the mouse. *Lab Animal Science* 43:583-585
32. Hoit BD, Khoury SF, Kranias EG, Ball N, Walsh RA (1995) In vivo echocardiographic detection of enhanced left ventricular function in gene-targeted mice with phospholamban deficiency. *Circ Res* 77:632-637
33. Rockman HA, Ono S, Ross RS, Jones LR, Karimi M, Bhargava V, Ross J, Chien KR (1994) Molecular and physiological alterations in murine ventricular dysfunction. *Proc Natl Acad Sci USA* 91:2694-2698
34. Kaplan ML, Cheslow Y, Vikstrom K, Malhotra A, Geenen DL, Nakouzi A, Leinwand LA, Buttrick PM (1994) Cardiac adaptations to chronic exercise in mice. *Am J Physiol* 267:H1167-H1173
35. Grupp IL, Subramaniam A, Hewett TE, Robbins J, Grupp G (1993) Comparison of normal, hypodynamic, and hyperdynamic mouse hearts using isolated work-performing heart preparations. *Am J Physiol* 265:H1401-1410
36. Marber MS, Mestral R, Chi SH, Sayen MR, Yellon DM, Dillmann WH (1995) Overexpression of the rat inducible 70-kD heat stress protein in a transgenic mouse increases the resistance of the heart to ischemic injury. *J Clin Invest* 95:1446-1456
37. Plumier JC, Ross BM, Currie RW, Angelidis CE, Kazlaris H, Kollias G, Pagoulatos GN (1995) Transgenic mice expressing the human heat shock protein 70 have improved post-ischemic myocardial recovery. *J Clin Invest* 95:1854-1860
38. Burstein D (1991) MR imaging of coronary artery flow in isolated and in vivo hearts. *J Magn Reson Imaging* 1:337-346
39. Rose SE, Wilson SJ, Zelaya FO, Crozier S, Doddrell DM (1994) High resolution high field rodent cardiac imaging with flow enhancement suppression. *Magn Reson Imaging* 12:1183-1190
40. Radford NB, Fina M, Benjamin JJ, Moreadith RW, Graves KH, Zhao PY, Gavva S, Wiethoff A, Sherry AD, Malloy CR, Williams RS (1996) Cardioprotective effects of 70-kDa heat shock protein in transgenic mice. *Proc Natl Acad Sci USA* 93:2339-2342
41. Lockhart SP, Hill D, King S, Down JD (1991) A semi-automated method of breathing rate measurement in the mouse. *Radiother Oncol* 22:68-70
42. Nielsen GD, Petersen SH, Vinggaard AM, Hansen LF, Wolkoff P (1993) Ventilation, CO<sub>2</sub> production, and CO<sub>2</sub> exposure effects in conscious, restrained CF-1 mice. *Pharin Toxicol* 72:163-168
43. Martin TR, Gerard NP, Galli SJ, Drazen JM (1988) Pulmonary responses to bronchoconstrictor agonists in the mouse. *J Appl Physiol* 64:2318-2323
44. Vijayaraghavan R, Schaper M, Thompson R, Stock MF, Boylstein LA, Luo JE, Alarie Y (1994) Computer assisted recognition and quantitation of the effects of airborne chemicals acting at different areas of the respiratory tract in mice. *Arch Toxicol* 68:490-499
45. Sidwell RW, Huffman JH, Gilbert J, Moscon B, Pedersen G, Burger R, Warren RP (1992) Utilization of pulse oximetry for the study of the inhibitory effects of antiviral agents on influenza virus in mice. *Antimicrobial Agents Chemother* 36:473-476
46. Kida K, Fujino Y (1993) Lung structure and elastic recoil properties in hereditary diabetes mellitus in KK-mice, C57 black mice, and F<sub>1</sub> hybrids. *J Lab Clin Med* 122:524-532
47. DiCosmo BF, Geba GP, Picarella D, Elias JA, Rankin JA, Stripp BR, Whitsett JA, Flavell RA (1994) Airway epithelial cell expression of interleukin-6 in transgenic mice. *J Clin Invest* 94:2028-2035
48. Roy RR, Edgerton VR (1995) Response of mouse plantaris muscle to functional overload: comparison with rat and cat. *Comp Biochem Physiol* 111A:569-575
49. Tsika RW, Hauschka SD, Gao L (1995) M-creatine kinase gene expression in mechanically overloaded skeletal muscle of transgenic mice. *Am J Physiol* 269:C665-C674
50. Dunn JF, Tracey I, Radda GK (1993) Exercise metabolism in duchenne muscular dystrophy: a biochemical and <sup>31</sup>P-nuclear magnetic resonance study of *mdx* mice. *Proc R Soc Lond* 251:201-206
51. van Deursen J, Heerschap A, Oerlemans F, Ruitenbeek W, Jap P, Laak HT, Wieringa B (1993) Skeletal muscles of mice deficient in muscle creatine kinase lack burst activity. *Cell* 74:621-631
52. Brosnan MJ, Raman SP, Chen L, Koretsky AP (1993) Altering creatine kinase isoenzymes in transgenic mouse muscle by overexpression of the B subunit. *Am J Physiol* 264:C151-C160
53. Dunn JF, Tracey I, Radda GK (1992) A <sup>31</sup>P-NMR study of muscle exercise metabolism in *mdx* mice: evidence for abnormal pH regulation. *J Neurol Sci* 113:108-113
54. Pemberton M, Anderson G, Barker J (1994) In vivo microscopy of microcirculatory injury in skeletal muscle following ischemia/reperfusion. *Microsurg* 15:374-382
55. Pachner AR, Itano A, Ricalton N, Choe S (1991) Chronic murine experimental myasthenia gravis: strength testing and serology. *Clin Immunol Immunopath* 59:398-406
56. Munasinghe JP, Tyler JA, Carpenter A, Hall LD (1995) High resolution MR imaging of joint degeneration in the knee of the STR/ORT mouse. *Magn Reson Imaging* 13:421-428
57. Townner RA, Yamaguchi T, Philbrick DJ, Holub BJ, Janzen EG, Takahashi H (1991) In vivo proton magnetic resonance imaging and localized spectroscopic analysis of polycystic kidney disease in DBA/2FG-*pcy* mice. *Magn Reson Imaging* 9:429-434
58. Fabry ME, Costantini F, Pachnis A, Suzuka SM, Bank N, Aynedjian HS, Factor SM, Nagel RL (1992) High expression of human  $\beta$ - and  $\alpha$ -globins in transgenic mice: erythrocyte abnormalities, organ damage, and the effect of hypoxia. *Proc Natl Acad Sci USA* 89:12155-12159
59. Brosnan MJ, Chen L, Van Dyke TA, Koretsky AP (1990) Free ADP levels in transgenic mouse liver expressing creatine kinase. *J Biol Chem* 265:20849-20855
60. Kauppinen RA, Halmekyto M, Alhonen L, Janne J (1992) Nuclear magnetic resonance spectroscopy study on energy metabolism, intracellular pH, and free Mg<sup>2+</sup> concentration in the brain of transgenic mice overexpressing human ornithine decarboxylase gene. *J Neurochem* 58:831-836
61. Pollock JD, Williams DA, Gifford MAC, Li LL, Du X, Fisherman J, Orkin SH, Doerschuk Dinuer MC (1995) Mouse model of X-linked chronic granulomatous disease, an inherited defect in phagocyte superoxide production. *Nat Genet* 9:202-209
62. Yamaguchi F, Richards SJ, Beyreuther K, Salbaum M, Carlson GA, Dunnett SB (1991) Transgenic mice for the amyloid precursor protein 695 isoform have impaired spatial memory. *Neuroreport* 2:781-784

63. Silva AJ, Paylor R, Wehner JM, Tonegawa S (1992) Impaired spatial learning in  $\alpha$ -calcium-calmodulin kinase II mutant mice. *Science* 257:206-211
64. Mayford M, Abel T, Kandel ER (1995) Transgenic approaches to cognition. *Curr Opin Neurobiol* 5:141-148
65. Benquet C, Krzystyniak K, Savard R, Guertin F (1994) Modulation of exercise-induced immunosuppression by dietary polyunsaturated fatty acids in mice. *J Toxicol Env Health* 43:225-237
66. Malloy CR, Buster DC, Castro MC, Gerald CF, Jeffrey FMH, Sherry AD (1990) Influence of global ischemia on  $\text{Na}^+$  in the perfused rat heart. *Magn Reson Med* 15:33-44
67. Kost GJ (1990) pH standardization for phosphorus-31 magnetic resonance heart spectroscopy at different temperatures. *Magn Reson Med* 14:496-506
68. Malloy CR, Thompson JR, Jeffrey FMH, Sherry AD (1990) Contribution of exogenous substrates to acetyl coenzyme A: measurement by  $^{13}\text{C}$  NMR under non-steady state conditions. *Biochem* 29:6756-6761
69. Malloy CR, Sherry AD, Jeffrey FMH (1990) Analysis of tricarboxylic acid cycle of the heart using  $^{13}\text{C}$  isotope isomers. *Am J Physiol* 259:H987-H995
70. Doetschman T, Williams P, Maeda N (1988) Establishment of hamster blastocyst-derived embryonic stem (ES) cells. *Dev Biol* 127:224-227
71. Evans MJ, Notarianni E, Laurie S, Moor RM (1990) Derivation and preliminary characterization of pluripotent cell lines from porcine and bovine blastocysts. *Theriogenology* 33:125-128
72. Notarianni E, Laurie S, Moor RM, Evans MG (1990) Maintenance and differentiation in culture of pluripotential embryonic cell lines from pig blastocysts. *J Reprod Fert* 40:51-56
73. Piedrahita JA, Anderson GB, BonDurant RH (1990) On the isolation of embryonic stem cells: comparative behavior of murine, porcine and ovine embryos. *Theriogenology* 34:879-891
74. Strojek M, Reed MA, Hoover JL, Wagner TE (1990) A method for cultivating morphologically undifferentiated embryonic stem cells from porcine blastocysts. *Theriogenology* 33:901-913
75. Talbot NC, Caird ER Jr, Vernon GP, Powell AM, Nel ND (1993) Culturing the pig epiblast cells of the pig blastocyst. *In Vitro Cell Dev Biol* 29A:543-554
76. Saito S, Strelchenko N, Niemann H (1992) Bovine embryonic stem cell-like cell lines cultured over several passages. *Roux Arch Dev Biol* 201:134-141
77. Graves KH, Moreadith RW (1993) Derivation and characterization of putative pluripotential embryonic stem cells from preimplantation rabbit embryos. *Mol Reprod Dev* 36:424-433
78. Iannaccone PM, Taborn GU, Garton RL, Caplice MD, Brenin DR (1994) Pluripotent embryonic stem cells from the rat are capable of producing chimeras. *Dev Biol* 163:288-292
79. Sukoyan MA, Golubitsa AN, Zhelezova AI, Shilov AG, Vatinin SY, Maximovsky LP, Andreeva LE, Mc Whir J, Pack SD, Bayborodin SI, Kerkis AY, Kizilova HL, Serov OL (1992) Isolation and cultivation of blastocyst-derived stem cell lines from American mink. *Mol Reprod Dev* 33:418-431
80. Thomson JA, Kalishman J, Golos TG, During M, Harris CP, Becker RA, Hearn JP (1995) Isolation of a primate embryonic stem cell line. *Proc Natl Acad Sci USA* 92:7844-7848
81. Bongso A, Fong C-Y, Ng S-C, Ratman S (1994) Isolation and culture of inner cell mass cells from human blastocyst. *Hum Reprod* 9:2110-2117



# Perspectives Series: Molecular Medicine in Genetically Engineered Animals

## Transgenesis in the Rat and Larger Mammals

Linda J. Mullins and John J. Mullins

Centre for Genome Research, The University of Edinburgh, Edinburgh EH9 3JQ, United Kingdom

Advances in biotechnology over the last ten years have made it possible for the researcher to alter gene expression *in vivo* in many diverse ways (1). With the establishment of embryonic stem (ES)<sup>1</sup> cell technology (2), more subtle and precise alterations can now be achieved than were previously possible using microinjection techniques. However, to date germline transmission has only been achieved with mouse ES cells, and microinjection continues to be the method most widely used for other species. While the mouse has a number of advantages, not least the depth of our knowledge of its genetics, other species are being increasingly used for transgenic studies due to their greater suitability for addressing specific questions. We will briefly review the application of transgenic technology to nonmurine species as it stands at present, with particular emphasis on developments appertaining to biomedical research.

### *Transgenesis by pronuclear injection*

A number of significant limitations regarding the application of pronuclear injection to nonmurine animals have been identified (3), not least being the time and cost. Such limitations are due to longer gestation and generation times, reduced litter sizes, and higher maintenance costs. Further consideration must be given to the large numbers of fertilized eggs (and hence donor animals) required for microinjection, the high cost of carrying nontransgenic offspring to term, and the relatively low efficiency of gene integration. Such limitations are particularly severe for the production of bovine transgenics and, as a consequence, more significant departures from the standard procedures used for the mouse have been adopted for this species (4). For example, the use of *in vitro* embryo production in combination with gene transfer technology has played a large role in the development of transgenic cattle. The development of microinjected embryos through to the

morula/blastocyst stage in recipient rabbits or sheep, enables sexing, transgene screening, and cloning to take place before reintroduction into the natural host, providing that such screening methods are robust and reliable.

The major problem regarding pronuclear microinjection is that the exogenous DNA integrates randomly into chromosomal DNA. Position effects, where the transgene is influenced by its site of integration in the host chromosome (5), can have major consequences on the expression of the transgene, including loss of cell specificity, inappropriately high copy number-independent expression and complete silencing of the transgene. This is of greater concern in nonmurine transgenesis where the investment is higher. Position-independent, copy number-related expression can be achieved using sequences such as the locus control regions identified upstream of the  $\beta$ -globin gene cluster and downstream of the CD2 gene (6, 7), the A elements which flank the chicken lysozyme gene (8), and matrix attachment regions (9). Such elements have been shown to function across species barriers, and their incorporation into gene constructs can overcome position effects and improve expression of heterologous genes within specific cell types (5). In many cases, simply including large amounts of flanking sequences may be sufficient to overcome position effects and direct expression to specific tissues. To this end, the development and use of P1 (10), bacterial artificial chromosome (BAC) (11) and yeast artificial chromosome (YAC) vectors (12) for cloning of large segments of DNA, should greatly improve the chances of including important regulatory elements, including those involved in chromatin structure, within the transgene construct.

### *Embryonic stem cell technology*

With the development of ES cell technology in the mouse (2), genetic manipulations can be performed in cell culture using appropriate selection strategies to permit the directed integration of the transgene to a specific region of the chromosome via homologous recombination. With the advent of homologous recombination, the researcher is able to insertionally inactivate, replace, or introduce subtle alterations to the endogenous gene of interest. Once the intended genetic change has been verified, the appropriate ES cells are introduced into blastocysts by microinjection, and, during subsequent gestation, may contribute to the developing embryo. If such a contribution is made, then by definition the resulting animal would be chimeric, being derived in part from the ES cells originating in culture. Assuming that the chimerism extends to the germline, then an appropriate breeding strategy will lead to the recovery of nonchimeric heterozygotes and, if viable, mice which are homozygous for the genetic change.

Most attempts to isolate and culture inner cell mass (ICM) cells from other species are based on the methods used for the

Address correspondence to John J. Mullins, Centre for Genome Research, The University of Edinburgh, King's Buildings, West Mains Road, Edinburgh EH9 3JQ, United Kingdom. Phone: 44-131-650-6846; FAX: 44-131-667-0164.

Received for publication 29 January 1996 and accepted 5 February 1996.

1. Abbreviations used in this paper: DAF, decay accelerating factor; ES, embryonic stem; HAR, hyperacute rejection; ICM, inner cell mass.

J. Clin. Invest.

© The American Society for Clinical Investigation, Inc.

0021-9738/96/12/0S37/04 \$2.00

Volume 98, Number 11, Supplement 1996, S37-S40

mouse. ES cells are maintained in culture in the presence of mouse-derived differentiation-inhibiting agents, provided either as a media supplement or through cocultivation in the presence of feeder cells. It has been suggested that these mouse-derived agents do not adequately prevent differentiation of stem cells in species other than the mouse, and pluripotent rat ES cells, capable of producing chimeras, were found to grow best on primary rat embryonic fibroblasts as the feeder layer (13). Freshly isolated cells from ICMs have been injected into blastocysts to produce chimeric offspring in both sheep and cattle (14), and their totipotency at this stage is further demonstrated by their ability to produce offspring after transfer into enucleated oocytes (15). Such nuclear transfer techniques are potentially very useful for the production of clonal offspring and would avoid the initial chimeric generation necessitated by the injection of ES cells into blastocysts. Recently, bovine-specific culture methods have shown promise with cells of up to 27 d of age maintaining their ability to direct normal calf development following nuclear transfer (16). However, at the present time the reliable generation of bovine ES cell lines requires the pooling of ICMs from several blastocysts and further efforts are required to enable the long-term culture of clonal bovine ES cells. Although to date chimeric animals have been generated from several species including the pig (17), in no species other than the mouse has germline transmission of an ES cell been successfully demonstrated. This remains a major goal for the future and may well require the use of novel strategies which depart widely from the traditional methods used in the mouse.

#### *Nonmurine species in biomedical research*

Selected physiological questions may be more conveniently modelled in the rat or in larger species. Not only can physical size be an advantage for biochemical sampling and physiological analyses, but certain genes may provide useful information when introduced into, for example, the rat genome when parallel experiments in the mouse would be ineffective. Examples include the modulation of blood pressure by the mouse *Ren-2* gene (18) and the modeling of inflammatory disease (19). In both cases, but for different reasons, no phenotype was observed in the respective transgenic mice, highlighting one of the advantages of having alternative species for understanding physiological mechanisms and the etiology of disease. More recently, a number of transgenic experiments have been undertaken to investigate lipoprotein metabolism. The human apolipoprotein A-1 gene was successfully expressed in the rat (20), resulting in increased serum HDL cholesterol concentrations, and attempts to therapeutically lower apo B100, and hence LDL and lipoprotein(a) concentrations, in the rabbit were successful (21) but resulted in complications. Although the targeted expression of the apo B-editing protein in the liver of the transgenic rabbits resulted in reduced LDL and lipoprotein(a) concentrations as intended, many of the animals developed liver dysplasia, suggesting that high level expression of the editing protein had unforeseen and detrimental side effects, possibly via the editing of other important mRNAs. The rabbit has also been used in HIV-1 research, with the development of a line expressing the human CD4 protein on T lymphocytes (22). Susceptibility to HIV infection was demonstrated, and although the rabbits are less sensitive to infection than humans, they may represent an inexpensive alternative to primates for many studies.

Gene transfer in farm animals was initially aimed towards improving production efficiency, carcass quality (23), and disease resistance of livestock. However, it has been suggested that the simple over-expression of hormones such as growth hormone may have unacceptable side effects. Recently some elegant studies of growth using transgenic rats have been performed and are likely to yield valuable information on the biochemistry and physiology of growth (24, 25). A more successful application of transgenesis in farm animals has been the production of biomedically important proteins. The two most popular methods have been to direct expression to hematopoietic cells or to the lactating mammary gland. In the former case, transgenic swine expressing high levels of human hemoglobin were generated using the locus control region from the  $\beta$ -globin gene cluster to overcome positional effects and direct expression to the hematopoietic cells (26). However, due to its natural ability to synthesize and secrete large amounts of protein, the mammary gland has become the primary focus for the expression of heterologous proteins in large mammals. Transgene expression has been successfully directed to the mammary gland using promoter sequences from milk protein genes such as those encoding ovine  $\beta$ -lactoglobulin (BLG), goat  $\beta$ -casein, and murine whey acidic protein. The BLG promoter was used to direct expression of human  $\alpha_1$ -antitrypsin in lines of transgenic mice and sheep (27). Interestingly, a wide variation in expression was observed between mouse lines, and from one lactation to another within a single line. In sheep however, similar high levels of heterologous protein were expressed in milk over consecutive lactations and over several generations in a given transgenic line, allowing the viable development of a flock of transgenic sheep. In separate studies high levels of expression of human tissue plasminogen activator were obtained in goat's milk under the control of the goat  $\beta$ -casein promoter (28). The development of suitable purification methods and the use of transgenically produced proteins in clinical trials are well advanced, and, if successful, will have important implications for the production of human proteins in transgenic livestock. Poor expression of the ovine promoter in the mouse may reflect species differences in recognizing heterologous versus homologous promoters and raises questions concerning the predictive value of mouse models. At best therefore the generation of transgenic mice may, in certain cases, only be a guide to the potential success of a transgene construct in another species.

Gene transfer could equally be used to enhance the quality and suitability of milk derived from domesticated animals as a food for human consumption. Human milk is devoid of  $\beta$ -lactoglobulin, which is responsible for most of the allergies to cows' milk, and has a relatively high content of lactoferrin, which is important in iron transport and combating bacterial infections. One could envisage in the future the reduction of saturated fat content in cows' milk and the knock-out of unwanted proteins or their replacement with other more useful components. Through the manipulation of milk constituents it should be possible to more closely emulate the desirable components of human milk. The alteration of milk composition would appear to be a practical possibility given that milk micelles are remarkably tolerant to changes in composition, as demonstrated by the knock-out of the mouse  $\beta$ -casein gene (29). Ethical concerns regarding the generation of transgenic animals, which have been engineered specifically for pharmaceutical, medical, or nutritional reasons, lie outside the scope

of this overview, however it must be clearly ascertained that expression of a transgene does not compromise the animal.

### *Xenograft organs for transplantation surgery*

The shortage of human organs for transplantation has raised interest in the possibility of xenotransplantation, i.e. the use of animal organs (30). However, the major barrier to successful xenogeneic organ transplantation is the phenomenon of complement-mediated hyperacute rejection (HAR), brought about by high levels of circulating natural antibodies that recognize carbohydrate determinants on the surface of xenogeneic cells. After transplantation of the donor organ, a massive inflammatory response ensues through activation of the classical complement cascade. This leads to activation and destruction of the vascular endothelial cells and, ultimately, the donor organ. The membrane-associated complement inhibitors, endogenous to the donor organ, are species restricted and thus confer only limited resistance. The complement cascade is regulated at specific points by proteins such as decay accelerating factor (DAF), membrane cofactor protein, and CD59. These regulators of complement activation are species specific. The initial strategy used to address HAR in porcine-to-primate xenotransplantation was to produce transgenic pigs expressing high levels of the human terminal complement inhibitor, hCD59. This was shown to protect the xenogeneic cells from human complement-mediated lysis in vitro (31). More recently, organ transplantation has been achieved using donor pigs which expressed human DAF on their endothelium (32), or both DAF and CD59 on erythrocytes, such that the proteins translocated to the cell membranes of endothelial cells (33). After transplantation, the pig hearts survived in recipient baboons for prolonged periods without rejection (33). Clearly, such genetic manipulations are bringing xenotransplantation ever closer to reality. If the isolation of suitable ES cells and application of homologous recombination becomes a reality in the pig, it may be possible to knockout the antigenic determinants to which antispecies antibodies bind, as a further strategy for eliminating HAR.

### *Summary*

The use of nonmurine species for transgenesis will continue to reflect the suitability of a particular species for the specific questions being addressed, bearing in mind that a given construct may react very differently from one species to another. The application of transgenesis in the pig should produce major advances in the fields of transfusion and transplantation technology, while alterations in the composition of milk in a range of domesticated animals will have major effects on the production of pharmacologically important proteins and could eventually lead to the development of human milk substitutes. Despite the lack of germline transmission to date, major efforts continue to be directed towards the generation and use of ES cells from nonmurine species, using both traditional and new technologies, and the availability of such cells is likely to accelerate both the use of such species and the precision with which genetic changes can be introduced.

### **References**

1. Murphy, D., and D.A. Carter, editors. 1993. Transgenesis techniques: principals and protocols *In Methods in Molecular Biology*. Vol. 18. Humana Press Inc., Totowa, NJ.
2. Hooper, M.L. 1992. Embryonal Stem Cells. *Introducing Planned* Changes into the Animal Germline. Harwood Academic Publishers, Berks, UK.
3. Mullins, J.J., and L.J. Mullins. 1993. Transgenesis in non-murine species. *Hypertension (Dallas)*. 22:630-633.
4. Eyestone, W.H. 1994. Challenges and progress in the production of transgenic cattle. *Reprod. Fertil. Dev.* 6:647-652.
5. Clark, A.J., P. Bissinger, D.W. Bullock, S. Damak, R. Wallace, C.B.A. Whitelaw, and F. Yull. 1994. Chromosomal position effects and the modulation of transgene expression. *Reprod. Fertil. Dev.* 6:589-598.
6. Orkin, S.H. 1990. Globin gene regulation and switching. *Cell*. 63:665-672.
7. Lake, R.A., D. Wotton, and M.J. Owen. 1990. A 3' transcriptional enhancer regulates tissue-specific expression of the human CD2 gene. *EMBO (Eur. Mol. Biol. Organ.) J.* 9:3129-3136.
8. Bonifer, C., M. Vidal, F. Grosveld, and A.E. Sippel. 1990. Tissue specific and position independent expression of the complete gene for chicken lysozyme in transgenic mice. *EMBO (Eur. Mol. Biol. Organ.) J.* 9:2843-2848.
9. McKnight, R.A., A. Shamay, L. Sankaran, R.J. Wall, and L. Henninghausen. 1992. Matrix-attachment regions can impart position-independent regulation of a tissue-specific gene in transgenic mice. *Proc. Natl. Acad. Sci. USA*. 89:6943-6947.
10. Pierce, J.C., B. Sauer, and N. Sternberg. 1992. A positive selection vector for cloning high molecular weight DNA by the bacteriophage P1 system: improved cloning efficacy. *Proc. Natl. Acad. Sci. USA*. 89:2056-2060.
11. Shizuya, H., B. Birren, U.-J. Kim, V. Mancino, T. Slepak, Y. Tachiiri, and M. Simon. 1992. Cloning and stable maintenance of 300-kilobase-pair fragments of human DNA in *Escherichia coli* using an F-factor-based vector. *Proc. Natl. Acad. Sci. USA*. 89:8794-8797.
12. Larin, Z., A.P. Monaco, and H. Lehrach. 1991. Yeast artificial chromosome libraries containing large inserts of mouse and human DNA. *Proc. Natl. Acad. Sci. USA*. 88:4123-4127.
13. Iannaccone, P.M., G.U. Taborn, R.L. Garton, M.D. Caplice, and D.R. Brenin. 1994. Pluripotent embryonic stem cells from the rat are capable of producing chimeras. *Dev. Biol.* 163:288-292.
14. Anderson, G.B. 1992. Isolation and use of embryonic stem cells from livestock species. *Anim. Biotechnol.* 3:165-175.
15. Sims, M., and N.L. First. 1993. Production of calves by transfer of nuclei from cultured inner cell mass cells. *Proc. Natl. Acad. Sci. USA*. 90:6143-6147.
16. First, N.L., M.M. Sims, S.P. Park, and M.J. Kent-First. 1994. Systems for production of calves from cultured bovine embryonic cells. *Reprod. Fertil. Dev.* 6:553-562.
17. Wheeler, M.B. 1994. Development and validation of swine embryonic stem cells: a review. *Reprod. Fertil. Dev.* 6:563-568.
18. Mullins, J.J., J. Peters, and D. Ganten. 1990. Fulminant hypertension in transgenic rats harbouring the mouse Ren-2 gene. *Nature (Lond.)*. 344:541-544.
19. Hammer, R.E., S.D. Maika, J.A. Richardson, J.-P. Tang, and J.D. Taurog. 1990. Spontaneous inflammatory disease in transgenic rats expressing HLA-B27 and human  $\beta_2$ -m: an animal model of HLA-B27-associated human disorders. *Cell*. 63:1099-1112.
20. Swanson, M.E., T.E. Hughes, I. St. Denny, D.S. France, J.R. Paterniti, C. Tapparelli, P. Gfeller, and K. Burki. 1992. High level expression of human apolipoprotein A-I in transgenic rats raises total serum high density lipoprotein cholesterol and lowers rat apolipoprotein A-I. *Transgenic Res.* 1:142-147.
21. Yamanaka, S., M.E. Balestra, L.D. Ferrell, J. Fan, K.S. Arnold, S. Taylor, J. M. Taylor, and T.L. Innerarity. 1995. Apolipoprotein B mRNA-editing protein induces hepatocellular carcinoma and dysplasia in transgenic animals. *Proc. Natl. Acad. Sci. USA*. 92:8483-8487.
22. Dunn, C.S., M. Mehtali, L.M. Houdebine, J.-P. Gut, A. Kirn, and A.-M. Aubertin. 1995. Human immunodeficiency virus type 1 infection of human CD4-transgenic rabbits. *J. Gen. Virol.* 76:1327-1336.
23. Solomon, M.B., V.G. Pursel, E.W. Paroczay, and D.J. Bolt. 1994. Lipid composition of carcass tissue from transgenic pigs expressing a bovine growth hormone gene. *J. Anim. Sci.* 72:1242-1246.
24. Flavell, D.M., T. Wells, S.E. Wells, D.F. Carmignac, G.B. Thomas and I.C. A.F. Robinson. A new dwarf rat I: Dominant negative phenotype in GRF-GH transgenic growth retarded (Tgr) rats. 1995. Abstracts of the 77th Annual meeting of The Endocrine Society. P2-239.
25. Wells, T., D.M. Flavell, S.E. Wells, D.F. Carmignac, G.B. Thomas and I.C. A.F. Robinson. A new dwarf rat II: GH secretion, responses to GRF and somatostatin, and growth stimulation by GRF in the GRF-GH transgenic (Tgr) rat. 1995. Abstracts of the 77th Annual meeting of The Endocrine Society. P2-240.
26. Sharma, A., M.J. Martin, J.F. Okabe, R.A. Truglio, N.K. Dhanjal, J.S. Logan, and R. Kumar. 1994. An isologous porcine promoter permits high-level expression of human hemoglobin in transgenic swine. *Biotechnology*. 12:55-59.
27. Carver, A.S., M.A. Dalrymple, G. Wright, D.S. Cottom, D.B. Reeves, Y.H. Gibson, J.L. Keenan, J.D. Barrass, A.R. Scott, A. Colman, and I. Garner. 1993. Transgenic livestock as bioreactors: stable expression of human alpha-1-antitrypsin by a flock of sheep. *Biotechnology*. 11:1263-1270.
28. Ebert, K.M., J.P. Selgrath, P. DiTullio, J. Denman, T.E. Smith, M.A. Memon, J.E. Schindler, G.M. Monastersky, J.A. Vitale, and K. Gordon. 1991. Recombinant production of a variant of human tissue-type plasminogen activator in goat milk: generation of transgenic goats and analysis of expression. *Biotechnology*. 9:835-838.

29. Kumar, S., A.R. Clarke, M.L. Hooper, D.S. Horne, A.J.R. Law, J. Leaver, A. Springbett, E. Stevenson, and J.P. Simons. 1994. Milk-composition and lactation of beta-casein-deficient mice. *Proc. Natl. Acad. Sci. USA*. 91: 6138-6142.
30. Dorling, A., and R.I. Lechler. 1994. Prospects for xenografting. *Curr. Opin. Immunol.* 6:765-769.
31. Fodor, W.L., B.L. Williams, L.A. Matis, J.A. Madri, S.A. Rollins, J.W. Knight, W. Velander, and S.P. Squinto. 1994. Expression of a functional human-complement inhibitor in a transgenic pig as a model for the prevention of xenogenic hyperacute organ rejection. *Proc. Natl. Acad. Sci. USA*. 91:11153-11157.
32. Rosengard, A.M., N.R.B. Cary, G.A. Langford, A.W. Tucker, J. Wallwork, and D.J.G. White. 1995. Tissue expression of human-complement inhibitor, decay-accelerating factor, in transgenic pigs: a potential approach for preventing xenograft rejection. *Transplantation (Baltimore)*. 59:1325-1333.
33. McCurry, K.R., D.L. Kooyman, C.G. Alvarado, A.H. Cotterell, M.J. Martin, J.S. Logan, and J.L. Platt. 1995. Human complement regulatory proteins protect swine-to-primate cardiac xenografts from humoral injury. *Nature Med.* 1:423-427.

# Reproduction, Fertility and Development



The official journal of the Fertility Society of Australia  
and of the Australian Society for Reproductive Biology

Contents

Volume 6

Number 5

1994

**Papers from a Symposium on Embryonic Stem Cells and Transgenic Livestock, held on 12 January 1994, at the Monash Medical Centre, Melbourne.**

Symposium organized by Alan Trounson, Robert Seamark and Julian Wells; sponsored by the Department of Industry, Technology and Commerce, and Cook Australia Pty Ltd.

Introduction.

*Alan O. Trounson*

541

Studies of *in vitro* differentiation with embryonic stem cells.

*Roger A. Pedersen*

543

Systems for the production of calves from cultured bovine embryonic cells.

*N. L. First, M. M. Sims, S. P. Park and M. J. Kent-First*

553

Development and validation of swine embryonic stem cells: a review.

*Matthew B. Wheeler*

563

Strategies for the isolation and characterization of bovine embryonic stem cells.

*Robert A. Cherny, Tonya M. Stokes, Jennifer Merei, Lucia Lom, Mal R. Brandon and R. Lindsay Williams*

569

Germ line transmission of yeast artificial chromosomes in transgenic mice.

*Lluís Montoliu, Andreas Schedl, Gavin Kelsey, Hanswalter Zentgraf, Peter Lichter and Günther Schütz*

577

Site-specific transgene insertion: an approach.

*Peter Wigley, Christiane Becker, Juliana Beltrame, Timothy Blake, Lesley Crocker, Sharon Harrison, Ian Lyons, Zara McKenzie, Rick Tearle, Robert Crawford and Allan Robins*

585

Chromosomal position effects and the modulation of transgene expression.

*A. J. Clark, P. Bissinger, D. W. Bullock, S. Damak, R. Wallace, C. B. A. Whitelaw and F. Yull*

589

## Progress and Emerging Problems in Livestock Transgenesis: a Summary Perspective

R. F. Seamark

*Department of Obstetrics and Gynaecology, The University of Adelaide,  
Adelaide, S.A. 5005, Australia.*

**Abstract.** The creation of transgenic livestock is a complex multistep procedure the successful execution of which demands a high level of skill and application. Useful animals have been generated by transfer of genes to zygotes by microinjection, but further extension to livestock breeding is severely limited by the present low efficiency and lack of precision in gene transfer procedures. There are major developments in alternative approaches to gene transfer and those based on embryonic stem (ES) cell lines show particular promise as a broadly adaptable means of allowing precise manipulation of specific genes within the animal genome. Rapid progress is being made in adapting ES cell technology to livestock species but as yet no one has demonstrated the totipotency of the putative cell lines so far generated. The demonstration of the feasibility of the chimaeric route for reinstating an ES cell genome into the germ line of the pig is a major advance. For other livestock breeds, particularly those with long generation times and bearing single young where the chimaeric route is much less useful, there are encouraging developments in nucleus transfer (cloning) technology which could provide practical solutions. Overall, there are now good reasons to be optimistic that transgenesis will eventually be available to all livestock breeders with the proviso that there are no further unanticipated phenomena such as the effect of tissue culture on imprinting, to be discovered to threaten the predictability of outcome of ES cell-derived pregnancies and further limit the potential usefulness of this futuristic technology to the livestock industry.

### Introduction

It is clear that transgenesis remains the most exciting and far reaching of recent advances in animal biotechnology. To the livestock breeder, the potential applications are legend and ordained to stretch the boundaries of human imagination.

It is also clearly evident that the term transgenesis implies more now than it did a decade ago when it was first coined by Gordon and Ruddle (1983). Then it was used to describe a technical process enabling transfer of inheritable, functioning genes between organisms, irrespective of species barriers. Now, following the advent of embryonic stem (ES) cell technology, it encompasses a process which allows the full armoury of recombinant DNA technology to be applied to enable molecular tinkering at all sites within the animal genome.

Although various studies have provided insight into what this new technology could offer to the livestock breeder, scientific and technical challenges still confront the molecular and reproductive biologist attempting to make the technology available to serve this purpose.

This paper briefly overviews the progress and emerging problems in livestock transgenesis in the light of the preceding discussion to provide a summary update.

### Transgenesis: a Multistep Procedure

Transgenesis is a multistep procedure with each step testing the limits of advanced breeding knowledge and techniques. As such, the overall success rate is critically dependent on achieving the maximum efficiency for each of the individual steps. At present, no steps are 100% efficient and losses quickly compound resulting in the very low yields seen. Typically, by means of direct microinjection, purportedly the most efficient of the physical-chemical routes of gene transfer, only 1-2% of eggs injected result in transgenic young in livestock breeds. Furthermore, the transgenes insert at random sites within the genome to interrupt normal gene function on at least 10% of occasions. There is also frequent loss of the anticipated control of expression of the transgenes that are incorporated as a result of positional effects. Such inefficiency has major cost implications in livestock breeding and especially to cattle which produce single young and have a long generation time.

There have been various attempts to improve the efficiency of gene incorporation, by injecting oocytes and zygotes at different stages of the cell cycle (Powell *et al.* 1992) or by means of UV light (French *et al.* 1990), restriction enzymes, dyestuffs or other means



in association with microinjection to increase potential insertion sites within the host DNA; however, so far, there has been no significant improvement.

Embryo culture has proved helpful in allowing selection of viable embryos after injection (Powell *et al.* 1994) but reliable identification of pre-implantation embryos containing integrated transgenes through polymerase chain reaction (PCR), or other means, is proving elusive (Eyestone 1994). However, there now appear to be several promising ways of overcoming positional effects including: flanking injected transgenes with base sequences homologous to targeted insertion sites (Wilmot and Whitelaw 1994); the use of overlapping gene sequences (Clark *et al.* 1994); and the use of dicistronic targeting vectors to couple position-independent and position-dependent transgene sequences (Mountford *et al.* 1994). The proposed use of precisely-located FLP recombinase target sites within the genome to allow both insertion and exchange of transgene cassettes through the FLP recombinase system at an efficiency comparable with the zygote microinjection approach is a particularly exciting development (Wigley *et al.* 1994).

The creation of separate artificial mammalian chromosomes (MACs) to contain the transgenes as described by Montoliu *et al.* (1994) would be the ultimate approach towards obtaining precise transgene control, but whether MACs can be made large enough to persist in the livestock genome without loss remains speculative. Of the alternative biological routes, viral vectors are potentially a 100% efficient means of achieving gene transfer but have specific limitations in the size of the gene construct that can be incorporated and problems of regulation owing to their uncontrolled site of insertion. Research exploring this approach is also heavily constrained by institutional regulatory bodies because of concerns with respect to the potential biohazardous nature of the vectors.

Sperm-mediated transfer would be a serious contender in livestock transgenesis if the efficiencies claimed by some groups (5%) (Lavitrano *et al.* 1989; Laura and Gandolfi 1993) could be more readily duplicated. The major appeal of this type of transfer is that, procedurally, it is easily incorporated into routine breeding systems and would allow a practical means of enhancing, in a directed way, the genetic potential of a herd or flock within current husbandry practices. One useful extension of this approach currently under investigation, is to couple improved methods of sperm-mediated transfer with *in vitro* maturation (IVM) and *in vitro* fertilization (IVF) procedures (Bachiller *et al.* 1991; Gagné *et al.* 1991). This would reduce the amount of DNA required and allow better regulatory control if transformed zygotes could be identified before transfer. There have been recent claims of successful extension of sperm-mediated transfer to a sheep transgenesis programme in Beijing, China,

(Y. F. Dai, personal communication) and a resurgence of interest in this approach can be anticipated.

Intravenous DNA delivery (Zhu *et al.* 1993) as a means of generating germ line transgenics remains speculative, but it could have immediate potential usefulness for production of pharmaceuticals in livestock.

### ES Technology in Livestock: Current Progress

The exciting prospect of ES cell technology is that it can overcome the limitations relating to inefficiencies in gene transfer or manipulation by providing an abundance of totipotent ES cells required to allow genetic manipulation by conventional recombinant DNA techniques. A variety of procedures are now available to ensure that those cells transformed according to plan can be identified, cloned and maintained as isogenetic cell lines. The vision is that the modified ES cell genome can then be reinstated within the germ line, thus providing an almost inexhaustible source of identical, superior transgenic stock with revolutionary impact on the livestock industry.

There are now many encouraging reports which clearly indicate that pluripotent ES cells can be created for the major livestock breeds, most notably the pig (Wheeler 1994); however, as yet, no group has demonstrated totipotency of these cells through reinstating their genome within a germ line.

Furthermore, for reasons that any practitioner in this area of ES cell research would be aware of, even if such cell lines were already available, the brave new world envisaged for the livestock breeder could not be realized immediately as procedures for reinstating the ES cell genome into a germ line are still far from routine.

Several routes are potentially available for this purpose. In the mouse, the most commonly used approach is to inject about 10–15 isolated ES cells into a blastocoel of a host blastocyst and to allow the cells to mix with the cells of the inner cell mass. The resultant chimaeric blastocysts are then transferred to recipients for rearing. In skilled hands, about 30% of the chimaeric offspring are germ line chimaeras capable of producing young with the ES cell genotype. Potentially, this figure can be increased through the use of very early (8–16-cell) stage embryos (Tokunaga and Tsunoda 1992) and tetraploid or otherwise handicapped blastocysts (Nagy *et al.* 1990), as hosts for ES cells.

As now convincingly shown by Wheeler (1994), this route can be adopted without major modification for putative pig ES cells provided one is persistent enough and chooses the right breeds. Their success also augurs well for the application of the chimaeric route to other livestock breeds, accepting the obvious constraint that a successful outcome, i.e. the creation of germ line chimaeras, can only be known in the following generation, a delay of 3–4 years in the case of cattle.

The alternative, more desired and, thus, preferred route towards reinstating the ES genome in the germ line which is now under active consideration by all major groups, is by means of nucleus transfer. The feasibility of this approach for livestock species was first indicated by Smith and Wilmut (1989) when they successfully created viable sheep zygotes by fusing individual inner cell mass cells with enucleated oocytes. This route is preferred as, when applied to ES cells, it ensures that all the cells in the offspring, including the germ cells, are of the ES cell genotype. The technical approach presently favoured by researchers remains firmly based on the cloning procedures pioneered by Willadsen (1986) where nucleus transfer is achieved by electrofusing a karyoplast with a surgically enucleated oocyte (cytoplast) derived from *in vivo* or *in vitro* sources. However, when used in cloning 16–64-cell stage embryos, the overall success of this process is only 6–7 lambs or calves born per 100 karyoplasts (blastomeres) fused and success with the smaller inner cell mass cells or ES cells may be expected to be less. Within reasonable limits, this low efficiency would be negated by the abundance of ES cells available from a given cell line and the unlimited supply of oocytes from an abattoir source that could be generated by means of IVM-procedures. Simple non-surgical methods of enucleating oocytes are also under development to facilitate this approach (Fulka and Moor 1993; Tatham *et al.* 1993). However, it may be anticipated that the maintenance of high overall yields in a complex multistep procedure such as nucleus transfer will remain a significant technical challenge to the embryologist. In the improvement of efficiency, one area of active research relates to the need to develop simple procedures to ensure a higher yield of zygotes through the matching of the stage of cell cycle of recipient oocytes and nucleus donor cells. Concomitantly, new ways of achieving cell fusion need to be devised as electrofusion often activates oocytes inappropriately owing to the major changes in cellular ion flux it induces. As a consequence, there is renewed interest in the use of Sendai virus (Tsunoda and Kato 1993) and chemical fusagens as alternative routes to nucleus transfer. However, as yet, no procedures have been developed for achieving nucleus transfer and activating the oocyte as subtle as those used by the sperm at fertilization. The isolation and sequencing of the fusagens and the active principle(s) contained within the sperm head which evoke the normal activation response of the egg would be a major advance in this area.

Embryo culture is widely used in nucleus transfer programmes as a means of selecting purportedly viable zygotes suitable for transfer and thus minimizing the number of recipients needed. Most commonly, this entails transfer to the Fallopian tube of a temporary host, usually a sheep or a rabbit. A period of *in vitro*

culture would be more convenient for this purpose but the ideal choice of media and culture conditions required for this purpose is still far from resolved (Trounson *et al.* 1994). The simple culture media, favoured by several groups including this laboratory, is now known to have long-term adverse impact on embryo viability (Walker *et al.* 1992) and the usefulness of co-culture and more complex media remains to be fully evaluated. In part, the lack of resolution in this area can be ascribed to a reluctance by many researchers to accept that ultimate proof of new culture procedures does require embryo transfer and assessment of the viability of young. The various claims for many of the cell fusion procedures now extant are still based mainly on the numbers of blastocysts generated in culture, despite the increasing evidence of significant loss of these blastocysts after transfer. It remains to be determined to what extent such losses relate to the nucleus transfer process itself, or are artifacts of the various culture systems.

#### ES Technology in Livestock: Emerging Problems

There is now growing appreciation that development of the preimplantation embryo reflects not only the genomic contribution of both parents but the quality of the environment to which the embryo is exposed.

Even small changes in this environment can impact on development with long-term implications on health and welfare. For example, in the mouse, brief exposure of preimplantation embryos to *in vivo* culture conditions can both result in substantial phenotypic variation and predicate the subsequent expression and penetration of some transgenes (Kothary *et al.* 1992 and reviewed by De-Groot and Hochberg 1993). *in vivo* ~~extended period of embryo culture (3–5 days) can result in dramatically enhanced peri- and post-natal loss and abnormally large lambs (Walker *et al.* 1992).~~

Asynchrony between the stage of development of the embryo and tract at embryo transfer can also affect development as first indicated by Wilmut and Sales (1981) in the ewe; this was also recently substantiated by Kleeman *et al.* (1994) who found that fetal growth was enhanced abnormally by advancing the stage of development of the tract in recipient ewes through administering progesterone during the first three days of pregnancy. Similar results had been previously obtained in the cow (Garrett *et al.* 1988). Further study of the full range of epi-genetic factors influencing gene expression during this critical developmental period is thus clearly warranted.

Insight into the cellular and molecular biology underlying these phenomena has been provided by studies characterizing the tract in terms of the production of growth factor and cytokines and the embryo in terms of its receptors (Gandolfi 1994; Watson *et al.* 1992, 1994). These studies, together with others on the impact of



macromolecules (Hill *et al.* 1994), redox active substances and various substrates (Tounson *et al.* 1994), clearly indicate both the complexity and subtlety of the tubal and uterine environment and the communication networks influencing the development of the conceptus.

The contingencies imposed by culture and other embryo micromanipulation procedures used in ES cell culture and nucleus transfer on imprinted genes such as insulin-like growth factor 2 (IGF2) and its receptor (IGF2r) may provide particular insight in relation to anomalies in fetal growth and development, as would the study of cytokines and other growth factors which interact directly with the genome. Culture conditions are also known to alter the status of imprinted genes within ES cell lines and to change both the genotype and phenotype of cell lines in culture (Parchment and Natarayan 1992) with unanticipated implications for procedural outcomes (Pedersen 1994). The degree to which these or other wild cards yet to be discovered will curtail the eventual usefulness of transgenic ES cells to the livestock breeder remains a matter of speculation.

## References

- Jochiller, D., Schellander, K., Pell, J., and Ruther, U. (1991). Liposome-mediated DNA uptake by sperm cells. *Mol. Reprod. Dev.* 30, 194-200.
- Clark, A. J., Bissinger, P., Bullock, D. W., Damak, S., Wallace, R., Whitelaw, C. B. A., and Yull, F. (1994). Chromosomal position effects and the modulation of transgene expression. *Reprod. Fertil. Dev.* 6, 589-98.
- De-Groot, N., and Hochberg, A. (1993). Gene imprinting during placental and embryonic development. *Mol. Reprod. Dev.* 36, 390-406.
- Eyestone, W. H. (1994). Challenges and progress in the production of transgenic cattle. *Reprod. Fertil. Dev.* 6, 647-52.
- French, A., Du, Z., and Seamark, R. F. (1990). Ultraviolet light increased the integration frequency of microinjected DNA. *Proc. 22nd Annu. Conf. Aust. Soc. Reprod. Biol. Abstract No. 54.*
- Fulka, J. Jr, and Moor, R. M. (1993). Non-invasive chemical enucleation of mouse oocytes. *Mol. Reprod. Dev.* 34, 427-30.
- Gagné, M. B., Pothier, F., and Strard, M.-A. (1991). Electroporation of bovine spermatozoa to carry foreign DNA into oocytes. *Mol. Reprod. Dev.* 29, 6-15.
- Gandolfi, F. (1994). Autocrine, paracrine and environmental factors influencing embryonic development from zygote to blastocyst. *Theriogenology* 41, 95-100.
- Garrett, J. E., Gelsert, R. D., Zavy, M. T., and Morgan, G. L. (1988). Evidence for maternal regulation of early conceptus growth and development in beef cattle. *J. Reprod. Fertil.* 84, 437-46.
- Gordon, J. W., and Ruddle, F. H. (1983). Gene transfer in mouse embryos: production of transgenic mice by pronuclear injection. *Methods Enzymol.* 101, 411-33.
- Hill, J. C., Walker, S. K., and Nancarrow, C. D. E. (1994). The effects of an ovine oviducal estrus-associated glycoprotein on embryo cleavage and blastocyst formation rate. *Theriogenology* 41, 215. [Abstr.]
- Kleeman, D. O., Walker, S. K., and Seamark, R. F. (1994). Fetal growth in sheep is enhanced when progesterone is administered during the first three days of pregnancy. *J. Reprod. Fertil.* (In press.)
- Kothary, R. K., Allen, N. D., Barton, S. C., Norris, M. L., and Sorani, M. A. H. (1992). Factors affecting cellular mosaicism in the expression of a *lac 2* transgene in two cell stage mouse embryos. *Biochem. Cell Biol.* 70, 1097-104.
- Laura, A., and Gandolfi, F. (1993). Recent advances in sperm cell mediated transfer. *Mol. Reprod. Dev.* 36, 255-7.
- Lavitrano, M., Camaloui, A., Fazio, V. M., Dolle, S., Farace, M. G., and Spadofara, C. (1989). Sperm cells as vectors for introducing foreign DNA into eggs: genetic transformation of mice. *Cell* 57, 717-23.
- Montellu, L., Schedl, A., Kelsey, G., Zentgraf, H., Brandon, M. R., and Williams, R. L. (1994). Germ line transmission of yeast artificial chromosomes in transgenic mice. *Reprod. Fertil. Dev.* 6, 577-84.
- Mountford, P., Zevnik, B., Duwel, A., Nichols, J., Li, M., Dani, C., Robertson, M., Chambers, J., and Smith, A. (1994). Dicistronic targeting constructs: reporters and modifiers of mammalian gene expression. *Proc. Natl Acad. Sci. USA* 91, 4303-7.
- Nagy, A., Goeza, E., Diaz, E. M., Prideaux, V. R., Ivanyi, E., Marikula, M., and Rossant, J. (1990). Embryonic stem cells alone are able to support fetal development in the mouse. *Development* 110, 815-21.
- Parchment, R. E., and Natarayan, K. (1992). A free-radical hypothesis for the instability and evolution of genotype and phenotype *in vitro*. *Cytotechnology* 10, 93-124.
- Pedersen, R. (1994). Relationship between cell lineage and genomic imprinting in mammalian development. *Reprod. Fertil. Dev.* 6, 543-52.
- Powell, B. C., Walker, S. K., Bawden, C. S., Sivaprasad, A. V., and Rogers, G. E. (1994). Transgenic sheep and wool growth: possibilities and current status. *Reprod. Fertil. Dev.* 6, 615-23.
- Powell, D. J., Galli, C., and Moor, R. M. (1992). The fate of DNA injected into mammalian oocytes and zygotes at different stages of the cell cycle. *J. Reprod. Fertil.* 95, 211-20.
- Smith, L. C., and Wilmut, I. (1989). Influence of nuclear and cytoplasmic activity on the development *in vivo* of sheep embryo after nuclear transplantation. *Biol. Reprod.* 40, 1027-35.
- Tatham, B. G., Dowling, A. T., and Tounson, A. O. (1993). Enucleation by centrifugation for bovine nuclear transplantation. *Proc. 25th Annu. Conf. Aust. Soc. Reprod. Biol. Abstract No. 31.*
- Tokunaga, T., and Tsunoda, Y. (1992). Efficacious production of viable germ-line chimeras between embryonic stem (ES) cells and 8-stage embryos. *Dev. Growth & Differ.* 34, 561-6.
- Tounson, A., Pushett, D., MacLellan, L. J., Lewis, I., and Gardner, D. K. (1994). Current status of IVF/IVF and embryo culture in humans and farm animals. *Theriogenology* 41, 57-66.
- Tsunoda, Y., and Kato, Y. (1993). Nuclear transplantation of embryonic stem cells in mice. *J. Reprod. Fertil.* 98, 537-40.
- Walker, S. K., Heard, T. M., and Seamark, R. F. (1992). *In vitro* culture of sheep embryos without co-culture: successes and perspectives. *Theriogenology* 37, 111-26.
- Watson, A. J., Hogan, A., Hahnel, A., Welner, K. E., and Schultz, G. A. (1992). Expression of growth factor ligand and receptor genes in the pre-implantation bovine embryo. *Mol. Reprod. Dev.* 31, 87-95.
- Watson, A. J., Watson, P. H., Arcellana-Paulillo, M., Warnes, D., Walker, S. K., Schultz, G. A., Armstrong, D. T., and Seamark, R. F. (1994). A growth factor phenotype map for ovine preimplantation development. *Biol. Reprod.* 50, 725-33.
- Wheeler, M. B. (1994). Development and validation of swine embryonic stem cells: a review. *Reprod. Fertil. Dev.* 6, 563-8.

- Wigley, P., Becker, C., Beltrame, J., Blake, T., Crocker, L., Harrison, S., Lyons, I., McKenzie, Z., Tearle, R., Crawford, R., and Robins, A. (1994). Site-specific transgene insertion: an approach. *Reprod. Fertil. Dev.* 6, 585-8.
- Willadsen, S. M. (1986). Nuclear transplantation in sheep embryos. *Nature (Lond.)* 320, 63-5.
- Wilmut, I., and Sales, D. I. (1981). Effect of an asynchronous environment on embryonic development in sheep. *J. Reprod. Fertil.* 61, 179-84.
- Wilmut, I., and Whitelaw, C. B. A. (1994). Strategies for production of pharmaceutical proteins in milk. *Reprod. Fertil. Dev.* 6, 625-30.
- Zhu, N., Uggitt, D., Liu, Y., and Debs, R. (1993). Systemic gene expression after intravenous DNA delivery into adult mice. *Science* 261, 209-15.

Revised manuscript received and accepted 14 April 1994